The dark side of primary production in temperate forest soils

Dissertation

To fulfil the

Requirement for the Degree of

"doctor rerum naturalium" (Dr. rer. nat)

FRIEDRICH-SCHILLER-
UNIVERSITÄT
JENA

Submitted to the Council of the Faculty

of Biological Sciences

of the Friedrich Schiller University Jena

by **MSc. Rachael Oluwatoyin Akinyede**

born on 26th April 1990 in Enschede, The Netherlands.

Reviewers: 1. Prof. Dr. Kirsten Küsel, Faculty of Biological sciences (Jena)
2. Prof. Dr. Gerd Gleixner, Max Planck Institute for Biogeochemistry (Jena)
3. Prof. Dr. Steffen Kolb, Leipniz-Zentrum für Agrarlandschaftsforschung (Müncheberg)

Date of defense: 27.09.2022

Dissertation, Friedrich-Schiller-Universität Jena, 2022

Soil, Microbes, Carbon;

A tale of an intriguing interplay underfoot!

Contents

Abbreviations

16S rRNA	16S ribosomal RNA
aclA	ATP citrate lyase alpha subunit
CBB	Calvin Benson Bassham pathway
CO_2	Carbon dioxide
DNA	Deoxyribonucleic acid
EA	Elemental analyser
HPLC	High-performance liquid chromatography
IRMS	Isotope ratio mass spectrometry
KEGG	Kyoto Encyclopedia of Genes and Genomes
MB	Microbial biomass
MBC	Microbial biomass carbon
NADPH	Nicotinamide adenine dinucleotide phosphate
PC	Pyruvate carboxylase
PEP	Phosphoenolpyruvate
PEPC	Phosphoenolpyruvate carboxylase
Pg C	Petagram of carbon
PICRUSt2	Phylogenetic Investigation of Communities by Reconstruction of Unobserved States (v2.2.0 beta)
rTCA	Reverse tricarboxylic acid cycle
RuBisCO	Ribulose 1,5, Bisphosphate Carboxylase Oxygenase
SOC	Soil organic carbon
SOM	Soil organic matter
WLP	Wood Ljungdahl pathway

Summary

Soils are the largest terrestrial organic carbon pool and source of atmospheric CO_2. The fate of organic carbon in soils is chiefly controlled by microbial activities, mainly via mineralization by heterotrophs releasing CO_2. However, before it is released into the atmosphere, a portion of this CO_2 is refixed non-phototrophically by chemolithoautotrophic microbes. This process is called dark CO_2 fixation, and is expected to not only modulate CO_2 fluxes, but also contribute to soil organic carbon (SOC). Thus, CO_2 fixation could be linked to the increase of SOC stocks in soils like those of temperate forests, in addition to increased plant inputs. As SOC from plant litter decreases with depth, there is a reduced availability of nutrients for heterotrophs. But since CO_2 concentration increases with depth, the relative impact of chemolithoautotrophy likely increases with depth. This is expected to affect SOC and soil CO_2 fluxes and might vary with changes in biogeochemical and climatic factors. Thus, quantifying the inputs and chemolithoautotrophic potential for CO_2 fixation across temperate forest soil depths and the factors affecting this process, is required to determine its contribution to SOC and soil CO_2 fluxes, and its response to shifts in biogeochemical parameters and global climate change.

To evaluate the potential contribution of dark CO_2 fixation to SOC, dark CO_2 fixation rates were quantified across 1 m soil profiles in temperate forest soils using ^{13}C metabolic labelling incubations. This method enabled the tracing of ^{13}C-CO_2 into microbial biomass carbon (MBC) and SOC. Dark CO_2 fixation rates per gram of soil were highest in the top horizons and decreased with depth, along with a decrease in SOC and MBC content. Contributions to MBC and SOC were observed across the profile accounting for up to 1% and 0.01%, respectively. With these findings, dark CO_2 fixation is likely an important source of carbon to microbial biomass and is suggested to contribute to the entire soil organic matter pool across depth.

Additionally, the genomic potential for chemolithoautotrophy across depth was determined using high throughput *16S rRNA* gene sequencing of the bacterial community accompanied by PICRUSt2 predictions and quantitative PCR (qPCR) analysis of functional genes. The abundance of autotroph genes was mostly similar with depth and did not correlate with CO_2 fixation rates. Dark CO_2 fixation rates were rather correlated with microbial biomass, as reflected by a uniformity of the rates per gram MBC across depth. Further statistical modelling comparing CO_2 fixation rates over three temperate forests soils revealed a correlation with MBC. This suggests microbial biomass as the main driver of CO_2 fixation and thus, could be a proxy for predicting CO_2 fixation rates in temperate forest soils. Further screening to identify

the CO_2 fixation pathways showed that genes for non-autotrophic anaplerotic CO_2 fixation were predicted in bacterial OTUs that constituted ~70% of the community. These OTUs were mainly affiliated with the dominant bacterial phyla in the soils; *Proteobacteria*, *Acidobacteria,* and *Actinobacteria*. Bacterial OTUs predicted with autotrophic genes were 4 times less and made up less than 20% of the bacterial community. Most of these putative autotrophs possessed RuBisCO genes of the Calvin Benson Bassham (CBB) pathway. The qPCR analysis of these marker genes confirmed the predicted low potential for autotrophy with up to 5%. The correlation of CO_2 fixation rates with microbial biomass and the high potential for anaplerotic CO_2 fixation thus suggests that dark CO_2 fixation in temperate forest soils is likely a common cellular mechanism within the soil microbiome, and not specific for chemolithoautotrophs.

When comparing fixation rates across soils dominated by deciduous (beech) and coniferous (pine) trees, the correlation with microbial biomass was not universal. Pine subsoils featured lower rates than beech subsoils, despite comparable microbial biomass content. The lower rates in pine subsoils were linked to lower SOC inputs from shallow-rooted pine trees to the deep horizons, and this was accompanied by a distinct community composition like *Chloroflexi* with a lower CO_2 fixation potential. These suggest that a lower SOC input influenced the community composition, resulting in a lower CO_2 fixation rate. Thus, in addition to MBC, SOC is a key driver of CO_2 fixation. Fixation rates also correlated with pH across all forest soils investigated, and this was linked to the potential influence of pH on the SOC inputs and the community.

Extrapolating CO_2 fixation rates per unit area and to in-situ temperature conditions resulted in a fixation rate as high as 25 ± 7.2 g C m^{-2} yr^{-1} to 1 m depth, and this recycled 5.6% of CO_2 from soil respiration. Upscaling over the global temperate forest area suggests the fixation of 0.26 ± 0.07 Pg C annually. This amount is equivalent to the reported annual net carbon sink in temperate forests globally and likely accounts for 2% of global temperate forest soil respiration. This suggest that dark CO_2 fixation recycles a substantial amount of temperate forest soil CO_2 and maintains the carbon sink of temperate forests. Higher CO_2 concentrations increased fixation rates, with a linear 120% increase between 2% and 10% CO_2. Assuming this rate of increase, we estimated that CO_2 fixation across all temperate forest soils globally might increase by 35% under a projected 164% increase in atmospheric CO_2 by the year 2100. As this increase is 1.6-fold less than projected increase in soil respiration (120% increase), dark CO_2 fixation might recycle only 1.2% of CO_2 from soil respiration. Furthermore, CO_2 fixation showed a temperature sensitivity (Q_{10}) of 2.07, lower than the Q_{10} of net soil respiration with

2.98. Based on these Q_{10} values, we estimated that CO_2 fixation might increase by 33% under projected 4 °C warming by the end of this century. This increase is 1.16-fold less than that of soil respiration (55% more), and thus, might recycle ~1.7% of CO_2 from temperate forest soil respiration globally. These findings suggest that the impact of dark CO_2 fixation on temperate forest soil CO_2 fluxes might diminish under projected global climate change scenarios.

The findings presented in this thesis highlight the contributions of dark CO_2 fixation to SOC by recycling CO_2 produced from soil respiration across temperate forest soil profiles. Dark CO_2 fixation is likely a ubiquitous process among temperate forest soil microbiome and not restricted to chemolithoautotrophs. It is influenced by changes in geochemical parameters like SOC and pH. As CO_2 fixation also responds to higher CO_2 concentration and temperature, this thesis further highlights that dark CO_2 fixation might be affected by global climate change.

Zusammenfassung

Böden sind der größte terrestrische Pool an organischem Kohlenstoff und eine Quelle für atmosphärisches CO_2. Der Verbleib von organischem Kohlenstoff in Böden wird hauptsächlich durch mikrobielle Aktivität gesteuert, vor allem mittels der Mineralisierung durch Heterotrophe, die CO_2 freisetzen. Bevor es jedoch in die Atmosphäre freigesetzt wird, wird ein Teil dieses CO_2 durch chemolithoautotrophe Mikroben auf nicht-photrophe Weise refixiert. Dieser Prozess wird als dunkle CO_2-Fixierung bezeichnet und beeinflusst nicht nur die CO_2-Flüsse, sondern auch den organischen Kohlenstoff im Boden (SOC). So könnte die CO_2-Fixierung - zusätzlich zum erhöhten pflanzlichen Eintrag - mit dem Anstieg der SOC-Vorräte in Böden, wie denen gemäßigter Wälder, in Verbindung stehen. Da der SOC aus der Pflanzenstreu mit zunehmender Tiefe abnimmt, ist die Verfügbarkeit von Nährstoffen für heterotrophe Organismen geringer. Da die CO_2-Konzentration jedoch mit der Tiefe zunimmt, steigt der relative Einfluss der Chemolithoautotrophie wahrscheinlich ebenfalls mit zunehmender Tiefe. Es wird erwartet, dass sich dies auf die SOC- und CO_2-Flüsse im Boden auswirkt und mit Veränderungen der biogeochemischen und klimatischen Faktoren variiert. Um den Beitrag von dunkler CO_2-Fixierung zum SOC- und CO_2-Fluss in den Böden gemäßigter Wälder sowie dessen Reaktion auf Veränderungen der biogeochemischen Parameter und den globalen Klimawandel zu bestimmen, ist es daher erforderlich, den Input und das chemolithoautotrophe Potenzial für die CO_2-Fixierung über verschiedene Bodentiefen sowie einflussnehmender Faktoren zu quantifizieren.

Um den potenziellen Beitrag der dunklen CO_2-Fixierung zum SOC zu bewerten, wurden die Raten der dunklen CO_2-Fixierung in 1 m tiefen Bodenprofilen aus gemäßigten Wäldern mithilfe von ^{13}C-markierten Inkubationen quantifiziert. Diese Methode ermöglichte die Rückverfolgung von ^{13}C-CO_2 in den Kohlenstoff der mikrobiellen Biomasse (MBC) und den SOC. Die dunklen CO_2-Fixierungsraten pro Gramm Boden waren in den obersten Horizonten am höchsten und nahmen mit der Tiefe ab, zusammen mit einer Abnahme des SOC- und MBC-Gehalts. Die Beiträge zu MBC und SOC wurden über das gesamte Profil hinweg beobachtet und betrugen bis zu 1 % bzw. 0,01 %. Aufgrund dieser Ergebnisse ist die CO_2-Fixierung im Dunkeln wahrscheinlich eine wichtige Kohlenstoffquelle für die mikrobielle Biomasse und trägt somit zum gesamten Pool der organischen Bodensubstanz in der Tiefe bei.

Darüber hinaus wurde das genomische Potenzial für Chemolithoautotrophie in der Tiefe durch Hochdurchsatz-Sequenzierung von bakteriellen *16S rRNA*-Genen in Verbindung mit PICRUSt2-Vorhersagen und quantitativer PCR (qPCR)-Analyse funktioneller Gene bestimmt.

Die Häufigkeit der autotrophen Gene war in der Tiefe meist ähnlich und korrelierte nicht mit den CO_2-Fixierungsraten. Die CO_2-Fixierungsraten im Dunkeln waren eher mit der mikrobiellen Biomasse korreliert, was sich in einer Gleichmäßigkeit der Raten pro Gramm MBC in der Tiefe widerspiegelte. Eine weitere statistische Modellierung, bei der die CO_2-Fixierungsraten in drei Böden gemäßigter Wälder verglichen wurden, ergab eine Korrelation mit der MBC. Dies deutet darauf hin, dass die mikrobielle Biomasse die Haupttriebkraft der CO_2-Fixierung ist und somit ein Proxy für die Vorhersage der CO_2-Fixierungsraten in Böden gemäßigter Wälder sein könnte. Ein weiteres Screening zur Identifizierung der CO_2-Fixierungswege zeigte, dass Gene für die nicht-autotrophe anaplerotische CO_2-Fixierung in ~ 70 % der bakteriellen Gemeinschaft vorhergesagt wurden. Diese OTUs gehörten hauptsächlich zu den vorherrschenden bakteriellen Phyla in den Böden: *Proteobakterien, Acidobakterien* und *Actinobakterien*. Die Anzahl der bakteriellen OTUs, für die autotrophe Gene vorhergesagt wurden, war viermal geringer und machte weniger als 20 % der bakteriellen Gemeinschaft aus. Die meisten dieser mutmaßlichen Autotrophen besaßen RuBisCO-Gene des Calvin-Benson-Bassham-Zyklus (CBB). Die qPCR-Analyse dieser Markergene bestätigte das vorhergesagte geringe Potenzial für Autotrophie mit bis zu 5 %. Die Korrelation der CO_2-Fixierungsraten mit der mikrobiellen Biomasse und das hohe Potenzial für die anaplerotische CO_2-Fixierung lassen darauf schließen, dass die dunkle CO_2-Fixierung in Böden gemäßigter Wälder wahrscheinlich ein allgemeiner zellulärer Mechanismus innerhalb des Bodenmikrobioms und nicht spezifisch für Chemolithoautotrophe ist.

Beim Vergleich der Fixierungsraten in Böden, welche von Laubbäumen (Buche) oder Nadelbäumen (Kiefer) dominiert wurden, war die Korrelation mit der mikrobiellen Biomasse nicht universell. Kiefernunterböden wiesen trotz vergleichbarem Gehalt an mikrobieller Biomasse niedrigere Raten auf als Buchenunterböden. Die niedrigeren Raten in Kiefernunterböden waren mit einem geringeren SOC-Eintrag von den flach wurzelnden Kiefern in die tiefen Bodenhorizonte verbunden, was mit einer bestimmten Zusammensetzung der Gemeinschaft wie z.B. aus *Chloroflexi* und mit einem geringeren CO_2-Fixierungspotenzial einherging. Dies deutet darauf hin, dass ein geringerer SOC-Eintrag die Zusammensetzung der Gemeinschaft beeinflusste, was auch zu einer geringeren CO_2-Fixierungsrate führte. Somit ist der SOC neben dem MBC ein wichtiger Faktor für die CO_2-Fixierung. Die Fixierungsraten korrelierten in allen untersuchten Waldböden auch mit dem pH-Wert, was mit dem potenziellen Einfluss des pH-Werts auf den SOC-Eintrag und die mikrobielle Gemeinschaft in Verbindung steht.

Die Extrapolation der CO_2-Fixierungsraten pro Flächeneinheit auf In-situ-Temperaturbedingungen ergab eine Fixierungsrate von 25 ± 7,2 g C m^{-2} yr^{-1} in 1 m Tiefe, was einem Recycling von 5,6 % des CO_2 aus der Bodenatmung entsprach. Ein Upscaling über das globale Gebiet der gemäßigten Wälder ergab eine Fixierung von 0,26 ± 0,07 Pg C jährlich. Diese Menge entspricht der bekannten jährlichen Nettokohlenstoffsenke in den Wäldern der gemäßigten Zonen weltweit und macht wahrscheinlich 2 % der globalen Bodenatmung in den Wäldern der gemäßigten Zone aus. Dies deutet darauf hin, dass durch die CO_2-Fixierung im Dunkeln ein erheblicher Teil des CO_2 im Boden der Wälder der gemäßigten Breiten recycelt wird und die Kohlenstoffsenke der Wälder gemäßigter Breiten erhalten bleibt. Höhere CO_2-Konzentrationen steigerten die Fixierungsraten mit einem linearen Anstieg von 120 % zwischen 2 % und 10 % CO_2. Ausgehend von dieser Steigerungsrate schätzten wir, dass die CO_2-Fixierung in allen Böden gemäßigter Wälder bei einem prognostizierten Anstieg des atmosphärischen CO_2 um 164 % bis zum Jahr 2100 weltweit um 35 % zunehmen könnte. Da dieser Anstieg um das 1,6-fache geringer ist als der prognostizierte Anstieg der Bodenatmung (120 %), könnte die CO_2-Fixierung im Dunkeln nur 1,2 % des CO_2 aus der Bodenatmung zurückgewinnen. Darüber hinaus zeigte die CO_2-Fixierung eine Temperaturempfindlichkeit (Q_{10}) von 2,07, die niedriger ist als die Q_{10} der Netto-Bodenatmung von 2,98. Auf der Grundlage dieser Q_{10}-Werte schätzten wir, dass die CO_2-Fixierung bei einer prognostizierten Erwärmung von 4 °C bis zum Ende dieses Jahrhunderts um 33 % zunehmen könnte. Dieser Anstieg ist um das 1,16-fache geringer als der der Bodenatmung (55 % mehr) und könnte somit weltweit ~1,7 % des CO_2 aus der Bodenatmung gemäßigter Wälder recyceln. Diese Ergebnisse deuten darauf hin, dass der Einfluss der dunklen CO_2-Fixierung auf die CO_2-Flüsse der Böden gemäßigter Wälder unter den prognostizierten Szenarien des globalen Klimawandels abnehmen könnte.

Die in dieser Arbeit vorgestellten Ergebnisse unterstreichen den Beitrag der dunklen CO_2-Fixierung zum SOC durch die Wiederverwertung von CO_2 aus der Bodenatmung in Bodenprofilen gemäßigter Wälder. Die dunkle CO_2-Fixierung ist wahrscheinlich ein allgegenwärtiger Prozess im Bodenmikrobiom gemäßigter Wälder und nicht auf chemolithoautotrophe Organismen beschränkt. Sie wird durch Veränderungen geochemischer Parameter wie dem SOC und dem pH-Wert beeinflusst. Da die CO_2-Fixierung auch auf eine höhere CO_2-Konzentration und Temperatur reagiert, zeigt diese Arbeit außerdem, dass die dunkle CO_2-Fixierung durch den globalen Klimawandel beeinflusst werden könnte.

1 Introduction

1.1 The cycling of carbon in soils

Soils can be thought of as a dynamic, heterogenous, and biologically active porous matter on the Earth's surface (Schoonover and Crim, 2015; Totsche et al., 2017), serving as a medium for plant growth, ground water recharge, nutrient cycling, and habitat for microorganisms (Thies and Grosssman, 2006; Schwilch et al., 2015; Wood, 1995). As part of the vital role of soil in sustaining life on Earth (Schoonover and Crim, 2015), soils function as the principal terrestrial repository of carbon (Jobbágy and Jackson, 2000; Lal, 2005).

The world's soils store ~2300 Pg C (total carbon pool) in the top 1 m depth (Batjes, 1996), exceeding atmospheric levels and all living plants on Earth combined (Jobbágy and Jackson, 2000; Lal, 2008). Most of this carbon is stored as soil organic matter (SOM) (1500 Pg C) (Lal, 2008; Scharlemann et al., 2014). SOM is composed of heterogeneous mixtures of primarily decaying plant matter at varying stages of decomposition, which is a blend of different simple to complex polymers like cellulose, lignin, proteins, and lipids, derived from above-ground litter and below-ground root exudates and symbiotic fungi (Gleixner et al., 2002; Kögel-Knabner, 2001; Trumbore and Czimczik, 2008). These complex polymers are subjected to oxidative, enzymatic, and hydrolytic degradation by microorganisms (mainly bacteria and fungi) across the profile (Gleixner et al., 2002; Lorenz and Lal, 2005). The by-products of this degradation can be assimilated by microorganisms to form new microbial biomass (Gleixner et al., 2002), decomposed to release carbon dioxide (CO_2) into the atmosphere (Trumbore and Czimczik, 2008), or stabilized into complex macromolecules like pyrogenic and humic substances (Lorenz and Lal, 2005; Six et al., 2002). It is, however, mostly the relatively simple molecules interacting with each other and with mineral surfaces that accumulate to form the large reserve of soil organic carbon (SOC) present in soils (Trumbore and Czimczik, 2008).

Through their biomass and residues (necromass), microbes are also a significant source of carbon in soils (Gleixner, 2013; Kallenbach et al., 2016; Kögel-Knabner, 2001). Microbial inputs as a significant source of stabilized SOM have been both conceptualized and described in soils (Kästner et al., 2021; Liang et al., 2019; Ma et al., 2018; Miltner et al., 2012) and are proposed to play an even greater role than plants in soil carbon sequestration (Kästner et al., 2021). SOC storage is considered highly influenced by microbial activities that even the most persistent SOC is made up of carbon that has initially passed through microbial biomass (Liang et al., 2019). Microbes are also metabolically flexible, with the ability to utilize other carbon

sources than plant-derived SOM (Gleixner, 2013). The uptake of different forms of carbon, particularly those present in soils in large amounts, like CO_2, has been observed in soils (Miltner et al., 2005; Nowak et al., 2015). Thus, CO_2 fixation by microorganisms likely also contributes to the large organic carbon stocks in the soil.

Due to the large and dynamic carbon pool in soils, the world's soils function as an important source and sink of atmospheric carbon (Gleixner et al., 2002). As a source of atmospheric CO_2, global soil respiration releases an estimated 60 Pg C into the atmosphere annually (Lal, 2008). A roughly equal amount of atmospheric carbon via plants is re-introduced into the soil (Lal, 2008), resulting in a neutral balance. Any shift in this carbon balance would determine whether soils act essentially as net sources or sinks of carbon. For instance, processes that influence the release of large amounts of CO_2 from soils, e.g., deforestation, may increase atmospheric CO_2 levels (Lal, 2004; 2008; Rastogi et al., 2002). Conversely, land-use changes like afforestation increase SOC stocks via increased photosynthetic CO_2 fixation by tree biomass (Grüneberg et al., 2014; Lal, 2004). Thus, carbon cycling in soil has significant effects on global climate change (Allison and Treseder, 2011). Considering that microbes are chiefly involved in the cycling and input of carbon in soil (Dell'Abate and Biro, 2015), the presence and activities of microbes, including the fixation of carbon from CO_2 in soils, might be affecting the large pools and fluxes of carbon in soils with consequences on global climate change.

1.2 Dark CO_2 fixation in soils: An overview

Responsible for the net fixation of 70 Pg C annually (Berg, 2011), CO_2 fixation is regarded as the most important biosynthetic process on Earth (Berg, 2011; Hügler et al., 2003). Various organisms, commonly plants and microbes in different ecosystems, can fix CO_2 using energy generated from sunlight (photo-autotrophy) or reduced inorganic compounds (chemolithoautotrophy), serving as the only path to generate new organic carbon in nature.

In soils, respiration (that is, the production of CO_2 from microbial decomposition of SOM using oxygen as an electron acceptor (Anderson, 1982)) leads to the release of CO_2. However, before emission into the atmosphere, small fractions of the CO_2 in the soil pore spaces can be fixed by chemolithoautotrophs and some heterotrophs to build their biomass (Miltner et al., 2005; Yuan et al., 2012), and this eventually becomes a part of SOM. Since soils are predominantly dark habitats, where light penetration is restricted, this process uses inorganic compounds, e.g., reduced nitrogen/sulphur compounds, as energy sources (Shively et al., 1998; Wu et al., 2014). This non-phototrophic assimilation of CO_2 is known as "dark CO_2 fixation" (Figure 1).

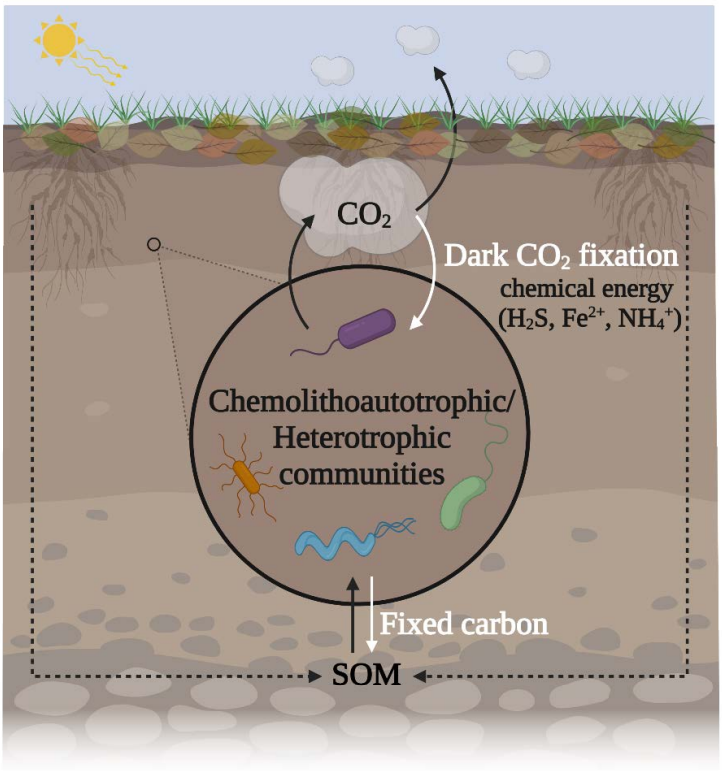

Figure 1| Scheme showing dark CO_2 fixation in soils. CO_2 is produced in mineral soils through the microbial decomposition of SOM (solid black arrows) derived from plant inputs (dashed black arrows). Dark CO_2 fixation by soil microbes may recycle some of the pore space CO_2 before it escapes into the atmosphere to form microbial biomass, which eventually forms a part of SOM (white arrows). As soils are mostly dark habitats, inorganic compounds are used as energy sources to power the fixation process.

Among the few findings documenting dark CO_2 fixation in soils, Miltner et al. (2005) reported a bulk dark CO_2 fixation rate of 0.19 µg C g (dw) $soil^{-1}$ d^{-1} in agricultural surface and subsoils (0 – 30 cm). The rate also correlated linearly with soil respiration and was enhanced by the addition of readily available organic carbon substrates. In a further study of dark CO_2 fixation in soils, Beulig et al. (2014) and Nowak et al. (2015) quantified a fixation rate of 0.14 - 0.51 µg C g (dw) $soil^{-1}$ d^{-1} in the subsoils (20 - 40 cm depth) of a mofette influenced by high subcrustal CO_2 degassing (Beulig et al., 2016), similar to rates reported by Miltner et al. (2005).

In addition to rate measurements, the genomic potential for dark CO_2 fixation, as reflected by the abundance of autotrophic CO_2 fixation genes, has long been reported in agricultural and forest soils (Selesi et al., 2005; Tolli and King, 2005) as well as in rice paddy soils (Wu et al., 2014), pointing towards a prevalence of chemoautotrophic CO_2 fixation in various soils. Furthermore, Liu et al. (2018) and Niederberger et al. (2015) demonstrated the potential for dark chemolithoautotrophic fixation of CO_2 in soils of semi-arid desert and Antarctic dry

valleys, indicating the occurrence and importance of this process for carbon accumulation in oligotrophic or extreme environments. Dark CO_2 fixation has also been suggested to be common among heterotrophs in soils (Santruckova et al., 2005). Recent studies showed high abundances of phosphoenolpyruvate carboxylase genes in arctic tundra soil profiles, indicative of non-autotrophic CO_2 fixation in these soils (Šantrůčková et al., 2018). Genomic potential for CO_2 fixation by both chemolithoautotrophs and heterotrophs has been reported in other soil types, e.g., soils of tropical forests (Nowak et al., unpublished result), and the arctics (Šantrůčková et al., 2018), suggesting this process to be common in different soils.

1.3 Role of dark CO_2 fixation in soil carbon cycling

Dark CO_2 fixation is suggested to modulate carbon emitted as CO_2 from soils and contribute to SOC content. According to Miltner et al. (2005), reported rates of dark CO_2 fixation accounted for 3 – 5% of CO_2 from soil respiration in agricultural soils. Similarly, Spohn et al. (2019) reported that dark CO_2 fixation recycled almost 4% of soil respiration across temperate forest soil horizons. Furthermore, Miltner et al. (2005) also showed that carbon derived via dark CO_2 fixation made up to ~0.05% of the total organic carbon present in agricultural soil after 80 days. As much as 27% of SOM at the top 10cm of a mofette soil was also suggested to be derived from dark CO_2 fixation (Nowak et al., 2015). Besides contributions to SOC content and modulation of CO_2 fluxes from soils, dark CO_2 fixation can also affect isotope signatures ($\delta^{13}C$ and $\Delta^{14}C$) of SOM. It is common for soils to exhibit enrichment of $\delta^{13}C$ signatures (Billings and Richter, 2006; Diochon and Kellman, 2008; Brunn et al., 2014) and depletion of $\Delta^{14}C$ signals of SOM with depth (Trumbore, 2009). The observed depth trends of $\Delta^{14}C$ signal are due to the natural radioactive decay of ^{14}C to ^{14}N (Nowak et al., 2015; Trumbore, 2009). Several mechanisms (e.g., depletion of $\delta^{13}C$ signals of atmospheric CO_2 or Suess effect, preferential decomposition of organic compounds, microbial fractionation during litter decomposition, or mixing of new and old SOC) have been proposed to explain the $\delta^{13}C$ enrichment across depth (Ehleringer et al., 2000). Biogeochemical reactions generally discriminate against ^{13}C (Cerling et al., 1991; Šantrůčková et al., 2018). Thus, carboxylation reactions involving microbial CO_2 incorporation in soils were explained as one of the most likely mechanisms responsible for the increase in $\delta^{13}C$ signatures with soil depth (Ehleringer et al., 2000). In agreement, positive discriminatory activities of the CO_2-fixing carboxylases were suggested to partly cause the positive shifts in $\delta^{13}C$ isotope signatures of SOC (Šantrůčková et al., 2018, 2000). Furthermore, in addition to the natural ^{14}C decay, more negative shifts in $\Delta^{14}C$ values of mofette SOM due to dark fixation of the ^{14}C depleted geogenic CO_2 have been documented (Nowak et al., 2015).

1.4 Pathways for dark CO_2 fixation in soils

1.4.1 Autotrophic CO_2 fixation

Generally, during CO_2 fixation, CO_2 with the oxidation state of +4 is assimilated into cellular carbon, having an average oxidation state of 0 (reduced cellular carbon, e.g., carbohydrates) (Berg, 2011). This reaction requires four electrons supplied by either NADPH or reduced ferredoxin (Bar-Even et al., 2012a; Fuchs, 2011). Reduced ferredoxin (E_0' ~400 mV) has a lower or more negative redox potential compared to NADPH (E_0' ~320 mV), that is, the half-reaction of reduced ferredoxin has a higher potential to donate electrons to reduce CO_2 (i.e., more energetic) than that of NADPH (Bar-Even et al., 2012a; Berg, 2011). Unlike NAPDH, the reducing carboxylases of ferredoxin are highly oxygen-sensitive as they contain iron-sulphur clusters and free radical intermediates that are easily oxidized (Bar-Even et al., 2012b; Erb, 2011). Hence, while reduced ferredoxin is used as reductants by anaerobes and limited to anoxic environments, aerobes often depend on NADPH as an electron donor and is commonly used in oxic environments (Bar-Even et al., 2012b). An input of energy is required for both reductants to drive the CO_2 reduction process, provided by ATP hydrolysis (Berg, 2011). Pathways that operate under anoxic conditions require less ATP than pathways employed under oxic conditions. A carboxylating enzyme is often required to link either CO_2 or HCO_3^- (bicarbonate), depending on the pH of the medium, with an organic acceptor molecule, and this enzyme must be regenerated in the subsequent steps of the pathway (Berg, 2011). The resulting drained-off products thus serve as the central metabolites from which macromolecules like nucleic acids, lipids, carbohydrates, and proteins are derived (Berg, 2011).

Chemolithoautotrophic bacteria are mostly known to fix CO_2 using six different metabolic pathways (Berg, 2011; Hügler and Sievert, 2011; Saini et al., 2011). The most predominant pathway is the Calvin-Benson-Bassham cycle (CBB) (Bassham et al., 1954). The other pathways include; the reductive citric acid (rTCA) cycle (Arnon–Buchanan cycle), the reductive acetyl-CoA pathway (Wood–Ljungdahl pathway (WLP)), the 3-hydroxypropionate/malyl-CoA cycle, the 3-hydroxypropionate/4-hydroxybutyrate cycle, and the dicarboxylate/4-hydroxybutyrate cycle (Berg et al., 2007; Buchanan and Arnon, 1990; Huber et al., 2008; Ljungdahl, 1986; Zarzycki et al., 2009). Due to the demand for reduced inorganic compounds, temperature, and O_2 preferences (Hügler and Sievert, 2011), some of these known pathways as well as other less known reported pathways are uncommon in soils. Only the first three mentioned autotrophic pathways, CBB, rTCA, and WLP, are mostly reported in soils and are thus discussed further (Figure 2).

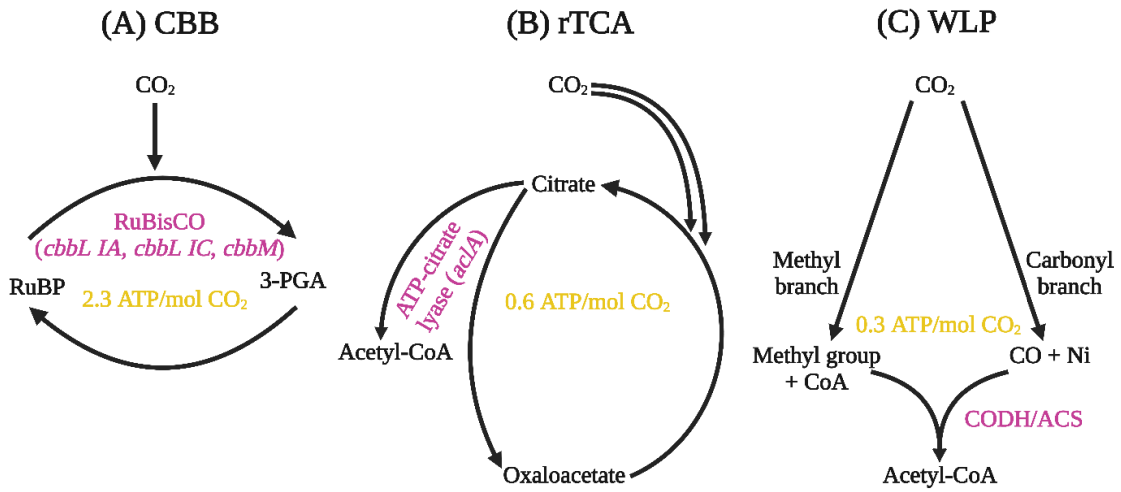

Figure 2| Simple scheme showing the prevalent autotrophic CO_2 fixation pathways in soils. Pink and yellow texts indicate the key enzymes (with encoding genes) and ATP requirements, respectively. References for the pathways, energy requirements and key enzymes/genes are found in the main text.

The Calvin Benson Bassham pathway (CBB). This is quantitatively the most significant CO_2 fixation pathway in nature (Berg, 2011; Fuchs, 2011). It depends on the activity of ribulose-1,5-bisphosphate carboxylase/oxygenase (RuBisCO). The CBB pathway has a high energy demand, requiring seven ATP equivalents and five NADPHs (2.3 mol ATP/ mol CO_2) to synthesize one molecule of glyceraldehyde-3-phosphate from three molecules of CO_2 (Bar-Even et al., 2012b; Erb, 2011a). This pathway begins with the electrophilic binding of CO_2 to ribulose-1,5-bisphosphate (RuBP), a C5 sugar in its enediolate form, catalysed by the enzyme RuBisCO. The formed product, an unstable C6 intermediate, is spontaneously split into two molecules of 3-phosphoglycerate (3-PGA) that get reduced by further gluconeogenic reactions driven by ATP hydrolysis. The final steps involve the phosphorylation of ribulose-5-phosphate by phosphoribulokinase (PRK) to regenerate RuBP (Berg, 2011) (Figure 2A).

The key enzyme, RuBisCO, is not efficient in discriminating between CO_2 and O_2 and consequently has a low catalytic affinity for CO_2 (Lorimer and Andrews, 1973). Due to adaptation to different environmental conditions (e.g., CO_2, O_2 concentrations), various forms of this enzyme, namely forms I, II, III, and IV, with different catalytic properties and oxygen sensitivity has evolved (Badger and Bek, 2008; Selesi et al., 2005; Tabita et al., 2008). Of these various forms, only forms I and II are known to participate in autotrophy (Berg, 2011). Form I RuBisCO is suggested to occur in all chemolithoautotrophs of the bacteria domain (Tolli and King, 2005) but is predominantly found in photosynthetic and aerobic chemolithoautotrophic organisms (Selesi et al., 2005). Form II RuBisCO is common among phototrophs (e.g.,

members of the non-sulphur purple bacteria) and some chemolithotrophs that grow under microoxic to anaerobic conditions (Watson and Tabita, 1997) like the facultatively anaerobic *Thiobacillus* spp. (Alfreider et al., 2003) and is encoded by the *cbbM* gene (Herrmann et al., 2015). Form I being more oxygen tolerant (Tabita et al., 2008), consists of four clades, IA to ID, encoded by the *cbbL* gene (Selesi et al., 2005; Wu et al., 2014). While obligate chemolithoautotrophs use the form IA RuBisCO, facultative chemolithoautotrophs predominately possess the form IC variant (Tolli and King, 2005; Wu et al., 2014). Mainly cyanobacteria and algae have the Clades IB and ID of form I (Tabita et al., 2008) and are less common in mineral soils where light as an energy source is a limiting factor. Form I is the most dominant RuBisCO variant in soils (Tcherkez et al., 2006; Wu et al., 2014; Yuan et al., 2012). Thus, form IA and IC, in addition to form II RuBisCO, have been the most commonly described CO_2 fixing mechanisms in soils like agricultural soils (Miltner et al., 2005; Yuan et al., 2012, 2013), wetland mofettes (Nowak et al., 2015) as well as in soils of the Arctics and Antarctica (Niederberger et al., 2015; Šantrůčková et al., 2018).

The reductive Tricarboxylic Acid pathway (rTCA). This pathway is a reversal of the oxidative TCA or Krebs cycle (Buchanan and Arnon, 1990). The rTCA pathway uses a similar set of enzymes as the TCA cycle, except that the enzymes: succinate dehydrogenase is replaced by fumarate reductase, NAD^+-dependent 2-oxoglutarate dehydrogenase by ferredoxin-dependent 2-oxoglutarate synthase, and citrate synthase by ATP-citrate lyase. (Alfreider et al., 2017; Fuchs, 2011; Hügler et al., 2005). The ATP-citrate lyase, encoded by the *aclA* gene, is regarded as a characteristic key enzyme of the pathway (Alfreider et al., 2017). It involves the cleavage of citrate by ATP citrate lyase and forms acetyl-CoA from two molecules of CO_2 (Fuchs, 2011) (Figure 2B). For bacterial assimilation, the formed acetyl-CoA is carboxylated to pyruvate by ferredoxin-dependent pyruvate synthase, which is further converted to central intermediates of carbon metabolism like phosphoenolpyruvate (PEP), oxaloacetate, and 2-oxoglutarate, before citrate is regenerated (Berg, 2011). This pathway uses both ferredoxin and NADPH as reductants. It is more energy-efficient than the CBB pathway (Berg, 2011; Campbell and Craig Cary, 2004; Hügler et al., 2005), requiring ~0.6 mol ATPs per mol of CO_2 for conversion to pyruvate and is thus, one of the most energy-efficient CO_2 fixation pathway (Bar-Even et al., 2012b; Erb, 2011a). It is mainly used by microbes dwelling under anoxic and microoxic conditions, such as green sulphur bacteria (*Chlorobium limicola*) (Fuchs, 2011; Saini et al., 2011), some members of the *Proteobacteria* and *Nitrospirae* (*Nitrospira*, *Leptospirillum*) phyla and among thermophiles (Berg, 2011). This cycle is also known to

exhibit some level of O_2 tolerance (Berg, 2011; Erb, 2011a; Hügler and Sievert, 2011) and was reported to be prevalent in oligotrophic soils with low SOC content (Liu et al., 2018).

The Wood-Ljungdahl pathway (WLP). This is also known as the reductive acetyl-CoA pathway (Ljungdahl, 1986). It is the only autotrophic pathway that can simultaneously fix CO_2 and generate ATP via substrate-level phosphorylation by converting acetyl-CoA to acetate (Fuchs, 2011). Hence, it is highly energy-efficient (~0.3 mol ATP/ mol CO_2) (Bar-Even et al., 2012b). With the aid of a coenzyme and an enzyme metal centre serving as CO_2 acceptors, two molecules of CO_2 forms acetyl CoA in a non-cyclic manner via two branches (methyl and carbonyl branches) (Figure 2C). One of the molecules of CO_2 is reduced to a methyl group and bound to a coenzyme, and the other CO_2 molecule is reduced to carbon monoxide (CO) and bound to nickel (Ni), using CO dehydrogenase/acetyl-CoA synthase (CODH/ACS) as the key enzyme (Berg et al., 2010; Hügler and Sievert, 2011; Ljungdahl, 1986). The reaction between the methyl group and CO forms an enzyme-bound Ni-acetyl group, leading to acetyl-CoA formation. The resultant assimilation of acetyl CoA via pyruvate is also as described for the rTCA cycle. The key enzymes of this pathway are very oxygen sensitive and are generally found among strict anaerobes (Saini et al., 2011). It is common among methanogens and acetogens, which synthesize methane and acetic acid respectively from CO_2, as well as sulphate reducing bacteria, some denitrifiers (Berg, 2011; Ragsdale and Pierce, 2008; Thauer et al., 2008), and some *Choloflexi* members (Hug et al., 2013; Probst et al., 2017). This pathway is prevalent in soil environments with fluctuating O_2 tensions like wetlands (Beulig et al., 2016, 2014). Thus, organisms possessing this pathway in such an environment can cope with oxidative stress by adopting strategies like synthesising oxidative response enzymes (catalase, peroxidase) or switching to favourable electron acceptors (Berg, 2011).

1.4.2 Non-autotrophic CO_2 fixation

Anaplerotic CO_2 fixation. Besides its role in cellular respiration, the tricarboxylic acid (TCA) cycle serves as a producer of cellular intermediates for monomers to build cellular macromolecules. Many of these intermediates are thus drained from the TCA cycle and used as precursors for amino acid biosynthesis and as nucleic acid building blocks (Berg et al., 2002). These intermediates must be replenished to maintain normal TCA cycle functions (Krebs, 1941). This is accomplished by anaplerotic reactions during which pyruvate or phosphoenolpyruvate (PEP) is carboxylated to oxaloacetate; hence CO_2 (as HCO_3^-) is fixed (Erb, 2011). These series of carboxylation reactions are catalyzed by biotin-dependent pyruvate carboxylase (PC) and phosphoenolpyruvate carboxylase (PEPC), respectively (Bar-Even et al.,

2010; Erb, 2011; Owen et al., 2002). Genes encoding both PC and PEPC occur together in many bacteria (Erb, 2011a; Sauer and Eikmanns, 2005), particularly those with a complete TCA cycle (Eichorst et al., 2018; Martins et al., 2019). Thus, many autotrophs and heterotrophs potentially fix CO_2 via anaplerotic reactions. Anaplerotic CO_2 fixation is not considered to lead to any net carbon accumulation (Alonso-Sáez et al., 2010; Merlin et al., 2003). However, this pathway has been described in many soils ranging from agricultural, afro-temperate forest, and arctic tundra soils (Miltner et al., 2005, 2004; Nel and Cramer, 2019; Šantrůčková et al., 2018; 2005), and is likely a widespread cellular mechanism within the soil microbiome (Figure 3).

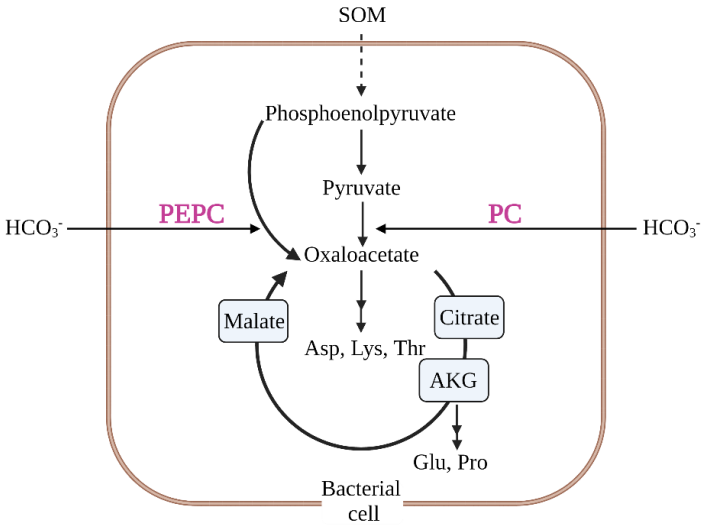

Figure 3| Metabolic routes for non-autotrophic CO_2 fixation via anaplerotic reactions during growth on soil organic matter (SOM). Carboxylation reaction by PEPC and PC enzymes (pinks texts) allows the fixation of CO_2 to form oxaloacetate, a precursor molecule required for the downstream synthesis of amino acids, like Aspartate (Asp), Lysin (Lys), Threonine (Thr), etc.

1.5 Factors influencing dark CO_2 fixation in soils

1.5.1 Soil organic carbon (SOC) input

SOC serves as the most important carbon source (Lladó et al., 2017) and regulator of soil microbes (Dalal, 1998; Su et al., 2020). Differences in SOC content and quality across depths are also reported to cause shifts in microbial community composition and abundance (Hackl et al., 2005; Lladó et al., 2017; Nacke et al., 2011; Urbanová et al., 2015), with resultant effects on their function (Dukunde et al., 2019; Kaiser et al., 2016) and likewise, rates of key processes, e.g., respiration (Walker et al., 2018). Past studies have indicated that soils with low organic carbon content likely feature higher chemolithoautotrophic activity and hence have higher CO_2 fixation rates. In a study by Xiao et al. (2018), the lower SOC content in depositional soils with

low SOC content featured about 5 times higher CO_2 fixation rates when compared to eroded sites with higher SOC due to the higher abundance of obligate autotrophs. CO_2 fixation has been suggested to be the primary carbon source in oligotrophic environments like soils from Antarctic Dry Valley soils (Niederberger et al., 2015) and semiarid desserts (Liu et al., 2018). This suggests that spatial variations of SOC inputs known to occur across soil profiles (Jobbágy and Jackson, 2000) and between soils due to differences in vegetation inputs (Liu et al., 2018; Vesterdal et al., 2013, 2008) might exert differential effects on CO_2 fixation activity in soils.

1.5.2 Soil CO_2 concentration

Another critical and known driver of dark CO_2 fixation in soils is the concentration of CO_2. CO_2 concentration in well-drained soils is several times higher than atmospheric levels, with concentrations usually ranging between 1 and 5% (Andrews and Schlesinger, 2001; Richter and Markewitz, 1995). Many microbes require CO_2 as part of their central metabolic process (e.g., replenishing TCA cycle intermediates) for their growth and function (Erb, 2011; Kreb, 1941). Some autotrophs employing the WLP pathway cannot be cultivated without the addition of a significant amount of inorganic carbon (Drake et al., 2006). Up to 2-folds increase in bacterial biomass were reported in agricultural soils exposed to elevated CO_2 (5 vol%) compared to soils incubated under ambient CO_2 concentration (0.05 vol%) (Santruckova et al., 2005). Under higher CO_2 concentrations, the energetics for autotrophic CO_2 fixation are favoured (Bar-Even et al., 2012b), and this is because biochemical reactions are substrate-dependent, with reaction rates being higher at higher substrate concentrations (Michaelis and Menten, 1913). Dark CO_2 fixation rates in the soil up to 30cm deep has also been reported to relate positively with CO_2 produced by soil respiration (Miltner et al., 2005; Spohn et al., 2019; Šantrůčková et al., 2018). As a result, an increase in CO_2 production within the soil pore spaces and its impact on dark CO_2 fixation rates will affect the amount of CO_2 emitted from soils. In comparison to surface soils, organic carbon and nutrient input are limiting in subsoils (Jobbágy and Jackson, 2000; Jones et al., 2018), but CO_2 concentrations are higher (Davidson et al., 2006). Since high abundances of chemolithoautotrophs were reported from carbon-limited soils (Li et al., 2018), an increase in CO_2 even in deep subsoils might also positively impact chemolithoautotrophic activity and the rates of dark CO_2 fixation.

1.5.3 Temperature

Temperature is one of the most important environmental factors jointly influencing soil biogeochemical processes, including the growth and activities of soil microbial communities (Biederbeck and Campbell, 1973; Brockett et al., 2012; Pietikäinen et al., 2005; Peltoniemi et

al., 2015). Higher temperature increases the kinetic energy of biomolecules and speeds up enzymatic reactions (Arrhenius, 1898; Davidson and Janssens, 2006). This leads to an increase in cellular metabolism and ATP synthesis (Boscolo-Galazzo et al., 2018), which may translate into increased rates of cellular processes, including CO_2 fixation rates. Studies showing the influence of temperature on dark CO_2 fixation in soils are scarce. A recent study reported a nearly 10-fold increase in dark CO_2 fixation rates with rising temperatures from 4 to 25 °C (Nel and Cramer, 2019). Since respiration rates increase with temperature (Hicks Pries et al., 2017; Melillo et al., 2002) and CO_2 fixation rates scale with soil respiration (Miltner et al., 2005; Spohn et al., 2019), dark CO_2 fixation may respond to temperature in a similar magnitude as soil respiration. Hence, dark CO_2 fixation rates might increase under future global warming scenarios and thus modulate the amount of CO_2 emitted from soils.

1.5.4 Soil pH

Soil pH has been reported as the best predictor of microbial communities and their functions in soils (Cheng et al., 2020; Dukunde et al., 2019; Kaiser et al., 2016; Lauber et al., 2009; Ren et al., 2018). Changes in soil pH may also affect the abundance of the CO_2 fixing communities themselves. High amounts of facultative autotrophs were reported to dominate soils with circumneutral pH over soils with low pH (Long et al., 2015; Yuan et al., 2012). A significant increase in CO_2 fixation with increasing pH was reported due to a positive correlation between pH and the abundance of specific bacteria groups like *Proteobacteria* (Long et al., 2015).

1.6 Dark CO_2 fixation in temperate forest soils: The knowns and unknowns

In response to projected threats from global climate change, there is growing interest in the capacity of forests to fix anthropogenically derived CO_2, and this is mainly due to the capacity of forest soils, particularly in temperate forests, to store carbon (Lal, 2005). The world's temperate forests serve as a net sink for an extra 0.26 Pg C yr^{-1} (Dixon et al., 1994), and ~60% of temperate forest carbon reserves are in the soil (Lal, 2005; Taggart and Cross, 2009) with 195 Pg C (1 m) (Jobbágy and Jackson, 2000). In recent decades, an increase in temperate forest SOC stocks was reported (Goodale et al., 2002; Lorenz et al., 2011) and attributed to increased tree biomass and litter inputs (Miao et al., 2019; Mobley et al., 2015; Schrumpf et al., 2014).

In addition to plant carbon inputs, previous findings indicate that many bacteria groups are capable of contributing to temperate forest SOC via CO_2 fixation (Szukics et al., 2012; VanInsberghe et al., 2015; Žifčáková et al., 2016). The presence of genes indicating the potential for autotrophic fixation of CO_2 via the CBB pathway has been documented in many

temperate forest soils (Dukunde et al., 2019; Kaiser et al., 2016; Tolli and King, 2005). In temperate forests, high concentrations of organic nutrients like dissolved organic nitrogen are constantly drained from forest floors (Qualls et al., 2000). Under favourable conditions, these may be transformed via microbial mineralization to produce ammonium and nitrite ions (Chen et al., 2019; Staelens et al., 2012), serving as potential energy sources for chemolithotrophs like ammonia and nitrite-oxidizing bacteria fixing CO_2 (Badger and Bek, 2008).

Carbon inputs into temperate forest soils through dark CO_2 fixation are suggested to be of minimum importance (Žifčáková et al., 2016) has been ignored (Lladó et al., 2017), but there are a few scattered proofs highlighting the role of dark CO_2 fixation in temperate forest soils. In a recent study, Spohn et al. (2019) observed dark CO_2 fixation rates of 0.34 μg C g soil $^{-1}$ d^{-1} in the top 0.7 m depth of a temperate forest soil. This rate accounted for up to 4% of CO_2 from soil respiration, and contributions to stable microaggregate of SOM were observed (Figure 4). However, the rate of CO_2 fixation in the deeper horizons is yet to be investigated. In fact, the majority of reported studies on dark CO_2 fixation investigated no deeper than the top 20 cm of soil depth (Ge et al., 2016; Lynn et al., 2017; Yuan et al., 2012). Considering that SOC in soils originating from plant litter typically decreases with depth (Jobbágy and Jackson, 2000), there is likely a reduced availability of nutrients for heterotrophic growth. However, CO_2 concentrations are higher (Davidson et al., 2006). Hence, diverse niches for the colonization of chemolithoautotrophic bacteria fixing CO_2 can be created across the soil profile (Ge et al., 2016; Wu et al., 2015, 2014). Past findings indicate that deep soils may harbour significant proportions of chemolithoautotrophs (Li et al., 2018), and subsoils have a high capacity to sequester substantial amounts of SOC due to the longer turnover time and chemical recalcitrance of SOM (Lorenz and Lal, 2005). Additionally, in situ CO_2 fixation is considered a consistent carbon source in organic carbon-limited soil environments (Liu et al., 2018; Niederberger et al., 2015). Therefore, the genomic potential and relative impact of chemolithoautotrophy might increase with depth (Figure 4). Consequently, CO_2 fixation likely occurs in the deeper profiles. This may serve as an additional yet important carbon source for many microbes in the subsoil and thus can affect SOC and soil CO_2 fluxes. Additionally, for global soil carbon surveys, a fixed soil depth is always considered, usually 1 m (Jobbágy and Jackson, 2000). Thus, to properly evaluate the inputs of CO_2 fixation to temperate forest SOC stocks and CO_2 fluxes, CO_2 fixation rates to 1 m deep should be quantified. Such information would be necessary to understand how microbial CO_2 assimilation modulates CO_2 fluxes from soils, and this could be tested under varying conditions, e.g., CO_2 concentration (Figure 4).

Furthermore, the apart from the potential for CO_2 fixation by gram-positive bacteria (Spohn et al., 2019) and the CBB pathway (Dukunde et al., 2019; Kaiser et al., 2016), the potential key players and other pathways for CO_2 fixation in temperate forest soils are unknown (Figure 4).

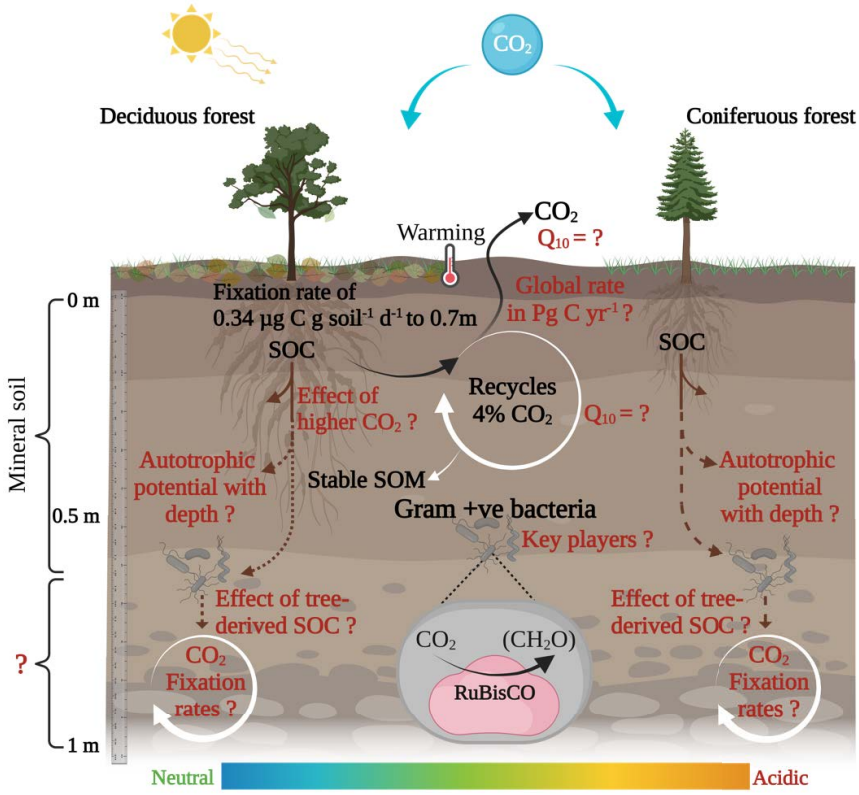

Figure 4| Dark CO_2 fixation in temperate forest soils: Black arrows close to the surface show soil respiration and while white circular arrows denote dark CO_2 fixation. SOC inputs (broken brown arrows down the profile) decrease with depth and are higher in deciduous than coniferous-dominated soils which are denoted by varying degrees of broken lines. Increase in faded gray circles with depth shows increasing soil CO_2 concentration. Red texts with question marks highlight the knowledge gaps**.**

The factors that mainly shape microbial communities in temperate forest soils, particularly SOC content (Kaiser et al., 2016; Lladó et al., 2017), also affect corresponding SOM dynamics like respiration rates in temperate forest soils (Hicks Pries et al., 2017; Melillo et al., 2002). As these factors affect dark CO_2 fixation in other soils, similar effects are expected in temperate forest soils. In temperate forests, tree inputs from litter and root exudates are the dominant source of SOC (Rasse et al., 2005, 2001) which are, in turn, important carbon sources for forest soil microbes (Lladó et al., 2017). Differences in tree species influence the content and quality of SOC (Vesterdal et al., 2013) and, consequently, microbial communities and their functional potentials across the soil profile (Hackl et al., 2005; Urbanová et al., 2015). Lower soil carbon inputs are more typical of coniferous than deciduous trees (Vesterdal et al., 2013).

Consequently, soils dominated by coniferous trees are associated with a different microbial community composition compared to deciduous soils (Lladó et al., 2017). This effect of low carbon on the community might stimulate chemolithoautotrophic activity leading to higher CO_2 fixation rates in coniferous than deciduous soils. A higher abundance of obligate autotrophs in response to lower SOC content was shown to positively influence CO_2 fixation in soils (Xiao et al., 2018). Yet, the influence of tree-derived SOC inputs on dark CO_2 fixation activity in temperate forest soils is not known (Figure 4). Furthermore, pH is another strong driver of microbial communities in temperate forest soils (Kaiser et al., 2016; Nacke et al., 2011). Temperate forest soils with higher pH also show higher microbial diversity, including high populations of autotrophic groups compared to acidic soils (Dukunde et al., 2019; Kaiser et al., 2016). Such higher diversity exerted through higher pH might in turn have positive impacts on their CO_2 fixation rates as reported in paddy soils (Long et al., 2015) (Figure 4).

Due to the importance of soil carbon on atmospheric CO_2 levels, another important aspect to consider is how dark CO_2 fixation responds to or is impacted by global climate change. Of particular interest within this context is temperature change. Beyond the knowledge that CO_2 fixation rates increase at higher temperatures (Nel and Cramer, 2019), it is crucial to quantify the temperature responses of dark CO_2 fixation rates. A commonly adopted way to do this is by measuring rates at a 10 °C rise in temperature to determine the temperature sensitivity (Q_{10}) (Conant et al., 2008; Davidson and Janssens, 2006). As Earth's temperature is expected to warm (4 °C) in the nearest future (2010) (Soong et al., 2020), soil CO_2 production is expected to be ~30% higher based on measured Q_{10} values (Hicks Pries et al., 2017). Thus, information on the Q_{10} of dark CO_2 fixation compared to that of respiration rates may be useful to predict future changes in net soil CO_2 fluxes (Figure 4).

1.7 Investigating dark CO_2 fixation in soils

1.7.1 How to investigate dark CO_2 fixation in soils: Methods adopted

Metabolic labelling with ^{13}C to determine dark CO_2 fixation rates. The use of stable carbon isotope, ^{13}C, as a metabolic tracer in laboratory incubation studies has been adopted to determine rates of CO_2 fixation by microbes into soil organic matter (Beulig et al., 2016; Miltner et al., 2004; Šantrůčková et al., 2018). Because ^{13}C is a rare (1.11%) carbon isotope (Craig, 1953), it serves as a valuable tool for studying soil carbon dynamics (Trumbore, 2009; Ehleringer et al., 2000). By entirely replacing the more abundant ^{12}C in CO_2 gas with ^{13}C label, the detection of this label above natural abundance levels in specific markers can be used to

monitor the flow of carbon derived from CO_2 within different SOM pools (typically microbial biomass carbon and soil organic carbon). This can be used to derive the rate of CO_2 fixation and the total proportion of carbon derived from CO_2 into different carbon pools (Miltner et al., 2004; Nowak et al., 2015; Spohn et al., 2019). Based on this principle, the ^{13}C-labelled CO_2 can be used at specific concentrations in soil microcosm incubations (Figure 5A), and the amount of fixed ^{13}C in the microbial biomass and the bulk soil can be quantified. To determine the amount of carbon fixed into microbial biomass, the soil microbial biomass carbon content (MBC) is extracted via Chloroform fumigation extraction (CFE) method (Figure 5B), a widely used approach to measure the microbial carbon in soils (Xu et al., 2013). This method involves lysing microbial cells with chloroform to release the cellular carbon in the form of dissolved organic carbon (DOC) (Vance et al., 1987). The carbon content and ^{13}C signals of the extracted DOC fractions can be measured using a "high OC" elemental analyser system and by isotope ratio mass spectrometry (HPLC-IRMS), respectively. The MBC content and its $\delta^{13}C$ signals are derived by taking the difference in carbon content measured from the chloroform-fumigated and unfumigated DOC fractions (Nowak et al., 2015). For the bulk soil, the carbon content and ^{13}C signal of SOC is measured directly from the dried soil using an elemental analyser coupled to an IRMS system (EA-IRMS) (Figure 5C). By applying an isotope mass balance and normalizing the ^{13}C signals of MBC and SOC to their respective carbon content, the CO_2 fixation rates per gram of MBC and per gram of soil, respectively (Figure 5D), are derived.

High throughput amplicon-based techniques to assess the metabolic potential for CO_2 fixation. Accompanying the rate derivations, techniques like quantitative PCR (qPCR) can be used to quantify specific functional marker genes involved in dark CO_2 fixation (Figure 5E). Genes encoding key enzymes, like RuBisCO, or ATP citrate lyase of the CBB and rTCA pathways, respectively, can be used to generate information on the metabolic CO_2 fixation potential present among the microbial communities. This can be used to draft conclusions about the potential pathways involved (Alfreider et al., 2018, 2012, 2003; Selesi et al., 2005). Amplicon sequencing of bacterial *16S rRNA* genes is suitable to provide insights into the taxonomic composition of the soil bacterial communities. Estimates of the relative abundance of different microbial groups can be derived from phylum to genus level, and this can be used to analyse dynamics in the microbial communities. Datasets from *16S rRNA* sequencing can be further employed for downstream predictions of functional potentials (CO_2 fixation pathways and key players involved). This can be done by analysing *16S rRNA* sequences on operational taxonomic units (OTU) level using software packages like Phylogenetic

Investigation of Communities by Reconstruction of Unobserved States (PICRUSt) (Douglas et al., 2020). However, these methods for assessing CO_2 fixation potential are not without shortcomings. Aside from that, both approaches are vulnerable to methodological (e.g., primer specificity for qPCR) and database (e.g., comprehensive reference genome for PICRUSt) biases (Agrawal et al., 2019), they may only indicate genomic potential and not an actual activity of the genes detected. However, when complemented with rate measurements via ^{13}C metabolic labelling, these methods serve as powerful tools to explore dark CO_2 fixation in soils.

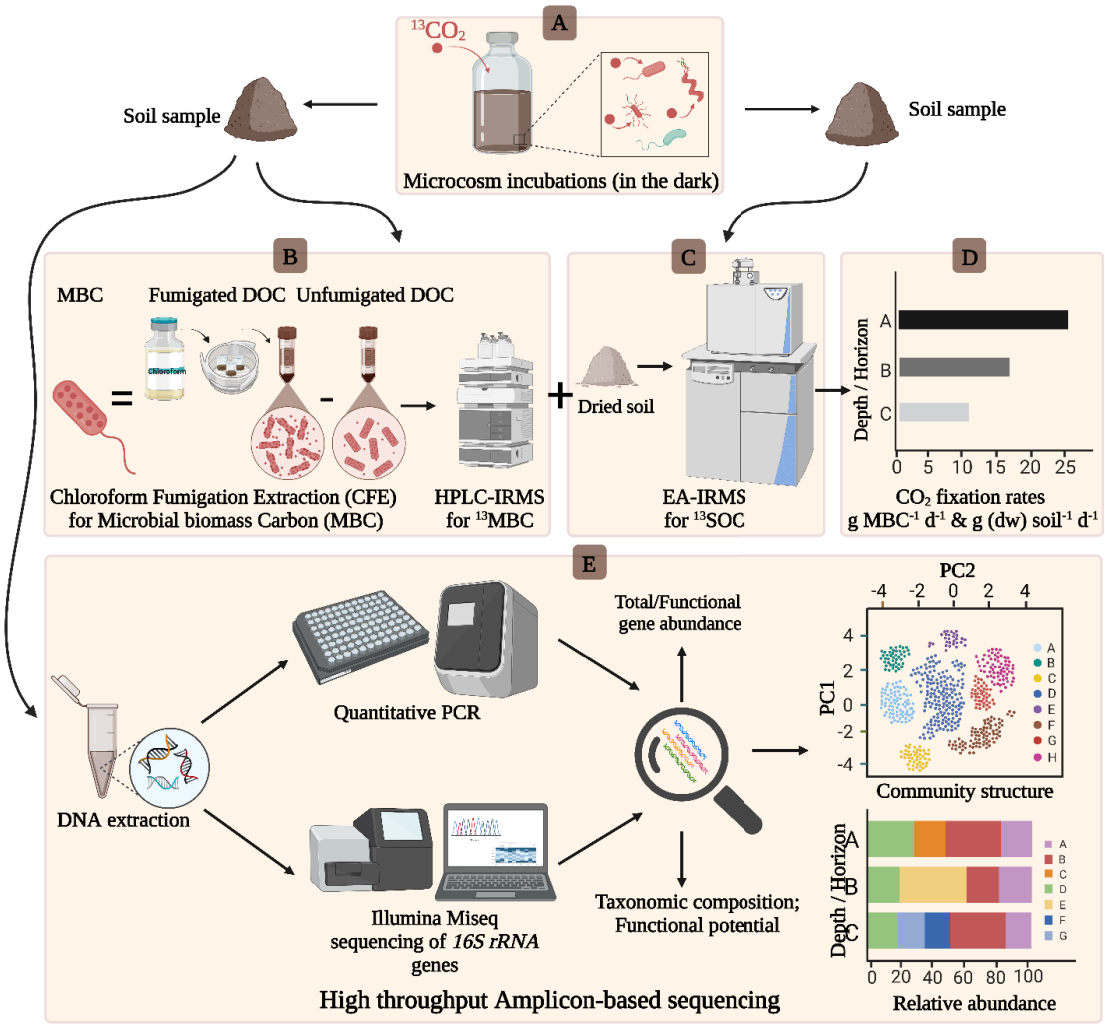

Figure 5| Overview of project workflow and methods used to investigate dark CO_2 fixation in soils. Soil samples are incubated in microcosms using ^{13}C labelled CO_2 and are used to trace the incorporation of CO_2-derived carbon from microbes into SOM (A). Incorporated carbon isotopes are traced into microbial biomass (B) and soil organic carbon (C) and used to determine CO_2 fixation rates per gram of MBC and per gram of soil dry weight (D). *16S rRNA* sequencing and qPCR are excellent high throughput amplicon-based tools used to determine the taxonomic composition and functional potential (CO_2 fixation genes and metabolic pathways) of the bacterial community (E).

1.7.2 Where to investigate dark CO_2 fixation: Selected study sites

Deciduous and coniferous forests are the two most important temperate forest types (Tyrrell et a., 2012). Hence for this thesis, study sites from well-established temperate forest plots within Germany were selected.

The Hainich National Park: The first experimental study site is located within the "Hainich National Park" near the village of "Weberstedt" in central Germany (Knohl et al., 2003; Mölder et al., 2006). Being one of the largest forests in central Europe, with an area covering ~7600 ha, the "Hainich National Park" was established in 1997 to preserve this vast forest landmass (Knohl et al., 2003; Schrumpf et al., 2014). It is dominated by a mixture of deciduous trees; old-growth beech (65% *Fagus sylvatica*), ash (25% *Fraxinus excelsior*), and maple (7% *Acer pseudoplantanus* and *Acer plantanoides*) trees, with a few interspersed European hornbeams (*Carpinus betulus*), elm (*Ulmus glabra*) and other deciduous species (Knohl et al., 2003). Mineral soils are typically *Cambisols*, characterised by pH of 4 -7 with high clay (40%, sand 4%) and SOC content of up to 8% (Knohl et al., 2003; Schrumpf et al., 2014).

The Schorfheide-Chorin Exploratory: The second experimental site is in the forested part of the Schorfheide-Chorin Biodiversity exploratory in North-Eastern Germany. Covering an area of 1300 km^2, the Schorfheide-Chorin Exploratory is a part of the German Biodiversity Exploratories established for the purpose of long-term and large-scale research on the relationships between land use, biodiversity changes, and ecosystem functions in central European forests and grasslands (Fischer et al., 2010). The dominant tree species of the mature age class forests in this region include a mixture of beech (*Fagus sylvatica*), pine (*Pinus sylvestris*), and oak (*Quercus spp*.) trees (Fischer et al., 2010). Mineral soils are classified as *Cambisols*, with a sandy texture (89%), a low pH (<5), and >3% of organic carbon content (Kaiser et al., 2016).

The Hummelshain Forest: The third experimental forest site is located in close proximity to the Hummelshain municipality in Thuringia, Central Germany. The study site establishment involved the planting of European beech trees within Norway spruce, and Scot's pine stands to counteract the low pH of the topsoil under the coniferous stands and for the biological activation of the forest floors (Graser 1928). European beech (*Fagus sylvatica.* Linné), Scot's pine (*Pinus sylvestris*), and Norway spruce (*Picea abies* (L.) H. Karst) stands are the dominant tree species present. The mineral soils are predominantly sandy (40 – 50% sand and silt), having a low pH (<4) and organic carbon content of between 2 – 3% (Achilles et al., 2020).

1.8 Aims and hypotheses of the study

This thesis aims to understand and quantify the role of dark CO_2 fixation across the soil profile, to elucidate the chemolithoautotrophic potential of the soil microbiome, and to identify the biogeochemical factors influencing this process in temperate forest soils. It involves investigating soils from well-established temperate forest plots in different regions in Germany that encompass various forest management regimes, tree species dominance, and edaphic soil properties. Such settings make it possible to address the following questions:

1. What are the rates of dark CO_2 fixation across depths, and how does this contribute to soil organic matter in temperate forest soils?
2. Which chemolithoautotrophic microorganisms and metabolic pathways are prevalent in temperate forest soils which can contribute to dark CO_2 fixation?
3. Which parameters influence the rates of dark CO_2 fixation in temperate forest soils?

To answer the above questions, a few hypotheses were highlighted:
The microbial assimilation of CO_2 across the profile is expected to contribute to SOC, but the inputs of CO_2 fixation to SOC and how it modulates CO_2 fluxes from temperate forest soils are currently poorly understood. Organic carbon originating from plant litter typically decreases with soil depth but CO_2 content increases. Thus, the relative impact of chemolithoautotrophy likely increases with depth. Thus, the first two hypotheses of this thesis were:

H_1 Dark CO_2 fixation occurs down to 1 m depth in temperate forest soils.

H_2 The genomic potential for chemolithoautotrophy will increase with soil depth.

In temperate forest soils, organic carbon content is lower in soils dominated by coniferous than deciduous tree species. As such differences in organic carbon inputs (quality and quantity) affect microbial community composition and abundance, consequences on dark CO_2 fixation rates are expected. Thus, the third hypothesis of this thesis was:

H_3 Lower SOC inputs in coniferous compared to deciduous dominated soils will lead to higher CO_2 fixation activity.

The decomposition of SOC is affected by temperature, increasing soil respiration rates. Since warming also increases dark CO_2 fixation rates, the fourth hypothesis was:

H_4 Dark CO_2 fixation has a similar sensitivity to higher temperatures as soil respiration.

1.9 Thesis structure

This thesis is organized into three results chapters, all of which jointly address the aim and hypotheses highlighted above.

Chapter 2, "**Rates of dark CO_2 fixation are driven by microbial biomass in a temperate forest soil"** (Akinyede *et al*., 2020; published in *Soil Biology & Biochemistry*), evaluated the potential role of dark CO_2 fixation for temperate forest SOC using a forest plot in the Hainich National Park as a study site. It involved using a ^{13}C metabolic labelling approach in soil microcosms to quantify CO_2 fixation rates per gram of soil dry weight and microbial biomass across 1 m depth, thus partly addressing hypothesis 1 (**H_1**) of this thesis. The potential contributions to temperate forest MBC, SOC stocks, and CO_2 fluxes were derived, and an extrapolation of the rates to global temperate forest area was done. Chapter 2 served as a proof of principle experimental for subsequent determination of dark CO_2 fixation rates in the other temperate forest soils, as seen in Chapters 2 and 3. The genomic potential for CO_2 fixation in the Hainich forest soils was further determined, thus partly addressing hypothesis 2 (**H_2**). Chapter 2 further explored how dark CO_2 fixation rates change under increasing CO_2 concentrations and how this affects CO_2 fluxes from soils under future changes in atmospheric CO_2 conditions.

The input of organic carbon to soils varies with temperate forest tree species, and this influences microbial community composition and function. Thus, Chapter 3, "**Dark CO_2 fixation in temperate beech and pine forest soils" (**Akinyede *et al*., 2022; published in *Soil Biology & Biochemistry***),** aimed to test whether differences in tree-specie specific SOC inputs will consequently affect dark CO_2 fixation rates. Two soil plots from the Schorfheide-Chorin Exploratory dominated by different tree species (deciduous-beech and coniferous-pine) were used as a proxy for differences in SOC content existing in deciduous and coniferous temperate forest soils. Using ^{13}C labelling incubations, we investigated the rates of dark CO_2 fixation across depths in the forest soils, and comparisons were made over three temperate deciduous and coniferous forest soils. Thus, hypothesis 3 (**H_3**) was addressed. Also, biotic and abiotic soil properties were statistically linked to dark CO_2 fixation rates to identify and validate existing relationships between dark CO_2 fixation rates and other measured soil properties linked to SOC in different temperate forest soils. The genomic potential for CO_2 fixation across depth was also determined as done in Chapter 2, and this also partly addresses hypothesis 2 (**H_2**). This involved a full assessment of the presence and abundance of known pathways for both

autotrophic and non-autotrophic CO_2 fixation in the soils. CO_2 fixation rates and contributions to MBC and SOC with depth were assessed in these soils. Thus, hypothesis 1 (**H_1**) was also partly addressed in this Chapter.

A future increase in global soil temperatures has been projected. Documented effects on temperate forest SOC have been mostly described to result in increased soil respiration leading to loss of SOC stocks. Thus, Chapter 4, **"Temperature sensitivity of dark CO_2 fixation in temperate forest soils"** (Akinyede et al., manuscript submitted to *Biogeosciences*), assessed the relationship between dark CO_2 fixation and temperature, otherwise known as the temperature sensitivity (Q_{10}), and how this compares to the temperature sensitivity of soil respiration. With this, hypothesis 4 (**H_4**) was addressed. We investigated soils dominated by deciduous-beech and coniferous-spruce trees from the Hummelshain forest. Dark CO_2 fixation rates and respiration rates were determined under two temperature conditions (4°C and 14°C) with depth, and the Q_{10} of both processes were also determined and compared. Using the derived Q_{10} values, changes in dark CO_2 fixation and respiration rates in response to projected soil warming were evaluated. The microbial community composition, potential key players, and metabolic pathways involved were likewise determined as done in Chapters 1 and 2, thus also partly addressing hypothesis 2 (**H_2**). Finally, differences in dark CO_2 fixation rates and Q_{10} values were also linked to soil texture, community composition, and microbial biomass turnover. Based on measured rates and inputs to MBC and SOC, hypothesis 1 (**H_1**) was also partly addressed in this Chapter.

2 Manuscript 1: Rates of dark CO_2 fixation are driven by microbial biomass in a temperate forest soil

Authors: Akinyede, R., Taubert, M., Schrumpf, M., Trumbore, S., Küsel, K

Bibliographic information (if published or accepted for publication: Citation): Akinyede, R., Taubert, M., Schrumpf, M., Trumbore, S., Küsel, K., 2020. Rates of dark CO_2 fixation are driven by microbial biomass in a temperate forest soil. *Soil Biology & Biochemistry* 150, 107950. doi:10.1016/j.soilbio.2020.107950

The candidate is (Please tick the appropriate box.)

☐✓ First author, ☐ Co-first author, ☐ Corresponding author, ☐ Co-author.

Status (if not published; "submitted for publication", "in preparation".): Published

For this study, Trumbore, S. and Küsel, K designed the project and, together with Taubert, M and Schrumpf, M, designed the experiments. I, Akinyede, R, Küsel, K, and Schrumpf, M conducted the soil sampling campaigns. I performed all isotope measurements and molecular analysis, analyzed and discussed data (including all figures), and wrote the manuscript. Taubert, M helped with the experimental design, supervised DNA extraction and sequence analysis, and helped with the data visualization and discussion. Taubert, M also edited the manuscript draft. Schrumpf, M., Trumbore, S., Küsel, K helped review and edit the manuscript draft. My contributions are summarized as follows.

Authors' contributions (in %) to the given categories of the publication

Author	Conceptual	Data analysis	Experimental	Writing the manuscript	Provision of material
Akinyede, R	20	70	70	50	0
Taubert, M	10	20	5	20	0
Schrumpf, M	10	0	0	5	0
Trumbore, S	30	10	0	5	50
Küsel, K	30	0	0	20	50
Others	0	0	15	0	0
Total:	100%	100%	100%	100%	100%

_____ _____

Signature candidate Signature supervisor (member of the Faculty)

Supplementary data for this article can be found at the end of the research article.

Soil Biology and Biochemistry 150 (2020) 107950

Contents lists available at ScienceDirect

Soil Biology and Biochemistry

journal homepage: http://www.elsevier.com/locate/soilbio

Rates of dark CO_2 fixation are driven by microbial biomass in a temperate forest soil

Rachael Akinyede [a,b], Martin Taubert [a], Marion Schrumpf [b], Susan Trumbore [b], Kirsten Küsel [a,c,*]

[a] Aquatic Geomicrobiology, Institute of Biodiversity, Friedrich Schiller University Jena, Dornburger Str. 159, 07743, Jena, Germany
[b] Department for Biogeochemical Processes, Max Planck Institute for Biogeochemistry, Hans-Knöll Str. 10, 07745, Jena, Germany
[c] German Centre for Integrative Biodiversity Research (iDiv) Halle-Jena-Leipzig, Deutscher Platz 5, 04103, Leipzig, Germany

ARTICLE INFO

Keywords:
Dark CO_2 fixation
Temperate forest soil
$^{13}CO_2$ labelling
Microbial biomass carbon
Soil organic matter

ABSTRACT

Soils substantially contribute to the terrestrial fluxes of CO_2 to the atmosphere. Dark CO_2 fixation, the microbial process by which pore space CO_2 is reduced to organic matter, may recycle and trap some of the CO_2 respired in soils before it can escape to the atmosphere. To evaluate its potential significance for global temperate forest soil carbon stocks, we quantified dark CO_2 fixation rates in a temperate beech forest soil down to 1 m depth over a range of 2–20% (v:v) headspace CO_2 concentrations, by tracing incorporation of a ^{13}C–CO_2 label into microbial biomass carbon and soil organic matter. We found that fixation rates under a concentration of 2% CO_2 decreased with depth from 0.86 to 0.06 μg C normalized to g(dw) soil^{-1} d^{-1}. However, when dark CO_2 fixation rates were normalized to soil microbial biomass carbon, no significant differences between depths were observed. Higher CO_2 concentrations increased fixation rates, with a linear 2-fold increase between 2% and 10% CO_2. Molecular analysis revealed the dominance of heterotrophs, along with the presence of autotrophs mainly employing the Calvin Benson Bassham (CBB) pathway followed by the reductive citric acid (rTCA) pathway. Although community composition varied with depth, the relative fraction of autotrophs determined by qPCR of RuBisCO (*cbbL* IA, *cbbL* IC) and ATP-citrate lyase (*aclA*) genes remained stable at approximately 0.5% of the total community. Dark CO_2 fixed carbon accounted for up to 1.1% of microbial biomass carbon and up to 0.035% of soil organic carbon after 28 days. We estimated a fixation flux of 25 ± 7.2 g C m^{-2} yr^{-1} to 1 m depth for the Hainich forest soil under field conditions. Without this process, Hainich forest soil CO_2 emissions would be 5.6% higher, recycling a fraction of carbon large enough to potentially affect carbon isotope signatures in SOC. If this is held for all temperate forest soils globally, the annual rate of dark CO_2 fixation would be 0.26 ± 0.07 Pg C yr^{-1} to a depth of 1 m, without considering contributions from other biomes. In conclusion, microbial biomass carbon and CO_2 concentration appear to be the main drivers of dark CO_2 fixation in temperate forest soils, and dark CO_2 fixation may maintain Hainich forest soil carbon stocks by moderating a significant fraction of soil CO_2 emissions annually.

1. Introduction

Forests are recognized as the largest and most important terrestrial carbon pool on Earth with up to 800 Pg of organic carbon in their soils (Whitehead, 2011; Domke et al., 2016). Of the major forest biomes, temperate forests represent a significant component of the global carbon cycle (Scott, 1996; Lorenz et al., 2011), with more than half of the global temperate forest total carbon reserves being stored in soils (Malhi et al., 1999). An increase of temperate forest soil organic carbon (SOC) stocks has been reported over the last decades (Goodale et al., 2002; Lorenz et al., 2011; Grüneberg et al., 2014). This has been largely attributed to increased forest biomass and litter input (Mobley et al., 2015; Miao et al., 2019) brought about by photosynthetic CO_2 fixation. However, in addition to organic carbon fixed by plants, soil microbes can fix CO_2 present in soil pore spaces through non-phototrophic CO_2 fixation, often referred to as dark CO_2 fixation. This process is carried out by both chemolithoautotrophic and heterotrophic microbes via several metabolic pathways and reactions (Miltner et al., 2004). Chemolithoautotrophic microorganisms fixing CO_2 use six known pathways, with the Calvin-Benson-Bassham cycle (CBB) being quantitatively the most significant (Berg, 2011; Hügler and Sievert, 2011). In soil environments, furthermore, the reductive citric acid cycle (rTCA) and, the

* Corresponding author. Aquatic Geomicrobiology, Institute of Biodiversity, Friedrich Schiller University Jena, Dornburger Str. 159, 07743, Jena, Germany.
E-mail address: kirsten.kuesel@uni-jena.de (K. Küsel).

https://doi.org/10.1016/j.soilbio.2020.107950
Received 19 April 2020; Received in revised form 31 July 2020; Accepted 3 August 2020
Available online 8 August 2020

Wood Ljungdahl pathway (WLP) are of relevance. These pathways are more energy-efficient than the CBB pathway but are restricted to microaerophilic and anaerobic organisms (Berg et al., 2010; Berg, 2011; Hügler and Sievert, 2011). Besides CO_2 fixation by chemolithoautotrophs, heterotrophs fix CO_2 via assimilatory carboxylations (Alonso-Sáez et al., 2010; Erb, 2011) and anaplerotic reactions in citric acid metabolism (Krebs, 1941).

Dark CO_2 fixation has been reported for a range of soils such as forest soils (Spohn et al., 2019), agricultural soils (Miltner et al., 2004, 2005; Wu et al., 2015), paddy soils (Yuan et al., 2012; Wu et al., 2014; Ge et al., 2016), wetland soils (Nowak et al., 2015; Beulig et al., 2016; Lynn et al., 2017), temperate grasslands soils (Nel and Cramer, 2019) as well as semi-arid desert soils (Liu et al., 2018) and arctic tundra soils (Šantrůčková et al., 2018). Moreover, the presence of genes involved in autotrophic fixation of CO_2 via the Calvin cycle has been reported in temperate forest soils (Kaiser et al., 2016; Dukunde et al., 2019), suggesting that dark CO_2 fixation may serve as an important source of SOC and thereby to global carbon storage in temperate forests.

Dark CO_2 fixation has been shown to be common among both autotrophs and heterotrophs in soils (Miltner et al., 2005; Šantrůčková et al., 2018; Nel and Cramer, 2019). However, anaplerotic CO_2 fixation by heterotrophs is not known to lead to any net carbon accumulation (Merlin et al., 2003; Alonso-Sáez et al., 2010). Consequently, only carbon fixed by chemolithoautotrophs is likely to directly affect SOC stocks. As most of these studies also focused on the top 20 cm of soil with a typically high SOC content (Yuan et al., 2012; Wu et al., 2014, 2015; Lynn et al., 2017), reports on the distribution of chemolithoautotrophs through deep soil profiles are rare. Thus, since high abundances of chemolithoautotrophs are reported from carbon-limited soils (Niederberger et al., 2015; Li et al., 2018), we speculate that their relative abundance is higher in deeper soil horizons, characterized by low SOC content (Jobbágy and Jackson, 2000). This shift in the microbial community composition towards a higher abundance of chemolithoautotrophs could also affect dark CO_2 fixation rates.

In incubation experiments, dark CO_2 fixation rates are enhanced by increasing concentrations of headspace CO_2 in soil microcosms (Beulig et al., 2016; Šantrůčková et al., 2018; Spohn et al., 2019). In diffusion-dominated soils, soil pore space CO_2 concentrations vary as a function of soil depth from 0.04 to 13.0% by volume in the upper several meters of soil (Amundson and Davidson, 1990). Other studies report ranges between 1 and 5% of CO_2 in the soil pore space (Richter and Markewitz, 1995; Andrews and Schlesinger, 2001). In nondiffusion-dominated mofette soils, which are characterized by subcrustal CO_2 degassing, concentrations can reach even more than 90% partial pressure CO_2 (Beulig et al., 2014), with stimulatory effects on microbial CO_2 fixation (Beulig et al., 2016). A systematic approach evaluating the effect of a broad range of CO_2 concentrations on dark CO_2 fixation across depth in forest soils is missing.

This study explores dark CO_2 fixation using a well-characterized *Eutric Cambisol* soil plot in the Hainich Forest National Park, Germany, which is currently regarded as a net carbon sink (Schrumpf et al., 2014). With the aim to assess the role and mechanisms of dark CO_2 fixation in temperate forest soils, we hypothesize that (i) the relative abundance of chemolithoautotrophs will increase down the soil profile, (ii) dark CO_2 fixation rate scales with the abundance of chemolithoautotrophs and (iii) this process is enhanced under high soil CO_2 concentrations. We further propose that dark CO_2 fixation contributes to microbial biomass carbon and SOC along the entire soil profile and describe the potential relevance of this process for temperate forest soils.

2. Materials and methods

2.1. Site description and soil classification

The location of the study site (51°04'46"N 10°27'08"E, 440 m a.s.l.) is within the "Hainich National Park'', near the city of Eisenach, central Germany, The vegetation at the sampling site is dominated by a mixture of old-growth beech (65% *Fagus sylvatica* L.), ash (25% *Fraxinus excelsior* L.) and maple (7% *Acer pseudoplantanus* L. and *Acer plantanoides* L.) trees, with a few interspersed European hornbeams (*Carpinus betulus* L.), elm (*Ulmus glabra* Huds.) and other deciduous species (Knohl et al., 2003; Mölder et al., 2006). The site is located in the footprint area of an eddy covariance system for monitoring CO_2 exchange between the forest ecosystem and the atmosphere, and it is also used for monitoring long-term changes in soil carbon. The "Hainich National Park" is positioned in a suboceanic/subcontinental climate on a gentle north-facing slope (2–3° inclination). Mean annual rainfall at the site is 720 mm and mean annual air temperature is 8.3 °C as in the year 2019 (https://gbov.acri.fr). The soil of the sampled plot is characterized by high clay (46–76%), and silt (22–57%) contents across a 60 cm depth gradient. The clay content is increasing with soil depths and the silt content declining due to a Pleistocene loess layer overlaying the clay-rich Triassic limestone residue in the subsoil. This slightly acidic soil is classified as a Eutric Cambisol with a thin mull type litter layer (IUSS Working Group WRB, 2015; Schrumpf et al., 2014). Further description of the forest vegetation and site can be found in Knohl et al. (2003), Kutsch et al. (2010), and Schrumpf et al. (2014).

2.2. Sampling design

The first soil sampling campaign was carried out in August 2017, representing the middle of the summer season. Soil was sampled in triplicate cores (1–2 m apart) at one subplot in the footprint of the eddy covariance tower. A closed auger was driven into the soil with a motor hammer (Cobra Combi, Atlas Copco AB, Nacka, Sweden) to obtain intact soil cores. The depth of the borehole and the length of the extracted core were compared to estimate soil compaction during the coring process. Ignoring the organic layer and beginning from the mineral horizon, three segments were extracted from the soil cores with depths chosen to sample comparable pedogenic horizons in each of the triplicate cores: 0–12 cm (A horizon), 35–45 cm (BC horizon), and 70–100 cm (C horizon). Soils from each of the triplicate cores were sieved separately onsite using a 2 mm sieve to remove stones and roots for the incubation experiments from which subsamples for DNA extraction were immediately frozen in liquid nitrogen.

For the second sampling campaign, soils were sampled in November 2017. Duplicate cores were sampled from the same subplot as described above. Soil cores were again cut into three segments according to the similarity of the horizon among the duplicate cores to obtain samples from 0 to 12 cm (A horizon), 45–60 cm (BC horizon), and 80–100 cm (C horizon). Segment length varied slightly between both sampling campaigns. Soils from the same depths of the duplicate cores were mixed and homogenized prior to sieving.

2.3. Geochemical parameters and ^{13}C isotope measurements of SOC

Total and inorganic carbon and nitrogen concentration of soil samples were determined on a "Vario Max" system (Elementar Analysesysteme GmbH, Hanau, Germany). Gravimetric water content was determined by weighing soil samples before and after drying at 105 °C for 24 h. Additionally, soil pH was determined in a 0.01 M KCl solution with a soil-to-solution ratio of 1:2.5 using a WTW pH meter (330, Weilheim, Germany). The ^{13}C isotope ratios of bulk soil samples were determined using an isotope ratio mass spectrometer (DELTA C; stable isotope monitoring system; Finnigan MAT, Germany) coupled to an elemental analyzer (EA 1100, CE Instruments, Milan, Italy) via a ConFlo III interface. All ^{13}C isotope ratios were then reported in the delta notation (δ) that expresses $^{13}C/^{12}C$ ratios as $\delta^{13}C$ values in per mil (‰), which is relative to the international reference material Vienna Pee Dee Belemnite (V-PDB) (Coplen et al., 2006).

$$\delta^{13}C = \left(\frac{\frac{^{13}C}{^{12}C}\text{sample}}{\frac{^{13}C}{^{12}C}\text{reference}} - 1 \right) \times 1000$$

2.4. ^{13}C–CO_2 labelling experiments

To determine CO_2 fixation rates, triplicate incubations for each sieved soil sample from the August sampling campaign were performed in sterilized 120 ml serum bottles with butyl rubber stoppers, containing 25 g (wet weight) of soil. Headspace was flushed with synthetic air (75% N_2 and 25% O_2), adjusted to 2% (v/v) ^{13}C–CO_2 and incubated statically in the dark at room temperature (20 °C) for a period of 7, 14 and 28 days. Likewise, triplicate control incubations with 2% (v/v) unlabelled CO_2 (^{12}C–CO_2) were set up. To obtain control samples without biological activity, soil samples were autoclaved thrice for 2 h at 130 °C at 60 bar and used in the incubation set-ups as described above. To account for soil respiration and to maintain the same headspace CO_2 concentration, the headspace of all incubations and controls was renewed every 3 days throughout the incubation periods. This was done by flushing out the headspace with synthetic air and inoculating all incubations and controls with 2% (v/v) ^{13}C–CO_2 or 2% (v/v) ^{12}C–CO_2, respectively.

A second labelling experiment was conducted to determine the influence of increased CO_2 concentrations on CO_2 fixation rates by using increasing headspace CO_2 concentrations. Duplicate soil microcosms were constructed by adding 30 g (wet weight) sieved soil from the November sampling campaign to sterile 100 ml incubation bottles sealed with butyl rubber stoppers. Bottles were flushed with synthetic air and adjusted to 2, 5, 10, and 20% (v/v) headspace CO_2 concentrations (24.5, 23.75, 22.5, and 20% (v:v) O_2 concentration, respectively). Microcosms were incubated for 7 days as described above. At the end of each incubation time, soils were homogenized and split into three parts. One part was dried at 40 °C and ground for bulk ^{13}C and organic carbon analysis, the second part was stored at −80 °C for later DNA analysis and the third was prepared immediately for the extraction of microbial biomass carbon (MBC) by chloroform fumigation extraction (CFE) using 0.05 M K_2SO_4 according to Vance et al. (1987). To enhance extraction efficiency and to minimize losses for extracted carbon by microbial degradation, the modified protocol from Nowak et al. (2015) was used.

2.5. Determination of delta ^{13}C ratios in MBC and mass-balance calculations

The concentration of carbon in the form of dissolved organic carbon from all bulk soil samples and soil incubations (including all controls) was determined in K_2SO_4 extracts derived from fumigated and unfumigated samples (6 g each) after chloroform fumigation extraction using a “high OC"(Elementar Analysesysteme GmbH, Hanau, Germany). Afterwards, the $\delta^{13}C$ ratios were determined by isotope ratio mass spectrometry (IRMS) using an isotope ratio mass spectrometer (DELTA C; stable isotope monitoring system; Finnigan MAT, Germany) coupled to an elemental analyzer (EA 1100, CE Instruments, Milan, Italy) via a ConFlo III interface as described above.

By subtracting the amount of the dissolved organic carbon content of the unfumigated samples (C_{unfum}) from that of the fumigated samples (C_{fum}) and dividing with a correction factor K_{EC} (of 0.45) (Joergensen and Mueller, 1996), which accounts for the extraction efficiency, the microbial biomass carbon (C_{mic}) content was determined:

$$C_{mic}\left[mg\right] = \frac{\left[C_{fum} - C_{unfum}\right]}{K_{EC}}$$

The isotope ratio ($\delta^{13}C$) of microbial biomass carbon (MBC) was then derived for both the bulk samples (natural abundance levels) and incubations by applying an isotope mass balance:

$$\delta^{13}C_{MB}\ (‰) = \frac{\left[^{13}C_{fum} \times C_{fum} - {}^{13}C_{unfum} \times C_{unfum}\right]}{C_{fum} - C_{unfum}}$$

The actual $^{13}C/^{12}C$ ratio was obtained for the mass balance calculated $\delta^{13}C$ values as follows:

$$\frac{^{13}C}{^{12}C} = \left[\frac{\delta^{13}C}{1000} + 1\right] \times 0.011180$$

Where 0.011180 is the $^{13}C/^{12}C$ ratio of the international V-PDB standard (Werner and Brand, 2001; Brand et al., 2010; Meija et al., 2016). The CO_2 fixation rate was calculated by determining the excess ^{13}C content, which is the increase in $^{13}C/^{12}C$ ratio between the labelled and the unlabelled control normalized to the carbon content of the microbial biomass (C_{mic}).

$$\text{Excess } ^{13}C[mg] = \frac{^{13}C_{labelled}}{^{12}C_{labelled}} \times C_{mic} - \frac{^{13}C_{unlabelled}}{^{12}C_{unlabelled}} \times C_{mic}$$

The CO_2 fixation rate was calculated from the excess ^{13}C incorporated divided by the time of exposure to the label. This rate was normalized to either the absolute microbial biomass carbon content or the dry weight of the bulk soil.

2.6. DNA extraction and 16S rRNA gene sequencing

DNA was extracted from 0.25 g of all bulk soil and incubation samples using the DNeasy PowerSoil DNA Kit (Qiagen, Hilden, Germany) following the manufacturer’s protocol. Total nucleic acid extraction efficiency and yield were quantified using a Nanodrop 1000 spectrophotometer (PeQLab, Biotechnologie GmbH, Erlangen, Germany) and 1% agarose gel electrophoresis.

Polymerase Chain Reaction (PCR) was performed in 20 µl reactions containing 10 µl HotstartTaq Mastermix (Qiagen Hilden, Germany), 10 µM each of forward (341F) and reverse (785R) primers targeting the V3 to V4 hypervariable regions (Klindworth et al., 2013), 0.67 mg ml $^{-1}$ BSA (Bovine Serum Albumin), 5.67 µl nuclease-free water, and 5–10 ng of genomic DNA. The following PCR conditions were used: initial denaturation at 95 °C for 15 min, followed by 30 cycles consisting of denaturation (94 °C for 45 s), annealing (55 °C for 45 s) and extension (72 °C for 45 s) and then a final extension step at 72 °C for 10 min. For samples with low DNA concentration, 35 cycles of amplification were used. The PCR products were purified using the NucleoSpin gel and PCR clean up kit (Macherey-Nagel, Dueren, Germany). PCR products libraries were prepared for Illumina sequencing using the NEBNext Ultra DNA library prep kit for Illumina (New England Biolabs, Hitchin, UK). Following the manufacturer’s protocol, the ends of the DNA were prepared by adding “end prep” reagents to 55.5 µl of purified PCR products followed by a PCR thermal cycling step. Afterwards, adaptors were ligated to the prepared ends and then cleaned up without size selection as the PCR products were all under 500 bp in length. Enrichment of the adapter-ligated DNA was carried out in a single PCR cycling step and the final PCR amplicons were then cleaned using magnetic beads. Details about the reagents used including the thermal cycle steps and conditions can be found in the manufacturer’s protocol. The prepared libraries were then sequenced by Illumina Miseq (Illumina, Inc., San Diego, USA) (2 × 250 bp) following our inhouse sequencing protocol.

Generated raw sequence data were analyzed using the MOTHUR sequence analysis pipeline according to Schloss et al. (2009) (http://www.mothur.org) and the MOTHUR MiSeq SOP as of 19th December 2018. Paired reads were combined, and only sequences between 360 bp and 500 bp were kept, while sequences outside this range and with ambiguous bases as well as homopolymer length of above 8 bp were removed. All sequences were aligned to the SILVA reference database v132 and sequences with differences of no more than four bases were pre-clustered. Afterwards, chimeras were removed by Uchime using the GOLD reference database and sequences were

classified according to the same SILVA database earlier described.

To predict functional potential (CO_2 fixation pathways) for the generated 16S rRNA sequences, representative sequences from OTUs generated from MOTHUR were analyzed using the version 2 of Phylogenetic Investigation of Communities by Reconstruction of Unobserved States (PICRUSt2) software package (Douglas et al., 2019). OTU sequences were de-gaped and placed in a reference taxonomic tree using the Integrated Microbial Genomes database, and KEGG orthologs were predicted for each OTU based on steps described previously (Barbera et al., 2019; Czech and Stamatakis, 2019; www.hmmer.org).

2.7. Quantification of the 16Sr RNA, RuBisCO and rTCA marker genes

Quantitative PCR (qPCR) targeting bacterial 16S rRNA genes, RuBisCO marker genes of the Calvin Benson Basham cycle and the ATP citrate lyase (*acl)* genes of the reductive citric acid cycle (rTCA) was carried out on the Mx3000P instrument (Agilent, C.A, U.S.A) using Maxima SYBR Green Mastermix (Agilent). For the RuBisCO marker genes, primer pairs F-cbbL IA/R-cbbL IA, F-cbbL IC/R-cbbL IC and F-cbbM/R-cbbM were used targeting gene variants *cbbL* IA, *cbbL* IC and *cbbM,* respectively (Alfreider et al., 2003, 2012), following cycling conditions previously specified (Herrmann et al., 2015). For the rTCA cycle, primer pair F-g-acl-Nit/R-g-acl-Nit, which targets the alpha subunit of ATP citrate lyase (aclA) gene and is specific for nitrite oxidizing and complete ammonia oxidizing (comammox) Nitrospira, was used (Alfreider et al., 2018). The cycling conditions were: 10 min at 95 °C, followed by 45 cycles of 45 s at 94 °C, 45 s at an annealing temperature of 56 °C, 60 s at 72 °C, and then 78 °C for 20 s for data acquisition. Standard curves were constructed from ten times dilution series of mixtures of plasmids from 5×10^8 to 5×10^1 copies, each containing *cbbL* IA, *cbbL* IC, *cbbM* or *aclA* inserts for *cbbL* IA, *cbbL* IC, *cbbM* or *aclA* qPCR, respectively obtained from groundwater for the RuBisCO gene variants and from soil for the *aclA* genes (Herrmann et al., 2015). As a template, 5 μl of DNA samples in triplicates were used from a mixture of 3 μl DNA (1–3 ng μl^{-1}) template and 22 μl of TE buffer. Samples with DNA concentrations higher than 10 ng μl^{-1} were pre-diluted 1:10. Quantifications were considered valid when samples were in the linear range of the calibration curve (5×10^8 to 5×10^1). For bacterial 16S rRNA genes, primer pair Bac 8Fmod and Bac 338R (Loy et al., 2002; Daims et al., 1999) and cycling conditions given as 10 min denaturation at 95 °C, followed by 45 cycles of 30 s at 95 °C, 30 s at 55 °C and 25 s at 72 °C for data capture (Herrmann et al., 2012) were used. For absolute quantification of the 16S rRNA gene copies, plasmids containing the 16S rRNA gene of *Escherichia coli* were used to construct the standard curves for 16S rRNA genes as described for the RuBisCO marker genes above. All primer specifications used in this study can be found in Table S3 of the supplementary information.

2.8. Sequence data deposition

Generated sequences have been submitted to the NCBI database with accession numbers: SAMN14151380, SAMN14151381, SAMN14151382, SAMN14151383, SAMN14151384, and SAMN14151385.

3. Results

3.1. Dark CO_2 incorporation into SOC and MBC to 1 m depth

We observed an increase of $\delta^{13}C$ of SOC and MBC in the incubations of soil samples with $^{13}CO_2$ among all treatments, in comparison to the controls (Fig. S1). Dark CO_2 fixation rates, expressed in relation to soil dry weight as μg carbon per gram dry weight (dw) of soil per day, decreased with increasing soil depth, with the highest rates of 0.86 ± 0.01 μg C g (dw) $soil^{-1}$ d^{-1} observed in the top 12 cm depth after 7 days (Fig. 1A). At 70–100 cm depth, a significantly lower rate of $0.06 \pm 1.61 \times 10^{-3}$ μg C g (dw) $soil^{-1}$ d^{-1} (Student's *t*-test, $P = 6.57 \times 10^{-4}$) was determined. However, when expressed in relation to MBC, in μg carbon per gram of MBC per day, no significant difference in rates was observed across the depths ($P = 0.77$), as MBC also declined from about 369.97 ± 20.46 μg C gdw^{-1} in 0–12 cm depth to 20.15 ± 6.25 μg C gdw^{-1} in 70–100 cm depth ($P = 4.69 \times 10^{-4}$) (Table 1 and Table S1). These normalized rates ranged from 484.40 ± 3.52 μg C $gMBC^{-1}$ d^{-1} at the topsoil to 458.37 ± 37.58 μg C $gMBC^{-1}$ d^{-1} in the deepest samples (Fig. 1B).

We observed a decline in the rates of CO_2 fixation with incubation time for all soil depths. For the top 12 cm, the rates decreased from 0.86 ± 0.01 μg C g(dw) $soil^{-1}$ d^{-1} at 7 days of incubation to 0.45 ± 0.01 μg C g(dw) $soil^{-1}$ d^{-1} ($P = 9.87 \times 10^{-3}$) after 28 days. Interestingly, the ratio of the rates between the top 12 cm depth, and the two lower depths remained constant across all incubation times. Compared to the topsoil, fixation rates were 80% lower in 35–45 cm depth and 93% lower in 70–100 cm after 7 days of incubation and this ratio did not change with incubation time. When expressed in relation to MBC, rates declined significantly only at the top 12 cm depth by almost 2-folds from 484.40 ± 3.52 μg C $gMBC^{-1}$ d^{-1} to 294.38 ± 4.63 μg C $gMBC^{-1}$ d^{-1} ($P = 0.02$) when incubated for 7 versus 28 days.

3.2. Effect of CO_2 concentration on dark CO_2 fixation rates

We observed a general increase in $\delta^{13}C$ (Fig. S2) and of dark CO_2 fixation rates when soil derived from the November sampling campaign was incubated under increasing CO_2 headspace concentrations ranging from 2 to 20% (v:v) (Fig. 2). Across all depths, a linear response was observed between 2 and 10% CO_2. For the top 12 cm, rates increased significantly from 0.53 ± 0.01 μg C g(dw) $soil^{-1}$ d^{-1} at 2% CO_2 to $1.01 \pm 1.40 \times 10^{-4}$ μg C g(dw) $soil^{-1}$ d^{-1} at 10% CO_2 (Student's t-test, $P = 5.35 \times 10^{-6}$), leveling off at $1.07 \pm 2.47 \times 10^{-4}$ μg C g(dw) $soil^{-1}$ d^{-1} at 20% CO_2 ($P = 1.24 \times 10^{-2}$) (Fig. 2A). Likewise, the CO_2 fixation rates expressed in relation to MBC for the same depth was over 2-fold higher at 10% CO_2 with 608.83 ± 25.97 μg C $gMBC^{-1}$ d^{-1} compared to 300.90 ± 9.79 μg C $gMBC^{-1}$ d^{-1} at 2% CO_2 ($P = 7.81 \times 10^{-4}$) and reached 698.32 ± 39.01 μg C $gMBC^{-1}$ d^{-1} at 20% CO_2 compared to rates at 2% CO_2 ($P = 1.98 \times 10^{-3}$) (Fig. 2B). Similar increases in CO_2 fixation rates in relation to soil dry weight and MBC with higher CO_2 concentrations were also observed for the lower depth intervals. Over the total CO_2 concentration range used, the increase in fixation rates was non-linear, indicating a saturation of the CO_2 fixation process in the soil microcosms.

As in our first experiment and independent of the CO_2 concentration used, we observed a decrease of CO_2 fixation rates with increasing soil depth in relation to soil dry weight, but no significant change was observed with depth when rates were expressed in relation to MBC (Fig. 2B). Soils obtained from the August and November campaigns did not show significant differences in dark CO_2 fixation rate in relation to soil dry weight and MBC under similar incubation conditions (i.e, 2% CO_2 at 7 days of incubation).

3.3. Contribution of microbial CO_2 fixation to SOC and MBC

The relative amount of carbon in MBC and SOC derived from CO_2 fixation increased with the time of incubation. After 7 days of incubation with 2% CO_2 (v:v), dark CO_2 fixation accounted for $0.02 \pm 2.86 \times 10^{-3}$% of SOC and 0.34 ± 0.11% of MBC at the top 12 cm depth (Fig. 3). After 28 days, this CO_2 derived carbon doubled to 0.03 ± 0.01% (Student's *t*-test, $P = 9.58 \times 10^{-5}$) in SOC and to 0.82 ± 0.15% ($P = 7.62 \times 10^{-5}$) in MBC. With depth, the contribution of newly fixed carbon to SOC typically decreased slightly, ($P = 0.01$) but no significant difference ($P = 0.74$) in the contribution to MBC was observed across depth after 28 days. The increase of headspace CO_2 concentrations from 2% up to 20% (v:v) also increased the relative amount of excess ^{13}C in SOC and MBC (Fig. 3). In the top 12 cm, e.g., excess ^{13}C in SOC roughly doubled with a 5-fold increase in CO_2, from $0.01 \pm 2.88 \times 10^{-4}$% at 2% $^{13}CO_2$ (v:v) to $0.02 \pm 4.55 \times 10^{-4}$% at 10% $^{13}CO_2$ (v:v) ($P = 1.67 \times 10^{-5}$), and

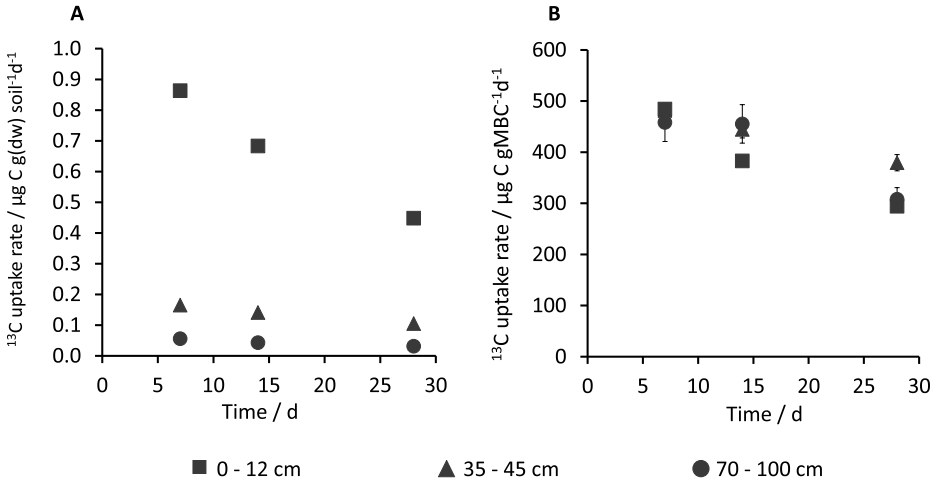

Fig. 1. Dark CO_2 fixation rate in soil microcosms with 2% $^{13}CO_2$. Shown are (A) ^{13}C uptake rates into SOC expressed in µg C g(dw) soil^{-1} d^{-1} (µg carbon per gram dry weight (dw) of soil per day) and (B) ^{13}C uptake rates in MBC expressed µg C gMBC^{-1} d^{-1} (µg carbon per gram microbial biomass carbon per day) after 7, 14 and 28 days of incubation. Error bars indicate standard deviation of three replicate incubations and are shown only where larger than symbols.

Table 1
Geochemical properties of soil cores obtained from the Hainich national park. Soil pH, soil organic carbon (SOC), carbon/nitrogen (C/N) ratio, microbial biomass carbon (MBC), and ^{13}C signatures, measured at 3 depth definitions from the Hainich forest soil cores during the August and November sampling campaigns. Reported values represent the mean of values measured from both campaigns. MBC values are obtained from the November campaign only.

Soil Depth (cm)	pH	SOC (%)	C/N ratio	MBC (µg C gdw^{-1})	SOC δ^{13}C (‰)
0–12	4.45 ± 0.44	3.46 ± 0.65	11 ± 0.80	369.97 ± 20.46	−26.75 ± 0.31
35–60	5.73 ± 0.18	0.85 ± 0.11	9 ± 0.52	29.74 ± 10.49	−24.72 ± 0.50
70–100	7.01 ± 0.04	0.44 ± 0.14	7 ± 0.81	20.15 ± 6.25	−24.69 ± 0.60

remained constant at 0.02 ± 2.44 × 10^{-3}% when $^{13}CO_2$ concentration increased from 2% to 20% ($P = 1.11 \times 10^{-2}$). Likewise, the excess ^{13}C in MBC in the top 12 cm increased from 0.21 ± 6.85 × 10^{-3}% at 2% (v:v) CO_2 to 0.43 ± 0.02% and 0.49 ± 0.03% under 10% and 20% $^{13}CO_2$ (v:v), respectively ($P = 7.81 \times 10^{-4}$ and $P = 1.98 \times 10^{-3}$, respectively). Similar effects of the increased CO_2 concentrations were also observed in the deeper soil depths.

3.4. Metabolic potential for autotrophic CO_2 fixation in the Hainich forest soil

Having observed the rates of dark CO_2 fixation and its contribution to SOC formation in the Hainich soil, we aimed to identify and characterize the microorganisms potentially playing the key role in this process. Taxonomic classification of OTUs revealed *Actinobacteria, Proteobacteria, Acidobacteria, Chloroflexi*, and *Verrucomicrobia* to be the predominant phyla identified across depth, together making up to 80% of the soil microbial communities (Fig. S3). These predominantly heterotrophic groups are typically found in temperate forest soils (López-Mondéjar et al., 2015; Lladó et al., 2017).

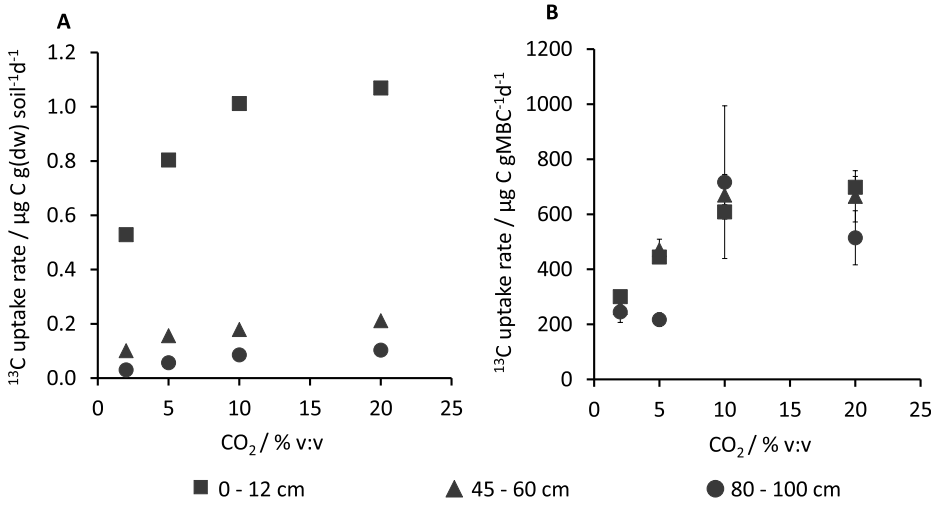

Fig. 2. Dark CO_2 fixation rates in soil microcosms with different $^{13}CO_2$ concentrations. Shown are (A) ^{13}C uptake rates into SOC expressed in µg C g(dw) soil^{-1} d^{-1} (µg carbon per gram dry weight (dw) of soil per day) and (B) ^{13}C uptakes expressed in MBC in µg C gMBC^{-1} d^{-1} (µg carbon per gram microbial biomass carbon per day) after 7 days of incubation with 2%, 5%, 10% and 20% $^{13}CO_2$. Error bars indicate standard deviation of three replicate incubations and are shown only where larger than symbols.

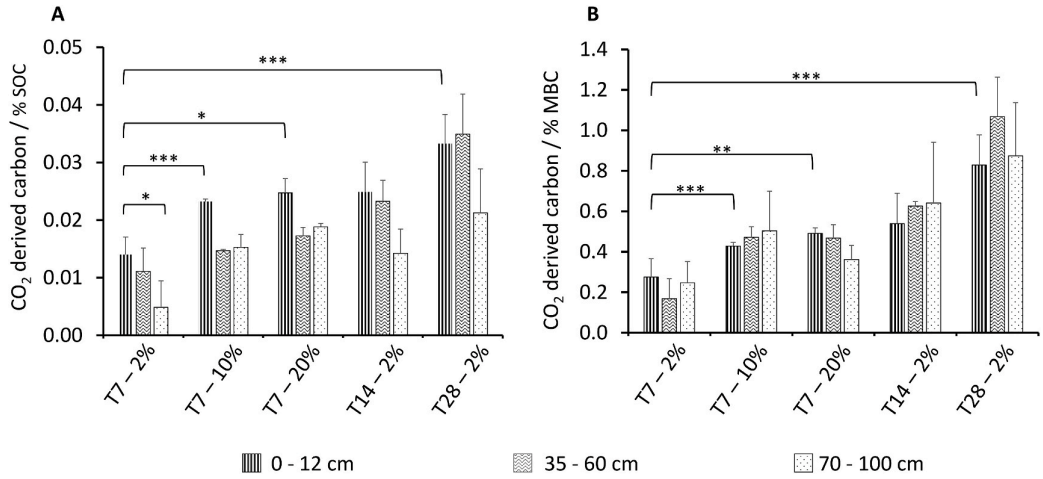

Fig. 3. Contribution of dark CO_2 fixation to SOC and MBC in soil microcosms with 2% and 20% $^{13}CO_2$ over time. Shown are the excess ^{13}C incorporation in SOC (A) and MBC (B) expressed as % of SOC and % of MBC at 2% $^{13}CO_2$ and 20% $^{13}CO_2$ after 7 days of incubation (T7-2%, T7-10% and T7-20% respectively) and at 2% $^{13}CO_2$ after 14 (T14-2%) and 28 (T28-2%) days of incubation. The depth definitions, 0–12 cm, 35–60 cm and 70–100 cm represent the depth range sampled for both campaigns. Error bars denote standard deviation of six replicate incubations from the August and November sampling campaigns (T7-2%), three incubations from the November campaign (T7-20%) and the August campaign (T14-2%, T28-2%). * denotes $P < 0.05$, ** denotes $P < 0.01$ and *** denotes $P < 0.001$.

Families that dominated the most abundant phyla across the soil profile included *Micromonosporaceae* (*Actinobacteria*), *Xanthobacteraceae* (*Proteobacteria*), *Roseiflexaceae* (*Chloroflexi*) and *Chthoniobacteraceae* (*Verrucomicrobia*). The microbial community differed distinctly with depth (Fig. S4). While members of the *Proteobacteria*, *Acidobacteria*, *Verrucomicrobia, Planctomycetes*, and *Bacteroidetes* phyla were observed to decrease in abundance across depth, bacteria phyla belonging to the *Chloroflexi* and *Actinobacteria* increased with depth and were the most predominant groups in lower depths.

To explore the metabolic potential for autotrophy, genes for key enzymes involved in CO_2 fixation pathways were predicted for bacterial OTUs by PICRUSt2. Putative autotrophic OTUs comprised up to 10% of the total bacterial community. Families of the most abundant putative autotrophic OTUs were identified as *Xanthobacteraceae, Nitrospiraceae, Nitrosomonadaceae*, and *Mycobacteriaceae* and were found to vary in abundance between the top 12 cm depth and the two lower depth intervals (Fig. 4). The autotrophic CO_2 fixation genes predicted were mostly related to the Calvin Benson Bassham (CBB) pathway (*Xanthobacteraceae, Nitrosomonadaceae*, and *Mycobacteriaceae*) followed by the reductive citric acid (rTCA) pathway (*Nitrospiraceae*) and the Wood-Ljungdahl pathway (WLP) being the least predominant pathway predicted (Fig. S5). Putative heterotrophs capable of CO_2 fixation, as denoted by the abundance of phosphoenolpyruvate carboxylase (PEPC) genes, were more abundant than the putative autotrophs across depth, constituting 45–50% of the total microbial community (Fig. S5).

To verify the potential for autotrophic CO_2 fixation, the abundance of marker genes for the CBB cycle and the rTCA pathway, RuBisCO (*cbbL* IA, *cbbL* IC, and *cbbM*) and ATP-citrate lyase alpha subunit (*aclA*), as well as of total bacterial 16S rRNA genes was determined using qPCR. In soil samples retrieved from both sampling campaigns, bacterial 16S rRNA gene copies were highest at 0–12 cm depth, ranging between 1.48×10^{10} and 2.41×10^{10} gene copies per gram dry weight of soil, and decreased substantially down the soil profile to between 1.06×10^{8} and 2.69×10^{8} gene copies per gram dry weight of soil (Table S2). Of the RuBisCO gene variants, *cbbL* IA and *cbbL* IC were detected in the soils, while *cbbM* was below the limit of detection (5×10^{3} gene copies per gram soil). Both detected gene variants showed similar distribution patterns in all soil depths of the two sampling campaigns (Fig. 5). Variant *cbbL* IC showed the highest abundance, between 0.18% and 0.40% relative to bacterial 16S rRNA gene copies. In comparison, abundances of *cbbL* IA were lower, with values between 0.009% and 0.040%. The *aclA* gene was detected in all soil depths in the November

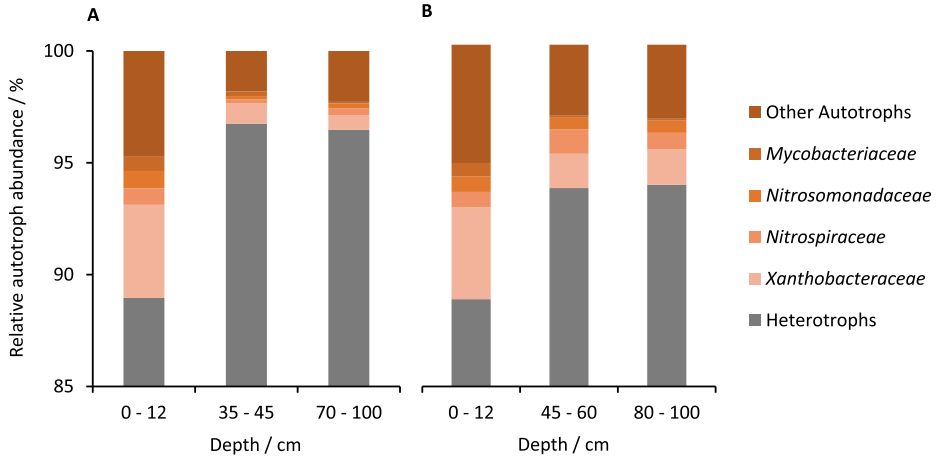

Fig. 4. Composition of the bacterial autotrophic community (family level). Shown are the relative abundance of assigned sequences for the most abundant putative autotrophic bacteria. (shades of orange bars) in comparison to the putative heterotrophs (gray bars) of bulk soil across depths for the August (A) and November (B) campaigns. Taxonomic selection is based on 16S rRNA predicted functions by PICRUSt2 (Phylogenetic Investigation of Communities by Reconstruction of Unobserved States, version 2). The scale on the y-axis begins from 85%. Data represent the mean of three replicate cores for the August campaign and two replicate soil samples from homogenized soil cores for the November campaign.

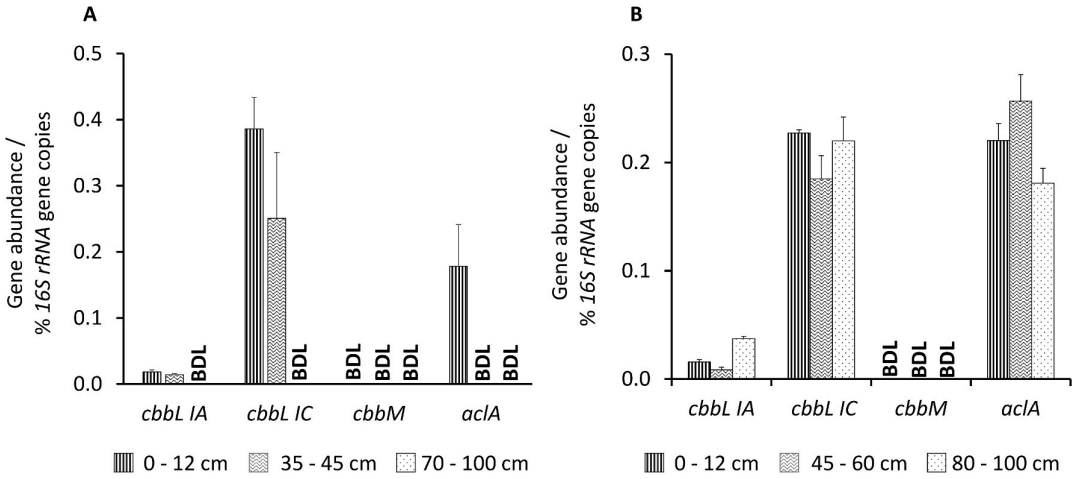

Fig. 5. Relative abundance of RuBisCO (*cbbL* IA, *cbbL* IC, and *cbbM) and ATP citrate lyase (aclA) marker gene copies in soil. Shown are the *cbbL* IA, *cbbL* IC, and *aclA* gene abundance in soil of the August (A) and November sampling campaigns (B) prior to incubation acquired by qPCR. Both are expressed as % of 16S rRNA gene copies in soil. Error bars indicate standard deviation of the mean of three replicate soil core samples for the August sampling campaign and two replicate soil samples from homogenized soil cores for the November sampling campaign. BDL denotes gene copies below detection limit.

campaign but was only above the detection limit at the top depth in the August campaign. This gene abundance was between 0.18% and 0.26% relative to bacterial 16S rRNA gene copies, showing a uniform distribution across depth. Taken together, the *cbbL* IA, *cbbL* IC, and *aclA* genes represented around 0.5% of the bacterial 16S rRNA gene copies in all samples and did not correlate with CO_2 fixation rates (Fig. S6B).

Interestingly, in the incubated soil samples, we observed a significant increase of RuBisCO gene copies in comparison to soils at the beginning of incubation (Fig. S7). This effect was most pronounced for *cbbL* IA after 7 days of incubation, where gene copy numbers had increased from $0.018 \pm 0.003\%$–$0.104\% \pm 0.024\%$ relative to bacterial 16S rRNA genes (Student's *t*-test, $P = 0.02$), and for *cbbL* IC after 14 days of incubation, where an increase from $0.39 \pm 0.05\%$ to $1.3 \pm 0.10\%$ ($P = 1.22 \times 10^{-3}$) had been observed. The abundance of *aclA* genes, however, was not different between incubation times. An increase of headspace CO_2 concentration had no effect on relative abundances of neither *cbbL* nor *aclA* genes (Fig. S8), even though a significant decrease in the 16S rRNA genes at the top 12 cm depth ($P = 0.002$) was observed when CO_2 increased from 2% (v:v) to 20% (v:v).

4. Discussion

Our data did not confirm our first hypothesis that the relative amount of chemolithoautotrophs will increase down the soil profile. The proportion of the autotrophs constituted a very small fraction of the soil microbial community with a constant relative gene abundance with depth (Fig. 5). Their abundance also did not correlate with dark CO_2 fixation rates across depth (Fig. S6B), thus contradicting our second hypothesis that dark CO_2 fixation rates would scale with the abundance of chemolithoautotrophs across depth. In agreement, the abundance of genes for autotrophic CO_2 fixation did not increase under higher (20%) CO_2 concentration (Fig. S8). This could be related to the typically slow growth rate of autotrophs (Lengeler et al., 1999; Jorgensen and Nelson, 2004; Lipsewers, 2017). However, an increase in autotroph gene abundance was observed after 7 days of incubation with 2% CO_2 (Fig. S7), showing the capacity for autotrophs to grow within that short period. Thus, higher CO_2 concentration did not affect chemolithoautotrophic growth. This suggests that the change in fixation rates observed was not caused by an increased abundance of autotrophs. However, as gene abundance does not necessarily reflect activity, we cannot completely exclude the contributions of autotrophs to the higher fixation rates observed. Also, PICRUSt2 predicted low abundances of obligate autotrophs such as members of the *Nitrospiraceae* family (Fig. 4). Obligate autotrophs specifically require inorganic electron donors like reduced nitrogen, sulfur, or iron compounds as energy sources for their growth (Brock et al., 2003; Alfreider et al., 2018). These compounds might be limited in deeper soils (Jones et al., 2018), restricting the activity of obligate autotrophs. In agreement, previous studies showed that chemolithoautotrophic CO_2 fixation can be stimulated in soils when amended with sulfur compounds as electron donors (Hart et al., 2013; Zhao et al., 2020). Facultative autotrophs like members of the *Xanthobacteraceae* family were the most abundant of all putative autotrophs identified in this study (Fig. 4). These groups are usually more widely distributed in soils than their obligate counterparts (Yuan et al., 2012; Wu et al., 2015; Xiao et al., 2018) due to their metabolic flexibility and predominantly mixotrophic lifestyle (Kappler and Nouwens, 2013; Oren, 2014; Xiao et al., 2018). CO_2 fixation by facultative autotrophs was shown to be enhanced under higher SOC (Yuan et al., 2012), therefore, their contributions to dark CO_2 fixation via the Calvin cycle may be impaired in deeper soils due to the limited SOC content (Xiao et al., 2018) in addition to the limited availability of inorganic electron donors required to support their growth. Therefore, autotrophs using the Calvin cycle, the rTCA pathway, or the Wood-Ljungdahl pathway seem to contribute little to the high dark CO_2 fixation rates observed in the forest soils. The soil microbial biomass was dominated, not surprisingly, by heterotrophic bacteria varying in their composition across the soil profile (Fig. S3). This dominance of heterotrophs over autotrophs has been previously reported for the Hainich forest soils (Dukunde et al., 2019) as well as for other soils shown to fix CO_2 (Liu et al., 2018; Šantrůčková et al., 2018) which could hint that heterotrophs are the main CO_2 fixers. Supporting this, PICRUSt2 analysis predicted a great abundance of phosphoenolpyruvate carboxylase (PEPC) genes across depth (Fig. S5), which may be indicative of the heterotrophic CO_2 fixation as suggested by previous findings (Bar-Even et al., 2012; Šantrůčková et al., 2018). The corresponding carboxylase genes of these heterotrophs were more abundant than functional genes of autotrophs in a study targeting CO_2 fixation in arctic soils (Šantrůčková et al., 2018). Heterotrophic CO_2 fixation was also shown to be enhanced under nutrient-limited conditions, potentially playing a role in cellular maintenance during stationary phase to enable longer survival under oligotrophic conditions (Alonso-Sáez et al., 2010). This increasing demand for inorganic carbon during cell starvation was suggested to result from the cells undergoing major shifts in protein and lipid composition during stationary growth phase (Merlin et al., 2003;

Table 2
Dark CO_2 fixation rates from a range of soils based on incubation experiments. Shown are measured rates of dark CO_2 fixation as reported by different soil incubation studies. Reported values are converted to dark CO_2 fixation rates per gram dry weight of soil and per gram of microbial biomass carbon (MBC) where applicable, for easy comparison.

Soil characteristics	Soil depth (cm/ Horizon)	Incubation conditions			Dark CO_2 fixation			Ref.
		CO_2 (vol %)	Temp (°C)	Time	Reported values	Rate per unit soil (μg C g(dw) soil-1 d-1)	Rate per unit MBC (μg C g MBC^{-1} d^{-1})	
Temperate forest soils	0 - 12 (A)	2	RT	7 days	30.48 ± 10.35 g C m^{-2} yr^{-1}	0.53 ± 0.01 - 0.86 ± 0.01	300.90 ± 9.79–484.40 ± 3.52	This study
	35 - 60 (BC)				18.78 ± 1.53 g C m^{-2} yr^{-1}	0.10 ± 1.57 × 10^{-5} - 0.16 ± 0.0037	260.88 ± 53.76–481.76 ± 7.08	
	70 - 100 (C)				7.81 ± 4.79 g C m^{-2} yr^{-1}	0.03 ± 2.42 × 10^{-5} - 0.06 ± 0.0016	245.23 ± 10.77–458.37 ± 37.58	
	0 - 5 (A)	1	15	7 days	132.6 ± 34.6–232.5 ± 12.6 μg C kg^{-1} soil d^{-1}	0.133–0.232	88.75 ± 11.42–112.21 ± 24.16	Spohn et al. (2019)
	30 - 40 (B1)				36.11 ± 1.61–47.8 ± 2.32 μg C kg^{-1} soil d^{-1}	0.036–0.048	50.34 ± 12.76–198.66 ± 21.96	
	60 - 70 (B2)				37.2 ± 3.02–55.64 ± 15.25 μg C kg^{-1} soil d^{-1}	0.037–0.056	42.93 ± 13.61 - 86.93 ± 24.58	
Temperate Agricultural soils	1–2	In situ	In situ	30 min	0.2–4.8 mg CO_2 m^{-2} h^{-1}.	nd	nd	Shimmel, 1987
	0–30	1	20	61 days	0.83 μmol C g^{-1} soil	0.163	nd	Miltner et al. (2004)
	0–30	nd	20	81 days	1.3 μmol C g^{-1} soil	0.19	nd	Miltner et al. (2005)
A range of temperate forest and field soils	5–15	0.05–5	RT	21 days	2.8–36.5 mg CO_2 $m^{-2}h^{-1}$,	1.82–23.56	nd	Šantrůčková et al. (2005)
	0–15	5	25	3 days	5.1–57 μmol C mol^{-1} C d^{-1}	nd	nd	Nel and Cramer, 2019
Temperate soils amended with S_2O_3	nd	0.1	RT	40 hr	4.52 ± 0.05 g CO_2 kg^{-1} soil	738	nd	Hart et al. (2013)
Temperate Mofette soils	0–10	100	12	28 days	494 ± 14 ng C g(dw) $soil^{-1}$ d^{-1}	0.494	nd	Beulig et al. (2014)
	25–40				512 ± 10 ng C g(dw) $soil^{-1}$ d^{-1}	0.512	nd	
	0–10	100	12	14 days	3.14 ± 0.44 μg C g(dw) $soil^{-1}$ d^{-1}	3.14	nd	Beulig et al. (2016)
	0–10	100	12	14 days	0.66–0.77 μg C gdw^{-1} d^{-1}	0.66–0.77	271–287	Nowak et al. (2015)
	0–10	100	12	7 days	1.07 ± 0.62 μg C gdw^{-1} d^{-1}	1.07 ± 0.62	nd	
	10–20				0.30–0.22 μg C gdw^{-1} d^{-1}	0.30 ± 0.22	nd	
	20–40				0.14 ± 0.03 μg C gdw^{-1} d^{-1}	0.14 ± 0.03	nd	
Tropical Forest soils	0–10	5	RT	7 days	0.10 ± 0.03–0.44 ± 0.13 μg C gdw^{-1} d^{-1}	0.10 ± 0.03 - 0.44 ± 0.13	nd	Nowak et al., (unpublished result)
	15–50				0.04 ± 0.01–0.12 ± 0.03 μg C gdw^{-1} d-1	0.04 ± 0.01 - 0.12 ± 0.03	nd	
	95–100				0.01 ± 0.00–0.04 ± 0.03 μg C gdw^{-1} d^{-1}	0.01 ± 0.00 - 0.04 ± 0.03	nd	
Arctic tundra soils	Cryoturbated	1	12	7 days	3.06 ± 0.59 μmol C mol $OC^{-1}d^{-1}$	0.04	nd	Šantrůčková et al. (2018).
	Mineral				7.37 ± 1.02 μmol C mol $OC^{-1}d^{-1}$	0.08	nd	
Semi-arid Desert soils	0–20	0.2	25	7 days	0.572 ± 0.04–1.45 ± 0.17 mg kg^{-1} soil	0.08–0.21	nd	Liu et al. (2018).

Temp: Temperature; RT: Room Temperature; nd: not determined.

Alonso-Sáez et al., 2010) and not from *de novo* synthesis of biomolecules, which would require additional nutrients, as lipid synthesis is also known to boost CO_2 demand (Cuellar-Bermudez et al., 2015; Sun et al., 2016; Eloka-Eboka and Inambao, 2017). Taken together, heterotrophs appear to be key players of dark CO_2 fixation in temperate forest soils.

Our average dark CO_2 fixation rates with 0.70–0.04 μg C g(dw) soil^{-1} d^{-1} across depths are within the magnitude of other studies covering a broad range of soils (Table 2) but are 2–6 times higher than those observed in a similar recent study of Spohn et al. (2019) with temperate forest soils. However, a direct comparison of the fixation rates is not always possible, due to differences in incubation conditions or due to the lack of specific data to convert rates to the same units. The lower values reported by Spohn et al. (2019) despite the higher SOC and microbial biomass carbon content of these soils, may have resulted from the lower incubation temperature or the long pre-incubation time of 10 days prior to the 7 days of incubation time. In agreement, previous studies have reported lower CO_2 fixation rates at temperatures below 25 °C (Nel and Cramer, 2019; Zhao et al., 2020) and we also observed a decline in fixation rates with increasing incubation time (Fig. 1). Similarly, our rates for the topsoil horizon were around 5 times higher than those of agricultural soils incubated for 61 and 81 days by Miltner and colleagues (2004 and 2005). Our values scale with those reported by Nowak et al. (2015), who recorded values between 1.07 and 0.14 μg C g(dw) soil^{-1} d^{-1} for the top 40 cm of a mofette soil, decreasing with depth, but were higher than those of a tropical forest soil (Nowak et al., unpublished result). Similar to this study, previous studies that included incubations of deeper soils show a strong decline of dark CO_2 fixation rates with depth (Table 2). As in our sites, these differences across depth diminished when rates were normalized to MBC (Figs. 1B and 2B, Nowak et al., 2015; Spohn et al., 2019). Strong relationships between dark CO_2 fixation rates and microbial biomass carbon exist despite distinct changes in microbial community structure with depth in Hainich forest soil (Fig. S3 and Fig. S6A), which are exemplary for most soils. Taken together, this suggests that it is not soil depth *per se* but microbial biomass, in particular heterotrophs, that is a determining factor for dark CO_2 fixation.

The second important driver for dark CO_2 fixation appears to be pore space CO_2 concentration. Our data showed a 2 to 3-fold rise of fixation rates when CO_2 concentrations increased from 2 to 20% independent of soil depth (Fig. 2), supporting our third hypothesis that this process is enhanced under high soil CO_2 concentrations. The response was linear between 2 and 10% CO_2, extending recent results of Spohn et al. (2019) that reported a ~2-fold linear increase between 1 and 6.1% CO_2. The increase of CO_2 fixation rates diminished from 10 to 20% CO_2 concentration. Since O_2 concentration throughout the incubation period was above 20%, this diminishing effect could result from a saturation of the CO_2 substrate. This reduced response to high CO_2 was also shown in wetland soils exposed to 100% CO_2 and explained by substrate saturation (Beulig et al., 2016). Forest soil microbes seem to reach saturation at lower CO_2 concentrations than wetland soils, probably due to community differences. Wetland microbes are more adapted to water-saturated anoxic conditions and harbor high fractions of anaerobes fixing CO_2 via the reductive acetyl-CoA pathway (acetogens, methanogens, and sulphate reducers) in addition to others using the Calvin cycle (Beulig et al., 2016). The linear response across a broad concentration range suggests that temperate forest soil fixation rates will respond to fluctuations in soil pore space CO_2, which can occur during both short term (hours to days) and seasonal periods of elevated temperature and soil moisture conditions (Lu et al., 2013).

The effect of increased CO_2 fixation rates upon elevated CO_2 conditions may play a role in the response of temperate forests to global change (Lorenz and Lal, 2009; Domke et al., 2016). Several studies have demonstrated a 30 to ~100% increase in soil CO_2 production and efflux if atmospheric CO_2 levels double, as is likely by 2050 (Hungate et al., 1997; Allen et al., 2000; Andrews and Schlesinger, 2001; Pendall et al., 2001; Oh et al., 2005), and which would also affect CO_2 concentration in soil. For example, in the Duke forest FACE experiment, Bernhardt et al. (2006), reported that elevating atmospheric CO_2 concentrations by 200 ppm (>50%) increased soil CO_2 concentration by > 7000 ppm (8–15% more) at 100 cm depth. A range of parameters, including soil diffusivity, the amount and depth distributions of roots, and microbial activities, as well as rates of soil CO_2 production will affect soil CO_2 levels (Oh et al., 2005). Despite predicted impacts on soil CO_2 concentrations, it is unclear whether elevated atmospheric CO_2 will directly affect soil microbial biomass, their community structure, or functions (Lladó et al., 2017). Since soil CO_2 concentrations are higher than atmospheric levels (<400 ppm), microbial response to elevated atmospheric CO_2 might be negligible (Dunbar et al., 2012; Brenzinger et al., 2017) especially as microbes may experience concentrations in microsites that are even higher than observed in pore space that may be more directly connected to the atmosphere. Also, inconsistencies exist on the effect of increased CO_2 on microbial functional traits from different forest ecosystems (Long et al., 2012; Schleppi et al., 2012) which may result from differences in local edaphic conditions. Therefore, such feedback is unpredictable across temperate forests globally. A potential outcome could be that increased atmospheric CO_2 levels may boost net primary productivity (Lladó et al., 2017) with unclear consequences on temperate forest carbon fluxes (Meier et al., 2015). For example, increased root exudation (Lladó et al., 2017) and litter input (Ahrens et al., 2015) can cause a shift in microbial community structure and enhance activities (Blagodatskaya et al., 2010; Fransson et al., 2016). Higher temperatures would further promote microbial SOC decomposition, leading to increased soil CO_2 concentration and release (Oh et al., 2005; Hicks Preis et al., 2018; Kravchenko et al., 2019) that may in return stimulate dark CO_2 fixation rates.

Our data show that up to 0.03% of SOC (1–13 mg C kg^{-1}) and up to 1% of MBC (0.2–4 mg C kg^{-1}) were derived from dark CO_2 fixation under 2% CO_2 after 28 incubation days. The low contribution of fixed carbon to the SOC pool (Fig. 3) is explained by its small proportion of microbial biomass with less than 5% (Rössner et al., 1996; Dalal, 1998). When we estimated dark CO_2 fixation rates per unit area (m^2) according to Xiao et al. (2018) and assuming a bulk density of 1 g cm^{-3} (Lorenz et al., 2011), an annual fixation rate of 57.1 ± 16.7 g C m^{-2} yr^{-1} to a depth of 1 m was achieved, which scales to 4.3 ± 1.3 Gg C yr^{-1} for the

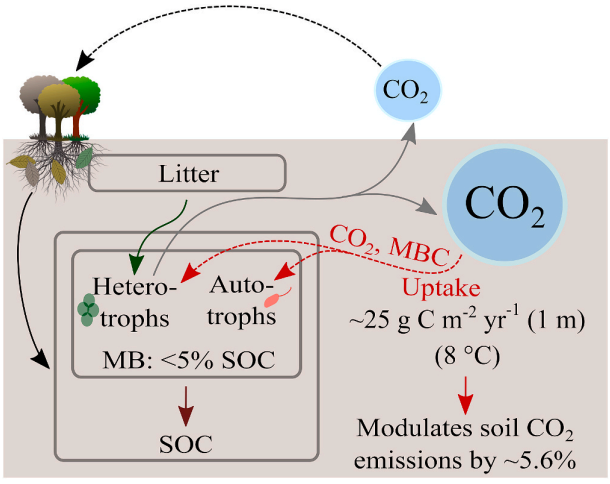

Fig. 6. Conceptual illustration of dark CO_2 fixation in Hainich forest soils. Curved squares represent litter, microbial biomass (MB), and SOC pools while arrows represent fluxes between pools. Photosynthetic CO_2 fixation is denoted by dashed black arrows and litter input into SOC can be directly (solid black arrow) or through decomposition (solid green arrow) by microbial biomass which is 5% of SOC. A part of the CO_2 released during decomposition can diffuse into the atmosphere (solid gray arrows) while 5.6% is fixed by the MB pool (dashed red arrows) at a rate governed by CO_2 concentration and the size of the microbial biomass which upon death, enters the SOC pool (solid brown arrows). (For interpretation of the references to colour in this figure legend, the reader is referred to the Web version of this article.)

total Hainich forest area (76 km^2; Knohl et al., 2003). Assuming this constant rate, it would take ~6 years to completely replace microbial biomass carbon and about 120 years (0–12 cm) to 220 years (below 70 cm) to replace all SOC in the Hainich forest soil with carbon fixed by dark CO_2 fixation. However, considering the mean annual temperatures in the Hainich forest soils of around 8 °C and assuming a Q_{10} of ~2, that is, a doubling of rates with a 10 °C rise in temperature (Moyano et al., 2008), the fixation rate under real field conditions is likely to be ~2.3 times less. This amount to ~25 ± 7.2 g C m^{-2} yr^{-1} (Fig. 6) and scales to ~1.9 ± 0.55 Gg C yr^{-1} for the total Hainich forest area. Under these conditions, fixation rate was higher than that of Spohn et al. (2019) extrapolated as ~14 g C m^{-2} yr^{-1} at 15 °C down to 70 cm depth. These rates are likely to be even higher if extrapolated to the same temperature and may be partly due to contributions from the deeper profiles, which were not accounted for in the previous studies. Accordingly, we would expect turnover times to be 2.3 times longer with values ranging from 280 years (0–12 cm) to 510 (below 70 cm) years for SOC and around 14 years for MBC under Hainich forest field conditions. These values are similar to estimated turnover times of 10–50 years for MBC and 270–880 years for SOC in tropical forest soils to 1 m depth (Nowak et al., unpublished result).

Our calculated annual uptake rates represent gross uptake and not necessarily evidence of net carbon gain (i.e, without accounting for carbon losses through heterotrophic respiration), as the Hainich forest soil also shows very small net carbon increase (Kutsch et al., 2010). Since gross carbon inputs of 441–452 g C m^{-2} yr^{-1} and CO_2 effluxes of 417–442 g C m^{-2} yr^{-1} down to 60 cm depth have been reported (Kutsch et al., 2010), our annual dark CO_2 fixation rate at 20 °C would account for ~13% of the forest soil gross carbon input, and thus be responsible for re-fixing a substantial amount (13%) of respired CO_2 into SOC. However, using the temperature corrected rates that more closely reflect the Hainich forest conditions (8 °C), this amounts to 5.6% of Hainich forest soil CO_2 emissions annually (Fig. 6). This is similar in range to those reported by Spohn et al. (2019), of up to 4% for temperate forest soil, and those of Miltner et al. (2005), of 3–5% of net respiration rate in agricultural soil. Based on our findings, we created a conceptual illustration of dark CO_2 fixation in the Hainich forest soil (Fig. 6). Here, photosynthetic CO_2 fixation promotes litter production. The latter can enter the SOC pool without passing through the microbial biomass (MB) pool (Trumbore, 2009) or can be decomposed by heterotrophs in the MB pool. During decomposition, respiration releases CO_2 into the soil air and a fraction diffuses out into the atmosphere. We predicted that 5.6% of respired CO_2 in the soil air is fixed by microbial biomass (autotrophs and heterotrophs) at a rate dependent on the CO_2 concentration and the MBC content.

Recycling of respired carbon will change the isotope signatures of SOC (Ehleringer et al., 2000). Soil pore space CO_2, mostly derived from root respiration (Rastogi et al., 2002), is usually more enriched in ^{13}C (by around 4‰) than SOC at corresponding depths due to restricted diffusion of the heavy $^{13}CO_2$ (Cerling et al., 1991). As a result, dark CO_2 fixation could provide a mechanism for higher $\delta^{13}C$ carbon to be incorporated directly into MBC and SOC in deep soils. This process has also been proposed as a cause for the commonly observed increase in ^{13}C signatures of SOC with depth (Šantrůčková et al., 2018).

Scaling up to a global temperate forest area of 10.4 million km^2 (Tyrrell et al., 2012), the rate of dark CO_2 fixation using temperature corrected rates measured from the Hainich forest soils at 2% CO_2 as reference, can be estimated as 0.26 ± 0.07 Pg C yr^{-1} to a depth of 1 m. This corresponds to 2.3% of the global anthropogenic carbon emissions in 2018 (~11.5 ± 0.9 Pg C; Friedlingstein et al., 2019) respectively. Based on the >7000 ppm increase in soil CO_2 upon a 200 ppm increase in atmospheric CO_2 concentration reported by Bernhardt et al. (2006), we further evaluated the effect of increased atmospheric CO_2 on the estimated annual dark CO_2 fixation rates. The 120 ppm increase in atmospheric CO_2 since 1750 would result in an increase of soil CO_2 by 0.42% (4200 ppm). Based on the 120% increase in fixation rates we observed when going from 2% to 10% CO_2, dark CO_2 fixation rates could currently be 6.3% higher than they were pre-industrially. Therefore, due to the rise of atmospheric CO_2, dark CO_2 fixation by the modern soil microbial community now fixes ~0.01 Pg C per year to 1 m depth more than it did in 1750. However, considering that the relationship between CO_2 concentration and fixation rate might depend on environmental conditions and the microbial community present, and that the geochemical conditions of all temperate forest soils globally was not accounted for, these values should be taken as back-of-the-envelope estimates with some degree of uncertainty.

Our results indicate that dark CO_2 fixation by microbial biomass is an important component of soil carbon fluxes and that the microbial biomass carbon pool likely represents a relatively dynamic pool of soil carbon that can respond to global environmental change on decadal to centurial timescales and thereby moderate the large stores of carbon found even in deep soils.

5. Conclusions

We estimated an average CO_2 fixation rate of 25 ± 7.2 g C m^{-2} yr^{-1} to a depth of 1 m for Hainich forest soil. Without this process, Hainich forest soil CO_2 emissions would be ~5.6% higher. Mitigation of soil CO_2 emissions by re-fixing a part of respired CO_2 will alter carbon isotope signatures across the soil profile. Although our global extrapolated rate at 0.26 ± 0.07 Pg C yr^{-1} is limited to temperate forests soils, it should be noted that other biomes may also contribute significantly to this process on a global scale. In addition, autotrophs constituted a small proportion of the community and showed a constant relative abundance with depth with no correlation with CO_2 fixation rates, while heterotrophs were the dominant groups. Although we cannot evaluate the proportion of carbon derived from both autotrophic and heterotrophic CO_2 fixation, heterotrophs appear to be the key mediators of this process, with the capacity to respond to increased pore space CO_2 concentrations with a 2 to 3-fold increase of the fixation rates. Our findings indicate that mostly heterotrophs are responsible for dark CO_2 fixation and that microbial biomass and CO_2 concentration are the main parameters affecting CO_2 fixation rates across the soil depth and may thus serve as a proxy to estimate dark CO_2 fixation rate in other temperate forest soils.

Declaration of competing interest

The authors declare that they have no known competing financial interests or personal relationships that could have appeared to influence the work reported in this paper.

Acknowledgements

This study was jointly supported by the Max Planck Institute for Biogeochemistry Jena (MPI-BGC), the International Max Planck Research School for Global Biogeochemical Cycles Jena (IMPRS-gBGC), Deutscher Akademischer Austauschdienst (DAAD) and the Collaborative Research Centre 1076 AquaDiva (CRC AquaDiva), Germany. We acknowledge the contributions of Marco Pöhlmann, Jens Wurlitzer, and Stefan Riedel for soil sampling and incubation set-ups. Further, indebted gratitude goes to Martin Nowak for his invaluable suggestions, Iris Kuhlmann for her support in carrying out CFE extractions and the routine measurements and analytical departments of the Max-Planck Institute for Biogeochemistry, Jena.

Appendix A. Supplementary data

Supplementary data to this article can be found online at https://doi.org/10.1016/j.soilbio.2020.107950.

References

Ahrens, B., Braakhekke, M.C., Guggenberger, G., Schrumpf, M., Reichstein, M., 2015. Contribution of sorption, DOC transport and microbial interactions to the ^{14}C age of a soil organic carbon profile: insights from a calibrated process model. Soil Biology and Biochemistry 88, 390–402.

Alfreider, A., Vogt, C., Hoffmann, D., Babel, W., 2003. Diversity of ribulose-1,5-bisphosphate carboxylase/oxygenase large-subunit genes from groundwater and aquifer microorganisms. Microbial Ecology 45, 317–328.

Alfreider, A., Schirmer, M., Vogt, C., 2012. Diversity and expression of different forms of RuBisCO genes in polluted groundwater under different redox conditions. FEMS Microbiology Ecology 79, 649–660.

Alfreider, A., Grimus, V., Luger, M., Ekblad, A., Salcher, M.M., Summerer, M., 2018. Autotrophic carbon fixation strategies used by nitrifying prokaryotes in freshwater lakes. FEMS Microbiology Ecology 94, 1–12.

Allen, A.S., Andrews, J.A., Finzi, A.C., Matamala, R., Richter, D.D., Schlesinger, W.H., 2000. Effects of free-air CO_2 enrichment (FACE) on belowground processes in a Pinus taeda forest. Ecological Applications 10, 437–448. https://doi.org/10.2307/2641105.

Alonso-Sáez, L., Galand, P.E., Casamayor, E.O., Pedrós-Alió, C., Bertilsson, S., 2010. High bicarbonate assimilation in the dark by Arctic bacteria. The ISME Journal 4, 1581–1590.

Amundson, R.G., Davidson, E.A., 1990. Carbon dioxide and nitrogenous gases in the soil atmosphere. Journal of Geochemical Exploration 38, 13–41. https://doi.org/10.1016/0375-6742(90)90091-N.

Andrews, J.A., Schlesinger, W.H., 2001. Soil CO_2 dynamics, acidification, and chemical weathering in a temperate forest with experimental CO_2 enrichment. Global Biogeochemical Cycles 15, 149–162.

Barbera, P., Kozlov, A.M., Czech, L., Morel, B., Darriba, D., Flouri, T., Stamatakis, A., 2019. EPA-ng: massively parallel evolutionary placement of genetic sequences. Systematic Biology 68, 365–369.

Bar-Even, A., Noor, E., Milo, R., 2012. A survey of carbon fixation pathways through a quantitative lens. Journal of Experimental Botany 63, 2325–2342.

Berg, I.A., Kockelkorn, D., Ramos-Vera, W.H., Say, R.F., Zarzycki, J., Hügler, M., Alber, B.E., Fuchs, G., 2010. Autotrophic carbon fixation in archaea. Nature Reviews Microbiology 8, 447–460. https://doi.org/10.1038/nrmicro2365.

Berg, I.A., 2011. Ecological aspects of the distribution of different autotrophic CO_2 fixation pathways. Applied and Environmental Microbiology 77, 1925–1936.

Bernhardt, E.S., Barber, J.J., Pippen, J.S., Taneva, L., Andrews, J.A., Schlesinger, W.H., 2006. Long-term effects of free air CO_2 enrichment (FACE) on soil respiration. Biogeochemistry 77, 91–116. https://doi.org/10.1007/s10533-005-1062-0.

Beulig, F., Heuer, V.B., Akob, D.M., Viehweger, B., Elvert, M., Herrmann, M., Hinrichs, K. U., Küsel, K., 2014. Carbon flow from volcanic CO_2 into soil microbial communities of a wetland mofette. The ISME Journal 9, 746–759. https://doi.org/10.1038/ismej.2014.148.

Beulig, F., Urich, T., Nowak, M., Trumbore, S.E., Gleixner, G., Gilfillan, G.D., Fjelland, K. E., Küsel, K., 2016. Altered carbon turnover processes and microbiomes in soils under long-term extremely high CO_2 exposure. Nature Microbiology 1, 1–9.

Blagodatskaya, E., Blagodatsky, S., Dorodnikov, M., Kuzyakov, Y., 2010. Elevated atmospheric CO_2 increases microbial growth rates in soil: results of three CO_2 enrichment experiments. Global Change Biology 16, 836–848. https://doi.org/10.1111/j.1365-2486.2009.02006.x.

Brand, W.A., Assonov, S.S., Coplen, T.B., 2010. Correction for the ^{17}O interference in $\delta(^{13}C)$ measurements when analyzing CO_2 with stable isotope mass spectrometry (IUPAC Technical Report). Pure and Applied Chemistry 82, 1719–1733. https://doi.org/10.1351/PAC-REP-09-01-05.

Brenzinger, K., Kujala, K., Horn, M.A., Moser, G., Guillet, C., Kammann, C., Müller, C., Braker, G., 2017. Soil conditions rather than long-term exposure to elevated CO_2 affect soil microbial communities associated with N-cycling. Frontiers in Microbiology 8, 1–14.

Brock, T.D., Madigan, M.T., Martinko, J.P., Parker, J., 2003. Brock Biology of Microorganisms, tenth ed. Prentice Hall, Upper Saddle River, New Jersey, pp. 565–575.

Cerling, T.E., Solomon, D.K., Quade, J., Bowman, J.R., 1991. On the isotopic composition of carbon in soil carbon dioxide. Geochimica et Cosmochimica Acta 55, 3403–3405.

Coplen, T.B., Brand, W.A., Gehre, M., Gröning, M., Meijer, H.A.J., Toman, B., Verkouteren, R.M., 2006. New guidelines for ^{13}C measurements. Analytical Chemistry 78, 2439–2441.

Cuellar-Bermudez, S.P., Romero-Ogawa, M.A., Vannela, R., Lai, Y.J.S., Rittmann, B.E., Parra-Saldivar, R., 2015. Effects of light intensity and carbon dioxide on lipids and fatty acids produced by *Synechocystis sp.* PCC6803 during continuous flow. Algal Research 12, 10–16. https://doi.org/10.1016/j.algal.2015.07.018.

Czech, L., Stamatakis, A., 2019. Scalable methods for analyzing and visualizing phylogenetic placement of metagenomic samples. PloS One 14, 1–50. https://doi.org/10.1371/journal.pone.0217050.

Daims, H., Brühl, A., Amann, R., Schleifer, K.-H., Wagner, M., 1999. The domain-specific probe EUB338 is insufficient for the detection of all bacteria: development and evaluation of a more comprehensive probe set. Systematic & Applied Microbiology 22, 434–444.

Dalal, R.C., 1998. Soil microbial biomass - what do the numbers really mean? Australian Journal of Experimental Agriculture 38, 649–665.

Domke, G.M., Perry, C.H., Walters, B.F., Woodall, C.W., Russell, M.B., Smith, J.E., 2016. Estimating litter carbon stocks on forest land in the United States. The Science of the Total Environment 557–558, 469–478.

Douglas, G.M., Maffei, V.J., Zaneveld, J., Yurgel, S.N., Brown, J.R., Taylor, C.M., Huttenhower, C., Langille, M.G.I., 2019. PICRUSt2: an Improved and Extensible Approach for Metagenome Inference, p. 672295. https://doi.org/10.1101/672295. BioRxiv.

Dukunde, A., Schneider, D., Schmidt, M., Veldkamp, E., Daniel, R., 2019. Tree species shape soil bacterial community structure and function in temperate deciduous forests. Frontiers in Microbiology 10, 1–17. https://doi.org/10.3389/fmicb.2019.01519.

Dunbar, J., Eichorst, S.A., Gallegos-Graves, L.V., Silva, S., Xie, G., Hengartner, N.W., Evans, R.D., Hungate, B.A., Jackson, R.B., Megonigal, J.P., Schadt, C.W., Vilgalys, R., Zak, D.R., Kuske, C.R., 2012. Common bacterial responses in six ecosystems exposed to 10 years of elevated atmospheric carbon dioxide. Environmental Microbiology 14, 1145–1158.

Ehleringer, J.R., Buchmann, N., Flanagan, L.B., 2000. Carbon isotope ratios in belowground carbon cycle processes. Ecological Applications 10, 412–422.

Eloka-Eboka, A.C., Inambao, F.L., 2017. Effects of CO_2 sequestration on lipid and biomass productivity in microalgal biomass production. Applied Energy 195, 1100–1111. https://doi.org/10.1016/j.apenergy.2017.03.071.

Erb, T.J., 2011. Carboxylases in natural and synthetic microbial pathways. Applied and Environmental Microbiology 77, 8466–8477.

Fransson, P., Andersson, A., Norström, S., Bylund, D., Bent, E., 2016. Ectomycorrhizal exudates and pre-exposure to elevated CO_2 affects soil bacterial growth and community structure. Fungal Ecology 20, 211–224.

Friedlingstein, P., Jones, M.W., O'Sullivan, M., Andrew, R.M., Hauck, J., Peters, G.P., Peters, W., Pongratz, J., Sitch, S., Le Quéré, C., DBakker, O.C.E., Canadell1, J.G., Ciais, P., Jackson, R.B., Anthoni, P., Barbero, L., Bastos, A., Bastrikov, V., Becker, M., Bopp, L., Buitenhuis, E., Chandra, N., Chevallier, F., Chini, L.P., Currie, K.I., Feely, R. A., Gehlen, M., Gilfillan, D., Gkritzalis, T., Goll, D.S., Gruber, N., Gutekunst, S., Harris, I., Haverd, V., Houghton, R.A., Hurtt, G., Ilyina, T., Jain, A.K., Joetzjer, E., Kaplan, J.O., Kato, E., Goldewijk, K.K., Korsbakken, J.I., Landschützer, P., Lauvset, S. K., Lefèvre, N., Lenton, A., Lienert, S., Lombardozzi, D., Marland, G., McGuire, P.C., Melton, J.R., Metzl, N., Munro, D.R., Nabel, J.E.M.S., Nakaoka, S.I., Neill, C., Omar, A.M., Ono, T., Peregon, A., Pierrot, D., Poulter, B., Rehder, G., Resplandy, L., Robertson, E., Rödenbeck, C., Séférian, R., Schwinger, J., Smith, N., Tans, P.P., Tian, H., Tilbrook, B., Tubiello, F.N., Van Der Werf, G.R., Wiltshire, A.J., Zaehle, S., 2019. Global carbon budget 2019. Earth System Science Data 11, 1783–1838. https://doi.org/10.5194/essd-11-1783-2019.

Ge, T., Wu, X., Liu, Q., Zhu, Z., Yuan, H., Wang, W., Whiteley, A.S., Wu, J., 2016. Effect of simulated tillage on microbial autotrophic CO_2 fixation in paddy and upland soils. Scientific Reports 6, 1–9.

Goodale, C.L., Apps, M.J., Birdsey, R.A., Field, C.B., Heath, L.S., Houghton, R.A., Jenkins, J.C., Kohlmaier, G.H., Kurz, W., Liu, S., Nabuurs, G.J., Nilsson, S., Shvidenko, A.Z., 2002. Forest carbon sinks in the northern hemisphere. Ecological Applications 12, 891–899.

Grüneberg, E., Ziche, D., Wellbrock, N., 2014. Organic carbon stocks and sequestration rates of forest soils in Germany. Global Change Biology 20, 2644–2662. https://doi.org/10.1111/gcb.12558.

Hart, K.M., Kulakova, A.N., Allen, C.C.R., Simpson, A.J., Oppenheimer, S.F., Masoom, H., Courtier-Murias, D., Soong, R., Kulakov, L.A., Flanagan, P.V., Murphy, B.T., Kelleher, B.P., 2013. Tracking the fate of microbially sequestered carbon dioxide in soil organic matter. Environmental Science and Technology 47, 5128–5137.

Herrmann, M., Hädrich, A., Küsel, K., 2012. Predominance of thaumarchaeal ammonia oxidizer abundance and transcriptional activity in an acidic fen. Environmental Microbiology 14, 3013–3025.

Herrmann, M., Rusznyák, A., Akob, D.M., Schulze, I., Opitz, S., Totsche, K.U., Küsel, K., 2015. Large fractions of CO_2-fixing microorganisms in pristine limestone aquifers appear to be involved in the oxidation of reduced sulfur and nitrogen compounds. Applied and Environmental Microbiology 81, 2384–2394.

Hicks Pries, C.E., Castanha, C., Porras, R., Phillips, C., Torn, M.S., 2018. Response to Comment on "The whole-soil carbon flux in response to warming.". Science 359, 1420–1423. https://doi.org/10.1126/science.aao0457.

Hungate, B.A., Holland, E.A., Jackson, R.B., Chapin, F.S., Mooney, H.A., Field, C.B., 1997. The fate of carbon in grasslands under carbon dioxide enrichment. Nature 388, 576–579.

Hügler, M., Sievert, S.M., 2011. Beyond the Calvin cycle: autotrophic carbon fixation in the ocean. Annual Review of Marine Science 3, 261–289.

IUSS Working Group WRB, 2015. World reference base for soil resources 2014, updated 2015 International soil classification system for naming soils and creating legends for soil maps. World Soil Resources Reports 106. https://doi.org/10.1017/S0014479706394902.

Jobbágy, E.G., Jackson, R.B., 2000. The vertical distribution of soil organic carbon and its relation to climate and vegetation. Ecological Applications 10, 423–436.

Joergensen, R.G., Mueller, T., 1996. The fumigation-extraction method to estimate soil microbial biomass: calibration of the kEN value. Soil Biology and Biochemistry 28, 25–31. https://doi.org/10.1016/0038-0717(95)00101-8.

Jorgensen, B.B., Nelson, D.C., 2004. Sulfide oxidation in marine sediments: geochemistry meets microbiology. Special Papers - Geological Society of America 379, 63–81. https://doi.org/10.1130/0-8137-2379-5.63.

Jones, R.M., Goordial, J.M., Orcutt, B.N., 2018. Low energy subsurface environments as extraterrestrial analogs. Frontiers in Microbiology 9, 1–18.

Kaiser, K., Wemheuer, B., Korolkow, V., Wemheuer, F., Nacke, H., Schöning, I., Schrumpf, M., Daniel, R., 2016. Driving forces of soil bacterial community structure, diversity, and function in temperate grasslands and forests. Scientific Reports 6, 1–12.

Kappler, U., Nouwens, A.S., 2013. Metabolic adaptation and trophic strategies of soil bacteria-C1-metabolism and sulfur chemolithotrophy in Starkeya novella. Frontiers in Microbiology 4, 1–12. https://doi.org/10.3389/fmicb.2013.00304.

Klindworth, A., Pruesse, E., Schweer, T., Peplies, J., Quast, C., Horn, M., Glöckner, F.O., 2013. Evaluation of general 16S ribosomal RNA gene PCR primers for classical and next-generation sequencing-based diversity studies. Nucleic Acids Research 41, 1–11.
Knohl, A., Schulze, E.D., Kolle, O., Buchmann, N., 2003. Large carbon uptake by an unmanaged 250-year-old deciduous forest in Central Germany. Agricultural and Forest Meteorology 118, 151–167. https://doi.org/10.1016/S0168-1923(03)00115-1.
Kravchenko, I.K., Tikhonova, E.N., Ulanova, R.V., Menko, E.V., Sukhacheva, M.V., 2019. Effect of temperature on litter decomposition, soil microbial community structure and biomass in a mixed-wood forest in European Russia. Current Science 116, 765–772.
Krebs, H.A., 1941. Carbon dioxide assimilation in heterotrophic organisms. Nature (London) 147, 560–563.
Kutsch, W.L., Persson, T., Schrumpf, M., Moyano, F.E., Mund, M., Andersson, S., Schulze, E.D., 2010. Heterotrophic soil respiration and soil carbon dynamics in the deciduous Hainich forest obtained by three approaches. Biogeochemistry 100, 167–183.
Lengeler, J.W., Drews, G., Schlegel, H.G., 1999. Biology of Prokaryotes, first ed. Blackwell Science, Oxford, p. 166.
Li, B., Li, Z., Sun, X., Wang, Q., Xiao, E., Sun, W., 2018. DNA-SIP reveals the diversity of chemolithoautotrophic bacteria inhabiting three different soil types in typical karst rocky desertification ecosystems in Southwest China. Microbial Ecology 76, 976–990.
Lipsewers, Y.A., 2017. Role of Chemolithoautotrophic Microorganisms Involved in Nitrogen and Sulfur Cycling in Coastal Marine Sediments. Doctoral dissertation. Utrecht University, Utrecht, The Netherlands. https://dspace.library.uu.nl/handle/1874/357552.
Liu, Z., Sun, Y., Zhang, Y., Feng, W., Lai, Z., Fa, K., Qin, S., 2018. Metagenomic and ^{13}C tracing evidence for autotrophic atmospheric carbon absorption in a semiarid desert. Soil Biology and Biochemistry 125, 156–166.
Lladó, S., López-Mondéjar, R., Baldrian, P., 2017. Forest soil bacteria: diversity, involvement in ecosystem processes, and response to global change. Microbiology and Molecular Biology Reviews 81, 1–27. https://doi.org/10.1128/MMBR.00063-16.
Long, X., Chen, C., Xu, Z., Oren, R., He, J.Z., 2012. Abundance and community structure of ammonia-oxidizing bacteria and archaea in a temperate forest ecosystem under ten-years elevated CO_2. Soil Biology and Biochemistry 46, 163–171.
Lorenz, K., Lal, R., 2009. Carbon Sequestration in Forest Ecosystems. Springer, Dordrecht Heidelberg London New York, pp. 159–194.
Lorenz, K., Lal, R., Shipitalo, M.J., 2011. Stabilized soil organic carbon pools in subsoils under forest are potential sinks for atmospheric CO_2. Forest Science 57, 19–25.
López-Mondéjar, R., Voříšková, J., Větrovský, T., Baldrian, P., 2015. The bacterial community inhabiting temperate deciduous forests is vertically stratified and undergoes seasonal dynamics. Soil Biology and Biochemistry 87, 43–50.
Loy, A., Lehner, A., Lee, N., Adamczyk, J., Meier, H., Ernst, J., Schleifer, K.H., Wagner, M., 2002. Oligonucleotide microarray for 16S rRNA gene-based detection of all recognized lineages of sulfate-reducing prokaryotes in the environment. Applied and Environmental Microbiology 68, 5064–5081.
Lu, X., Fan, J., Yan, Y., Wang, X., 2013. Responses of soil CO_2 fluxes to short-term experimental warming in alpine steppe ecosystem, Northern Tibet. PloS One 8, 2–9. https://doi.org/10.1371/journal.pone.0059054.
Lynn, T.M., Ge, T., Yuan, H., Wei, X., Wu, X., Xiao, K., Kumaresan, D., Yu, S.S., Wu, J., Whiteley, A.S., 2017. Soil carbon-fixation rates and associated bacterial diversity and abundance in three natural ecosystems. Microbial Ecology 73, 645–657.
Malhi, Y., Baldocchi, D.D., Jarvis, P.G., 1999. The carbon balance of tropical, temperate and boreal forests. Plant, Cell and Environment 22, 715–740.
Meier, I.C., Pritchard, S.G., Brzostek, E.R., Mccormack, M.L., Phillips, R.P., 2015. The rhizosphere and hyphosphere differ in their impacts on carbon and nitrogen cycling in forests exposed to elevated CO_2. New Phytologist 205, 1164–1174.
Meija, J., Coplen, T.B., Berglund, M., Brand, W.A., De Bievre, P., Gröning, M., Holden, N. E., Irrgeher, J., Loss, R.D., Walczyk, T., Prohaska, T., 2016. Atomic weights of the elements 2013 (IUPAC technical report). Pure and Applied Chemistry 88, 265–291.
Merlin, C., Mcateer, S., Coulson, A., 2003. Why is carbonic anhydrase essential to *Escherichia coli*. Journal of Bacteriology 185, 6415–6424. https://doi.org/10.1128/JB.185.21.6415.
Miao, R., Ma, J., Liu, Yinzhan, Liu, Yanchun, Yang, Z., Guo, M., 2019. Variability of aboveground litter inputs alters soil carbon and nitrogen in a coniferous-broadleaf mixed forest of Central China. Forests 10, 1–12. https://doi.org/10.3390/f10020188.
Miltner, A., Richnow, H.H., Kopinke, F.D., Kästner, M., 2004. Assimilation of CO_2 by soil microorganisms and transformation into soil organic matter. Organic Geochemistry 35, 1015–1024.
Miltner, A., Kopinke, F.D., Kindler, R., Selesi, D., Hartmann, A., Kästner, M., 2005. Non-phototrophic CO_2 fixation by soil microorganisms. Plant and Soil 269, 193–203.
Mobley, M.L., Lajtha, K., Kramer, M.G., Bacon, A.R., Heine, P.R., Richter, D.D., 2015. Surficial gains and subsoil losses of soil carbon and nitrogen during secondary forest development. Global Change Biology 21, 986–996. https://doi.org/10.1111/gcb.12715.
Moyano, F.E., Kutsch, W.L., Rebmann, C., 2008. Soil respiration fluxes in relation to photosynthetic activity in broad-leaf and needle-leaf forest stands. Agricultural and Forest Meteorology 148, 135–143. https://doi.org/10.1016/j.agrformet.2007.09.006.
Mölder, A., Bernhardt-Römermann, M., Schmidt, W., 2006. Forest ecosystem research in Hainich National Park (Thuringia): first results on flora and vegetation in stands with contrasting tree species diversity. Waldoekologie Online 3, 83–99.
Nel, J.A., Cramer, M.D., 2019. Soil microbial anaplerotic CO_2 fixation in temperate soils. Geoderma 335, 170–178.
Niederberger, T.D., Sohm, J.A., Gunderson, T., Tirindelli, J., Capone, D.G., Carpenter, E. J., Cary, S.C., 2015. Carbon-fixation rates and associated microbial communities residing in arid and ephemerally wet antarctic dry valley soils. Frontiers in Microbiology 6, 1–9.
Nowak, M.E., Beulig, F., Von Fischer, J., Muhr, J., Küsel, K., Trumbore, S.E., 2015. Autotrophic fixation of geogenic CO_2 by microorganisms contributes to soil organic matter formation and alters isotope signatures in a wetland mofette. Biogeosciences 12, 7169–7183.
Oh, N.H., Kim, H.S., Richter, D.D., 2005. What regulates soil CO_2 concentrations? A modeling approach to CO_2 diffusion in deep soil profiles. Environmental Engineering Science 22, 38–45.
Oren, A., 2014. The family, *Xanthobacteraceae*. In: Rosenberg, E., DeLong, E.F., Lory, S., Stackebrandt, E., Thompson, F. (Eds.), The Prokaryote. Springer, Berlin Heidelberg, pp. 709–726.
Pendall, E., Leavitt, S.W., Brooks, T., Kimball, B.A., Pinter, P.J., Wall, G.W., LaMorte, R. L., Wechsung, G., Wechsung, F., Adamsen, F., Matthias, A.D., Thompson, T.L., 2001. Elevated CO_2 stimulates soil respiration in a FACE wheat field. Basic and Applied Ecology 2, 193–201.
Rastogi, M., Singh, S., Pathak, H., 2002. Emission of carbon dioxide from soil. Current Science 82, 510–517.
Richter, D.D., Markewitz, D., 1995. How deep is soil? BioScience 45, 600–609.
Rössner, H., Kuhnert-Finkernagel, R., Öhlinger, R., Beck, T., Baumgarten, A., Heilmann, B., 1996. Indirect estimation of microbial biomass. In: Schinner, F., Öhlinger, R., Kandeler, E., Margesin, R. (Eds.), Methods in Soil Biology. Springer, Berlin, Heidelberg, p. 47.
Šantrůčková, H., Bird, M.I., Elhottová, D., Novák, J., Picek, T., Šimek, M., Tykva, R., 2005. Heterotrophic fixation of CO_2 in soil. Microbial Ecology 49, 218–225.
Šantrůčková, H., Kotas, P., Bárta, J., Urich, T., Čapek, P., Palmtag, J., Eloy Alves, R.J., Biasi, C., Diáková, K., Gentsch, N., Gittel, A., Guggenberger, G., Hugelius, G., Lashchinsky, N., Martikainen, P.J., Mikutta, R., Schleper, C., Schnecker, J., Schwab, C., Shibistova, O., Wild, B., Richter, A., 2018. Significance of dark CO_2 fixation in arctic soils. Soil Biology and Biochemistry 119, 11–21.
Schleppi, P., Bucher-Wallin, I., Hagedorn, F., Körner, C., 2012. Increased nitrate availability in the soil of a mixed mature temperate forest subjected to elevated CO_2 concentration (canopy FACE). Global Change Biology 18, 757–768.
Schloss, P.D., Westcott, S.L., Ryabin, T., Hall, J.R., Hartmann, M., Hollister, E.B., Lesniewski, R.A., Oakley, B.B., Parks, D.H., Robinson, C.J., Sahl, J.W., Stres, B., Thallinger, G.G., Van Horn, D.J., Weber, C.F., 2009. Introducing mothur: open-source, platform-independent, community-supported software for describing and comparing microbial communities. Applied and Environmental Microbiology 75, 7537–7541. https://doi.org/10.1128/AEM.01541-09.
Schrumpf, M., Kaiser, K., Schulze, E.D., 2014. Soil organic carbon and total nitrogen gains in an old growth deciduous forest in Germany. PloS One 9, 1–8.
Scott, M.J., 1996. Human settlements in a changing climate: impacts and adaptation. In: Watson, R.T., Zinyowera, M.C., Moss, R.H. (Eds.), Climate Change: Impacts, Adaptation and Mitigation of Climate Change: Scientific-Technical Analyses. Contribution of Working Group II of the Intergovernmental Panel on Climate Change. Cambridge University Press, Cambridge, United Kingdom and New York, pp. 116–117.
Shimmel, S.M., 1987. Dark fixation of carbon dioxide in an agricultural soil. Soil Science 144, 20–23.
Spohn, M., Müller, K., Höschen, C., Mueller, C.W., Marhan, S., 2019. Dark microbial CO_2 fixation in temperate forest soils increases with CO_2 concentration. Global Change Biology 26, 1926–1935. https://doi.org/10.1111/gcb.14937.
Sun, Z., Chen, Y.F., Du, J., 2016. Elevated CO_2 improves lipid accumulation by increasing carbon metabolism in *Chlorella sorokiniana*. Plant Biotechnology Journal 14, 557–566. https://doi.org/10.1111/pbi.12398.
Trumbore, S., 2009. Radiocarbon and soil carbon dynamics. Annual Review of Earth and Planetary Sciences 37, 47–66. https://doi.org/10.1146/annurev.earth.36.031207.124300.
Tyrrell, M.L., Ross, J., Kelty, M., 2012. Carbon dynamics in the temperate forest. In: Ashton, M.S., Tyrrell, M.L., Spalding, D., Gentry, B. (Eds.), Managing Forest Carbon in a Changing Climate. Springer, Dordrecht, The Netherlands, pp. 77–107.
Vance, E.D., Brookes, P.C., Jenkinson, D.S., 1987. An extraction method for measuring soil microbial biomass carbon. Soil Biology and Biochemistry 19, 703–707.
Werner, R.A., Brand, W.A., 2001. Referencing strategies and techniques in stable isotope ratio analysis. Rapid Communications in Mass Spectrometry 15, 501–519. https://doi.org/10.1002/rcm.258.
Whitehead, D., 2011. Forests as carbon sinks - benefits and consequences. Tree Physiology 31, 893–902.
Wu, X., Ge, T., Yuan, H., Li, B., Zhu, H., Zhou, P., Sui, F., O'Donnell, A.G., Wu, J., 2014. Changes in bacterial CO_2 fixation with depth in agricultural soils. Applied Microbiology and Biotechnology 98, 2309–2319.
Wu, X., Ge, T., Wang, W., Yuan, H., Wegner, C.E., Zhu, Z., Whiteley, A.S., Wu, J., 2015. Cropping systems modulate the rate and magnitude of soil microbial autotrophic CO_2 fixation in soil. Frontiers in Microbiology 6, 1–10. https://doi.org/10.3389/fmicb.2015.00379.
Xiao, H., Li, Z., Chang, X., Deng, L., Nie, X., Liu, C., Liu, L., Jiang, J., Chen, J., Wang, D., 2018. Microbial CO_2 assimilation is not limited by the decrease in autotrophic bacterial abundance and diversity in eroded watershed. Biology and Fertility of Soils 54, 595–605.
Yuan, H., Ge, T., Chen, C., O'Donnell, A.G., Wu, J., 2012. Significant role for microbial autotrophy in the sequestration of soil carbon. Applied and Environmental Microbiology 78, 2328–2336.
Zhao, Y., Liu, P., Rui, J., Cheng, L., Wang, Q., Liu, X., Yuan, Q., 2020. Dark carbon fixation and chemolithotrophic microbial community in surface sediments of the cascade reservoirs, Southwest China. The Science of the Total Environment 698, 1–9.

Rates of dark CO_2 fixation are driven by microbial biomass in a temperate forest soil

Supplementary Information

Rachael Akinyede[a,b], Martin Taubert[a], Marion Schrumpf[b], Susan Trumbore[b], Kirsten Küsel[a,c]

[a]Aquatic Geomicrobiology, Institute of Biodiversity, Friedrich Schiller University Jena, Dornburger Str. 159, 07743 Jena, Germany

[b]Department for Biogeochemical Processes, Max Planck Institute for Biogeochemistry, Hans-Knöll Str. 10, 07745 Jena, Germany

[c]German Centre for Integrative Biodiversity Research (iDiv) Halle-Jena-Leipzig, Deutscher Platz 5, 04103 Leipzig, Germany

Correspondence: Kirsten Küsel, Friedrich Schiller University Jena, Dornburger Str. 159, 07743 Jena, Germany. Email: kirsten.kuesel@uni-jena.de

Materials and Methods

Radiocarbon measurements

To measure the radiocarbon content of soil samples, accelerator mass spectrometry (AMS) with a 3-MV Tandetron ion accelerator (HVEE, Amersfoort, Netherlands) was used (Steinhof et al., 2004). Subsamples of soil containing 1 mg of carbon were combusted quantitatively and the developed CO_2 was catalytically reduced to graphite at 625 °C by H_2 reduction. Radiocarbon data are reported as $\Delta^{14}C$, which is the ‰ deviation of the $^{14}C/^{12}C$ ratio from the international oxalic acid universal standard (ox1). The $\Delta^{14}C$ value of the sample was corrected for mass-dependent isotope fractionation to a common value of -25‰ (Mook and van der Plicht, 1999). The $\Delta^{14}C$ values of the standards were also corrected appropriately for radioactive decay between 1950 and the year "*y*" of the measurement (Nowak et al., 2015; Trumbore, 2009). As expected, the measured bulk ^{14}C values decreased significantly with depth from 11.80 ± 12.06 ‰ at the top 12 cm to -371.97 ± 29.10 ‰ at the bottom depth (p = 4.34 x 10^{-8}) (Table S1). This observed decrease in radiocarbon signal with depth is a common feature in most soils, due to the radioactive decay of ^{14}C to ^{14}N, and reflects the mean time elapsed since the C in SOC was originally fixed from the atmosphere(Nowak et al., 2015; Trumbore, 2009).

$$\Delta^{14}C = \left[\frac{\frac{^{14}C}{^{12}C} sample - 25}{0.95 \frac{^{14}C}{^{12}C} ox1 - 19 \times exp^{\left(y - \frac{1950}{8267}\right)}} \right] \times 1000$$

Results

Supplementary figures and tables

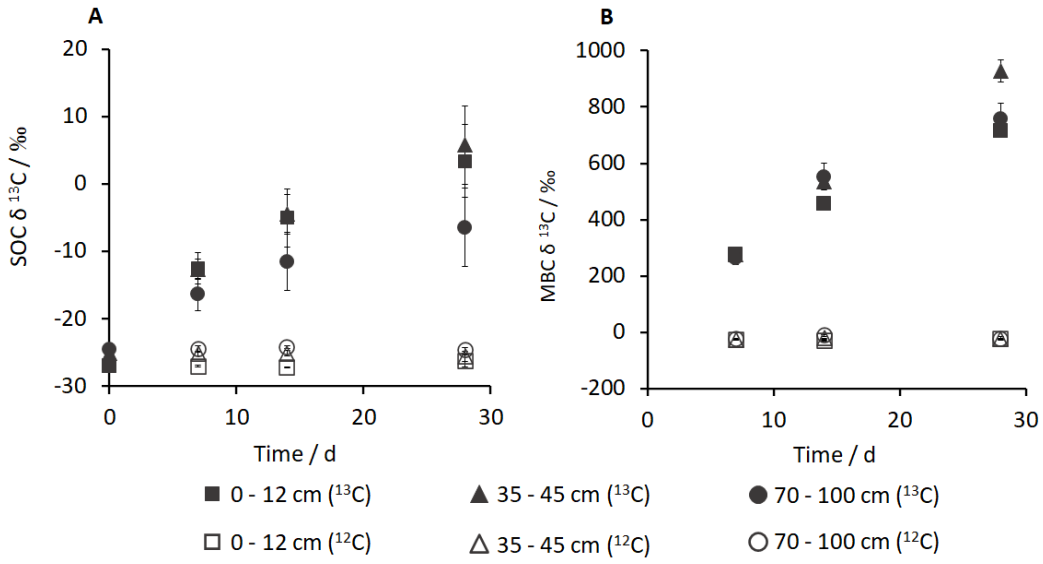

Figure S1: $\delta^{13}C$ signals of SOC and MBC in microcosms throughout incubation time. Shown are (A) ^{13}C signal in SOC (B) ^{13}C signal in MBC after 7, 14, and 28 days of incubation with 2% CO_2. Incubations with ^{12}C labelled CO_2 are denoted with empty symbols and incubations with ^{13}C labelled CO_2 are denoted with filled symbols. Day 0 reflects natural abundant values of SOC measured from bulk soil. Error bars indicate standard deviation of three replicate incubations and are shown only where larger than symbols.

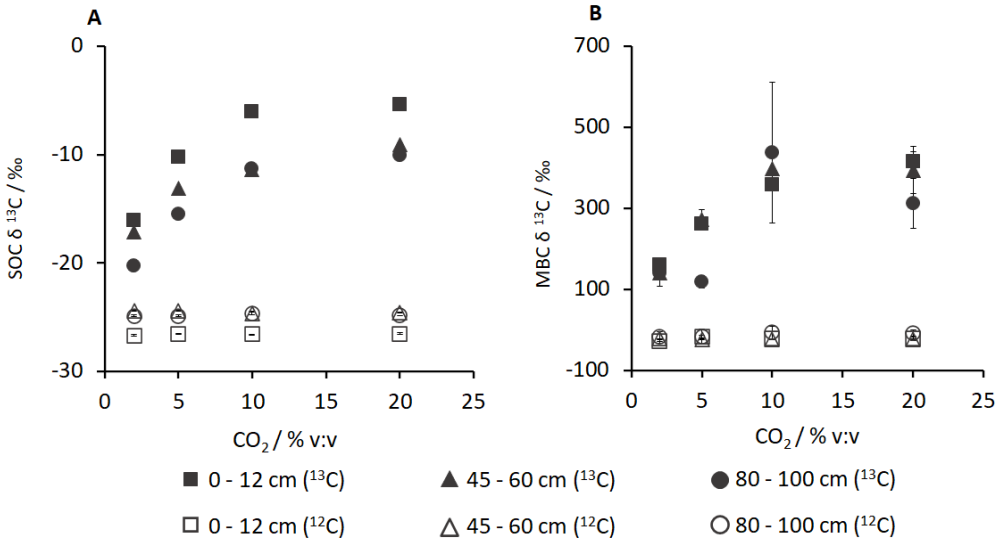

40

41 ***Figure S2: $\delta^{13}C$ signals of SOC and MBC in microcosms with different CO_2 concentrations in***
42 ***soil microcosms.*** Shown are (A) $\delta^{13}C$ signal in SOC and (B) $\delta^{13}C$ signal in MBC at 2%, 5%,
43 10% and 20%. CO_2 concentration expressed as % v:v in microcosm headspace. Filled symbols
44 depict incubations with $^{12}CO_2$ and empty symbols depict incubations with $^{13}CO_2$. Error bars
45 indicate standard deviation of three replicate incubations and are shown only where larger than
46 symbols.

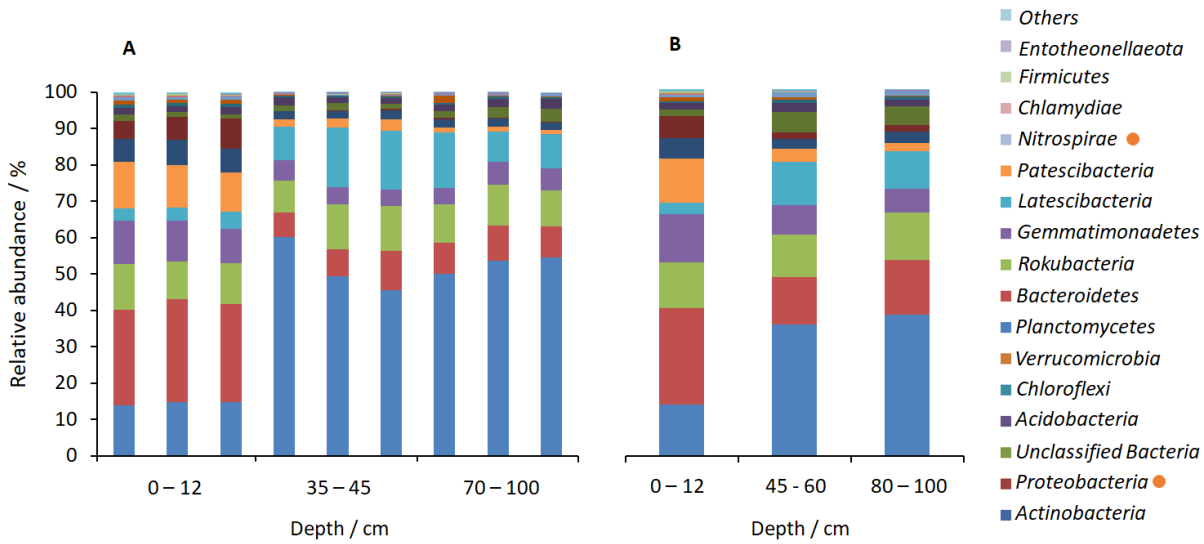

47

Figure S3: Composition of bacterial community (phylum level) in the Hainich forest soil. Shown are the relative abundance of assigned sequences of the bulk soil samples across depths for the August (A) and November (B) sampling campaign. Taxonomic assignments is based on the SILVA database implemented on the MOTHUR sequence analysis pipeline. Data represent three replicates cores per depth for the August sampling campaign and the mean of two sample replicates for the November sampling campaign. Bacteria Phyla containing the most abundant chemolithoautotrophic groups found are denoted by orange filled circles.

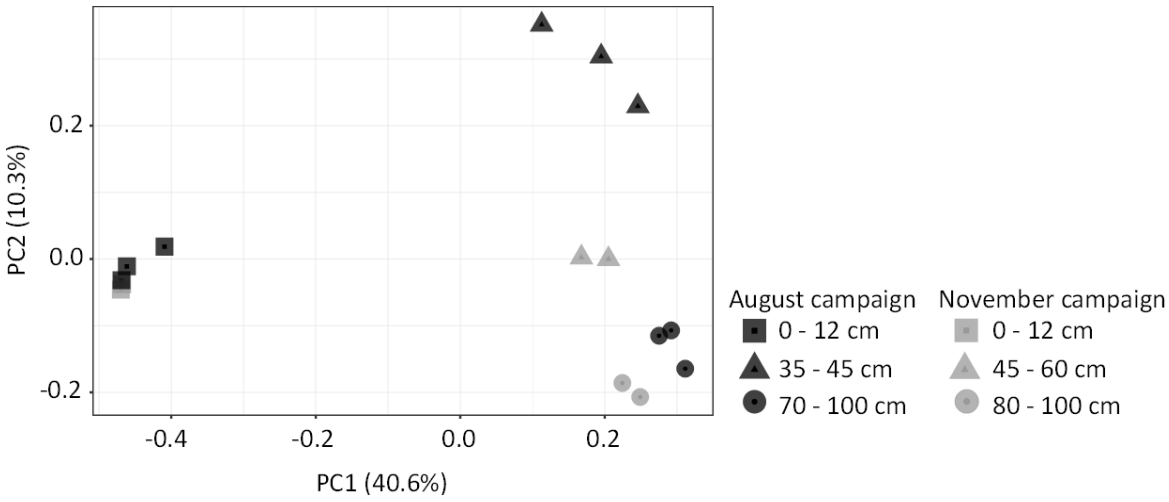

Figure S4: PCoA of Hainich forest soil bacterial community structure from August and November sampling campaigns. Plot based on OTU level analysis of 16S rRNA gene amplicons generated by Illumina Miseq sequencing. Shown are five independent data points per depth for both the August and November campaign and represented by three replicate soil cores from the August campaign (dark gray symbols) and two replicate soil samples from a single soil core from the November campaign (light gray symbols). Soil bacterial community composition shows significant change with depth for the August sampling campaign only (R^2 = 0.59, P = 0.004, PERMANOVA). This is caused largely by a distinct community in the top 12 cm soil layer (R^2 =

65 0.44, $P = 0.011$). The bacterial community in the two lower soil layers, 35 – 45 cm and

66 70 – 100 cm did not differ significantly from one another ($R^2 = 0.35$, $P = 0.10$).

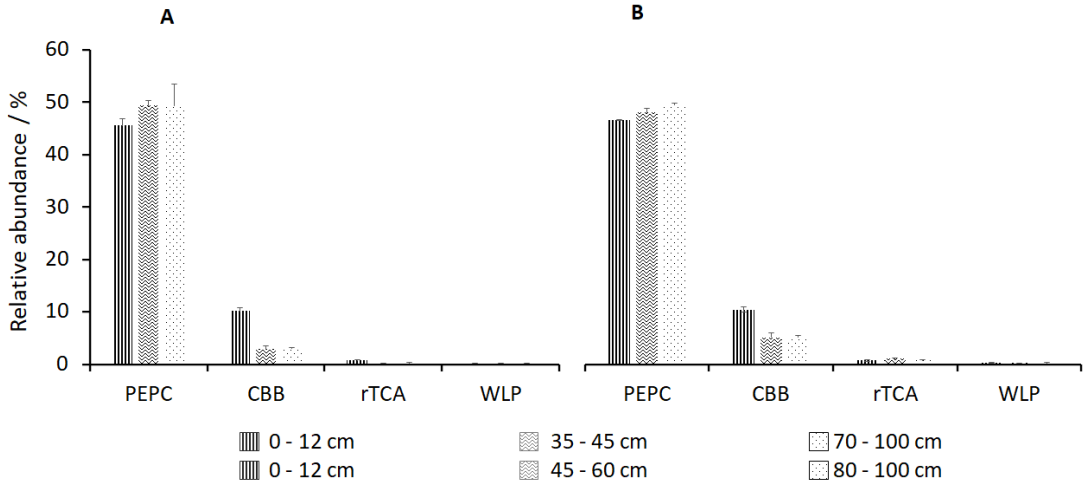

67

68 ***Figure S5: Predicted abundance of carboxylase genes involved in dark CO_2 fixation.*** Shown

69 are the relative abundance of key enzymes involved in dark CO_2 fixation predicted by PICRUSt2

70 analysis of bacterial 16S rRNA gene amplicon sequence data. Specific key enzymes are

71 combined for the Calvin Benson Basham pathway (CBB), reverse tricarboxylic acid pathway

72 (rTCA), and the Wood–Ljungdahl pathway (WLP). Phosphoenolpyruvate carboxylase (PEPC)

73 gene is reported for heterotrophic CO_2 fixation by anaplerotic reactions.

74

75

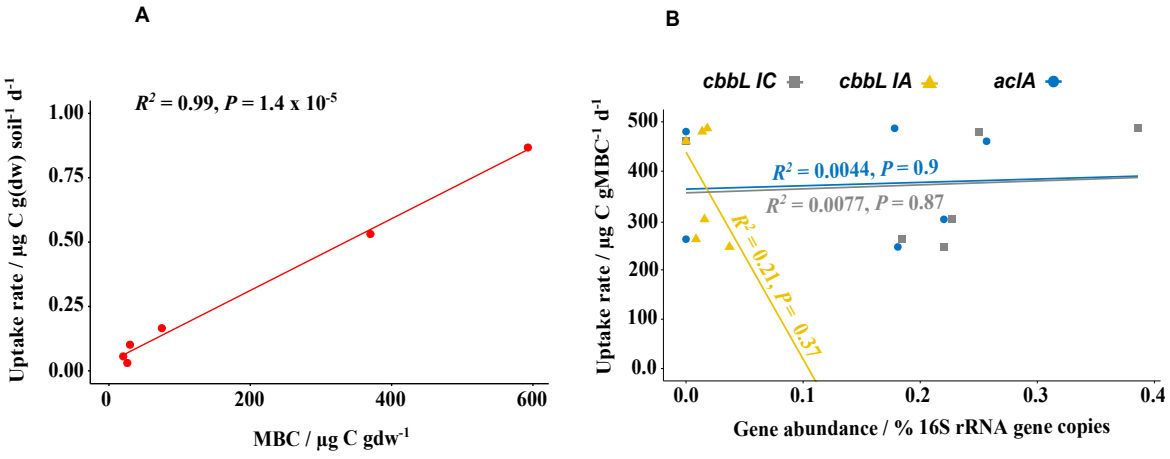

Figure S6: Correlation of microbial biomass and autotroph abundance (based on RuBisCO and aclA gene variants) with measured uptake rates. Shown are correlations between the measured dark CO_2 fixation rates per gram dry weight (dw) of soil and microbial biomass carbon (MBC) (A) and between dark CO_2 fixation per gram microbial biomass and the abundance of marker genes encoding for RuBisCO (*cbbL IA, cbbLIC)* and rTCA cycle (*aclA*) (B) measured in the August and November campaigns across 0 – 100 cm depth profile.

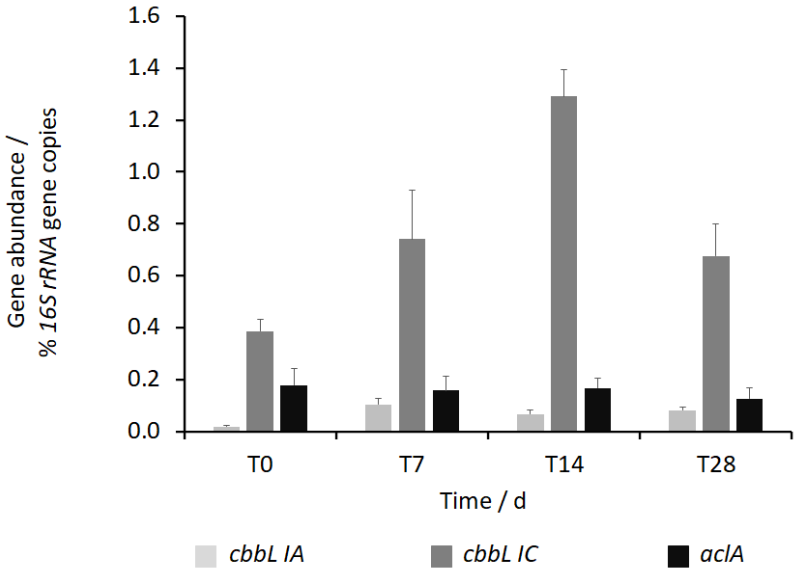

Figure S7: Abundance of RuBisCO (cbbL IA, cbbL IC) and ATP citrate lyase (aclA) marker gene copies at 2% v:v CO_2 in soil. Shown are the *cbbL IA, cbbL IC*, and *aclA* gene abundance based on qPCR from the August sampling campaign at the top 0 – 12 cm depth from days 7, 14, and 28 incubation with 2% v:v CO_2 expressed as % of 16S rRNA gene copies. The scale on the y-axis is logarithmic. Error bars indicate standard deviation of three replicate incubations.

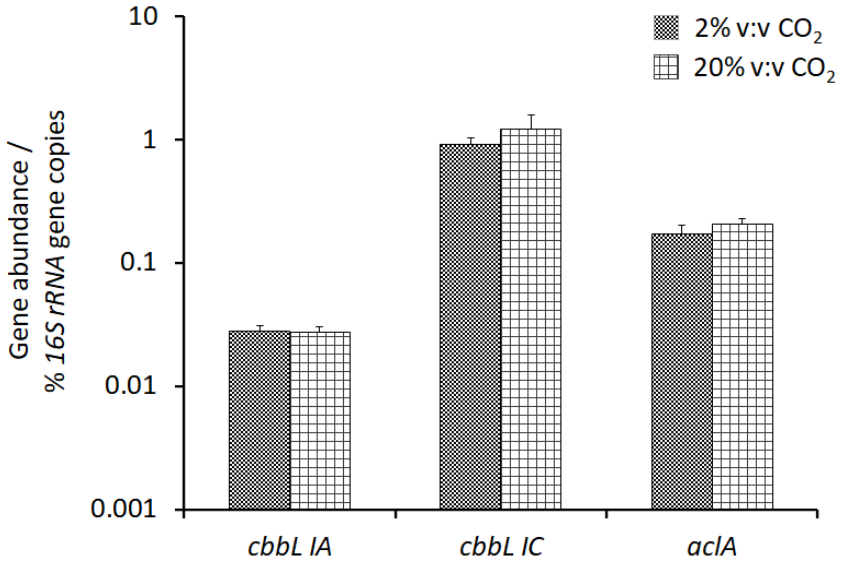

Figure S8: Abundance of RuBisCO (cbbL IA, cbbL IC) and ATP citrate lyase (aclA) marker gene copies at 2% and 20% CO_2 in soil. Shown are the *cbbL* IA, *cbbL* IC, and *aclA* gene abundance based on qPCR analysis from the November sampling campaign at the top 0 – 12 cm depth after 7 days incubation with 2% v:v and 20% v:v CO_2 expressed as % of 16S rRNA gene copies. The scale on the y-axis is logarithmic. Error bars indicate standard deviation of three replicate incubations.

Table S1: Geochemical properties of soil cores obtained from the Hainich national park from two sampling campaigns. Soil pH, moisture content, soil organic carbon (SOC), carbon/nitrogen (C/N) ratio, microbial biomass carbon (MBC), and natural abundance ^{13}C and ^{14}C signatures of SOC, reported for 3 depths definitions for the August and November campaign. Reported average values for the August campaign are individual and mean values of three replicate cores. $\delta^{13}C$ and $\Delta^{14}C$ values of the individual cores from the August campaign represent the mean of analytical replicates. All reported values for the November campaign represent the mean of three sample replicates. "nd" denotes samples where no measurement was determined.

Sampling Campaign / Soil cores		Depth (cm)	pH	Moisture Content (%)	SOC (%)	C/N	MBC (µgCgd w^{-1})	MBC $\delta^{13}C$ (‰)	$\delta^{13}C$ (‰)	$\Delta^{14}C$ (‰)
August	1	0 - 12	4.1	24.60	4.4	11	nd	nd	-26.60 ± 0.02	-3.20 ± 4.40
		35 - 45	5.7	18.62	1.03	9	nd	nd	-25.10 ± 0.05	-309.40 ± 3.30
		70 - 100	7.0	21.76	0.72	7	nd	nd	-25.00 ± 0.07	-309.40 ± 3.90
	2	0 - 12	4.6	25.87	4.18	12	nd	nd	-27.10 ± 0.02	30.30 ± 3.80
		35 - 45	5.7	20.64	0.7	8	nd	nd	-24.64 ± 0.21	-292.20 ± 20
		70 - 100	7.0	21.32	0.31	8	nd	nd	-25.16 ± 0.21	-367.00 ± 3.60
	3	0 - 12	5.3	30.72	2.89	13	nd	nd	-27.20 ± 0.05	26.00 ± 3.80
		35 - 45	5.4	23.79	0.85	9	nd	nd	-25.55 ± 0.01	-147.10 ± 3.20
		70 - 100	7.0	25.26	0.44	8	nd	nd	-23.50 ± 0.40	-388.40 ± 3.80
	Average	0 - 12	4.7 ± 0.60	27.06 ± 3.23	3.82 ± 0.82	12 ± 0.93	nd	nd	-26.97 ± 0.32	17.7 ± 18.23
		35 - 45	5.6 ± 0.14	21.02 ± 2.61	0.86 ± 0.17	9 ± 0.82	nd	nd	-25.10 ± 0.45	-249.57 ± 89.15
		70 - 100	6.98 ± 0.02	22.78 ± 2.16	0.49 ± 0.21	8 ± 0.61	nd	nd	-24.55 ± 0.92	-354.93 ± 40.86
November		0 - 12	4.24 ± 0.06	30.3	3.10 ± 0.01	11 ± 0.03	369.97 ± 20.46	-25.29 ± 0.77	-26.53 ± 0.07	4.8 ± 1.56
		45 - 60	5.88 ± 0.01	25.0	0.86 ± 0.003	9 ± 0.06	29.74 ± 10.49	-19.11 ± 5.49	-24.34 ± 0.05	-397.4 ± 1.13
		80 - 100	7.04 ± 0.04	23.5	0.39 ± 0.01	7 ± 0.22	20.15 ± 6.25	-22.74 ± 2.98	-24.84 ± 0.02	-382.85 ± 9.12

nd: not determined

Table S2: Quantification of 16S rRNA, cbbL IA, cbbL IC, cbbM and aclA marker genes.

Shown are the gene copies for the 16S rRNA, *cbbL* IA, *cbbL* IC, *cbbM* and *aclA* marker genes expressed per gram dry weight of soil and their ratios (*cbbL* IA, *cbbL* IC, and *aclA* only) expressed as a % of 16S rRNA gene copies in bulk soil for both the August and November sampling campaign. Data is based on quantitative PCR analysis. Errors indicate standard deviation of the mean of three replicate soil cores samples for the August campaign and two replicate soil samples from a homogenized soil core for the November campaign. BDL denotes gene copies below detection limit.

Sampling campaign	Depth (cm)	16S rRNA	*cbbL*_IA	*cbbL*_IC	*cbbM*	*aclA*	*cbbL* IA / 16S rRNA (%)	*cbbL* IC / 16S rRNA (%)	*aclA* / 16S rRNA (%)
August	0 - 12 cm	$2.41 \times 10^{10} \pm 8.31 \times 10^{9}$	$4.20 \times 10^{6} \pm 5.24 \times 10^{5}$	$9.13 \times 10^{7} \pm 2.31 \times 10^{7}$	BDL	$4.05 \times 10^{7} \pm 8.22 \times 10^{6}$	0.018 ± 0.003	0.386 ± 0.048	0.178 ± 0.063
	35 - 45 cm	$3.16 \times 10^{8} \pm 3.53 \times 10^{8}$	$9.70 \times 10^{4} \pm 9.18 \times 10^{3}$	$1.06 \times 10^{6} \pm 3.58 \times 10^{5}$	BDL	BDL	0.014 ± 0.002	0.250 ± 0.100	BDL
	70 - 100 cm	$1.06 \times 10^{8} \pm 4.58 \times 10^{6}$	BDL	BDL	BDL	BDL	BDL	BDL	BDL
November	0 - 12 cm	$1.48 \times 10^{10} \pm 2.14 \times 10^{9}$	$2.31 \times 10^{6} \pm 2.57 \times 10^{4}$	$3.36 \times 10^{7} \pm 4.44 \times 10^{6}$	BDL	$2.81 \times 10^{7} \pm 1.97 \times 10^{6}$	0.016 ± 0.0021	0.227 ± 0.003	0.220 ± 0.016
	45 - 60 cm	$9.67 \times 10^{8} \pm 1.50 \times 10^{8}$	$8.44 \times 10^{4} \pm 3.56 \times 10^{4}$	$1.77 \times 10^{6} \pm 6.89 \times 10^{4}$	BDL	$2.46 \times 10^{6} \pm 1.49 \times 10^{5}$	0.009 ± 0.0023	0.185 ± 0.022	0.257 ± 0.024
	80 - 100 cm	$2.69 \times 10^{8} \pm 6.88 \times 10^{7}$	$1.01 \times 10^{5} \pm 3.17 \times 10^{4}$	$6.98 \times 10^{5} \pm 7.44 \times 10^{4}$	BDL	$4.91 \times 10^{5} \pm 1.61 \times 10^{5}$	0.037 ± 0.0023	0.220 ± 0.022	0.181 ± 0.014

BDL: Below Detection Limit

117 ***Table S3: Primer specifications used for bacterial quantification and detection of CO_2 fixation***

118 ***pathways.***

Pathway / Function	Target gene	Primer name	Sequences (5' -3')	bp[1]	Ta[2]	References
CBB-cycle	RubisCO form IA	cbbL_IA_f	CGGCACSTGGACCACSGTSTGGAC	620	54	Alfreider et al., 2003
		cbbL_IA_r	GTARTCGTGCATGATGATRGG			
	RubisCO form IC	cbbL_IC_f	TGGTGCATCTGVCCGGCRTG	552	55	Alfreider et al., 2009, Alfreider et al., 2012
		cbbL_IC_r	GAACATCAAYTCKCAGCCCTT			
	RuBisCO form II	cbbM_f	GGCACCATCATCAAGCCCAAG	505	53	Alfreider et al., 2003
		cbbM_r	TCTTGCCGTAGCCCATGGTGC			
rTCA-cycle	ATP citrate lyase (*Nitrospira*)	q_aclA_Nit-f	TCSTTCGGCGTCATYACCAAG	320	56	Alfreider et al., 2018
		q_aclA_Nit-r	GCCSGCATGRCCGAAYTTCAT			
Phylogenetic identification	*16s rRNA*	Bac_ 341F	CCTACGGGNGGCWGCAG	444	55	Klindworth et al., 2012
		Bac_785R	GACTACHVGGGTATCTAATCC			
	16s rRNA qPCR	Bac_8_Fmod	AGAGTTTGATCMTGGCTCAG	510	52	Daims et al., 1999 Loy et al., 2002
		Bac_338_r				

119 1bp: size of primer product; 2Ta: Annealing temperature

120 **References**

121 Alfreider, A., Vogt, C., Hoffmann, D., Babel, W., 2003. Diversity of ribulose-1,5-bisphosphate
122 carboxylase/oxygenase large-subunit genes from groundwater and aquifer microorganisms.
123 Microbial Ecology 45, 317–328.
124 Alfreider, A., Vogt, C., Geiger-Kaiser, M., Psenner, R., 2009. Distribution and diversity of
125 autotrophic bacteria in groundwater systems based on the analysis of RubisCO genotypes.
126 Systematic and Applied Microbiology 32, 140–150. doi:10.1016/j.syapm.2008.11.005
127 Alfreider, A., Schirmer, M., Vogt, C., 2012. Diversity and expression of different forms of RuBisCO
128 genes in polluted groundwater under different redox conditions. FEMS Microbiology Ecology
129 79, 649–660.
130 Alfreider, A., Grimus, V., Luger, M., Ekblad, A., Salcher, M.M., Summerer, M., 2018. Autotrophic
131 carbon fixation strategies used by nitrifying prokaryotes in freshwater lakes. FEMS
132 Microbiology Ecology 94, 1–12.
133 Daims, H., Brühl, A., Amann, R., Schleifer, K.-H., Wagner, M., 1999. The domain-specific probe
134 EUB338 is insufficient for the detection of all bacteria: development and evaluation of a more
135 comprehensive probe set. Systemic and Applied Microbiology 22, 434–444.
136 Klindworth, A., Pruesse, E., Schweer, T., Peplies, J., Quast, C., Horn, M., Glöckner, F.O., 2013.
137 Evaluation of general 16S ribosomal RNA gene PCR primers for classical and next-generation
138 sequencing-based diversity studies. Nucleic Acids Research 41, 1–11.
139 Loy, A., Lehner, A., Lee, N., Adamczyk, J., Meier, H., Ernst, J., Schleifer, K.H., Wagner, M., 2002.
140 Oligonucleotide microarray for 16S rRNA gene-based detection of all recognized lineages of
141 sulfate-reducing prokaryotes in the environment. Applied and Environmental Microbiology 68,
142 5064–5081.
143 Mook, W. G.,Van der Plicht, J.,1999. Reporting C-14 activities and concentrations, Radiocarbon, 41,
144 227–239.

145 Nowak, M.E., Beulig, F., Von Fischer, J., Muhr, J., Küsel, K., Trumbore, S.E., 2015. Autotrophic
146 fixation of geogenic CO_2 by microorganisms contributes to soil organic matter formation and
147 alters isotope signatures in a wetland mofette. Biogeosciences 12, 7169–7183. doi:10.5194/bg-
148 12-7169-2015

149 Steinhof, A., Adamiec, G., Gleixner, G., van Klinken, G. J., and Wagner, T., 2004. The new C-14
150 analysis laboratory in Jena, Germany, Radiocarbon 46, 51–58.

151 Trumbore, S., 2009. Radiocarbon and soil carbon dynamics. Annual Review of Earth and Planetary
152 Sciences 37, 47–66. doi:10.1146/annurev.earth.36.031207.124300

3 Manuscript 2: Dark CO_2 fixation in temperate beech and pine forest soils

Authors: Akinyede, R., Taubert, M., Schrumpf, M., Trumbore, S., Küsel, K

Bibliographic information (if published or accepted for publication: Citation): Akinyede R., Taubert M., Schrumpf M., Trumbore S., Küsel K. 2022. Dark CO_2 fixation in temperate beech and pine forest soils. *Soil Biology & Biochemistry* 165, 108526. doi.org/10.1016/j.soilbio.2021.108526

The candidate is (Please tick the appropriate box.)

☐✓ First author, ☐ Co-first author, ☐ Corresponding author, ☐ Co-author.

Status (if not published; "submitted for publication", "in preparation".): Published

In this study, I, Akinyede, R Schrumpf, M and Küsel, K designed the concept and experiment. I conducted all soil sampling campaigns and laboratory experiments, performed all isotope measurements and molecular analysis, and analyzed all generated datasets, including the statistical modelling and figures. Taubert, M helped with experimental design, molecular analysis, data visualization, and discussion. He also edited the manuscript draft. Schrumpf, M., Trumbore, S., Küsel, K assisted with sampling design and editing the manuscript draft. The manuscript was written by me with contributions from all authors. My contributions are summarized as follows:

Authors' contributions (in %) to the given categories of the publication

Author	Conceptual	Data analysis	Experimental	Writing the manuscript	Provision of material
Akinyede, R	50	90	80	60	0
Taubert, M	10	10	0	15	0
Schrumpf, M	20	0	5	5	0
Trumbore, S	10	0	0	10	50
Küsel, K	10	0	0	10	50
Others	0	0	15	0	0
Total:	100%	100%	100%	100%	100%

_____ _____

Signature candidate Signature supervisor (member of the Faculty)

Supplementary data for this article can be found at the end of the research article.

Soil Biology and Biochemistry 165 (2022) 108526

Contents lists available at ScienceDirect

Soil Biology and Biochemistry

journal homepage: www.elsevier.com/locate/soilbio

Dark CO_2 fixation in temperate beech and pine forest soils

Rachael Akinyede [a,b], Martin Taubert [a], Marion Schrumpf [b], Susan Trumbore [b], Kirsten Küsel [a,c,*]

[a] Aquatic Geomicrobiology, Institute of Biodiversity, Friedrich Schiller University Jena, Dornburger Str. 159, 07743, Jena, Germany
[b] Department for Biogeochemical Processes, Max Planck Institute for Biogeochemistry, Hans-Knöll Str. 10, 07745, Jena, Germany
[c] German Centre for Integrative Biodiversity Research (iDiv) Halle-Jena-Leipzig, Puschstraße 4, 04103, Leipzig, Germany

ARTICLE INFO

Keywords:
Soil organic carbon
Microbial biomass carbon
$^{13}CO_2$ labelling
Anaplerotic reactions
Deciduous
Coniferous

ABSTRACT

Soils are the largest terrestrial organic carbon pool and the largest terrestrial source of atmospheric CO_2. Non-phototrophic CO_2 fixation by microbes re-fixes and recycles CO_2 respired in soils. Our previous study showed that in temperate deciduous forest soil profiles, rates of dark CO_2 fixation were proportional to microbial biomass, irrespective of soil depth. However, the amount and quality of organic matter entering different soil depths vary for different temperate forest types and these influence microbial communities with unknown consequences for CO_2 fixation rates. To test whether differences in the amount and quality of SOC caused by tree species affect dark CO_2 fixation rates with depth, we conducted a study using acidic soils from two forest plots from the Schorfheide-Chorin Exploratory, Germany. These soils, dominated by either beech (deciduous) or pine (coniferous) tree stands differ in their SOC content and quality. We traced the incorporation of 2% (v:v) ^{13}C–CO_2 label into microbial biomass and estimated the CO_2 fixation rates relative to microbial biomass carbon content (in μg C g MBC^{-1} d^{-1}) across the soil profiles. The rates of dark CO_2 fixation per g MBC were similar across the beech soil profiles, but significantly lower in the pine soils at the B2 and BC horizons, suggesting that while dark CO_2 fixation rates are linked to MBC in deciduous forest soils, other factors influence dark CO_2 fixation rates in coniferous forest soils. The pine subsoils had low SOC content and quality, with a microbial community enriched with heterotrophic fermenters like *Chloroflexi* that are predicted to have a lower potential for heterotrophic CO_2 fixation compared to the other dominant bacteria phyla. In contrast, the beech soil profiles, characterized by higher SOC inputs, featured higher fractions of copiotrophs like *Proteobacteria, Acidobacteria,* and *Actinobacteria* predicted to have high heterotrophic CO_2 fixation potential. We thus speculate that in contrast to the beech soils, lower SOC inputs in the pine subsoils affected the community composition, leading to lower CO_2 fixation rates. We further made comparisons to soils dominated by mixed deciduous trees and featuring a higher MBC and SOC content. Over this range of temperate forest soils, CO_2 fixation rates were highest in the mixed deciduous forest soils, with MBC and Shannon index (used as a proxy parameter for community composition) showing the strongest correlations with the varying CO_2 fixation rates. Our study suggests that predictions of dark CO_2 fixation rates need to consider tree-species specific or site-specific conditions, as these may alter root carbon inputs and affect microbial community composition and their metabolic CO_2 fixation potentials in soil.

1. Introduction

Soils are the largest terrestrial organic carbon pool on Earth (Batjes, 1992), storing around 1500 Pg C in the top 1 m depth (Jobbágy and Jackson, 2000). The microbial degradation of plant litter in soils releases CO_2 back into the atmosphere (Rastogi et al., 2002; Kravchenko et al., 2019). A portion of this CO_2, however, is re-fixed through dark CO_2 fixation in soil and thereby reduces the amount of CO_2 emitted from soils (Miltner et al., 2005; Šantrůčková et al., 2018). This process, the non-phototrophic assimilation of CO_2 by microbes, has been estimated to fix ~0.3 Pg C/yr, corresponding to 3–6% of annual soil CO_2 emissions in temperate forest soils (Spohn et al., 2019; Akinyede et al., 2020).

Dark CO_2 fixation is carried out by both chemolithoautotrophs and heterotrophs via various metabolic pathways. Chemolithoautotrophs fix CO_2 using one of the six known autotrophic pathways (Berg, 2011; Fuchs, 2011), with the Calvin Benson Bassham (CBB) pathway being the most important in soils (Tcherkez et al., 2006; Wu et al., 2014). This pathway depends on the activity of the key enzyme RuBisCO (ribulose-1,

* Corresponding author. Friedrich Schiller University Jena, Dornburger Str. 159, 07743, Jena, Germany.
E-mail address: kirsten.kuesel@uni-jena.de (K. Küsel).

https://doi.org/10.1016/j.soilbio.2021.108526
Received 29 September 2021; Received in revised form 13 December 2021; Accepted 14 December 2021
Available online 17 December 2021

5-bisphosphate carboxylase oxygenase). Of the different RuBisCO forms, only form I and form II variants are known to participate in bacterial autotrophy (Berg, 2011). Form I RuBisCO is common among obligate and facultative autotrophic bacteria, e.g., *Proteobacteria* (Tolli and King, 2005). Form II RuBisCO is found in facultative anaerobic bacteria like *Thiobacillus* spp. (Alfreider et al., 2003). The CBB pathway has a high energy cost (Bar-Even et al., 2012). Hence, alternative energy-efficient pathways, like the reductive citric acid cycle (rTCA) and the Wood Ljungdahl pathway (WLP), are employed by soil microbes (Beulig et al., 2016; Liu et al., 2018). Due to the demand for reduced inorganic compounds, temperature, and oxygen preferences (Hügler and Sievert, 2011), other known autotrophic pathways are less common in soils. Additionally, heterotrophic bacteria in soils also fix CO_2 (Akinyede et al., 2020; Šantrůčková et al., 2018) via carboxylation reactions in citric acid metabolism (Krebs, 1941; Erb, 2011).

Both chemolithoautotrophic and heterotrophic bacteria fixing CO_2 are ecologically and phylogenetically diverse (Berg, 2011; Hügler and Sievert, 2011; Saini et al., 2011; Braun et al., 2021), with different factors influencing their metabolism. Thus, various environmental factors are known to affect CO_2 fixation rates (Berg, 2011; Hügler and Sievert, 2011). In soils, extrinsic factors such as CO_2 concentration (Beulig et al., 2016; Spohn et al., 2019; Akinyede et al., 2020), water content, temperature (Nel and Cramer, 2019), soil organic carbon (SOC) (Miltner et al., 2005; Šantrůčková et al., 2018), and the availability of electron donors (Hart et al., 2013) have been linked to dark CO_2 fixation rates. In a recent study, dark CO_2 fixation rates correlated with microbial biomass, and this was independent of observed changes in the community structure with depth in a temperate deciduous forest soil (Akinyede et al., 2020). Additionally, in cropland soils, organic carbon content was described to best predict the variations in CO_2 fixation rates observed between eroding and depositional topsoils due to the potential effect of soil organic carbon (SOC) on the proportion of the autotrophic bacterial community (Xiao et al., 2018).

SOC is an important regulator of soil microbes (Dalal, 1998; Su et al., 2020), serving as the most important carbon source (Lladó et al., 2017). Thus, variations in the amount and quality of SOC correlate with microbial biomass (Cleveland and Liptzin, 2007; Fierer et al., 2009; Liddle et al., 2020). SOC composition and content is mainly influenced by tree species (Vesterdal et al., 2013; Guo et al., 2016), with root inputs suggested as the dominant source of SOC in temperate forests (Rasse et al., 2001, 2005). Differences in tree species lead to distinct patterns in depth distributions of SOC content and its decomposition rates (Vesterdal et al., 2008; Binkley and Giardina, 2014; Joly et al., 2017; Achilles et al., 2020). Shallower rooting depths of coniferous trees introduce the largest proportion of carbon inputs to the top 10 cm depth of soils. Thus, easily degradable rhizodeposits are mostly restricted to the topsoil (Finzi et al., 1998; Vesterdal et al., 2013; Achilles et al., 2020). Deciduous trees, however, have higher root biomass (Finér et al., 2007; Ostonen et al., 2007) and distribute more of the easily degradable root-derived carbon into deeper soil layers (15–30 cm) (Vesterdal et al., 2013; Cha et al., 2019). Furthermore, the degradability of SOC is lower in topsoils under coniferous than deciduous tree species (Don and Kalbitz, 2005; Cuss and Guéguen, 2013) due to a higher portion of complex carbon substrates like lignin as well as the higher C/N ratios of the originating aboveground litter (Vesterdal et al., 2008; Thieme et al., 2019). These differences in SOC vertical distribution and quality also affect bacterial community composition across soil depths (Hackl et al., 2005; Urbanová et al., 2015; Nacke et al., 2016). Here, we compare dark CO_2 fixation rates in acidic deciduous and coniferous soil profiles to test whether differences in soil organic matter inputs, quality, and their influence on microbial communities lead to differences in CO_2 fixation rates with depth.

We examined dark CO_2 fixation rates using soil plots in the Schorfheide-Chorin Biodiversity Exploratory, Germany, having a sandy texture and acidic pH (Fischer et al., 2010; Kaiser et al., 2016). Two soil plots differing in their dominant tree species (beech and pine) and soil characteristics were selected. The beech plot was reported to have 30% higher mineral SOC content and >40% higher root decomposition rates, as well as 30% lower mineral soil C/N ratios than the pine plot (Solly et al., 2013; Kaiser et al., 2016; Schöning et al., 2019), indicating a higher SOC input and quality in the beech compared to the pine plots (Bauhus and Khanna, 1999; Lai et al., 2016; Achilles et al., 2020). Based on these plots, this study aimed to test whether differences in the amount and quality of SOC caused by tree species will affect dark CO_2 fixation rates across soil profiles. We traced the incorporation of $^{13}CO_2$ label into microbial biomass carbon and soil organic matter in soils dominated by beech and pine trees down to 1 m depth and estimated the CO_2 fixation rates relative to microbial biomass carbon content (μg C g MBC^{-1} d^{-1}) and to soil dry weight (μg C g (dw) $soil^{-1}$ d^{-1}) across the soil profiles. Additionally, we analysed the soil microbial community structures and used open-source tools for predicting genomic potential of known CO_2 fixation pathways, and identified potential biogeochemical factors that may influence rates of dark CO_2 fixation in temperate forest soils.

2. Materials and methods

2.1. Site description and soil classification

The study sites (SEW 49: N52°56′32.6′′ E13°49′38.0′′ and SEW 17: N52°53′07.6′′ E13°53′28.3′′) are two plots (beech and pine respectively) located within the forested area of the Schorfheide-Chorin Exploratory, North-eastern Germany (3–140 m a.s.l.) (Fischer et al., 2010). The Schorfheide-Chorin Exploratory is a part of the German Biodiversity Exploratories established to investigate the relationships between land use, biodiversity changes, and ecosystem functioning in forests and grasslands of central Europe (Fischer et al., 2010; https://www.biodiversity-exploratories.de). While beech (*Fagus sylvatica.* L.), pine (*Pinus sylvestris* L.), and oak (*Quercus* spp. L.) can be dominant tree species of mature age class forests of the Schorfheide-Chorin region (Fischer et al., 2010; Kaiser et al., 2016), the two study plots investigated are each composed of only beech and pine trees. Each of the experimental plots has a size of 100 × 100 m, located ~8 km apart. Mean annual precipitation (MAP) at these sites ranges between 500 and 600 mm annually and mean annual air temperature (MAT) is between 8.0 and 8.5 °C (Fischer et al., 2010). Soils are generally characterized by a high sand content (89%) due to the dominance of glacio-fluvial or aeolian sand with glacial till as the main geological substrate, resulting in a young glacial landscape (Fischer et al., 2010; Kaiser et al., 2016). Soils are mostly acidic (pH < 5), have low moisture and SOC content (Kaiser et al., 2016, Table 1), and are classified as *Cambisols* (Fischer et al., 2010; IUSS Working Group WRB, 2015; Kaiser et al., 2016). Further description of the forest sites can be found in Fischer et al. (2010), Kaiser et al. (2016), Thieme et al. (2019), and the Biodiversity Exploratory website (https://www.biodiversity-exploratories.de).

The soils in our previous study were sampled from a mixed deciduous (mostly beech) forest in the Hainich region, also part of the German Biodiversity Exploratories, located in central Germany, having a higher MAP but similar MAT. These soils were higher in pH, clay content, SOC, and microbial biomass carbon content. Data from this previous study (Akinyede et al., 2020) are used here to compare with those from the two new sites in the Schorfheide-Chorin Exploratory.

2.2. Sampling design

Soil sampling was carried out on December 2, 2018 (beginning of the winter season). With the aid of a closed auger (84 mm in diameter) driven into the soil with a motor hammer (Cobra Combi, Atlas Copco AB, Nacka, Sweden), three replicate soil cores were sampled (individual cores: 1–2 m apart) from each of the two plots (beech and pine). All soil cores were taken ~2 m away from the base of the trees to avoid direct impact from stem flow and to prevent larger roots from impeding the soil

Table 1
Biogeochemical properties of bulk soil cores obtained from the beech and pine plots. Soil pH, moisture content, soil organic carbon (SOC), total nitrogen (TN), carbon/nitrogen (C/N) ratio, microbial biomass carbon (MBC), MBC/SOC ratio, natural abundance $\delta^{13}C$ of SOC and MBC, $\Delta^{14}C$ signatures of SOC, 16S rRNA gene copies, and Shannon index for the beech and pine soils. Values are the mean of 3 replicate soil cores taken during the sampling campaign.

Plot (Dominant tree species)	Depth (Horizon)	pH	Moisture (%)	SOC (%)	TN (%)	C/N ratio	MBC (μg C g dw^{-1})	MBC /SOC (%)	δ^{13}SOC (‰)	δ^{13}MBC (‰)	Δ^{14}C (‰)	16S rRNA (copies/g dw^{-1})	Shannon index (H′)
Beech	AB	3.54 ± 0.11	7.96 ± 0.44	1.54 ± 0.40	0.09 ± 0.01	15.60 ± 1.21	224.70 ± 48.87	1.47 ± 0.06	−27.19 ± 0.15	−24.65 ± 0.26	91.00 ± 29.39	$1.97 \times 10^{10} \pm 5.02 \times 10^{9}$	5.86 ± 0.05
	BC	3.74 ± 0.19	3.95 ± 0.60	0.40 ± 0.13	0.02 ± 0.009	17.19 ± 2.06	30.18 ± 9.22	0.76 ± 0.1	−26.52 ± 0.41	−23.55 ± 1.75	−66.67 ± 52.49	$2.94 \times 10^{9} \pm 1.42 \times 10^{9}$	5.82 ± 0.09
	C	3.57 ± 0.28	2.74 ± 1.04	0.2 ± 0.04	0.02 ± 0.003	12.19 ± 1.84	35.21 ± 7.84	1.83 ± 0.51	−26.26 ± 0.50	−23.60 ± 1.32	−103.33 ± 64.47	$9.57 \times 10^{8} \pm 2.96 \times 10^{8}$	5.82 ± 0.22
Pine	AB	3.16 ± 0.38	8.91 ± 2.76	2.33 ± 0.79	0.09 ± 0.03	24.34 ± 0.23	215.15 ± 63.35	0.94 ± 0.14	−27.19 ± 0.17	−24.03 ± 0.63	39.73 ± 18.42	$1.77 \times 10^{10} \pm 5.30 \times 10^{9}$	4.89 ± 0.04
	B2	4.30 ± 0.03	3.10 ± 1.64	0.57 ± 0.08	0.03 ± 0.004	20.81 ± 0.30	90.64 ± 16.98	1.58 ± 0.06	−25.90 ± 0.2	−25.71 ± 0.72	−85.23 ± 39.50	$2.67 \times 10^{9} \pm 7.37 \times 10^{8}$	5.23 ± 0.10
	BC	4.54 ± 0.05	1.30 ± 0.22	0.08 ± 0.01	BDL	BDL	44.48 ± 3.88	5.37 ± 0.91	−25.14 ± 0.07	−24.30 ± 0.45	−163.43 ± 77.57	$2.41 \times 10^{8} \pm 5.18 \times 10^{7}$	4.53 ± 0.15

BDL: Below Detection Limit.

coring process. To estimate soil compaction during the coring process, the length of the borehole and the extracted cores were measured and compared, and soil compaction was minor with ~7%. The organic layer was removed before coring, and sampling began from the mineral horizon. The soil cores were then cut into 3 segments according to the similarity of the horizon boundaries among the triplicate cores to obtain samples representing the AB horizon (0–15 cm), BC horizon (24–65 cm), and C horizon (57–100 cm) for beech plot, and the AB horizon (0–10 cm), B2 horizon (23–44 cm), and BC horizon (40–80 cm) for the pine plot. Afterwards, samples from the soil core segments of both plots were sieved using a 2 mm sieve to remove stones and roots prior to use for incubation experiments in soil microcosms. Fresh samples were also taken for later geochemical analysis and DNA extraction (stored in liquid nitrogen).

2.3. Geochemical parameters, $\delta^{13}C$ and radiocarbon ($\Delta^{14}C$) measurements

Total and inorganic carbon and nitrogen content, pH, and gravimetric water content of soil samples were determined as previously described (Akinyede et al., 2020). The ^{13}C signature of total organic carbon was analysed using an elemental analyser coupled to an isotope ratio mass spectrometer according to Akinyede et al. (2020). The ^{13}C isotope ratios were reported in the delta notation (δ) expressed as $\delta^{13}C$ values ($^{13}C/^{12}C$ ratios) in per mil (‰), in relation to the international reference material Vienna Pee Dee Belemnite (Coplen et al., 2006).

$$\delta^{13}C\left(‰\right) = \left(\frac{\frac{^{13}C}{^{12}C_{\text{sample}}}}{\frac{^{13}C}{^{12}C_{\text{reference}}}} - 1\right) \times 1000 \quad (1)$$

The radiocarbon content of the soil samples was measured by accelerator mass spectrometry (AMS) with a MICADAS system (Ionplus, Dietikon, Switzerland) using graphite preparation method described by Steinhof et al. (2017). As with the ^{13}C isotope ratios, radiocarbon values were reported as the ‰ deviation of the $^{14}C/^{12}C$ ratio from the international oxalic acid universal standard (ox1) in $\Delta^{14}C$. The $\Delta^{14}C$ value of the sample was then corrected appropriately as previously described (Mook and Van der Plicht, 1999; Trumbore, 2009).

$$\Delta^{14}C = \left[\frac{\frac{^{14}C}{^{12}C}_{sample,\ -25}}{0.95\frac{^{14}C}{^{12}C}_{OX1,\ -19} \times exp\left(\frac{(y-1950)}{8267}\right)}\right] \times 1000 \quad (2)$$

2.4. ^{13}C–CO_2 labelling experiment, determination of delta ^{13}C ratios in microbial biomass carbon (MBC), and mass-balance calculations of CO_2 fixation rates

As in our previous study (Akinyede et al., 2020), rates of dark CO_2 fixation were determined using ^{13}C–CO_2 labelling incubations. Triplicate incubations for each sieved soil sample (30 g wet weight) obtained from all three soil cores for both the beech and pine plots were set up in sterilized 100 mL serum bottles sealed with butyl rubber stoppers. The headspace of the serum bottles was flushed with synthetic air (75% N_2 and 25% O_2), adjusted to 2% (v/v) (~20,000 ppm of CO_2) ^{13}C–CO_2, and incubated statically for 7 days in the dark at room temperature (20 °C). At the same time, control incubations with 2% (v/v) unlabelled CO_2 (^{12}C–CO_2) were performed in triplicate. To maintain similar CO_2 and isotopic concentrations in the microcosms, the headspace of all microcosms was flushed with synthetic air and inoculated with 2% (v/v) ^{13}C–CO_2 thrice within the 7-day incubation period as described in Akinyede et al. (2020). Data from previous incubation studies conducted at the same sites (Schöning et al., 2013a) indicated that the amount of dilution of the isotope label in the 2 days between flushing events amounted to only a few ppm, and so we ignored this in our calculation of CO_2 fixation rates. At the end of the 7-day incubation period, soil incubations were sacrificed and soils from all incubations were subsampled and prepared for bulk ^{13}C and organic carbon analysis. The extraction of microbial biomass carbon (MBC) and ^{13}C was done using the chloroform fumigation extraction (CFE) method with 0.05 M K_2SO_4 (Nowak et al., 2015; Vance et al., 1987). The $\delta^{13}C$ ratios in the extracts were determined by isotope ratio mass spectrometry (IRMS) (Nowak et al., 2015; Akinyede et al., 2020). Portions of the soil samples were also stored at −80 °C for later DNA analysis.

To determine the microbial biomass carbon content for all labelled and unlabelled samples, the carbon concentration in the form of dissolved organic carbon was first determined in K_2SO_4 extracts in two fractions per sample: chloroform-fumigated and unfumigated fractions.

The MBC contents for both the labelled and unlabelled samples were calculated as the carbon released into 0.05 M K_2SO_4 solution after chloroform treatment of fumigated (C_{fum}) sample minus that released from unfumigated (C_{unfum}) samples, divided by a correction factor K_{EC} (of 0.45) that accounts for the extraction efficiency (Joergensen and Mueller, 1996):

$$MBC[mg] = \frac{[C_{fum} - C_{unfum}]}{K_{EC}} \quad (3)$$

The amount of ^{13}C label uptake, that is, the $\delta^{13}C$ in per mil (‰) of microbial biomass carbon (MBC) was derived by applying an isotope mass balance to ^{13}C signals measured for both the fumigated and unfumigated DOC (Spohn et al., 2019; Akinyede et al., 2020):

$$\delta^{13}C_{MB}\ (‰) = \left[\delta \frac{^{13}C_{fum} \times C_{fum} - \delta^{13}C_{unfum} \times C_{unfum}}{C_{fum} - C_{unfum}}\right] \quad (4)$$

Using the derived $\delta^{13}C$ (‰), the $^{13}C/^{12}C$ ratios for MBC was then calculated for all treatments (^{13}C labelled) and controls (^{13}C unlabelled/natural abundance) based on the $^{13}C/^{12}C$ ratio of the international V-PDB standard with 0.011180 (Werner and Brand, 2001) as follows:

$$\frac{^{13}C}{^{12}C} = \left[\frac{\delta^{13}C}{1000} + 1\right] \times 0.0111802 \quad (5)$$

Subsequently, the excess ^{13}C was derived, which is the increase in $^{13}C/^{12}C$ ratio between the ^{13}C labelled treatment and the unlabelled controls (^{13}C natural abundance level) normalized to the carbon content of the microbial biomass (MBC):

$$Excess\ ^{13}C\ [mg] = \frac{^{13}C}{^{12}C_{labelled}} \times MBC[mg] - \frac{^{13}C}{^{12}C_{unlabelled}} \times MBC[mg] \quad (6)$$

This was divided by the incubation time to derive the CO_2 fixation rates per gram of MBC (g MBC^{-1} d^{-1}) (Spohn et al., 2019; Akinyede et al., 2020).

For CO_2 fixation rates in the total soil pool, the $^{13}C/^{12}C$ ratio measured in the bulk soil for all treatments and controls was derived using the ^{13}C signals measured in the bulk soil and the $^{13}C/^{12}C$ ratio of the V-PDB standard as similarly described for $^{13}C/^{12}C$ ratio of MBC in equation (5). By taking the difference of the derived $^{13}C/^{12}C$ ratios between the labelled treatment (^{13}C labelled) and unlabelled controls (^{13}C unlabelled/natural abundance), each normalized to the soil carbon content, the excess ^{13}C (mg) fixed to the soil pool was obtained as described in equation (6). Subsequently, the CO_2 fixation rates per gram of soil dry weight (g (dw) $soil^{-1}$ d^{-1}) were calculated by dividing the excess ^{13}C in the soil pool by the incubation time (Akinyede et al., 2020).

2.5. DNA extraction, 16S rRNA gene sequencing, and PICRUSt2 analysis

DNA was extracted from 0.25 g of all bulk soil samples using the DNeasy PowerSoil DNA Kit (Qiangen, Hilden, Germany) and following the manufacturer's instructions. Prior to Illumina Miseq sequencing, DNA was amplified by Polymerase Chain Reaction (PCR) using forward (341F) and reverse (785R) primers targeting the V3 to V4 hypervariable regions (Klindworth et al., 2013). The following PCR conditions were used; initial denaturation at 95 °C for 45 min, followed by 27 cycles consisting of denaturation (94 °C for 45 s), annealing (55 °C for 45 s) and extension (72 °C for 45 s) and then a final extension step at 72 °C for 10 min. All samples were run on a 1% agarose gel to ensure all amplicons were ~500 bp in length as described in the NEBNext Ultra DNA library prep kit for Illumina (New England Biolabs, Hitchin, UK). Further details on the reagents used as well as library preparation process are found in the manufacturer's protocol. Subsequently, the prepared libraries were sequenced by Illumina Miseq (Illumina, Inc, San Diego, USA) (2 x 250 bp following our inhouse sequencing protocol). The raw sequence data were analysed using the MOTHUR (v.1.39) sequence pipeline (Schloss et al., 2009; http://www.mothur.org) and the MOTHUR MiSeq SOP as of September 9, 2019. After paired reads were combined, sequences were trimmed leaving only sequences with lengths between 360 bp and 500 bp. Sequences were aligned to the SILVA reference database v132 (Quast et al., 2013) after which all sequences with differences of four bases or less were pre-clustered with a 0.03 cut-off for the OTU assignment, and chimeras removed using Uchime and the GOLD reference database (Edgar et al., 2011). On MOTHUR, taxonomic classification against the SILVA database as well as OTU binning was performed, and alpha diversity index (Shannon) of bacteria community structure was also determined.

Functional potential for CO_2 fixation was predicted for all generated 16S rRNA sequences. The representative sequences from OTUs generated from MOTHUR were analysed using version 2 (v2.2.0 beta) of the PICRUSt (Phylogenetic Investigation of Communities by Reconstruction of Unobserved States) software package (Douglas et al., 2020). PICRUSt2 prediction combines the use of multiple high-throughput and open-source tools for predicting genomic potential based on environmentally sampled 16S rRNA gene sequences (Douglas et al., 2020). Functional prediction involves phylogenetic placement, hidden-state prediction, and gene abundance tabulation for each sample. Here, OTU sequences are taken as input, used as the basis of the functional predictions, and gene family and pathway abundances are produced as the output. Using HMMER (www.hmmer.org), de-gapped OTU sequences were aligned to a reference taxonomic tree containing 20,000 full 16S rRNA gene sequences from prokaryotic genomes obtained from the Integrated Microbial Genomes database. After this, EPA-ng (Evolutionary Placement Algorithm) and GAPPA tools were used to determine the best position of these placed OTUs in a reference phylogeny and to visualize phylogenetic placement data for the most likely OTU placement (Barbera et al., 2019; Czech and Stamatakis, 2019). This resulted in a phylogenetic tree containing both the reference genomes and the sampled OTUs. This was used to infer (based on the KEGG database) individual gene family, and gene copy numbers for each OTU. Using the derived KEGG Orthology (KO) numbers for different key genes involved in CO_2 fixation, the six known autotrophic pathways namely: the Calvin Benson Bassham (CBB) pathway, the reductive citric acid (rTCA) pathway, the Wood Ljungdahl (WLP) pathway, the 3-hydroxypropionate/malyl-CoA (3HP) cycle, the 3-hydroxypropionate/4-hydroxybutyrate (HP/HB) cycle, and the dicarboxylate/4-hydroxybutyrate (DC/HB) cycle were deduced. Genes targeting heterotrophs involved in CO_2 assimilation via anaplerotic carboxylation reactions in the TCA cycle as well as via the serine cycle were also predicted.

2.6. Quantification of the 16S rRNA, RuBisCO, and rTCA marker genes

Gene abundances of bacterial 16S rRNA were determined by quantitative PCR (qPCR) on the Mx3000P instrument (Agilent, C.A, U.S.A) using Maxima SYBR Green Mastermix (Agilent). Primer pair Bac 8Fmod and Bac 338R was used to target the 16S rRNA genes (Loy et al., 2002; Daims et al., 1999) using cycling conditions and standards described in (Herrmann et al., 2012). Based on the most prevalent pathways predicted by PICRUSt2: the CBB pathway, and the rTCA pathway, we also determined the abundance of functional genes belonging to these selected CO_2 fixation pathways by qPCR. To quantify genes for the CBB pathway, primer pairs F-cbbL IA/R-cbbL IA, F-cbbL IC/R-cbbL IC, F-cbbM/R-cbbM were used to target the RuBisCO marker genes, *cbbL* IA, *cbbL* IC (form I RuBisCO), *cbbM* (form II RuBisCO) respectively (Alfreider et al., 2003, 2012; Herrmann et al., 2015). For the rTCA pathway, primer pair F-g-acl-Nit/R-g-acl-Nit, targeting the alpha subunit of the ATP citrate lyase (*aclA*) gene (encoding the ATP citrate lyase enzyme) was used. This primer pair is specific for nitrite-oxidizing and complete ammonia-oxidizing (comammox) bacteria like *Nitrospira* (Alfreider et al., 2018). All genes were quantified employing cycling conditions and standards previously described in Akinyede et al. (2020). As no reliable standardized qPCR protocols and primer sets were

available to target key genes of the WLP pathway as well as the remaining known autotrophic and heterotrophic CO_2 fixation pathways, the presence of these pathways was based on PICRUSt2 predictions only.

2.7. Statistical analysis

Statistical analyses were conducted using the R environment (v.3.6.1) and RStudio (v1.1.463). The CO_2 fixation rates per gram of soil and per gram of MBC as well as all soil geochemical parameters were compared separately for the pine and beech soil plots across the three horizons using one-way ANOVA and Tukey's test. Comparisons between the beech and pine plots at corresponding depths were done by Student's *t*-test. When comparing the CO_2 fixation rates over a broader range of deciduous and coniferous forest plots across the profiles, all datasets generated in this study were combined with those obtained from the Hainich forest (Akinyede et al., 2020) and differences were analysed also using ANOVA and Tukey's test. To analyse the contributions of soil abiotic and biotic properties to the variations in dark CO_2 fixation rates among the combined forest plots, multiple stepwise regression model was performed. As we combined two different datasets in the regression model, the possibility for random effect resulting from the different sampling periods was tested and found to be insignificant. Even when tested as a fixed effect (predictor) in the full and final model, the sampling period explained less than 3% ($P < 0.001$) of the variation and this is likely due to stronger variations in other measured parameters. Thus, we ignored sampling period in the full and final model. Categorical variables like depth and vegetation correlated strongly with some of the measured parameters. Since the effect of depth and vegetation on soil microbial communities is due to changes in abiotic properties, we aimed to test for direct causal relationships. As a result, depth and vegetation were excluded from the regression model. When accounting for the total community composition, the use of individual bacteria taxon was avoided due to the risk of overfitting the regression model. Thus, in the absence of a definite parameter, Shannon diversity index was used as a proxy variable for the variations in the total community between the forest plots, though we do not infer that Shannon index per se is a predictor of CO_2 fixation rates. Overall, seven abiotic (SOC, MBC, MBC/SOC ratio, $\Delta^{14}C$, water content, pH, C/N ratio) and three biotic (autotroph bacterial abundance (*cbbL* IC), PEPC abundance, and Shannon index) parameters were selected as predictors in the full model. All predictors were checked for multicollinearity, leaving only variables with variance inflation factors (VIFs) of <10 (Hair et al., 2014). Thus, a total of seven predictors (MBC, $\Delta^{14}C$, pH, C/N ratio, autotroph bacterial abundance (*cbbL* IC), PEPC abundance, and Shannon index) were used in the final model.

To determine the variations in the bacterial community between the beech and pine plots, beta diversity was measured by performing Principal Coordinate Analysis (PCoA) based on Bray-Curtis dissimilarity using the vegan package in R (Oksanen et al., 2008). Thus, the bacterial community from all soil samples in the beech and pine plots were clustered based on their similarity/dissimilarity. The significance of the factors accounting for OTU variances shown in the PCoA plot both between the two study plots and across depth was determined by performing Permutational Multivariant Analysis of Variance (PERMANOVA) using "adonis" functions with 999 permutations. The effects of measured geochemical parameters and CO_2 fixation rates on the variation in the bacterial communities between the plots were analysed by generating Non-metric Multidimensional Scaling (NMDs) plots also based on Bray-Curtis dissimilarity, using the "envfit" function as described previously (Kaiser et al., 2016). All functions used for the analyses of the bacterial community structure are contained in the vegan package in R. Differences in the abundance of all predicted and quantified genes involved in CO_2 fixation between the beech and pine plots and across depth were also analysed using ANOVA and Tukey's test. For all tests conducted, differences with $P < 0.05$ were considered statistically significant.

2.8. Nucleotide sequence deposition

All generated sequences obtained in this study are deposited in NCBI databases with accession numbers: SAMN19324419, SAMN19324420, SAMN19324421, SAMN19324422, SAMN19324423, and SAMN19324424 under bio project accession number: PRJNA607916.

3. Results

3.1. Lower soil layers of pine plots have lower dark CO_2 fixation rates

An increase of $\delta^{13}C$ of SOC and MBC was observed in all incubations of beech and pine soils amended with ^{13}C–CO_2, in comparison to the controls (Fig. S1). The calculated dark CO_2 fixation rates decreased significantly with depth in both the beech ($P = 2.9 \times 10^{-10}$, ANOVA and Tukey's test) and pine soils ($P = 7.2 \times 10^{-16}$) in relation to soil dry weight (expressed as μg C g (dw) soil^{-1} d^{-1}) (Fig. 1A). In the beech soils, fixation rates decreased by a factor of 4 from 0.18 ± 0.06 μg C g (dw) soil^{-1} d^{-1} in the AB horizon to 0.044 ± 0.007 μg C g (dw) soil^{-1} d^{-1} in the lower BC horizon ($P = 7.2 \times 10^{-5}$, Student's *t*-test). Compared to the top AB horizon ($P = 2.6 \times 10^{-5}$), values ~7 times lower with 0.023 ± 0.005 μg C g (dw) soil^{-1} d^{-1} were observed in the lowest C horizon of the beech soils. Rates in the pine plot were 14 times lower in the lowest BC horizon at 0.01 ± 0.002 μg C g (dw) soil^{-1} d^{-1} compared to the top AB horizon with 0.14 ± 0.03 μg C g (dw) soil^{-1} d^{-1} ($P = 1.4 \times 10^{-7}$). Differences in rates between pine and beech soils at comparable depths were significant only in the lower BC horizons ($P = 5.2 \times 10^{-8}$).

When expressed in relation to MBC content (as μg C g MBC^{-1} d^{-1}), dark CO_2 fixation rates were similar across depths for the beech soils ($P = 0.19$) (Fig. 1B) with values ranging between 348.3 ± 132.5 μg C g MBC^{-1} d^{-1} (AB horizon) and 277.9 ± 105.7 μg C g MBC^{-1} d^{-1} (C horizon). Similar fixation rates of 266.9 ± 28.2 μg C g MBC^{-1} d^{-1} were also observed in the top horizon (AB) of the pine soils ($P = 0.07$). Significantly lower rates were observed in the B2 (88.0 ± 23.3 μg C g MBC^{-1} d^{-1}, $P = 5.6 \times 10^{-9}$) and BC (40.3 ± 26.2 μg C g MBC^{-1} d^{-1}, $P = 7.2 \times 10^{-12}$) horizons compared to the top AB horizon of the pine plot. These rates, almost an order of magnitude lower than any other rates observed in this study, suggested that factors other than microbial biomass are required to explain dark CO_2 fixation rates in the deeper soil layers of the pine plot.

3.2. Pine plots have lower contributions of dark CO_2 fixation to SOC and MBC at depth

After 7 days of incubation, the fraction of SOC derived from dark CO_2 fixation in the beech soils ranged between 0.0083 ± 0.004% (AB horizon) and 0.0091 ± 0.001% (C horizon), and no significant difference in this relative fraction was observed between the depths ($P = 0.47$) (Fig. 2A). Similarly, the excess ^{13}C in MBC in the beech soils maintained uniform proportions across depths ($P = 0.19$), ranging between 0.24 ± 0.09% (AB horizon) and 0.19 ± 0.08% (C horizon) (Fig. 2B). In the pine soils, however, contributions of incorporated ^{13}C labels increased significantly from 0.0045 ± 0.001% of SOC in the AB horizon to 0.0074 ± 0.001% in the BC horizon ($P = 4.9 \times 10^{-6}$). In contrast, ^{13}C incorporation in MBC decreased with depth in the pine soils from 0.19 ± 0.02% in the AB horizon to 0.03 ± 0.02% in the BC horizon ($P = 7.2 \times 10^{-12}$). Across the entire soil profiles, the relative fraction of ^{13}C in SOC was 1.8-fold higher in the beech plot than in the pine plot ($P = 3.2 \times 10^{-8}$). In comparison, the relative fraction of ^{13}C in MBC was 2.7-fold higher also at the beech plot ($P = 9.6 \times 10^{-9}$). As carbon losses through respiration were not accounted for, calculated CO_2 fixation rates and contributions to SOC/MBC represent gross inputs and are no evidence of net carbon gains.

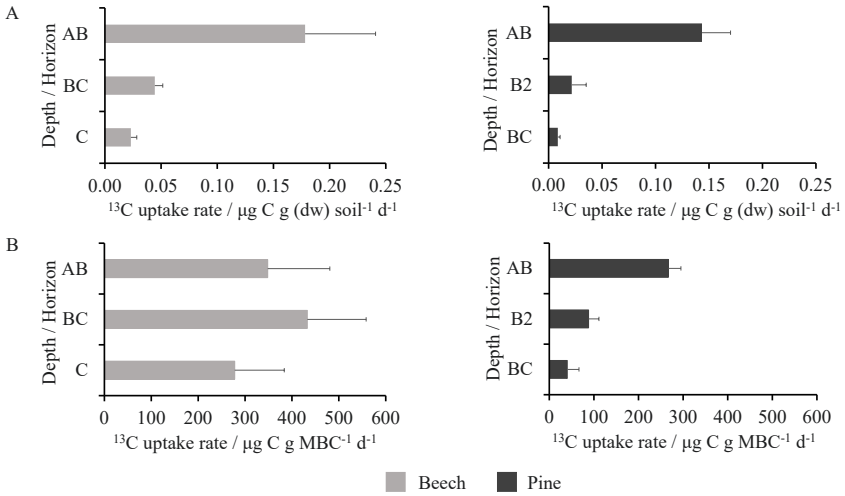

Fig. 1. Dark CO_2 fixation rate in soil incubations with 2% $^{13}CO_2$. Shown are (A) ^{13}C uptake rates in soil expressed in µg C g (dw) $soil^{-1}$ d^{-1} (µg carbon per gram dry weight (dw) of soil per day) and (B) ^{13}C uptake rates into MBC expressed in µg C g MBC^{-1} d^{-1} (µg carbon per gram of MBC per day) after 7 days of incubation in beech (light gray bars) and pine (dark gray bars) soil profiles. Error bars indicate standard deviations for 3 replicate incubations.

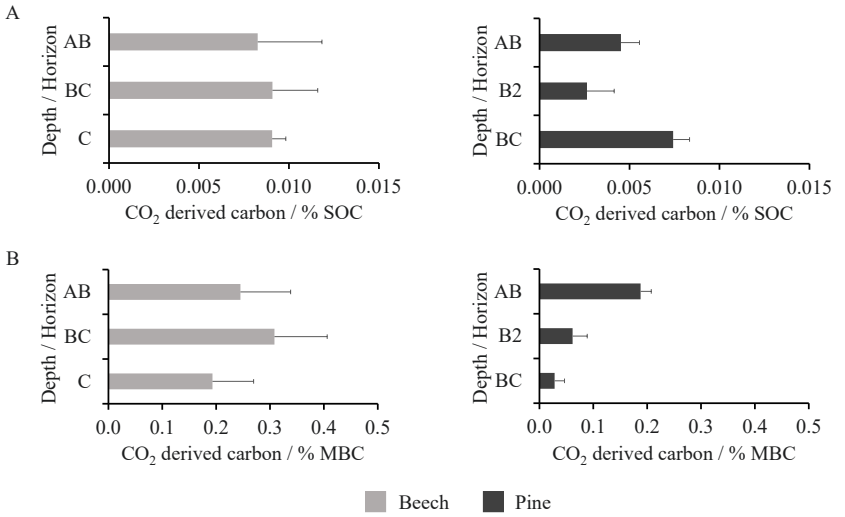

Fig. 2. Contributions of dark CO_2 fixation to SOC and MBC in soil incubations with 2% $^{13}CO_2$. Shown are the excess ^{13}C incorporation in SOC (A) expressed as a % of SOC and in MBC (B) expresses as a % of MBC after 7 days of incubation in beech (light gray bars) and pine (dark gray bars) soil profiles. Error bars indicate standard deviations for 3 replicate incubations.

3.3. Selected soil biogeochemical properties differ between the beech and pine soil profiles

We aimed to determine if the lower fixation rates in the deeper pine soils were related to differences in soil properties other than microbial biomass, especially microbial community composition (Table 1). All measured soil parameters described showed similar values before and after the incubation period for both the beech and pine soils. The pine plot featured a higher SOC content than the beech plot in the top AB horizon ($P = 0.009$). Both soils displayed a decline in SOC content with depth. This decline in SOC across depth was noticeably greater across the top and bottom profiles of the pine than the beech ($P = 2.8 \times 10^{-6}$) soils and led to beech soils having higher SOC contents in the BC horizon ($P = 3.6 \times 10^{-5}$). C/N ratio was much higher in the pine than the beech soils across depth with up to 24.34 ± 0.23 and 15.6 ± 1.2 respectively in the top AB horizon ($P = 4.47 \times 10^{-11}$). SOC in the pine plot featured a higher fraction of older carbon compared to the beech plot, as evident from the significantly lower $\Delta^{14}C$ values across the soil profiles ($R^2 = 0.83$, $P = 3.4 \times 10^{-5}$, ANCOVA).

MBC content, representing the soil microbial biomass, showed a sharper decrease with depth in the beech plot than in the pine plot, leading to significantly lower values in the BC horizon of the beech soils than in the BC horizon of pine soils ($P = 0.002$). In the topsoil, however, similar MBC contents were observed in both plots ($P = 0.7$). Bacterial 16S rRNA gene copy numbers, an index of soil bacterial biomass, also decreased significantly across depth in both the beech ($P = 6.1 \times 10^{-6}$) and the pine ($P = 0.03$) soils. However, no significant differences between beech and pine soils were observed at the top AB ($P = 0.58$) and lower BC ($P = 0.08$) horizons. Thus, the higher MBC content in the lower pine depths may be caused by other microbial groups than bacteria, like fungi (Awad et al., 2019).

MBC/SOC ratio at the top horizon of both soils were 0.9% and 1.5% for pine and beech soils respectively, increasing significantly to about 5% in the deep pine soils ($P = 6.6 \times 10^{-7}$) and only slightly to ~2% in

the deep beech soils (P = 0.04). As with MBC, a significantly higher MBC/SOC ratio was observed in the BC horizon of the pine than the beech soils ($P = 4.9 \times 10^{-7}$), while this ratio was higher in the AB horizon of the beech compared to the pine soils ($P = 3.8 \times 10^{-7}$).

Bacterial diversity decreased with depth in the pine plot, with Shannon index (H′) declining from 4.89 ± 0.04 in the AB horizon to 4.53 ± 0.15 in the BC horizon (P = 0.005). In contrast, the diversity with depth was more uniform in the beech plot with Shannon index ranging between 5.87 ± 0.05 in the AB horizon to 5.82 ± 0.22 in the C horizon (P = 0.6). Collectively, beech soils showed higher bacterial diversity than pine soils at both the comparable AB ($P = 4.2 \times 10^{-4}$) and BC horizons (P = 0.02).

3.4. Soil properties explain variations in dark CO_2 fixation rates

For the beech and pine soils, linear correlation analysis showed that MBC, SOC content and $\Delta^{14}C$ values, and water content formed positive correlations with measured uptake rates per gram dry weight of soil. Fixation rates normalized to MBC were mostly correlated with Shannon index (Fig. S2A), suggesting an influence of community composition. This was supported by the observed correlation of rates per gram of MBC with the community beta diversity ($R^2 = 0.99$, P = 0.001; Fig. S2B). To account for a broader range of soil characteristics, the data on dark CO_2 fixation rates and soil biotic and abiotic properties from both the beech and pine soils in this study were combined with those from our previous study (Akinyede et al., 2020) for a mixed deciduous forest in the Hainich Exploratory region (65% *Fagus sylvatica.* L.), a soil characterized by lower acidity, clay-rich texture, and higher SOC and MBC content. Rates of dark CO_2 fixation expressed both per gram of soil dry weight and per gram of MBC for identical experimental conditions were higher for the Hainich forest soils than observed in the current study ($P = 2.5 \times 10^{-5}$ and $P = 3.2 \times 10^{-11}$ for rates per gram dry weight of soil and per gram of MBC, respectively). When expressed per gram of soil weight, rates to 1 m depth were 0.22 ± 0.06 μg C g (dw) $soil^{-1}$ d^{-1} in the beech and 0.17 ± 0.03 g (dw) $soil^{-1}$ d^{-1} for the pine forest soil profiles, 4 to 5 times lower than those measured in the Hanich forest soils with 0.87 ± 0.24 g (dw) $soil^{-1}$ d^{-1} across 1 m depth (Fig. 3). To determine the contributions of the measured soil biogeochemical parameters to the variations in dark CO_2 fixation rates observed across the three forest plots, multiple stepwise regression analysis was performed. Multiple stepwise regression analysis with predictors in the final model revealed that MBC was the most important contributing factor, explaining 70.3% ($P < 0.001$) of the variations observed in the CO_2 fixation rates (per gram dry weight of soil) between the three forest soil plots across all depths ($R^2 = 0.78$, $P = 2.2 \times 10^{-16}$) (Fig. 3). The Shannon index, representing community composition, was the second-best predictor and explained 7.4% ($P < 0.001$) variation.

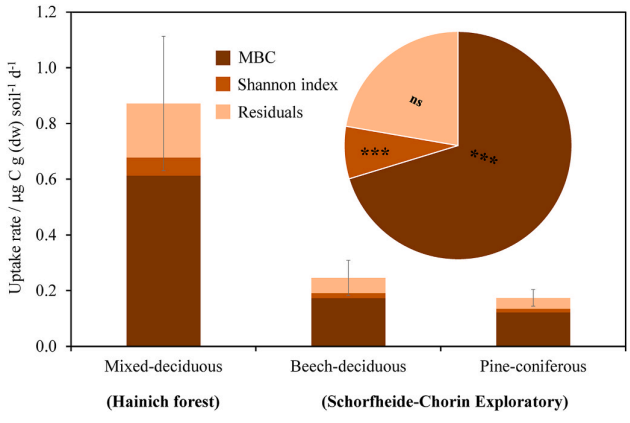

Fig. 3. Biogeochemical predictors of dark CO_2 fixation rates in beech, pine (Schorfheide-Chorin), and Hainich forest soils. Shown are the relative contributions (%) of measured soil biotic and abiotic properties (pie chart) as determined by multiple stepwise regression model to CO_2 fixation rates expressed as μg C g (dw) $soil^{-1}$ d^{-1} (bar chart). Data used are obtained from incubation and geochemical measurements from the beech and pine plots (Schorfheide-Chorin Exploratory) and a mixed-deciduous plot from the Hainich Exploratory region (Akinyede et al., 2020). *** denotes $P < 0.001$, ns denotes not significant.

3.5. The bacterial community structure varies between beech and pine soils

As the bacterial diversity in the soil explained some of the observed differences in dark CO_2 fixation rates across the beech and pine soil profiles, we further investigated the bacterial community structure by amplicon sequencing targeting bacterial 16S rRNA genes. Principal coordinate analysis (PCoA) at operational taxonomic unit (OTU) level revealed changes in the bacterial community structure with soil plot ($R^2 = 0.303$, P = 0.001, PERMANOVA) and soil depth ($R^2 = 0.300$, P = 0.002) (Fig. 4A). The effect of depth on the bacterial community structure was stronger in the pine plots ($R^2 = 0.76$, P = 0.004) compared

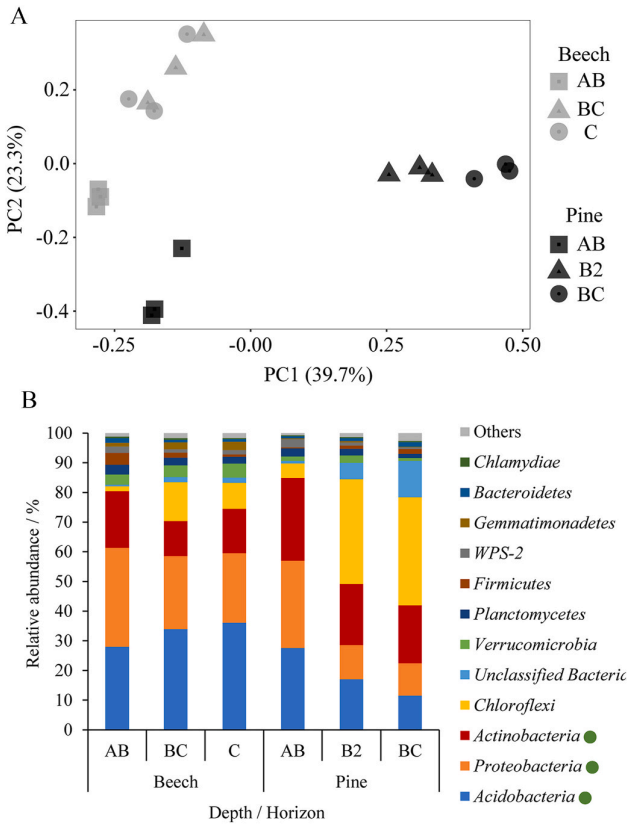

Fig. 4. Bacterial community structure (PCoA) and composition (Phylum level) of the beech and pine soil profiles. Shown are (A) PCoA of soil bacteria community structure based on OTU level analysis of 16S rRNA gene amplicons and (B) the relative abundance of assigned bacterial sequences of the bulk soil samples across depths obtained from the beech and pine soils. In the PCoA plot, 3 independent data points per depth are shown for both the beech (light gray symbols) and pine (dark gray symbols) soil plots. Phylum level taxonomic assignment in the bar plot is based on the SILVA database implemented on the MOTHUR sequence analysis pipeline. Data represent 3 replicate soil cores per depth for both soil plots. Phyla with green circular symbols contain the most abundant potential CO_2 fixing communities found in this study. (For interpretation of the references to colour in this figure legend, the reader is referred to the Web version of this article.)

to the beech plots ($R^2 = 0.51$, P = 0.022). This observed change in the community between both soil plots was largely a result of distinct communities in the lower horizons ($R^2 = 0.62$, P = 0.001), whereas the bacterial communities inhabiting the AB horizon did not differ significantly between the beech and pine soils ($R^2 = 0.61$, P = 0.1).

Taxonomic classification of the bacterial OTUs identified *Actinobacteria*, *Proteobacteria*, and *Acidobacteria* as the most dominant bacterial phyla in both soils (Fig. 4B), constituting 60–80% of the bacterial community. Strikingly, while these three groups were uniformly distributed across the beech soil profiles (P = 0.15, P = 0.19, and P = 0.13, respectively), they decreased strongly in relative abundance with depth in the pine soils (P = 0.04, P = 0.001, and P = 0.01, respectively). Instead, members of the *Chloroflexi* phylum dominated the bacterial community at the B2 and BC horizons of the pine plot, with relative abundances of up to 36%. This represented a 7-fold increase compared to the AB horizon of the pine soils, suggesting that *Chloroflexi* were the major group driving the differentiation in community structure observed in the PCoA. Members of this group also increased with depth in the beech soils (P = 0.01) but made up no more than 13% of the entire beech soil community, hence were ~3 times more abundant in the pine than the beech soils at the lower BC horizon ($P = 4.1 \times 10^{-4}$).

3.6. Beech soils have a higher potential for CO_2 fixation than pine soils

Based on the observed differences in the community structure, we used measures of genetic potential for CO_2 fixation to further understand the differences between the beech and pine soils. PICRUSt2 was used to predict genes for key enzymes involved in chemolithoautotrophic and heterotrophic CO_2 fixation for all 16S rRNA bacterial OTUs present in both the beech and pine forest plots. OTUs of putative autotrophs constituted <20% of the total bacterial community in both the beech and pine soils (Fig. S3A). Most of the autotrophic CO_2 fixation genes predicted were related to the CBB pathway and this pathway was predicted in ~15% of the total bacterial community. Putative autotrophs using the CBB pathway decreased significantly with depth in the pine soils from 13.6 ± 0.5% in the AB horizon to 3.8 ± 0.2% in the BC horizon ($P = 1.3 \times 10^{-4}$). No significant difference in the proportion of OTUs predicted with the CBB pathway was found across the beech soil horizons, with values between 14.6 ± 0.9% at the top AB depth and 11.2 ± 2.0% at the lower C horizon (P = 0.09). The WLP and rTCA pathways were the least predominant autotrophic pathways predicted, constituting ~2% and <1% respectively of the total bacterial community in the beech and pine soils. Predicted key genes for the remaining known autotrophic CO_2 fixation pathways: the 3HP cycle, the HP/HB cycle, and the DC/HB cycle were not detected in both soil plots. Together, all predicted autotrophic genes correlated with CO_2 fixation rates expressed per gram of MBC in the pine plots, but the beech plots showed no such correlations (Fig. S4A).

To verify putative chemolithoautotrophs able to fix CO_2, marker genes belonging to the CBB (RuBisCO (*cbbL* IA, *cbbL* IC, *cbbM*)) and rTCA (*aclA*) pathway were quantified by qPCR. All autotroph genes detected constituted <3% of the bacterial 16S rRNA gene copies across depth for both the beech and pine soils (Fig. S5). The *cbbL* IC genes were the most abundant, reaching values between 1.06 ± 0.66% and 2.25 ± 1.14% relative to 16S rRNA gene copies (Table S1). We found no difference in *cbbL* IC gene abundance between soils (P = 0.59) and across the beech (P = 0.09) and pine (P = 0.43) soil profiles. Other RuBisCO and *aclA* genes constituted <0.3% and <0.2% of the 16S rRNA gene copies respectively and no correlations between the RuBisCO and *aclA* genes with CO_2 fixation rates were found.

We further explored the potential for CO_2 fixation by type II methanotrophs using PICRUSt2. Members of this group, which are also present in soils (Lee et al., 2015a), can derive ~60% of their cell carbon from CO_2 fixation mostly via the serine cycle (Yang et al., 2013). As genetic markers for type II methanotrophs, fractions of predicted *pmoA* and *mmoX* genes made up <1% of the total bacterial community in the beech and pine soils.

As a marker for putative heterotrophs with CO_2 fixation potential, phosphoenolpyruvate carboxylase (PEPC) and pyruvate carboxylase (PC) genes (Fig. S3B) were predicted by PICRUSt2 in 30–70% of the total community in both the beech and pine soils. Remarkably, the predicted PEPC and PC genes decreased significantly in abundance with depth in the pine soils from 69.5 ± 9.8% in the AB horizon to 30.5. ± 6.8% in the BC horizon (P = 0.007) and correlated with CO_2 fixation rates expressed per gram of MBC (Fig. S4B). No significant difference in the distribution of these genes was observed across the beech soil horizons, with values between 63.5 ± 1.6% in the top AB depth and 55.8 ± 5.1% in the C horizon (P = 0.11). Accordingly, no correlation with fixation rates per gram of MBC was observed in the beech plot.

Taken together, the predicted PEPC and PC genes involved in heterotrophic CO_2 fixation were the most prevalent of all the CO_2 fixation pathways predicted, being over 4 times more abundant than the predicted autotrophic genes. Thus, the relative proportion of PEPC and PC genes among each of the dominant bacteria phyla identified was further explored. Among the dominant bacteria phyla, ~90% of all *Proteobacteria*, up to 73% of all *Actinobacteria*, and 60% of all *Acidobacteria* were predicted to possess PEPC or PC genes. In contrast, only 7–25% of members of *Chloroflexi* were predicted to possess these genes. The observed decline of the potential for heterotrophic CO_2 fixation in the lower depths of the pine plots could thus be explained by the increasing abundance of *Chloroflexi* in these soils (Fig. 5).

4. Discussion

In our previous experiments, we observed that rates of dark CO_2 fixation in soils of a mixed deciduous forest strongly correlated with the MBC content, suggesting MBC content to be a main predictor for dark CO_2 fixation rates in temperate forest soils (Akinyede et al., 2020). As variations in the amount and quality of SOC strongly influence microbial communities, we tested whether such differences in SOC caused by tree species will also affect dark CO_2 fixation rates with depth. The rates of dark CO_2 fixation per gram of MBC were uniform across soil depth for the beech forest plot as well as the topsoil of the pine forest plot but were significantly lower in the subsoils of the pine forest plot. These lower rates in the pine subsoils indicated that other factors besides the abundance of the microbial biomass control dark CO_2 fixation rates in soils under coniferous trees. Previous studies have also reported differences in dark CO_2 fixation rates between spruce and beech soils and suggested

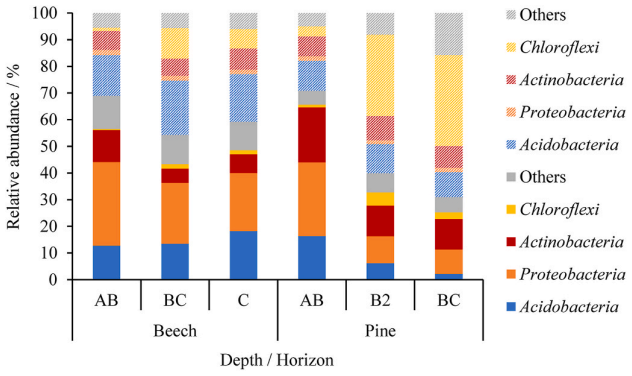

Fig. 5. Relative proportion of bacterial community based on the presence and absence of PEPC/PC carboxylase genes for each dominant phylum in the beech and pine soil profiles. Shown are the relative abundances of bacterial taxa with (filled bars) and without (striped bars) PEPC/PC carboxylase genes across 3 horizons in the beech and pine soils. Taxonomic selection is based on 16S rRNA predicted functions determined by PICRUSt2 (Version 2 of the Phylogenetic Investigation of Communities by Reconstruction of Unobserved States). Data represents 3 replicate soil cores per depth in both the beech and pine soil plots.

differences in the soil microbial community to be the reason (Spohn et al., 2019). Here we showed that pine soil profiles have stronger shifts in the bacterial community structure with soil depth and overall lower bacterial diversity than the beech soils. The pine subsoils were particularly enriched in *Chloroflexi* but strongly depleted in *Proteobacteria*, *Acidobacteria*, and *Actinobacteria* that formed the dominant groups in the beech soils. As the distribution of bacterial communities through the soil profile is also a reflection of their functional traits (Khlifa et al., 2017; Lladó et al., 2017), this suggests that the lower fixation rates in the deep pine layers may have been evoked by community shifts in favour of groups having a lower capacity to fix CO_2. In agreement, a much lower proportion of PEPC and PC genes was predicted for *Chloroflexi* as opposed to *Proteobacteria*, *Acidobacteria,* and *Actinobacteria*, which displayed a higher proportion of these genes. The products of these genes mark central entry points of CO_2 into the microbial metabolism in anaplerotic reactions during heterotrophic growth, which we found to be the lifestyle of the overwhelming majority of the soil microbes (Akinyede et al., 2020). Thus, we speculate that while the higher abundance of PEPC/PC genes in *Proteobacteria*, *Acidobacteria,* and *Actinobacteria* in the beech soils may explain the higher CO_2 fixation rates observed in these soils, the lower abundance of the PEPC/PC genes in *Chloroflexi* suggests that they fix no or less CO_2 during heterotrophic growth. The dominance of *Chloroflexi* in the pine subsoils could thus offer an explanation for the lower fixation rates observed.

Chloroflexi encompasses a metabolically versatile group of bacteria (Nierychlo et al., 2019; Speirs et al., 2019). Various *Chloroflexi* members are known to fix CO_2 by anoxygenic photosynthesis (3HP cycle) (Pierson and Castenholz, 1992; Berg, 2011; Hanada, 2014), but due to the lack of light, this lifestyle is not feasible in deep, mineral soil horizons. Chemolithoautotrophic growth via the Wood-Ljungdahl pathway was reported for some strains (Hug et al., 2013; McGonigle et al., 2019), but is unlikely due to the oxygen sensitivity of the key enzymes and the limited availability of suitable electron donors like H_2 in these soils (Berg, 2011; Beulig et al., 2014, 2016). When growing heterotrophically, *Chloroflexi* are typically fermenters able to break down complex plant-derived polymers, like polysaccharides, N-acetylglucosamine, organic acids, protein hydrolysate, and pyrogallol (Okabe et al., 2005; Xia et al., 2007, 2016; Kragelund et al., 2007, 2011; Hug et al., 2013; Wasmund et al., 2014). Acetate (acetyl-CoA) typically is the end product of fermentation, formed from pyruvate or phosphoenolpyruvate via pyruvate:ferredoxin oxidoreductase (PFOR) (Hug et al., 2013; Klatt et al., 2013; Sewell et al., 2017). These organisms typically feature a partial or non-functional "horseshoe" TCA cycle lacking succinyl-CoA synthetase (Wood et al., 2004; Berg, 2011; Hug et al., 2013; Vuillemin et al., 2020). Thus, acetyl-CoA is usually assimilated via the glyoxylate pathway, a variant of the TCA cycle (Wood et al., 2004; Kremer et al., 2019). During this process, acetyl-CoA is directly converted to malate via the cleavage of isocitrate to succinate and glyoxylate using isocitrate lyase and malate synthase as key enzymes (Erb et al., 2010; Kremer et al., 2019). Hence, no carboxylation reactions are required to generate oxaloacetate.

Contrastingly, members of the *Proteobacteria*, *Acidobacteria,* and *Actinobacteria* found in soils are typically copiotrophic in nature, preferring more labile forms of organic carbon (Eilers et al., 2010; Lladó et al., 2017). The primary product from their catabolic breakdown of organic carbon is mainly PEP and pyruvate (Romano and Conway, 1996; Liu et al., 2013; Martins et al., 2019). A complete TCA cycle is common in many strains (Moreno and Moriyo, 2006; Lee et al., 2015b; Eichorst et al., 2018; Martins et al., 2019), and PEPC/PC genes are present in many members of these groups (Šantrůčková et al., 2018; Akinyede et al., 2020). Hence, assimilation of PEP and pyruvate involves the generation of oxaloacetate, (Berg, 2011; Lee et al., 2015b; Thakur and Sen, 2016; Eichorst et al., 2018; Martins et al., 2019), the TCA cycle intermediate (Erb, 2011). Transformation to oxaloacetate involves the carboxylation of PEP or pyruvate which is catalysed by carboxylase enzymes, PEPC/PC (Kornberg, 1965; Owen et al., 2002; Bar-Even et al., 2010; Erb, 2011). These carboxylation reactions thus allow the use of CO_2 as a carbon source during heterotrophic growth.

Low CO_2 fixation rates in soils have also been linked to a low abundance of facultative and/or obligate autotrophs (Wu et al., 2014, 2015; Lynn et al., 2017; Xiao et al., 2018). Predicted and quantified genes linked to the CBB pathway (Kaiser et al., 2016) were generally low in abundance in both the beech and the pine soils. Also, type II methanotrophs constituted a minute proportion of the communities in both plots, likely due to the acidic conditions (pH $<$ 5). Type II methanotrophs thrive mostly under circumneutral to basic (pH 6–9) pH conditions (Nguyen et al., 2021), and occur mostly in upland soils and in the oxic-anoxic interface of wetland soils like rice paddies where both oxygen and methane are present (Macalady et al., 2002; Lee et al., 2015a; Hakobyan and Liesack, 2020). Thus, the observed low fraction of autotrophs and type II methanotrophs in both plots support our speculation that the higher abundance of heterotrophs lacking PEPC and PC genes in the pine subsoils might explain the lower CO_2 fixation rates observed. However, as the abundance of a gene does not necessarily reflect activity in that they do not provide information on their transcriptionally activity or level of expression (Milanese et al., 2019), the genomic potential for CO_2 fixation described here cannot be directly linked to the CO_2 fixation activity. Thus, reported correlations with fixation rates may only be used to speculate about the potential key players involved.

Much of the SOC available to microbes for heterotrophic growth in soils is derived from specific sources associated with the tree cover: litter input and root exudation (Nguyen, 2003; Rasse et al., 2005). Although significant inputs from fungal biomass turnover have also been reported (Liang et al., 2019; Wallander et al., 2004), tree-species specific differences in fungal biomass as potential SOC sources are mostly found in the topsoil (Wallander et al., 2004; Awad et al., 2019). Decomposing litter of soils dominated by coniferous trees feature lower fractions of labile dissolved organic carbon (DOC) than those under deciduous trees (Don and Kalbitz, 2005), but this effect is mostly restricted to the topsoil horizons (Achilles et al., 2020). The specific root lengths and root area of coniferous trees are smaller than those of deciduous tree species (Finér et al., 2007; Ostonen et al., 2007). Deep roots contribute significantly to the large carbon stocks in forest subsoils (Jobbágy and Jackson, 2000; Rasse et al., 2001, 2005), suggesting that soils under shallow-rooted coniferous trees will receive lower carbon inputs from root exudates compared to subsoils of deep-rooted deciduous trees. Accordingly, we observed a steeper decline in SOC content in the lower depths of the pine than in the beech soils. High carbon contents in deep soil horizons affect microbial communities and enhance microbial mineralization of forest soil organic matter via root-induced priming effect (Tefs and Gleixner, 2012; Adamczyk et al., 2019; Lladó et al., 2017). Such positive priming enhances the decomposition of not just labile but also older, complex organic carbon pools (Zhang et al., 2019). Thus, as opposed to the beech soils, the lower carbon inputs in the deep pine horizons might have influenced the microbial community composition leading to an overall slower decomposition rate and hence, accumulation of older, complex organic carbon fractions. In agreement, we observed lower $\Delta^{14}C$ signatures of SOC and higher C/N ratios with depth in pine soils suggesting that the pine soils contained older organic carbon substrates of lower quality when compared to the beech soils. These pine soils with a lower clay content also showed 20–30% lower mineral soil respiration rates (both as absolute values and relative to SOC content), and $>$2 folds lower enzymatic activities (e.g., N-acetyl-glucosaminidase and phosphatase) compared to the beech soils (Schöning et al., 2013a, 2013b; Kaiser et al., 2016), likewise indicating a lower organic carbon input and quality (Bauhus and Khanna, 1999; Craine et al., 2010; Veum et al., 2014; Meyer et al., 2018). Such differences in SOC content and quality were shown to affect microbial CO_2 fixation rates in soils (Miltner et al., 2005; Šantrůčková et al., 2018). Accordingly, the variations in bacterial community structure observed in forest soils under different tree species as reported here and by previous studies (Urbanová et al., 2015; Nacke et al., 2016; Dukunde et al., 2019) are often linked to such differences in

organic carbon input and quality (Thoms et al., 2010; Urbanová et al., 2015; Kaiser et al., 2016; Lladó et al., 2017; Liu et al., 2019a, 2019b).

Coniferous trees tend to exert a greater influence on microbial community structure than deciduous species (Hackl et al., 2005; Nacke et al., 2016). In agreement with our results, fermenting organisms using complex carbon substrates such as *Chloroflexi* and *Firmicutes* were repeatedly shown to dominate the bacteria community in coniferous soils (Baldrian et al., 2012; Uroz et al., 2013; Nacke et al., 2016; Lladó et al., 2017). Conversely, microbial groups like *Proteobacteria, Acidobacteria,* and *Actinobacteria* tend to be less enriched in coniferous than deciduous soils (Eilers et al., 2010; Urbanová et al., 2015). Thus, based on our observations, we speculate that the variations in SOC input between the beech and pine soils and the known influence on community composition might explain the differences in the CO_2 fixation rates between the beech and pine soil profiles (Fig. 6).

Furthermore, it should be considered that the extraction of MBC was based on the chloroform fumigation method which does not distinguish between active and dormant microbes (Blagodatsky et al., 2000). Thus, lower CO_2 fixation rates per gram of MBC in the pine than in the beech subsoils despite higher MBC/SOC ratios could also indicate that a larger portion of the extracted MBC in pine subsoils was not active, possibly due to the lower SOC input. As we did not measure respiration rates or the proportion of the active bacterial community in the beech and pine soils, this hypothesis would need to be proven in further studies.

Over a broader range of soil characteristics under deciduous and coniferous tree stands, fixation rates both per gram of soil dry weight and per gram of microbial biomass were higher in the Hainich forest soils than observed in our current study. A potential explanation for this is the higher MBC and SOC input, as the Hainich soils, despite differences in texture and pH, displayed a similar proportion of potential functional communities involved in CO_2 fixation, including type II methanotrophs, when compared to this study (Akinyede et al., 2020). It should be noted that the samples from the Hainich forest were taken in summer when microbial activities and root inputs might be higher (López-Mondéjar et al., 2015). Thus, it is likely that a larger portion of microbes was potentially active, and fresh inputs from root exudation were probably also larger than in winter when samples from the beech and pine plots were taken. This might also add to the higher MBC in the Hainich forest soil compared to the other two plots. Multiple stepwise regression revealed that MBC showed the strongest correlation with CO_2 fixation rates across the three compared forest plots while Shannon index formed the second strongest correlations. This highlights the importance of microbial community composition and their metabolic CO_2 fixation potentials on CO_2 fixation dynamics. SOC content and quality, being tree species-specific, could affect CO_2 fixation rates in the beech and pine forest soils via influence on microbial communities and their CO_2 fixation activities. Such tree-species specific effects might also exist in other temperate forest soils.

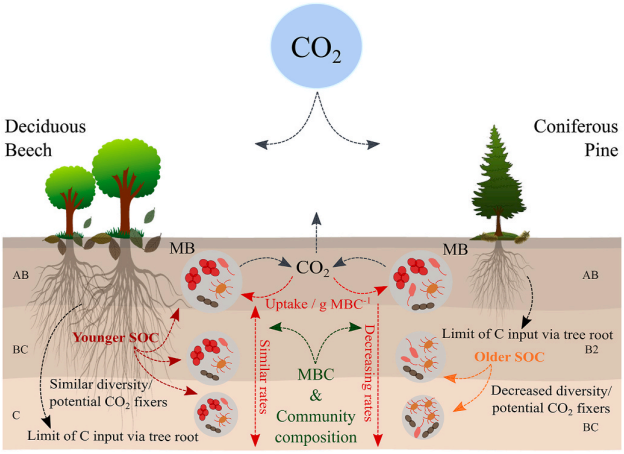

Fig. 6. Conceptual illustration of dark CO_2 fixation in temperate deciduous vs temperate coniferous forest soils. The distinct root system of each tree species determines the vertical distribution of SOC input and quality through the soil profile (black arrows). The deeper root systems typical of deciduous trees increase the rate of delivery of younger SOC at deeper soil depths compared to soils with shallower-rooted coniferous trees. This influences the bacterial composition of the microbial biomass (MB) pool that normally decreases with depth (denoted by the decreasing size of circles across the horizon). The resultant effect is a relatively uniform microbial community composition across the beech soil depths (dark red arrows) as opposed to the pine soils (orange arrows) which select for a different community composition in the deeper profiles that have a low CO_2 fixation potential. Hence, this leads to lower CO_2 uptake rates per gram of MBC in the pine than in the beech subsoils (bright red arrows). Overall, MBC and community composition showed the strongest correlations (green arrows) with dark CO_2 fixation rates. Fluxes of CO_2 between the soil and the atmosphere are denoted by gray arrows. (For interpretation of the references to colour in this figure legend, the reader is referred to the Web version of this article.)

5. Conclusions

Dark CO_2 fixation rates per unit of MBC were uniform through deciduous beech soil profiles but lower in the deeper horizons of soils dominated by coniferous pine trees. The pine subsoils featured a different bacterial community structure which was accompanied by a much lower potential for heterotrophic CO_2 fixation when compared to the beech subsoils. We speculate that lower SOC inputs in the deeper pine horizons favoured the dominance of oligotrophic bacteria phyla that feature a lower heterotrophic CO_2 fixation potential and hence, lower CO_2 fixation rates. The acidic coniferous and deciduous soil plots displayed lower rates than soils of mixed deciduous forest with higher pH, MBC, and SOC content. Among these forest plots, MBC and Shannon index also showed the strongest correlations with CO_2 fixation rates, suggesting that microbial community composition and their CO_2 fixation potential in soils influenced dark CO_2 fixation rates. As SOC is a regulator of microbial communities and their activities in soil, differences in the amount and quality of SOC, as evoked by tree species, may affect the metabolic potential for CO_2 fixation and exert a strong influence on dark CO_2 fixation rates between the beech and pine forest soils. Finally, this study suggests that the influence of tree-derived SOC inputs on microbial communities might also exist in other temperate forest soils, and thus, may play an important role in the dynamics of dark CO_2 fixation in temperate deciduous and coniferous forest soils.

Declaration of competing interest

The authors declare that they have no known competing financial interests or personal relationships that could have appeared to influence the work reported in this paper.

Acknowledgment

This study was jointly supported by the Max Planck Institute for Biogeochemistry Jena (MPI BGC), the International Max Planck Research School for Global Biogeochemical Cycles Jena (IMPRS-gBGC), Deutscher Akademischer Austauschdienst (DAAD), and the Collaborative Research Centre 1076 AquaDiva (CRC AquaDiva), Germany. Martin Taubert gratefully acknowledges funding by the DFG under Germany's Excellence Strategy - EXC 2051 - Project-ID 390713860. Our gratitude also goes to Iris Kuhlmann, Marco Pöhlmann, Jens Wurlitzer, and Stefan Riedel for soil sampling, incubation set-ups, and CFE-extractions and the routine measurements departments of the Max-Planck Institute for Biogeochemistry, Jena. We wish to acknowledge the contributions of members of the Biodiversity Exploratories, Germany for access to the study site. We thank the manager of the Schorfheide-Chorin Biodiversity Exploratory, Miriam Teuscher, and all former managers for their work in

maintaining the plot and project infrastructure; Christiane Fischer for giving support through the central office, Andreas Ostrowski for managing the central database, and Markus Fischer, Eduard Linsenmair, Dominik Hessenmöller, Daniel Prati, Ingo Schöning, François Buscot, Ernst-Detlef Schulze, Wolfgang W. Weisser and the late Elisabeth Kalko for their role in setting up the Biodiversity Exploratories project. We thank the administration of the Hainich national park, the UNESCO Biosphere Reserve Swabian Alb, and the UNESCO Biosphere Reserve Schorfheide-Chorin as well as all landowners for the excellent collaboration. The work has been (partly) funded by the DFG Priority Program 1374 "Biodiversity-Exploratories" (Grant ID SCHR 1181/2-3 and Grant ID TR 1054/4–3). Fieldwork permits were issued by the responsible state environmental offices of Baden-Württemberg, Thüringen, and Brandenburg.

Appendix A. Supplementary data

Supplementary data to this article can be found online at https://doi.org/10.1016/j.soilbio.2021.108526.

References

Achilles, F., Tischer, A., Bernhardt-Römermann, M., Heinze, M., Reinhardt, F., Makeschin, F., Michalzik, B., 2020. European beech leads to more bioactive humus forms but stronger mineral soil acidification as Norway spruce and Scots pine – results of a repeated site assessment after 63 and 82 years of forest conversion in Central Germany. For. Ecol. Manag. 483, 118769. https://doi.org/10.1016/j.foreco.2020.118769.

Adamczyk, B., Sietiö, O.M., Straková, P., Prommer, J., Wild, B., Hagner, M., Pihlatie, M., Fritze, H., Richter, A., Heinonsalo, J., 2019. Plant roots increase both decomposition and stable organic matter formation in boreal forest soil. Nat. Commun. 10, 1–9. https://doi.org/10.1038/s41467-019-11993-1.

Akinyede, R., Taubert, M., Schrumpf, M., Trumbore, S., Küsel, K., 2020. Rates of dark CO_2 fixation are driven by microbial biomass in a temperate forest soil. Soil Biol. Biochem. 150, 107950. https://doi.org/10.1016/j.soilbio.2020.107950.

Alfreider, A., Vogt, C., Hoffmann, D., Babel, W., 2003. Diversity of ribulose-1,5-bisphosphate carboxylase/oxygenase large-subunit genes from groundwater and aquifer microorganisms. Microbial Ecology 45, 317–328.

Alfreider, A., Schirmer, M., Vogt, C., 2012. Diversity and expression of different forms of RuBisCO genes in polluted groundwater under different redox conditions. FEMS Microbiol. Ecol. 79, 649–660.

Alfreider, A., Grimus, V., Luger, M., Ekblad, A., Salcher, M.M., Summerer, M., 2018. Autotrophic carbon fixation strategies used by nitrifying prokaryotes in freshwater lakes. FEMS Microbiol. Ecol. 94, 1–12.

Awad, A., Majcherczyk, A., Schall, P., Schröter, K., Schöning, I., Schrumpf, M., Ehbrecht, M., Boch, S., Kahl, T., Bauhus, J., Seidel, D., Ammer, C., Fischer, M., Kües, U., Pena, R., 2019. Ectomycorrhizal and saprotrophic soil fungal biomass are driven by different factors and vary among broadleaf and coniferous temperate forests. Soil Biology and Biochemistry 131, 9–18. https://doi.org/10.1016/j.soilbio.2018.12.014.

Baldrian, P., Kolaiřík, M., Štursová, M., Kopecký, J., Valášková, V., Větrovský, T., Žifčáková, L., Šnajdr, J., Rídl, J., Vlček, Č., Voříšková, J., 2012. Active and total microbial communities in forest soil are largely different and highly stratified during decomposition. The ISME J. 6, 248–258. https://doi.org/10.1038/ismej.2011.95.

Barbera, P., Kozlov, A.M., Czech, L., Morel, B., Darriba, D., Flouri, T., Stamatakis, A., 2019. EPA-ng: massively parallel evolutionary placement of genetic sequences. Systematic Biology 68, 365–369. https://doi.org/10.1093/sysbio/syy054.

Bar-Even, A., Noor, E., Lewis, N.E., Milo, R., 2010. Design and analysis of synthetic carbon fixation pathways. Proc. Natl. Acad. Sci. U.S.A. 107, 8889–8894. https://doi.org/10.1073/pnas.0907176107.

Bar-Even, A., Noor, E., Milo, R., 2012. A survey of carbon fixation pathways through a quantitative lens. Journal of Experimental Botany 63, 2325–2342. https://doi.org/10.1093/jxb/err417.

Batjes, N.H., 1992. Organic Matter and Carbon Dioxide, A Review of Soil Factors and Processes that Control Fluxes of Heat, Moisture and Greenhouse Gases. Technical Paper 23. International Soil Reference and Information Centre, Wageningen, pp. 97–148.

Bauhus, J., Khanna, P.K., 1999. The significance of microbial biomass in forest soils. In: Rastin, N., Bauhus, J. (Eds.), Going Underground - Ecological Studies in Forest Soils. Research Signpost, Trivandrum, India, pp. 77–110.

Blagodatsky, S.A., Heinemeyer, O., Richter, J., 2000. Estimating the active and total soil microbial biomass by kinetic respiration analysis. Biology and Fertility of Soils 32, 73–81. https://doi.org/10.1007/s003740000219.

Berg, I.A., 2011. Ecological aspects of the distribution of different autotrophic CO_2 fixation pathways. Applied and Environmental Microbiology 77, 1925–1936. https://doi.org/10.1128/AEM.02473-10.

Beulig, F., Heuer, V.B., Akob, D.M., Viehweger, B., Elvert, M., Herrmann, M., Hinrichs, K. U., Küsel, K., 2014. Carbon flow from volcanic CO_2 into soil microbial communities of a wetland mofette. The ISME Journal 9, 746–759. https://doi.org/10.1038/ismej.2014.148.

Beulig, F., Urich, T., Nowak, M., Trumbore, S.E., Gleixner, G., Gilfillan, G.D., Fjelland, K. E., Küsel, K., 2016. Altered carbon turnover processes and microbiomes in soils under long-term extremely high CO_2 exposure. Nat. Microbiol. 1, 1–9. https://doi.org/10.1038/nmicrobiol.2015.25.

Binkley, D.A.N., Giardina, C., 2014. Why do tree species affect soils ? The warp and woof of tree – soil interactions. Biogeosciences 42, 89–106. https://doi.org/10.1023/A.

Braun, A., Spona-Friedl, M., Avramov, M., Elsner, M., Baltar, F., Reinthaler, T., Herndl, G., Griebler, C., 2021. Reviews and syntheses: heterotrophic fixation of inorganic carbon – significant but invisible flux in global carbon cycling. Biogeosciences 18, 3689–3700. https://doi.org/10.5194/bg-2020-465.

Cha, J.Y., Cha, Y.K., Oh, N.H., 2019. The effects of tree species on soil organic carbon content in South Korea. Journal of Geophysical Research: Biogeosciences 124, 708–716. https://doi.org/10.1029/2018JG004808.

Cleveland, C.C., Liptzin, D., 2007. C:N:P stoichiometry in soil: is there a “Redfield ratio” for the microbial biomass? Biogeochemistry 85, 235–252. https://doi.org/10.1007/s10533-007-9132-0.

Coplen, T.B., Brand, W.A., Gehre, M., Groning, M., Meljer, L.H.A.J., Toman, B., Verkouteren, R.M., 2006. New guidelines for $\delta^{13}C$ measurements. Analytical Chemistry 78, 2439–2441.

Craine, J.M., Fierer, N., McLauchlan, K.K., 2010. Widespread coupling between the rate and temperature sensitivity of organic matter decay. Nature Geoscience 3, 854–857. https://doi.org/10.1038/ngeo1009.

Cuss, C.W., Guéguen, C., 2013. Distinguishing dissolved organic matter at its origin: size and optical properties of leaf-litter leachates. Chemosphere 92, 1483–1489.

Czech, L., Stamatakis, A., 2019. Scalable methods for analyzing and visualizing phylogenetic placement of metagenomic samples. PLoS One 14, 1–50.

Daims, H., Brühl, A., Amann, R., Schleifer, K.-H., Wagner, M., 1999. The domain-specific probe EUB338 is insufficient for the detection of all Bacteria: development and evaluation of a more comprehensive probe set. Systematic & Applied Microbiology 22, 434–444.

Dalal, R.C., 1998. Soil microbial biomass - what do the numbers really mean? Australian J. Experimental Agriculture 38, 649–665. https://doi.org/10.1071/EA97142.

Don, A., Kalbitz, K., 2005. Amounts and degradability of dissolved organic carbon from foliar litter at different decomposition stages. Soil Biol. Biochem. 37, 2171–2179. https://doi.org/10.1016/j.soilbio.2005.03.019.

Douglas, G.M., Maffei, V.J., Zaneveld, J.R., Yurgel, S.N., James, R., Taylor, C.M., Huttenhower, C., Langille, M.G.I., 2020. Nat. Biotechnol. 38, 685–688. https://doi.org/10.1038/s41587-020-0548-6. PICRUSt2.

Dukunde, A., Schneider, D., Schmidt, M., Veldkamp, E., Daniel, R., 2019. Tree species shape soil bacterial community structure and function in temperate deciduous forests. Front. Microbiol. 10, 1–17. https://doi.org/10.3389/fmicb.2019.01519.

Edgar, R.C., Haas, B.J., Clemente, J.C., Quince, C., Knight, R., 2011. UCHIME improves sensitivity and speed of chimera detection. Bioinformatics 27, 2194–2200. https://doi.org/10.1093/bioinformatics/btr381.

Eichorst, S.A., Trojan, D., Roux, S., Herbold, C., Rattei, T., Woebken, D., 2018. Genomic insights into the *Acidobacteria* reveal strategies for their success in terrestrial environments. Environ. Microbiology 20, 1041–1063. https://doi.org/10.1111/1462-2920.14043.

Eilers, K.G., Lauber, C.L., Knight, R., Fierer, N., 2010. Shifts in bacterial community structure associated with inputs of low molecular weight carbon compounds to soil. Soil Biol. Biochem. 42, 896–903. https://doi.org/10.1016/j.soilbio.2010.02.003.

Erb, T.J., 2011. Carboxylases in natural and synthetic microbial pathways. Appl. Environ. Microbiology 77, 8466–8477. https://doi.org/10.1128/AEM.05702-11.

Erb, T.J., Frerichs-Revermann, L., Fuchs, G., Alber, B.E., 2010. The apparent malate synthase activity of *Rhodobacter sphaeroides* is due to two paralogous enzymes, (3S)-malyl-coenzyme A (CoA)/β-methylmalyl-CoA lyase and (3S)-malyl-CoA thioesterase. J. Bacteriology 192, 1249–1258. https://doi.org/10.1128/JB.01267-09.

Fierer, N., Strickland, M.S., Liptzin, D., Bradford, M.A., Cleveland, C.C., 2009. Global patterns in belowground communities. Ecology Letters 12, 1238–1249.

Finér, L., Helmisaari, H.S., Lõhmus, K., Majdi, H., Brunner, I., Børja, I., Eldhuset, T., Godbold, D., Grebenc, T., Konôpka, B., Kraigher, H., Möttönen, M.R., Ohashi, M., Oleksyn, J., Ostonen, I., Uri, V., Vanguelova, E., 2007. Variation in fine root biomass of three European tree species: beech (*Fagus sylvatica* L.), Norway spruce (*Picea abies* L. Karst.), and Scots pine (*Pinus sylvestris* L.). Plant Biosyst. 141, 394–405. https://doi.org/10.1080/11263500701625897.

Finzi, A.C., Breemen, N. Van, Canham, C.D., 1998. Canopy tree-soil interactions within temperate forests: species effects on soil carbon and nitrogen. Ecological Appl. 8, 440–446. https://doi.org/10.2307/2641083.

Fischer, M., Bossdorf, O., Gockel, S., Hänsel, F., Hemp, A., Hessenmöller, D., Korte, G., Nieschulze, J., Pfeiffer, S., Prati, D., Renner, S., Schöning, I., Schumacher, U., Wells, K., Buscot, F., Kalko, E.K.V., Linsenmair, K.E., Schulze, E.D., Weisser, W.W., 2010. Implementing large-scale and long-term functional biodiversity research: the Biodiversity Exploratories. Basic and Applied Ecology 11, 473–485. https://doi.org/10.1016/j.baae.2010.07.009.

Fuchs, G., 2011. Alternative pathways of carbon dioxide fixation: insights into the early evolution of life? Annual Review of Microbiology 65, 631–658.

Guo, X., Meng, M., Zhang, J., Chen, H.Y.H., 2016. Vegetation change impacts on soil organic carbon chemical composition in subtropical forests. Scientific Reports 6, 1–9.

Hackl, E., Pfeffer, M., Donat, C., Bachmann, G., Zechmeister-Boltenstern, S., 2005. Composition of the microbial communities in the mineral soil under different types of natural forest. Soil Biol. Biochem. 37, 661–671. https://doi.org/10.1016/j.soilbio.2004.08.023.

Hair, J., Black, W.C., Babin, B.J., Anderson, R.E., 2014. In: Multivariate Data Analysis, seventh ed., pp. 200–201 Upper Saddle River, New Jersey.
Hakobyan, A., Liesack, W., 2020. Unexpected metabolic versatility among type II methanotrophs in the Alphaproteobacteria. Biological Chemistry 401, 1469–1477. https://doi.org/10.1515/hsz-2020-0200.
Hanada, S., 2014. The phylum Chloroflexi, the family *Chloroflexaceae*, and the related phototrophic families *Oscillochloridaceae* and *Roseiflexaceae*. In: Rosenberg, E., DeLong, E.F., Lory, S., Stackebrandt, E., Thompson, F. (Eds.), The Prokaryotes. Springer, Berlin, Heidelberg, pp. 515–532. https://doi.org/10.1007/978-3-642-38954-2_165.
Hart, K.M., Oppenheimer, S.F., Moran, B.W., Allen, C.C.R., Kouloumbos, V., Simpson, A. J., Kulakov, L.A., Barron, L., Kelleher, B.P., 2013. CO_2 uptake by a soil microcosm. Soil Biol. Biochem. 57, 615–624. https://doi.org/10.1016/j.soilbio.2012.10.036.
Herrmann, M., Hädrich, A., Küsel, K., 2012. Predominance of thaumarchaeal ammonia oxidizer abundance and transcriptional activity in an acidic fen. Environ. Microbiology 14, 3013–3025. https://doi.org/10.1111/j.1462-2920.2012.02882.x.
Herrmann, M., Rusznyák, A., Akob, D.M., Schulze, I., Opitz, S., Totsche, K.U., Küsel, K., 2015. Large fractions of CO_2-fixing microorganisms in pristine limestone aquifers appear to be involved in the oxidation of reduced sulfur and nitrogen compounds. Appl. Environ. Microbiol. 81, 2384–2394. https://doi.org/10.1128/AEM.03269-14.
Hug, L.A., Castelle, C.J., Wrighton, K.C., Thomas, B.C., Sharon, I., Frischkorn, K.R., Williams, K.H., Tringe, S.G., Banfield, J.F., 2013. Community genomic analyses constrain the distribution of metabolic traits across the *Chloroflexi* phylum and indicate roles in sediment carbon cycling. Microbiome 1, 1–17. https://doi.org/10.1186/2049-2618-1-22.
Hügler, M., Sievert, S.M., 2011. Beyond the Calvin cycle: autotrophic carbon fixation in the ocean. Annual Review of Marine Sci. 3, 261–289. https://doi.org/10.1306/06210404037.
IUSS Working Group WRB, 2015. In: World Reference Base for Soil Resources 2014, Updated 2015. International Soil Classification System for Naming Soils and Creating Legends for Soil Maps, World Soil Resources Reports No. 106. https://doi.org/10.1017/S0014479706394902.
Jobbágy, E.G., Jackson, R.B., 2000. The vertical distribution of soil organic carbon and its relation to climate and vegetation. Ecological Appl. 10, 423–436. https://doi.org/10.1890/1051-0761(2000)010 [0423:TVDOSO]2.0.CO;2.
Joergensen, R.G., Mueller, T., 1996. The fumigation-extraction method to estimate soil microbial biomass: calibration of the kEN value. Soil Biology and Biochemistry 28, 25–31. https://doi.org/10.1016/0038-0717(95)00101-8.
Joly, F.X., Milcu, A., Scherer-Lorenzen, M., Jean, L.K., Bussotti, F., Dawud, S.M., Müller, S., Pollastrini, M., Raulund-Rasmussen, K., Vesterdal, L., Hättenschwiler, S., 2017. Tree species diversity affects decomposition through modified micro-environmental conditions across European forests. New Phytologist 214, 1281–1293. https://doi.org/10.1111/nph.14452.
Kaiser, K., Wemheuer, B., Korolkow, V., Wemheuer, F., Nacke, H., Schöning, I., Schrumpf, M., Daniel, R., 2016. Driving forces of soil bacterial community structure, diversity, and function in temperate grasslands and forests. Scientific Reports 6, 1–12.
Khlifa, R., Paquette, A., Messier, C., Reich, P.B., Munson, A.D., 2017. Do temperate tree species diversity and identity influence soil microbial community function and composition? Ecology and Evolution 7, 7965–7974. https://doi.org/10.1002/ece3.3313.
Klatt, C.G., Liu, Z., Ludwig, M., Kühl, M., Jensen, S.I., Bryant, D.A., Ward, D.M., 2013. Temporal metatranscriptomic patterning in phototrophic *Chloroflexi* inhabiting a microbial mat in a geothermal spring. The ISME Journal 7, 1775–1789. https://doi.org/10.1038/ismej.2013.52.
Klindworth, A., Pruesse, E., Schweer, T., Peplies, J., Quast, C., Horn, M., Glöckner, F.O., 2013. Evaluation of general 16S ribosomal RNA gene PCR primers for classical and next-generation sequencing-based diversity studies. Nucleic Acids Res. 41, 1–11.
Kornberg, H.L., 1965. Anaplerotic sequences in microbial metabolism. Angewandte Chemie International Edition 4, 558–565. https://doi.org/10.1002/anie.196505581.
Kragelund, C., Levantesi, C., Borger, A., Thelen, K., Eikelboom, D., Tandoi, V., Kong, Y., Van Der Waarde, J., Krooneman, J., Rossetti, S., Thomsen, T.R., Nielsen, P.H., 2007. Identity, abundance and ecophysiology of filamentous *Chloroflexi* species present in activated sludge treatment plants. FEMS Microbiology Ecology 59, 671–682. https://doi.org/10.1111/j.1574-6941.2006.00251.x.
Kragelund, C., Thomsen, T.R., Mielczarek, A.T., Nielsen, P.H., 2011. Eikelboom's morphotype 0803 in activated sludge belongs to the *genus Caldilinea* in the phylum *Chloroflexi*. FEMS Microbiology Ecology 76, 451–462. https://doi.org/10.1111/j.1574-6941.2011.01065.x.
Kravchenko, I.K., Tikhonova, E.N., Ulanova, R.V., Menko, E.V., Sukhacheva, M.V., 2019. Effect of temperature on litter decomposition, soil microbial community structure and biomass in a mixed-wood forest in European Russia. Current Science 116, 765–772.
Krebs, H.A., 1941. Carbon dioxide assimilation in heterotrophic organisms. Nature (London) 147, 560–563.
Kremer, K., van Teeseling, M.C.F., von Borzyskowski, L., Bernhardsgrütter, I., van Spanning, R.J.M., Gates, A.J., Remus-Emsermann, M.N.P., Thanbichler, M., Erb, T.J., 2019. Dynamic metabolic rewiring enables efficient acetyl coenzyme A assimilation in *Paracoccus denitrificans*. mBio 10, 1–15. https://doi.org/10.1128/mBio.00805-19.
Lai, Z., Zhang, Y., Liu, J., Wu, B., Qin, S., Fa, K., 2016. Fine-root distribution, production, decomposition, and effect on soil organic carbon of three revegetation shrub species in northwest China. Forest Ecology and Management 359, 381–388. https://doi.org/10.1016/j.foreco.2015.04.025.
Lee, H.J., Jeong, S.E., Kim, P.J., Madsen, E.L., Jeon, C.O., 2015a. High resolution depth distribution of Bacteria, Archaea, methanotrophs, and methanogens in the bulk and rhizosphere soils of a flooded rice paddy. Frontiers in Microbiology 6, 1–13.
Lee, K.C.Y., Morgan, X.C., Power, J.F., Dunfield, P.F., Huttenhower, C., Stott, M.B., 2015b. Complete genome sequence of the thermophilic *Acidobacteria, Pyrinomonas methylaliphatogenes* type strain K22T. Stand. Genomic Sci. 10, 1–8.
Liang, C., Amelung, W., Lehmann, J., Kästner, M., 2019. Quantitative assessment of microbial necromass contribution to soil organic matter. Global Change Biology 25, 3578–3590. https://doi.org/10.1111/gcb.14781.
Liddle, K., McGonigle, T., Koiter, A., 2020. Microbe biomass in relation to organic carbon and clay in soil. Soil Syst. 4, 1–10. https://doi.org/10.3390/soilsystems4030041.
Liu, H., Sun, Y., Ramos, K.R.M., Nisola, G.M., Valdehuesa, K.N.G., Lee, W.K., Park, S.J., Chung, W.J., 2013. Combination of Entner-Doudoroff pathway with MEP increases isoprene production in engineered Escherichia coli. PLoS One 8, 1–8.
Liu, Z., Sun, Y., Zhang, Y., Feng, W., Lai, Z., Fa, K., Qin, S., 2018. Metagenomic and 13C tracing evidence for autotrophic atmospheric carbon absorption in a semiarid desert. Soil Biol. Biochem. 125, 156–166. https://doi.org/10.1016/j.soilbio.2018.07.012.
Liu, M., Sui, X., Hu, Y., Feng, F., 2019a. Microbial community structure and the relationship with soil carbon and nitrogen in an original Korean pine forest of Changbai Mountain, China. BMC Microbiol. 19, 1–14. https://doi.org/10.1186/s12866-019-1584-6.
Liu, X., Lin, T.-C., Vadeboncoeur, M.A., Yang, Z., Chen, S., Xiong, D., Xu, C., Li, Y., Yang, Y., 2019b. Root litter inputs exert greater influence over soil C than does aboveground litter in a subtropical natural forest. Plant and Soil 444, 489–499.
Lladó, S., López-Mondéjar, R., Baldrian, P., 2017. Forest soil bacteria: diversity, involvement in ecosystem processes, and response to global change. Microbiol. Mol. Biol. Rev. 81, 1–27. https://doi.org/10.1128/MMBR.00063-16.
López-Mondéjar, R., Voříšková, J., Větrovský, T., Baldrian, P., 2015. The bacterial community inhabiting temperate deciduous forests is vertically stratified and undergoes seasonal dynamics. Soil Biology and Biochemistry 87, 43–50. https://doi.org/10.1016/j.soilbio.2015.04.008.
Loy, A., Lehner, A., Lee, N., Adamczyk, J., Meier, H., Ernst, J., Schleifer, K.H., Wagner, M., 2002. Oligonucleotide microarray for 16S rRNA gene-based detection of all recognized lineages of sulfate-reducing prokaryotes in the environment. Appl. Environ. Microbiol. 68, 5064–5081.
Lynn, T.M., Ge, T., Yuan, H., Wei, X., Wu, X., Xiao, K., Kumaresan, D., Yu, S.S., Wu, J., Whiteley, A.S., 2017. Soil carbon-fixation rates and associated bacterial diversity and abundance in three natural ecosystems. Microbial Ecology 73, 645–657.
Macalady, J.L., Mcmillan, A.M.S., Dickens, A.F., Tyler, S.C., Scow, K.M., 2002. Population dynamics of type I and II methanotrophic bacteria in rice soils. Environ. Microbiol. 4, 148–157.
Martins, P.D., Frank, J., Mitchell, H., Markillie, L.M., Wilkins, M.J., 2019. Wetland sediments host diverse microbial taxa capable of cycling alcohols. Appl. Environ. Microbiol. 85, 1–15. https://doi.org/10.1128/AEM.00189-19.
McGonigle, J.M., Lang, S.Q., Brazelton, W.J., 2019. Genomic evidence for formate metabolism by *Chloroflexi* as the key to unlocking deep carbon in lost city microbial ecosystems. App. Environ. Microbiol. 86, 1–12. https://doi.org/10.1101/831230.
Meyer, N., Welp, G., Amelung, W., 2018. The temperature sensitivity (Q_{10}) of soil respiration: controlling factors and spatial prediction at regional scale based on environmental soil classes. Global Biogeochemical Cycles 32, 306–323. https://doi.org/10.1002/2017GB005644.
Milanese, A., Mende, D.R., Paoli, L., Salazar, G., Ruscheweyh, H.J., Cuenca, M., Hingamp, P., Alves, R., Costea, P.I., Coelho, L.P., Schmidt, T.S.B., Almeida, A., Mitchell, A.L., Finn, R.D., Huerta-Cepas, J., Bork, P., Zeller, G., Sunagawa, S., 2019. Microbial abundance, activity and population genomic profiling with mOTUs2. Nature Communications 10, 1014. https://doi.org/10.1038/s41467-019-08844-4.
Miltner, A., Kopinke, F.D., Kindler, R., Selesi, D., Hartmann, A., Kästner, M., 2005. Non-phototrophic CO_2 fixation by soil microorganisms. Plant Soil 269, 193–203. https://doi.org/10.1007/s11104-004-0483-1.
Moreno, E., Moriyo, I., 2006. Introduction to the Proteobacteria. In: Dworkin, M., Falkow, S., Rosenberg, E., Schleifer, K.H., Stackebrandt, E. (Eds.), The Prokaryotes. Springer, New York, pp. 315–456. https://doi.org/10.1007/0-387-30745-1_1.
Mook, W.G., Van der Plicht, J., 1999. Reporting ^{14}C activities and concentrations. Radiocarbon 41, 227–239.
Nacke, H., Goldmann, K., Schöning, I., Pfeiffer, B., Kaiser, K., 2016. Fine spatial scale variation of soil microbial communities under European beech and Norway spruce. Front. Microbiol. 7, 1–14. https://doi.org/10.3389/fmicb.2016.02067.
Nel, J.A., Cramer, M.D., 2019. Soil microbial anaplerotic CO_2 fixation in temperate soils. Geoderma 335, 170–178. https://doi.org/10.1016/j.geoderma.2018.08.014.
Nguyen, C., 2003. Rhizodeposition of organic C by plants: mechanisms and controls. Agronomie 23, 375–396.
Nguyen, D.T.N., Lee, O.K., Nguyen, T.T., Lee, E.Y., 2021. Type II methanotrophs: a promising microbial cell-factory platform for bioconversion of methane to chemicals. Biotechnol. Adv. 47, 107700. https://doi.org/10.1016/j.biotechadv.2021.107700.
Nierychlo, M., Miłobędzka, A., Petriglieri, F., McIlroy, B., Nielsen, P.H., McIlroy, S.J., 2019. The morphology and metabolic potential of the *Chloroflexi* in full-scale activated sludge wastewater treatment plants. FEMS Microbiol. Ecol. 95, 1–11.
Nowak, M.E., Beulig, F., Von Fischer, J., Muhr, J., Küsel, K., Trumbore, S.E., 2015. Autotrophic fixation of geogenic CO_2 by microorganisms contributes to soil organic matter formation and alters isotope signatures in a wetland mofette. Biogeosciences 12, 7169–7183. https://doi.org/10.5194/bg-12-7169-2015.
Okabe, S., Kindaichi, T., Ito, T., 2005. Fate of ^{14}C-labeled microbial products derived from nitrifying bacteria in autotrophic nitrifying biofilms. Appl. Environ. Microbiol. 71, 3987–3994. https://doi.org/10.1128/AEM.71.7.3987-3994.2005.

Oksanen, J., Kindt, R., Legendre, P., O'Hara, B., Simpson, G.L., Solymos, P.M., Stevens, M.H.H., Wagner, H., 2008. The Vegan Package. Community Ecology Package, p. 190.
Ostonen, I., Püttsepp, Ü., Biel, C., Alberton, O., Bakker, M.R., Lõhmus, K., Majdi, H., Metcalfe, D., Olsthoorn, A.F.M., Pronk, A., Vanguelova, E., Weih, M., Brunner, I., 2007. Specific root length as an indicator of environmental change. Plant Biosystems 141, 426–442. https://doi.org/10.1080/11263500701626069.
Owen, O.E., Kalhan, S.C., Hanson, R.W., 2002. The key role of anaplerosis and cataplerosis for citric acid cycle function. J. Biol. Chem. 277, 30409–30412.
Pierson, B.K., Castenholz, R.W., 1992. The family Chloroflexaceae. In: Balows, A., Trüper, H.G., Dworkin, M., Harder, W., Schleifer, K.H. (Eds.), The Prokaryotes. Springer, New York, pp. 3754–3774. https://doi.org/10.1007/978-1-4757-2191-1_44.
Quast, C., Pruesse, E., Yilmaz, P., Gerken, J., Schweer, T., Yarza, P., Peplies, J., Glöckner, F.O., 2013. The SILVA ribosomal RNA gene database project: improved data processing and web-based tools. Nucleic Acids Res. 41, 590–596. https://doi.org/10.1093/nar/gks1219.
Rasse, D.P., Longdoz, B., Ceulemans, R., 2001. TRAP: a modelling approach to below-ground carbon allocation in temperate forests. Plant Soil 229, 281–293.
Rasse, D., Rumpel, C., Dignac, M., 2005. Is soil carbon mostly root carbon? Mechanisms for a specific stabilisation. Plant Soil 269, 341–356.
Rastogi, M., Singh, S., Pathak, H., 2002. Emission of carbon dioxide from soil. Current Sci. 82, 510–517.
Romano, A.H., Conway, T., 1996. Evolution of carbohydrate metabolic pathways. Res. Microbiol. 147, 448–455. https://doi.org/10.1016/0923-2508(96)83998-2.
Saini, R., Kapoor, R., Kumar, R., Siddiqi, T.O., Kumar, A., 2011. CO_2 utilizing microbes - a comprehensive review. Biotechnol. Adv. 29, 949–960. https://doi.org/10.1016/j.biotechadv.2011.08.009.
Šantrůčková, H., Kotas, P., Bárta, J., Urich, T., Čapek, P., Palmtag, J., Eloy Alves, R.J., Biasi, C., Diáková, K., Gentsch, N., Gittel, A., Guggenberger, G., Hugelius, G., Lashchinsky, N., Martikainen, P.J., Mikutta, R., Schleper, C., Schnecker, J., Schwab, C., Shibistova, O., Wild, B., Richter, A., 2018. Significance of dark CO_2 fixation in arctic soils. Soil Biol. Biochem. 119, 11–21. https://doi.org/10.1016/j.soilbio.2017.12.021.
Schloss, P.D., Westcott, S.L., Ryabin, T., Hall, J.R., Hartmann, M., Hollister, E.B., Lesniewski, R.A., Oakley, B.B., Parks, D.H., Robinson, C.J., Sahl, J.W., Stres, B., Thallinger, G.G., Van Horn, D.J., Weber, C.F., 2009. Introducing mothur: open-source, platform-independent, community-supported software for describing and comparing microbial communities. App. Environ. Microbiol. 75, 7537–7541.
Schöning, I., Solly, E., Klötzing, T., Trumbore, S., Schrumpf, M., 2013a. MinSoil 2011 mineral soil respiration. Version 3. In: Biodiversity Exploratories Information System. Dataset. https://www.bexis.uni-jena.de/ddm/data/Showdata/17026#information.
Schöning, I., Solly, E., Klötzing, T., Trumbore, S., Schrumpf, M., 2013b. MinSoil 2011 mineral soil enzymes. Version 3. In: Biodiversity Exploratories Information System. Dataset. https://www.bexis.uni-jena.de/ddm/data/Showdata/17166#information.
Schöning, I., Apostolakis, A., Klötzing, T., Schrumpf, M., Trumbore, S., 2019. MinSoil 2017 – soil carbon and nitrogen concentrations. Version 10. In: Biodiversity Exploratories Information System. Dataset. https://www.bexis.uni-jena.de/ddm/data/Showdata/23846#information.
Sewell, H., Kaster, A.-K., Spormann, A., 2017. Homoacetogenesis in deep-sea *Chloroflexi*, as inferred by single-cell genomics, provides a link to reductive dehalogenation in terrestrial *Dehalococcoidetes*. Am. Soc. Microbiol. 8, 1–22.
Speirs, L.B.M., Rice, D.T.F., Petrovski, S., Seviour, R.J., 2019. The phylogeny, biodiversity, and ecology of the *Chloroflexi* in activated sludge. Front. Microbiol. 10, 1–19.
Solly, E., Schöning, I., Klötzing, T., Schrumpf, M., 2013. MinSoil 2011 root decomposition. Version 2. In: Biodiversity Exploratories Information System. Dataset. https://www.bexis.uni-jena.de/ddm/data/Showdata/16666#information.
Spohn, M., Müller, K., Höschen, C., Mueller, C.W., Marhan, S., 2019. Dark microbial CO_2 fixation in temperate forest soils increases with CO_2 concentration. Global Change Biol. 26, 1926–1935. https://doi.org/10.1111/gcb.14937.
Steinhof, A., Altenburg, M., Machts, H., 2017. Sample preparation at the Jena ^{14}C laboratory. Radiocarbon 59, 815–830. https://doi.org/10.1017/RDC.2017.50.
Su, Y., He, Z., Yang, Y., Jia, S., Yu, M., Chen, X., Shen, A., 2020. Linking soil microbial community dynamics to straw-carbon distribution in soil organic carbon. Scientific Reports 10, 1–12. https://doi.org/10.1038/s41598-020-62198-2.
Tcherkez, G.G.B., Farquhar, G.D., Andrews, T.J., 2006. Despite slow catalysis and confused substrate specificity, all ribulose bisphosphate carboxylases may be nearly perfectly optimized. Proc. Natl. Acad. Sci. U.S.A. 103, 7246–7251. https://doi.org/10.1073/pnas.0600605103.
Tefs, C., Gleixner, G., 2012. Importance of root derived carbon for soil organic matter storage in a temperate old-growth beech forest - evidence from C, N and ^{14}C content. For. Ecol. Manag. 263, 131–137. https://doi.org/10.1016/j.foreco.2011.09.010.
Thakur, S., Sen, A., 2016. Comparative analysis of metabolic machinery of Frankia along with other selected actinobacteria. Symbiosis 70, 59–68. https://doi.org/10.1007/s13199-016-0410-2.
Thieme, L., Graeber, D., Hofmann, D., Bischoff, S., Schwarz, M.T., Steffen, B., Meyer, U.N., Kaupenjohann, M., Wilcke, W., Michalzik, B., Siemens, J., 2019. Dissolved organic matter characteristics of deciduous and coniferous forests with variable management: different at the source, aligned in the soil. Biogeosciences 16, 1411–1432.
Thoms, C., Gattinger, A., Jacob, M., Thomas, F.M., Gleixner, G., 2010. Direct and indirect effects of tree diversity drive soil microbial diversity in temperate deciduous forest. Soil Biol. Biochem. 42, 1558–1565. https://doi.org/10.1016/j.soilbio.2010.05.030.
Tolli, J., King, G.M., 2005. Diversity and structure of bacterial chemolithotrophic communities in pine forest and agroecosystem soils. Appl. Environ. Microbiol. 71, 8411–8418. https://doi.org/10.1128/AEM.71.12.8411-8418.2005.
Trumbore, S., 2009. Radiocarbon and soil carbon dynamics. Annu. Rev. Earth Planet Sci. 37, 47–66. https://doi.org/10.1146/annurev.earth.36.031207.124300.
Urbanová, M., Šnajdr, J., Baldrian, P., 2015. Composition of fungal and bacterial communities in forest litter and soil is largely determined by dominant trees. Soil Biol. Biochem. 84, 53–64. https://doi.org/10.1016/j.soilbio.2015.02.011.
Uroz, S., Ioannidis, P., Lengelle, J., Cébron, A., Morin, E., Buée, M., Martin, F., 2013. Functional assays and metagenomic analyses reveals differences between the microbial communities inhabiting the soil horizons of a Norway spruce plantation. PLoS One 8, 1–13. https://doi.org/10.1371/journal.pone.0055929.
Vance, E.D., Brookes, P.C., Jenkinson, D.S., 1987. An extraction method for measuring soil microbial biomass C. Soil Biol. Biochem. 19, 703–707. https://doi.org/10.1016/0038-0717(87)90052-6.
Vesterdal, L., Clarke, N., Sigurdsson, B.D., Gundersen, P., 2013. Do tree species influence soil carbon stocks in temperate and boreal forests? For. Ecol. Manag. 309, 4–18. https://doi.org/10.1016/j.foreco.2013.01.017.
Vesterdal, L., Schmidt, I.K., Callesen, I., Nilsson, L.O., Gundersen, P., 2008. Carbon and nitrogen in forest floor and mineral soil under six common European tree species. For. Ecol. Manag. 255, 35–48. https://doi.org/10.1016/j.foreco.2007.08.015.
Veum, K.S., Goyne, K.W., Kremer, R.J., Miles, R.J., Sudduth, K.A., 2014. Biological indicators of soil quality and soil organic matter characteristics in an agricultural management continuum. Biogeochemistry 117, 81–99. https://doi.org/10.1007/s10533-013-9868-7.
Vuillemin, A., Kerrigan, Z., D'Hondt, S., Orsi, W.D., 2020. Exploring the abundance, metabolic potential and gene expression of subseafloor *Chloroflexi* in million-year-old oxic and anoxic abyssal clay. FEMS Microbiol. Ecol. 96, 1–14.
Wallander, H., Göransson, H., Rosengren, U., 2004. Production, standing biomass and natural abundance of ^{15}N and ^{13}C in ectomycorrhizal mycelia collected at different soil depths in two forest types. Oecologia 139, 89–97. https://doi.org/10.1007/s00442-003-1477-z.
Wasmund, K., Schreiber, L., Lloyd, K.G., Petersen, D.G., Schramm, A., Stepanauskas, R., Jørgensen, B.B., Adrian, L., 2014. Genome sequencing of a single cell of the widely distributed marine subsurface Dehalococcoidia, phylum *Chloroflexi*. The ISME J. 8, 383–397. https://doi.org/10.1038/ismej.2013.143.
Werner, R.A., Brand, W.A., 2001. Referencing strategies and techniques in stable isotope ratio analysis. Rapid Communications in Mass Spectrometry 15, 501–519.
Wood, A.P., Aurikko, J.P., Kelly, D.P., 2004. A challenge for 21st century molecular biology and biochemistry: what are the causes of obligate autotrophy and methanotrophy? FEMS Microbiol. Rev. 28, 335–352. https://doi.org/10.1016/j.femsre.2003.12.001.
Wu, X., Ge, T., Yuan, H., Li, B., Zhu, H., Zhou, P., Sui, F., O'Donnell, A.G., Wu, J., 2014. Changes in bacterial CO_2 fixation with depth in agricultural soils. Appl. Microbiol. Biotechnol. 98, 2309–2319. https://doi.org/10.1007/s00253-013-5179-0.
Wu, X., Ge, T., Wang, W., Yuan, H., Wegner, C.E., Zhu, Z., Whiteley, A.S., Wu, J., 2015. Cropping systems modulate the rate and magnitude of soil microbial autotrophic CO_2 fixation in soil. Front. Microbiol. 6, 1–10. https://doi.org/10.3389/fmicb.2015.00379.
Xia, Y., Kong, Y., Nielsen, P.H., 2007. In situ detection of protein-hydrolysing microorganisms in activated sludge. FEMS Microbiol. Ecol. 60, 156–165.
Xia, Y., Wang, Yubo, Wang, Yi, Chin, F.Y.L., Zhang, T., 2016. Cellular adhesiveness and cellulolytic capacity in *Anaerolineae* revealed by omics-based genome interpretation. Biotechnol. Biofuels 9, 1–13. https://doi.org/10.1186/s13068-016-0524-z.
Xiao, H., Li, Z., Chang, X., Deng, L., Nie, X., Liu, C., Liu, L., Jiang, J., Chen, J., Wang, D., 2018. Microbial CO_2 assimilation is not limited by the decrease in autotrophic bacterial abundance and diversity in eroded watershed. Biol. Fertil. Soils 54, 595–605. https://doi.org/10.1007/s00374-018-1284-7.
Yang, S., Matsen, J.B., Konopka, M., Green-Saxena, A., Clubb, J., Sadilek, M., Orphan, V.J., Beck, D., Kalyuzhnaya, M.G., 2013. Global molecular analyses of methane metabolism in methanotrophic alphaproteobacterium, methylosinus trichosporium OB3b. Part II. metabolomics and 13C-labeling study. Front. Microbiol. 4, 1–13.
Zhang, Z., Wang, W., Qi, J., Zhang, H., Tao, F., Zhang, R., 2019. Priming effects of soil organic matter decomposition with addition of different carbon substrates. J. Soils Sediments 19, 1171–1178. https://doi.org/10.1007/s11368-018-2103-3.

Dark CO_2 fixation in temperate beech and pine forest soils

Rachael Akinyede[a,b], Martin Taubert[a], Marion Schrumpf[b], Susan Trumbore[b], Kirsten Küsel[a,c]

[a]Aquatic Geomicrobiology, Institute of Biodiversity, Friedrich Schiller University Jena, Dornburger Str. 159, 07743 Jena, Germany

[b]Department for Biogeochemical Processes, Max Planck Institute for Biogeochemistry, Hans-Knöll Str. 10, 07745 Jena, Germany

[c]German Centre for Integrative Biodiversity Research (iDiv) Halle-Jena-Leipzig, Puschstraße 4, 04103 Leipzig, Germany

Correspondence: Kirsten Küsel, Friedrich Schiller University Jena, Dornburger Str. 159, 07743 Jena, Germany. Email: kirsten.kuesel@uni-jena.de

Results

Supplementary figures and table

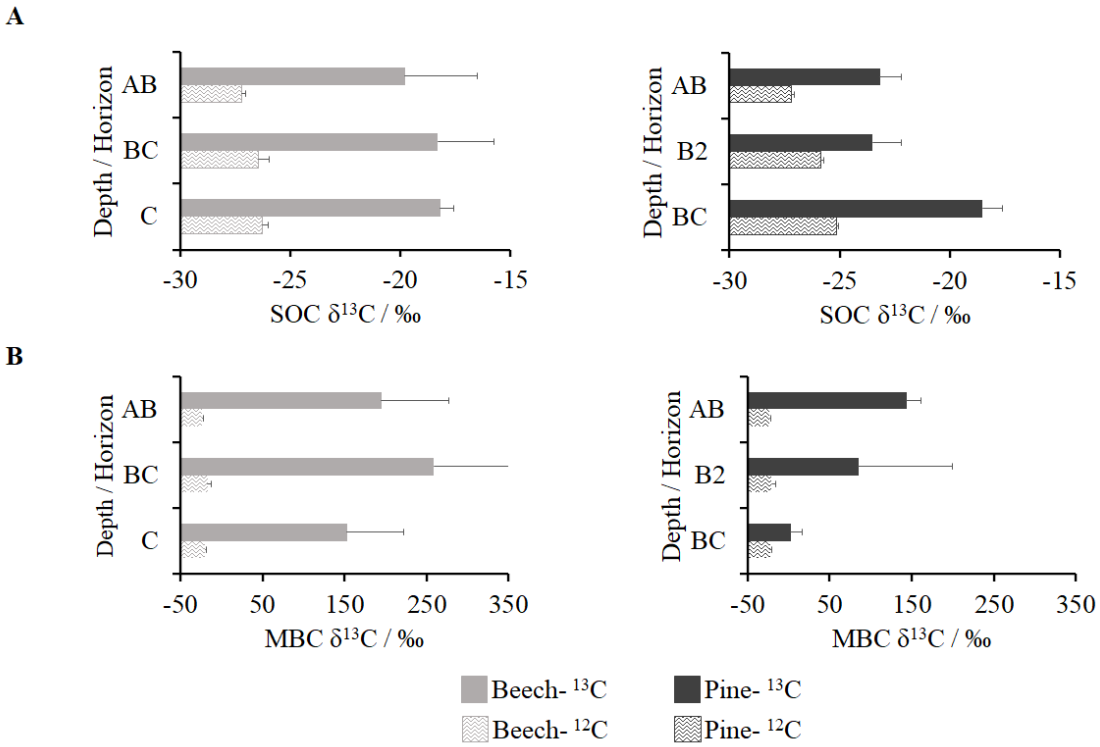

Figure S1: $\delta^{13}C$ signals of SOC and MBC in soil incubations supplemented with 2% $^{13}CO_2$. Shown are (A) ^{13}C signal in SOC and (B) ^{13}C signal in MBC after 7 days of incubation with 2% CO_2 in beech (light gray bars) and pine (dark gray bars) soils. Treatment incubations with ^{13}C labelled CO_2 are denoted with filled symbols while control incubations with ^{12}C are denoted by patterned symbols. Error bars indicate the standard deviation of incubations from three replicate soil cores.

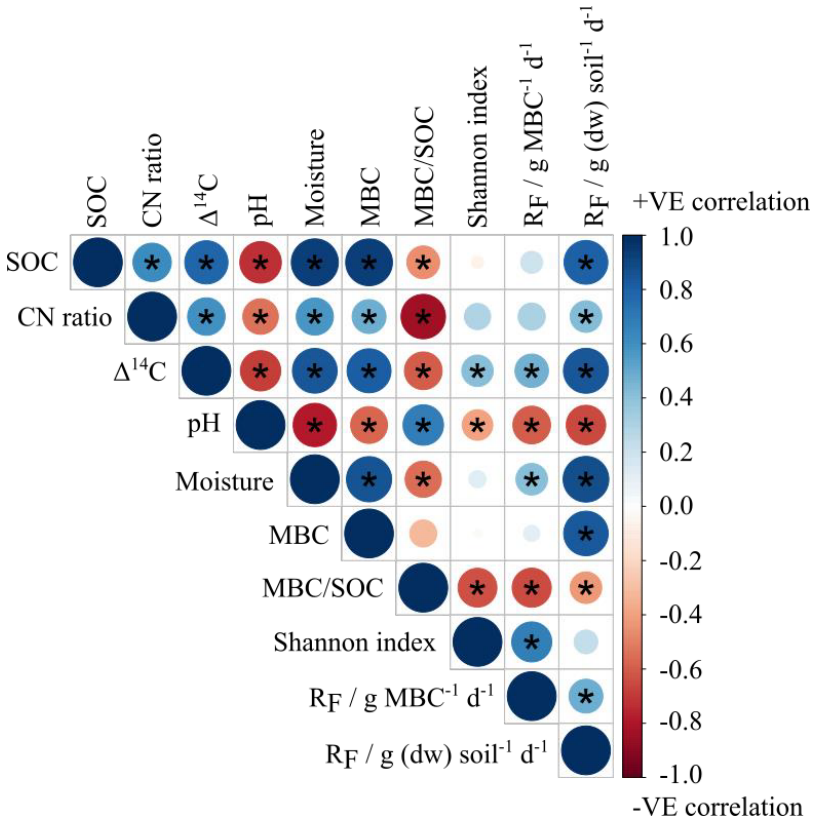

Figure S2A: Correlation between dark CO_2 fixation rates and soil abiotic and biotic properties in beech and pine soils. Shown are multiple correlations between measured dark CO_2 fixation rates (per gram dry weight (dw) of soil and per gram of MBC and some measured soil geochemical properties (SOC, C/N ratio, $\Delta^{14}C$, pH, moisture content, MBC, MBC/SOC, and Shannon index) obtained from the beech and pine soil plots of the Schorfheide-Chorin Exploratory. Red colours denote negative correlation and blue colours denote positive correlation. The intensity of the colours and size of the circles represent the strength of the correlation. R_F / g (dw) $soil^{-1}$ d^{-1} and R_F / g MBC^{-1} d^{-1} denote fixation rates normalised to soil dry weight and MBC respectively. Correlation is by Pearson's ranking, * denotes $P < 0.05$.

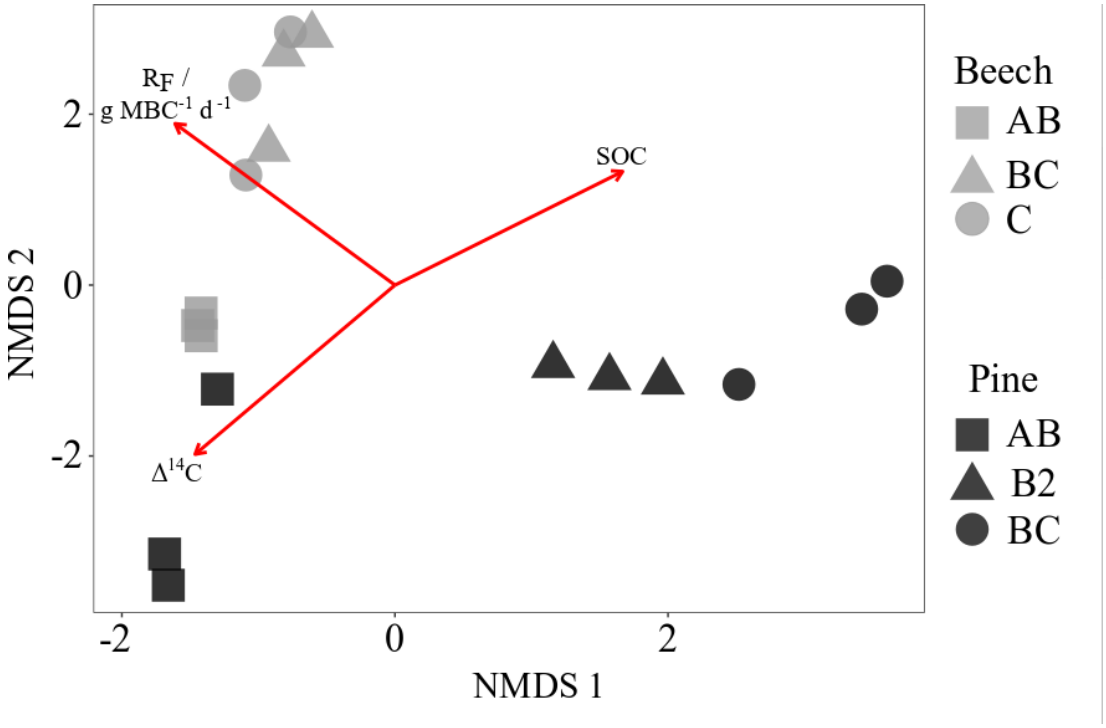

Figure S2B: Correlation of microbial community structure with dark CO_2 fixation rates and the most correlated soil abiotic properties in beech and pine soils. NMDS plot is based on OTU level analysis (Bray Curtis dissimilarities) of bacterial 16S rRNA gene amplicons generated by Illumina Miseq sequencing. Plot shows significant statistical correlation of the bacterial community structure with CO_2 fixation rates per gram of MBC; R_F /g MBC^{-1} d^{-1} (R^2 = 0.99, P = 0.001), with SOC (R^2 = 0.72, P = 0.001) and with $\Delta^{14}C$ (R^2 = 0.97, P = 0.001), indicated by red arrows. The beech soil samples are represented by light gray symbols while the pine soil samples are denoted by dark gray symbols. Samples at each depth are represented by three data points which are distinguished by the different symbols.

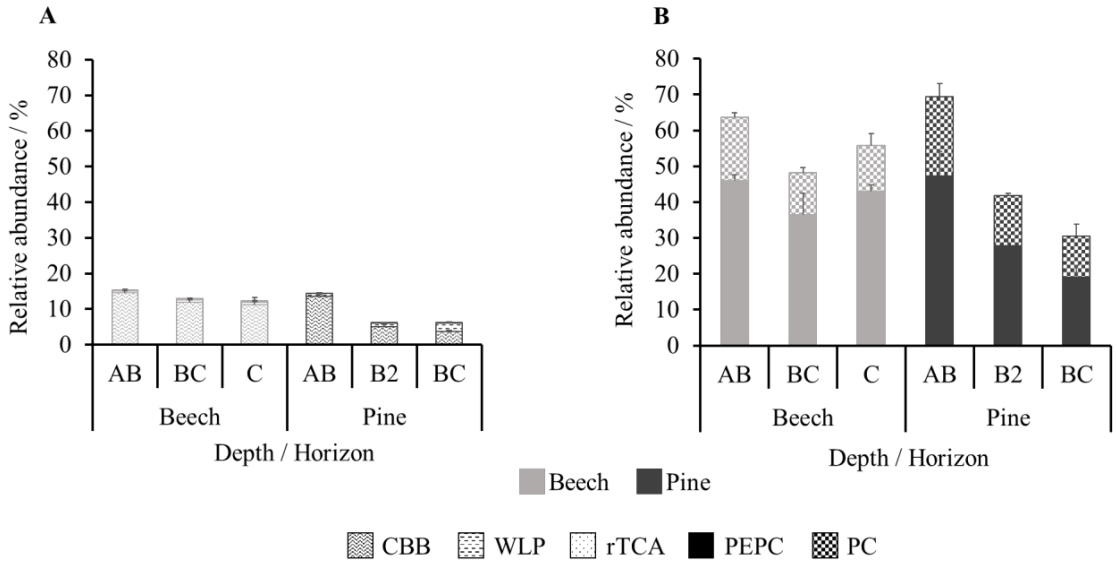

Figure S3: Predicted relative abundance of carboxylase genes involved in autotrophic and heterotrophic CO_2 fixation in the bulk soil. Shown is the relative abundance of genes coding for the key enzymes involved in (A) autotrophic CO_2 fixation and (B) heterotrophic CO_2 fixation, predicted by PICRUSt2 analysis of bacterial 16S rRNA gene amplicon sequence data in the bulk soils of beech and pine soil plots across 1 m depth. Phosphoenolpyruvate carboxylase (PEPC) and Pyruvate carboxylase (PC) genes are reported for heterotrophic CO_2 fixation by anaplerotic reactions. Key genes coding for RuBisCO enzymes, carbon monoxide dehydrogenase and acetyl COA synthase enzymes, and ATP citrate lyase enzyme are reported for autotrophic CO_2 fixation by the CBB, WLP, and rTCA pathway respectively. Gene abundances are expressed as % of bacterial 16S rRNA gene copies in soil. Error bars indicate the standard deviation of bulk soil samples from three replicate soil cores.

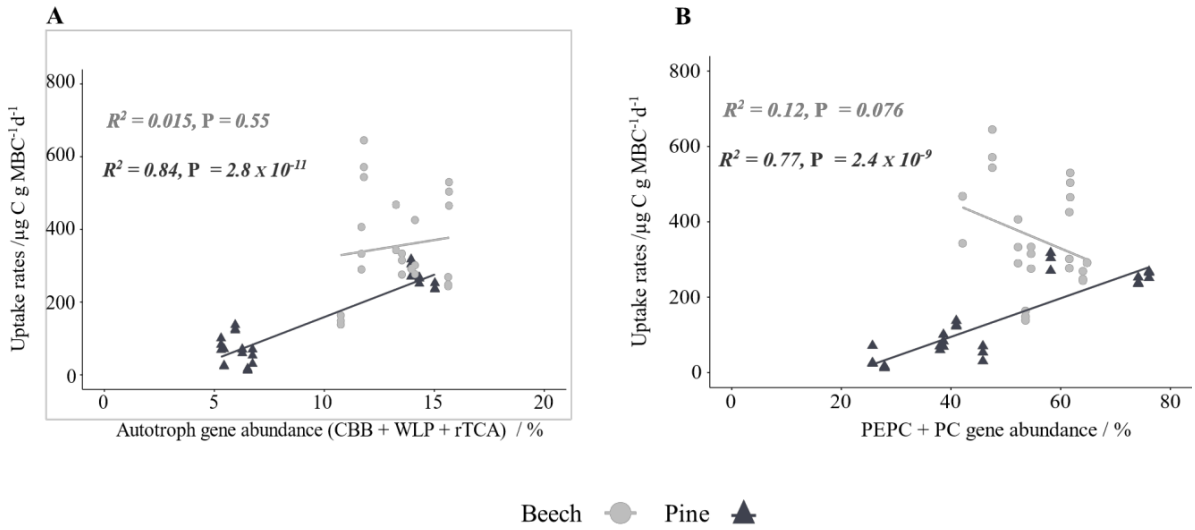

Figure S4: Correlation of predicted CO_2 fixing genes (based on PICRUST2 predictions) with measured uptake rates in beech and pine soils. Shown are correlations between dark CO_2 fixation rates per gram of MBC and (A) CO_2 fixing autotroph gene abundances (CBB, WLP, and rTCA pathway) and (B) CO_2 fixing heterotroph gene abundance (Phosphoenolpyruvate carboxylase (PEPC) and Pyruvate carboxylase (PC) genes) measured in bulk soils of the beech and pine soil plots across 1 m depth profiles. Gene abundances are expressed as % of bacterial 16S rRNA gene copies in soil.

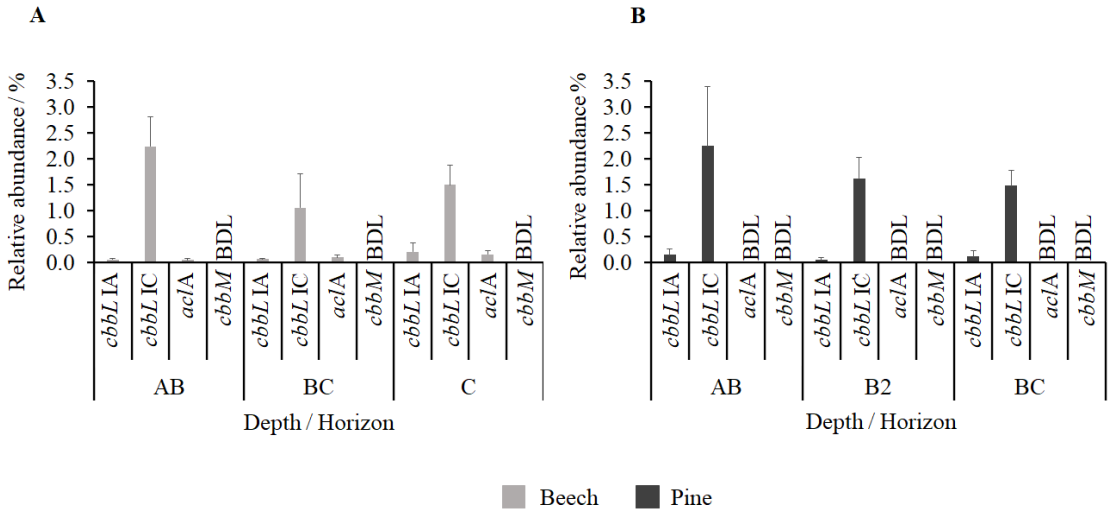

62

63 ***Figure S5: Measured relative abundance of RuBisCO (cbbL IA, cbbL IC,* and *cbbM) and***

64 ***ATP citrate lyase (aclA) marker genes involved in dark CO_2 fixation in the bulk soil.***

65 Shown are the *cbbL* IA, *cbbL* IC, *cbbM,* (CBB pathway), and *aclA* (rTCA pathway) gene

66 abundance in soils of the beech (A) and pine (B) plots across 1 m depth prior to incubation

67 acquired by qPCR. Gene abundances are expressed as % of bacterial 16S rRNA gene copies

68 in soil. Error bars indicate the standard deviation of bulk soil samples from three replicate soil

69 cores. BDL denotes gene copies below detection limit.

70

Table S1: Quantification of 16S rRNA, cbbL IA, cbbL IC, cbbM, and aclA marker genes. Shown are *cbbL* IA, *cbbL* IC, *cbbM,* and *aclA* marker genes expressed per gram dry weight of soil and (g dw^{-1}) their ratios (*cbbL* IA, *cbbL* IC, and *aclA* only) expressed as a percentage (%) of total bacterial 16S rRNA gene copies for both the beech and pine soil plots. Data is based on quantitative PCR (qPCR) analysis. Errors indicate the standard deviation of the mean of three replicate soil cores in both soil plots.

Plot (Dominant tree spp.)	Beech			Pine		
Depth (Horizon)	AB	BC	C	AB	B2	BC
cbbL IA (copies/g dw^{-1})	$1.04 \times 10^7 \pm 3.43 \times 10^6$	$1.99 \times 10^6 \pm 1.29 \times 10^6$	$1.68 \times 10^6 \pm 9.99 \times 10^5$	$2.84 \times 10^7 \pm 2.34 \times 10^7$	$2.13 \times 10^6 \pm 1.35 \times 10^6$	$4.23 \times 10^5 \pm 1.84 \times 10^5$
cbbL IC (copies/g dw^{-1})	$4.41 \times 10^8 \pm 1.08 \times 10^8$	$2.54 \times 10^7 \pm 4.97 \times 10^6$	$1.49 \times 10^7 \pm 6.93 \times 10^6$	$4.05 \times 10^8 \pm 2.69 \times 10^8$	$4.17 \times 10^7 \pm 4.32 \times 10^6$	$3.64 \times 10^6 \pm 1.28 \times 10^6$
cbbM (copies/g dw^{-1})	BDL	BDL	BDL	BDL	BDL	BDL
aclA (copies/g dw^{-1})	$8.68 \times 10^6 \pm 6.59 \times 10^6$	$2.87 \times 10^6 \pm 2.03 \times 10^6$	$1.43 \times 10^6 \pm 5.55 \times 10^6$	BDL	BDL	BDL
cbbL IA / 16S rRNA (%)	0.05 ± 0.02	0.05 ± 0.01	0.20 ± 0.17	0.15 ± 0.10	0.05 ± 0.04	0.11 ± 0.12
cbbL IC / 16S rRNA (%)	2.25 ± 0.56	1.06 ± 0.66	1.50 ± 0.37	2.25 ± 1.14	1.63 ± 0.40	1.48 ± 0.30
aclA / 16S rRNA (%)	0.04 ± 0.03	0.10 ± 0.05	0.16 ± 0.07	BDL	BDL	BDL

BDL: Below Detection Limit.

4 Manuscript 3: Temperature sensitivity of dark CO_2 fixation in temperate forest soils

Authors: Akinyede, R., Taubert, M., Schrumpf, M., Trumbore, S., Küsel, K

Bibliographic information (if published or accepted for publication: Citation): Akinyede, R., Taubert, M., Schrumpf, M., Trumbore, S., Küsel, K., 2022. Temperature sensitivity of dark CO_2 fixation in temperate forest soils. *Biogeosciences* 2, 4011–4028. doi.org/10.5194/bg-19-4011-2022

The candidate is (Please tick the appropriate box.)

☐✓ First author, ☐ Co-first author, ☐ Corresponding author, ☐ Co-author.

Status (if not published; "submitted for publication", "in preparation".): Published.

Authors' contributions (in %) to the given categories of the publication

For this manuscript, I, Akinyede, R, conceptualized the study with help from all co-authors. I designed and conducted the soil sampling and experiments. I performed all isotope measurements, analyzed the data, and produced all figures. I also wrote the manuscript draft. Taubert, M was part of the experimental design, data visualization and discussion, and editing of the manuscript. Schrumpf, M., Trumbore, S., Küsel, K helped with the study and experimental design, as well as reviewed and edited the manuscript draft. My contributions are summarized as follows:

Author	Conceptual	Data analysis	Experimental	Writing the manuscript	Provision of material
Akinyede, R	70	90	85	70	0
Taubert, M	5	10	0	15	0
Schrumpf, M	5	0	0	5	0
Trumbore, S	10	0	0	5	50
Küsel, K	10	0	0	5	50
Others	0	0	15	0	0
Total:	100%	100%	100%	100%	100%

_____ _____

Signature candidate Signature supervisor (member of the Faculty)

Supplementary data for this manuscript can be found at the end of this manuscript draft

Biogeosciences, 19, 4011–4028, 2022
https://doi.org/10.5194/bg-19-4011-2022

Biogeosciences Open Access EGU

Temperature sensitivity of dark CO_2 fixation in temperate forest soils

Rachael Akinyede[1,2], Martin Taubert[1], Marion Schrumpf[2], Susan Trumbore[2], and Kirsten Küsel[1,3]

[1]Aquatic Geomicrobiology, Institute of Biodiversity, Friedrich Schiller University Jena, Dornburger Str. 159, 07743 Jena, Germany
[2]Department of Biogeochemical Processes, Max Planck Institute for Biogeochemistry, Hans-Knöll Str. 10, 07745 Jena, Germany
[3]German Centre for Integrative Biodiversity Research (iDiv) Halle–Jena–Leipzig, Puschstraße 4, 04103 Leipzig, Germany

Correspondence: Kirsten Küsel (kirsten.kuesel@uni-jena.de)

Received: 1 April 2022 – Discussion started: 28 April 2022
Revised: 28 July 2022 – Accepted: 4 August 2022 – Published: 1 September 2022

Abstract. Globally, soil temperature to 1 m depth is predicted to be up to 4 °C warmer by the end of this century, with pronounced effects expected in temperate forest regions. Increased soil temperatures will potentially increase the release of carbon dioxide (CO_2) from temperate forest soils, resulting in important positive feedback on climate change. Dark CO_2 fixation by microbes can recycle some of the released soil CO_2, and CO_2 fixation rates are reported to increase under higher temperatures. However, research on the influence of temperature on dark CO_2 fixation rates, particularly in comparison to the temperature sensitivity of respiration in soils of temperate forest regions, is missing. To determine the temperature sensitivity (Q_{10}) of dark CO_2 fixation and respiration rates, we investigated soil profiles to 1 m depth from beech (deciduous) and spruce (coniferous) forest plots of the Hummelshain forest, Germany. We used ^{13}C-CO_2 labelling and incubations of soils at 4 and 14 °C to determine CO_2 fixation and net soil respiration rates and derived the Q_{10} values for both processes with depth. The average Q_{10} for dark CO_2 fixation rates normalized to soil dry weight was 2.07 for beech and spruce profiles, and this was lower than the measured average Q_{10} of net soil respiration rates with ∼ 2.98. Assuming these Q_{10} values, we extrapolated that net soil respiration might increase 1.16 times more than CO_2 fixation under a projected 4 °C warming. In the beech soil, a proportionally larger fraction of the label CO_2 was fixed into soil organic carbon than into microbial biomass compared to the spruce soil. This suggests a primarily higher rate of microbial residue formation (i.e. turnover as necromass or release of extracellular products). Despite a similar abundance of the total bacterial community in the beech and spruce soils, the beech soil also had a lower abundance of autotrophs, implying a higher proportion of heterotrophs when compared to the spruce soil; hence this might partly explain the higher rate of microbial residue formation in the beech soil. Furthermore, higher temperatures in general lead to higher microbial residues formed in both soils. Our findings suggest that in temperate forest soils, CO_2 fixation might be less responsive to future warming than net soil respiration and could likely recycle less CO_2 respired from temperate forest soils in the future than it does now.

1 Introduction

Most of Earth's terrestrial carbon stock is found in soils, with ∼ 36 % occurring in the top 1 m depth of forest soils (Jobbágy and Jackson, 2000) based on the new carbon inventory of the global soil carbon pool (Hugelius et al., 2014; Schuur et al., 2015). Decomposition of soil organic carbon (SOC) provides one of the largest sources of carbon dioxide (CO_2) to the atmosphere (Rastogi et al., 2002; Lal, 2004). Microbes can refix 3 %–6 % of CO_2 in temperate forest mineral soils before its release to the atmosphere (Akinyede et al., 2020; Spohn et al., 2019), through so-called dark CO_2 fixation (Miltner et al., 2005; Šantrůčková et al., 2018). Dark CO_2 fixation in soils is mediated by chemolithoautotrophic bacteria, largely via the Calvin–Benson–Bassham (CBB) path-

Published by Copernicus Publications on behalf of the European Geosciences Union.

way (Niederberger et al., 2015; Wu et al., 2014), the Wood–Ljungdahl pathway (WLP), or the reverse tricarboxylic acid (rTCA) pathway (Beulig et al., 2016; Liu et al., 2018). Heterotrophic bacteria can also contribute to dark CO_2 fixation via anaplerotic carboxylation reactions associated with central microbial metabolism (Erb, 2011). The genetic potential for both autotrophic and heterotrophic CO_2 fixation has been demonstrated in various soils (Miltner et al., 2005; Šantrůčková et al., 2018) including temperate forest soils (Akinyede et al., 2022a, 2020; Kaiser et al., 2016).

The biomass of microbial communities serves as the entry point of carbon fixed from CO_2 into SOC, which includes both the intact microbial biomass carbon (MBC) pool and released microbial residues (Miltner et al., 2004, 2005; Spohn et al., 2019). Microbial residues constitute any non-living organic material of microbial origin including necromass and extracellular metabolites (Geyer et al., 2020). Since the transformation of CO_2 and release of the fixed carbon via microbial residues vary for different microbial groups (Berg et al., 2011; Miltner et al., 2005), the composition and abundance of microbial communities play a vital role in CO_2 fixation rates in soils. High CO_2 fixation rates in soils have been reportedly associated with higher abundance of obligate autotrophs and specific bacterial groups like Proteobacteria (Long et al., 2015; Xiao et al., 2018). As the microbial communities fixing CO_2 are sensitive to changes in edaphic conditions (Berg, 2011; Hügler and Sievert, 2011), various biotic and abiotic predictors of CO_2 fixation rates have been identified. Factors like CO_2 concentration (Beulig et al., 2016; Spohn et al., 2019; Akinyede et al., 2020), SOC content and quality (Miltner et al., 2005; Šantrůčková et al., 2018; Xiao et al., 2018; Akinyede et al., 2022a), and pH (Šantrůčková et al., 2005; Long et al., 2015) affect dark CO_2 fixation rates in many soils including those of temperate forests.

Here, we focus on temperature as a factor determining soil CO_2 fixation rates. Biological processes are generally faster under higher temperatures due to accelerated rates of enzymatic reactions (Arrhenius, 1889; Van 't Hoff, 1898; Davidson and Janssens, 2006). Hence, temperature presumably affects dark CO_2 fixation rates but also the rates of CO_2 production through decomposition. If moisture is not limiting, warmer temperatures increase CO_2 emission from temperate forest soils (Melillo et al., 2017, 2011, 2002; Walker et al., 2018; Winkler et al., 1996), and the degree of response is similar to depths of 1 m (Hicks Pries et al., 2017; Soong et al., 2021). Such responses coincide with a reduction in the total SOC pool and have been mostly attributed to increased microbial respiration (Melillo et al., 2011). The net change in total CO_2 efflux from soil (net soil respiration) includes the effects of temperature on both CO_2 production (decomposition) and CO_2 fixation. These effects may change with soil depth from the relatively organic carbon-rich surface soils to the more carbon-limited deeper soils.

A previous study describing the influence of temperature on CO_2 fixation rates described ~ 10 times higher fixation rates at 25 °C than at 4 °C in a range of mostly Alisol and Retisol soils in afro-temperate forest and grassland ecosystems of the lower-latitude regions (Nel and Cramer, 2019), suggesting potentially large temperature effects on CO_2 fixation rates. However, a systematic study comparing the responses of dark CO_2 fixation and net soil respiration from temperate forest soils is currently lacking. The relative temperature responses of these processes are important because globally, soil temperatures are projected to warm by ~ 4 °C until 2100 (based on simulations under the Representative Concentration Pathway (RCP) 8.5 scenario; IPCC, 2013; Soong et al., 2020).

The temperature sensitivity (Q_{10}), the increase in reaction rates for a 10 °C rise in temperature, is a commonly reported value when describing the response of soil microbial processes to higher temperatures (Davidson and Janssens, 2006; Fang et al., 2005; Leifeld and Fuhrer, 2005). Hicks Pries et al. (2017) reported a Q_{10} of 2.4 for net respiration rates in temperate coniferous forest soil. Similar Q_{10} values of between 2 and 3 for net respiration rates have also been described for other soil environments (Conant et al., 2008; Li et al., 2021). Considering that dark CO_2 fixation rates and soil respiration rates increase with temperature as described above and that dark CO_2 fixation rates have been shown to correlate linearly with net soil respiration rates (Miltner et al., 2005; Šantrůčková et al., 2018), the Q_{10} values of dark CO_2 fixation rates with depth might correlate with those of net soil respiration rates.

This study describes the temperature sensitivity (Q_{10}) of dark CO_2 fixation rates and compares it to that of net soil respiration rates across soil profiles of deciduous and coniferous forests, the two temperate forests based on vegetation (Dreiss and Volin, 2014; Adams et al., 2019). Soils of two acidic forest plots from the Hummelshain forest, Germany, dominated by beech (deciduous) and spruce (coniferous) tree species were incubated under two temperature conditions (4 and 14 °C). We used a $^{13}CO_2$-labelling approach to quantify dark CO_2 fixation rates. We also measured net soil respiration rates and determined the Q_{10} values of both processes across depth. We thus hypothesize that the Q_{10} values of dark CO_2 fixation rates with depth correlate with those of net soil respiration rates. Using the derived Q_{10} values, we evaluated the potential changes in dark CO_2 fixation rates and net soil respiration rates under projected increase in global soil temperature. We further explored the microbial community composition in the beech and spruce soil, with the aim to assess potential differences in the community that might influence dark CO_2 fixation rates and, thereby, its Q_{10} across temperate forest soil profiles.

2 Materials and methods

2.1 Site description and soil classification

The study sites (beech plot 50°45′28.0″ N, 11°37′21.0″ E; spruce plot 50°45′30.0″ N, 11°37′23.0″ E) are located within the forested areas of the Hummelshain municipality (∼ 362 m a.s.l.) in Thuringia, central Germany. The study site was established on a former coniferous forest, and it involved the planting of European beech trees within Norway spruce and Scot's pine stands. The main purpose for this conversion was to counteract the low pH of the topsoil under the coniferous stands and, thus, biologically activate the forest floors (Graser, 1928). The mean annual rainfall in this area is about 630 mm, and the mean annual air temperature is around 7.8 °C (Achilles et al., 2020). The two study plots located < 1 km apart are dominated by European beech (*Fagus sylvatica* L.) and Norway spruce (*Picea abies* (L.) H.Karst.) tree stands, respectively, and feature similar soil geology (Achilles et al., 2020). The soils are mostly sandy (40 %–50 % sand and silt) with a clay enrichment with depth (Table 1; Eckelmann et al., 2006; Bormann, 2007) due to the Triassic sandstone bedrock in the Hummelshain area (Achilles et al., 2020). The soils in this region are predominantly quartz-rich (50 %–60 % quartz), consisting of sandstones and silt–mud stones, and are classified as Luvisols with an F-mull-over-loess layer (IUSS Working Group WRB, 2015; Achilles et al., 2020). Both soils feature a low pH (< 4) and a high C/N ratio (Table 1). The beech soil was slightly lower in SOC, MBC, total nitrogen (TN), and moisture content than the spruce soil across depth. The beech soil profile also featured a lower clay but higher sandy texture when compared to the spruce soil profile. Further description of the forest sites and the soil characteristics in the Hummelshain locality can be found in Achilles et al. (2020).

2.2 Sampling design

The sampling was carried out in September 2020, towards the end of the summer season. By driving in an 84 mm wide closed auger into the soil with the aid of a motor hammer (Cobra Combi, Atlas Copco AB, Nacka, Sweden), 6 replicate soil cores, 1–2 m apart, were obtained from each of the sampling plots, leading to a total of 12 soil cores for the beech and spruce plots. To avoid direct impact from stem flow and to prevent larger roots from impeding the soil coring process, all soil cores were taken ∼ 2 m away from the base of the trees. Soil sampling began from the mineral horizon, and the organic layer was ignored. Three segments were extracted from each soil core by depths chosen according to the similarity of the horizon among all replicate cores to obtain samples representing the AB horizon (0–20 cm), Bv horizon (20–55 cm), and BvT horizon (55–100 cm) for the beech plot and the AB horizon (0–20 cm), Bv horizon (20–55 cm), and BvT horizon (55–92 cm) for the spruce sample plot. Soil samples from the same depth intervals of each of the six replicate cores were homogenized in pairs to yield three replicate cores each for the beech and spruce forest plot. Afterwards, all soil samples were sieved using a 2 mm sieve to remove stones and roots prior to the incubation experiments. Fresh subsamples for later DNA extraction and geochemical analysis were also taken and immediately stored by freezing in liquid nitrogen.

2.3 Geochemical parameters and isotope measurements

The total and inorganic carbon and nitrogen concentration, pH, and gravimetric water content as well as carbon isotope signatures of all soil samples were determined as previously described by Akinyede et al. (2020) with values reported in Tables 1 and S1 in the Supplement. The ^{13}C signature of the bulk soil total organic carbon was analysed using an elemental analyser isotope ratio mass spectrometer (EA-IRMS) (EA 1110, CE Instruments, Milan, Italy) coupled to a Delta$^+$ IRMS (Thermo Finnigan, Bremen, Germany) through a ConFlo III interface. The extraction of microbial biomass carbon content was performed by chloroform fumigation extraction (CFE) (Nowak et al., 2015; Vance et al., 1987) using 0.05 M K_2SO_4 following methods described previously (Akinyede et al., 2020). The microbial biomass carbon content (MBC) extracted as the chloroform soluble carbon content was derived by taking the difference between the dissolved organic carbon (DOC) content in the unfumigated (C_{unfum}) and the fumigated soil extract fractions (C_{fum}) for all soil samples. Values from all samples were divided by a correction factor K_{EC} (of 0.45) that accounts for the extraction efficiency. This factor corrects for the incomplete release of carbon from the living microbial cells into the solution and is widely applied to different soils (Joergensen and Mueller, 1996; Joergensen et al., 2011; Wu et al., 1990) as CFE only measures the fraction of microbial biomass rendered extractable in K_2SO_4 solution after lysis with chloroform, which is likely the very labile microbial fraction (e.g. the cytoplasm) (Ocio and Brookes, 1990; Wu et al., 1990). The MBC content was thus calculated as follows:

$$\text{MBC (mg)} = \frac{[C_{fum} - C_{unfum}]}{K_{EC}}. \quad (1)$$

Despite previous studies showing no strong variations in the K_{EC} of 0.45 between soils or incubation temperatures (Martens, 1995; Joergensen et al., 2011), we cannot exclude possible effects resulting from differences in CFE efficiency on our results, especially in comparisons of the rates across the different soil depths or between the beech and spruce soils.

To determine the $\delta^{13}C$ signature of the bulk soil MBC, the ^{13}C signature of the DOC from the fumigated and unfumigated CFE fractions was analysed using an isotope ratio mass spectrometer (DELTA V IRMS, Thermo Fisher Scien-

Table 1. Geochemical properties of soil cores obtained from beech and spruce soil plots at the Hummelshain forest. Soil pH, moisture content, soil organic carbon (SOC), carbon / nitrogen (C/N) ratio, microbial biomass carbon (MBC), total nitrogen (TN), MBC / SOC ratio, natural abundance of ^{13}C of SOC and MBC, bacterial abundance (*16S rRNA* gene copies), and soil texture class are reported for three depths definitions for the beech and spruce soils of the Hummelshain forest. Each reported value represents the mean of three replicate soil cores taken from bulk soils during the sampling campaign. The abbreviation "dw" denotes dry weight.

	Depth – horizon (cm)					
	Beech			Spruce		
	AB (0–20)	Bv (20–55)	BvT (55–100)	AB (0–20)	Bv (20–55)	BvT (55–100)
pH	3.32 ± 0.08	3.47 ± 0.03	3.13 ± 0.03	2.84 ± 0.03	3.16 ± 0.02	3.07 ± 0.06
Moisture (%)	8.65 ± 1.30	8.28 ± 0.84	11.27 ± 1.41	10.34 ± 2.22	10.95 ± 0.66	14.27 ± 1.07
SOC (%)	0.90 ± 0.12	0.28 ± 0.11	0.12 ± 0.03	1.56 ± 0.07	0.33 ± 0.13	0.21 ± 0.05
C/N ratio	20.42 ± 1.77	11.23 ± 3.02	5.59 ± 0.83	19.13 ± 1.02	9.97 ± 2.37	6.38 ± 1.02
MBC ($\mu g\,C\,g^{-1}$ (dw))	74.14 ± 3.08	21.92 ± 6.53	14.26 ± 6.30	84.83 ± 9.42	25.39 ± 12.85	19.43 ± 6.71
TN (%)	0.04 ± 0.004	0.02 ± 0.002	0.02 ± 0.002	0.08 ± 0.005	0.03 ± 0.005	0.03 ± 0.002
MBC/SOC (%)	0.84 ± 0.15	0.80 ± 0.09	1.05 ± 0.34	0.55 ± 0.08	0.74 ± 0.10	0.96 ± 0.07
δ^{13}C-SOC (‰)	-27.14 ± 0.41	-25.96 ± 0.16	-25.37 ± 0.27	-27.62 ± 0.16	-25.53 ± 0.31	-25.25 ± 0.14
δ^{13}C-MBC (‰)	-23.62 ± 0.97	-22.45 ± 0.59	-22.71 ± 0.22	-21.57 ± 0.64	-22.05 ± 0.85	-22.67 ± 0.66
16S rRNA (copies g^{-1} (dw))	$1.83 \times 10^9 \pm 8.18 \times 10^8$	$7.0 \times 10^8 \pm 2.37 \times 10^8$	$1.19 \times 10^8 \pm 1.06 \times 10^8$	$2.40 \times 10^9 \pm 3.68 \times 10^8$	$5.47 \times 10^8 \pm 2.67 \times 10^8$	$3.89 \times 10^8 \pm 2.22 \times 10^8$
Soil texture class (Eckelmann et al., 2006; Bormann, 2007)	Highly silty sand (Su4)	Loamy silty sand (Slu)	Slightly clay loam (Lt2)	Loamy sandy silt (Uls)	Medium clayey silt (Ut3)	Loamy clay (Tl)

tific, Bremen, Germany) coupled to a high-performance liquid chromatography (HPLC) system (UltiMate 3000, Dionex Softron GmbH, Germering, Germany) via an LC IsoLink interface (Thermo Fisher Scientific, Bremen, Germany). All ^{13}C isotope ratios were reported in the delta notation (δ) expressed as $\delta^{13}C$ values ($^{13}C/^{12}C$ ratios) in per mil (‰), relative to the international reference material Vienna Pee Dee Belemnite (V-PDB) (Coplen et al., 2006).

$$\delta^{13}\mathrm{C}\ (‰) = \left[\frac{\frac{^{13}\mathrm{C}}{^{12}\mathrm{C}}\ \text{sample}}{\frac{^{13}\mathrm{C}}{^{12}\mathrm{C}}\ \text{reference}} - 1 \right] \times 1000 \tag{2}$$

Afterwards, the $\delta^{13}C$ in per mil (‰) of microbial biomass carbon (MBC) was derived by applying an isotope mass balance to the measured ^{13}C signals measured for all fumigated and unfumigated DOC fractions from CFE as previously described (Akinyede et al., 2020).

$$\delta^{13}\mathrm{C_{MB}}\ (‰) = \frac{\left[\delta^{13}\mathrm{C_{fum}} \times \mathrm{C_{fum}} - \delta^{13}\mathrm{C_{unfum}} \times \mathrm{C_{unfum}}\right]}{\mathrm{C_{fum}} - \mathrm{C_{unfum}}} \tag{3}$$

2.4 ^{13}C-CO_2-labelling incubation experiment

The CO_2 fixation rates were determined using microcosm incubations. Four replicates for each sieved soil sample (60 g wet weight) obtained from all six soil cores in both the beech and the spruce sampling plots were placed in sterilized 1000 mL serum bottles, closed with butyl rubber stoppers. The large headspace-to-soil-volume ratio was chosen to ensure minimal changes in the headspace CO_2 concentration and the ^{13}C isotope signatures as no further additions to the headspace CO_2 were performed throughout the incubation period with labelled $^{13}CO_2$. The four replicate jars were split into two pairs of two replicates each prior to a 4 d preincubation period. The first pair was preincubated at 4 °C and the second at 14 °C. Before preincubation, all jars were opened for several minutes to allow the CO_2 concentration in the jar to equilibrate with the ambient concentration. After the preincubation period, gas samples were obtained with the aid of a gas syringe for CO_2 measurement. Afterwards, the jars were opened, and homogenized soil samples were subsampled for (1) the determination of total and organic carbon and nitrogen content as well as ^{13}C isotope signatures of the bulk soil, (2) extraction to determine initial microbial biomass carbon content and its ^{13}C isotope signature, and (3) storage for later DNA analysis.

The remainder of the soil ($\sim$ 30 g) was placed in the incubation jar, which was then flushed with synthetic air (75 % N_2 and 25 % O_2). One replicate of each temperature set was adjusted to 2 % (v/v) ^{13}C-CO_2 in the headspace, and the second replicate was adjusted to 2 % (v/v) headspace ^{12}C-CO_2 concentration, serving as treatments and controls, respectively. All soils exposed to the 2 % (v/v) ^{13}C-CO_2, and con-

trols were then incubated statically in the dark for 21 d under the same temperature as used in the preincubation phase (4 and 14 °C). At the end of the incubation period, microcosms were opened and soil samples from all incubations were split into three parts, and geochemical parameters were analysed as after the preincubation phase. Parameters like SOC, MBC, the C/N ratio, and water content measured after incubation for the beech and spruce plots are described in Table S2 in the Supplement and did not differ with temperature and throughout the incubation period. In addition, the $\delta^{13}C$ signals of MBC and SOC from all incubated soil samples were measured as done for the bulk soil prior to the start of the rate measurements.

2.5 Determination of CO_2 fixation rates, respiration rates, and temperature sensitivity (Q_{10})

To calculate the CO_2 fixation rates for all soil incubations at both 4 and 14 °C, the actual $^{13}C/^{12}C$ ratio taken up into the total soil pool and into microbial biomass carbon (MBC) pool was measured as described in Sect. 2.3. This was derived from the measured and derived ^{13}C values (for all treatments (^{13}C labelled) and controls (^{13}C unlabelled/natural abundance)) of SOC and MBC, respectively.

The $^{13}C/^{12}C$ ratios were calculated based on the $^{13}C/^{12}C$ ratio of the international V-PDB standard as done previously (Akinyede et al., 2020, 2022a), where 0.0111802 is taken as the $^{13}C/^{12}C$ ratio of the international V-PDB standard (Werner and Brand, 2001):

$$\frac{^{13}C}{^{12}C} = \left[\frac{\delta^{13}C}{1000} + 1\right] \times 0.0111802. \quad (4)$$

Subsequently, the excess ^{13}C ratio for the soil pool and the MBC pool was derived from the increase in the $^{13}C/^{12}C$ ratio between the ^{13}C-labelled treatment and the ^{12}C-labelled controls (^{13}C natural abundance level) normalized to the respective carbon content of the soil and of the microbial biomass (MBC) as follows:

$$\text{excess } ^{13}C \text{ (mg)} = \frac{^{13}C_{\text{labelled}}}{^{12}C_{\text{labelled}}} \times \text{MBC/SOC} - \frac{^{13}C_{\text{unlabelled}}}{^{12}C_{\text{unlabelled}}} \times \text{MBC/SOC}. \quad (5)$$

These values were then divided by the incubation time and expressed per gram of the bulk soil dry weight and per gram of microbial biomass carbon to obtain the CO_2 fixation rates per gram of soil dry weight (g^{-1} (dw) soil d^{-1}) and per gram of MBC (g^{-1} MBC d^{-1}), respectively.

Following Spohn et al. (2019), the net respiration rates for all soil preincubations were determined based on the difference in the CO_2 concentrations of the glass jars measured at the beginning and at the end of the incubation period using a gas chromatograph system for trace gas analysis of air samples (Agilent 6890 GC FID ECD PDD, USA). Gas samples were taken from the headspace of the jars using a gas syringe attached to 250 mL evacuated vials. A period of 30 s was allowed for the gas vials to equilibrate with the incubation jars, after which the gas vials were disconnected from the vials and connected via a gas line to the gas chromatograph system for CO_2 measurement (in ppm). Using the ideal gas equation, net soil respiration rates were calculated according to Dossa et al. (2015), expressed as micrograms of carbon per gram of soil dry weight per day. As net respiration rates represent CO_2 produced minus CO_2 fixed, the total CO_2 production or decomposition rates were subsequently derived by adding the net respiration rates to the CO_2 fixation rates measured for all beech and spruce soil samples.

The temperature sensitivities of the CO_2 fixation (per unit soil and MBC) and net respiration rates (per gram of soil only), as well as the decomposition rate (per gram of soil only), were determined by calculating Q_{10} values according to Leifeld and Fuhrer (2005):

$$Q_{10} = \left[\frac{k_2}{k_1}\right]^{\left(\frac{10}{T_2 - T_1}\right)}, \quad (6)$$

where T_2 and T_1 denote the higher and lower temperatures (in °C) at which the soils were incubated, and k_2 and k_1 represent the corresponding derived CO_2 fixation rates, net respiration rate and decomposition rates for temperatures T_2 and T_1, respectively.

2.6 DNA extraction and *16S rRNA* gene sequencing

DNA was extracted from 0.25 g of all bulk soil and incubation samples using the DNeasy PowerSoil DNA kit (Qiagen, Hilden, Germany) according to the manufacturer's protocol. For Illumina MiSeq sequencing, libraries of amplicon sequences of bacterial *16S rRNA* genes were generated. All libraries were prepared with the NEBNext Ultra DNA Library Prep Kit for Illumina (New England Biolabs, Hitchin, UK) using a two-step barcoding approach. For the first step, forward (Bact_341F) and reverse (Bact_785R) primers targeting the V3 to V4 hypervariable regions of the bacterial *16S rRNA* gene were used (Klindworth et al., 2013). For Illumina sequencing, the primers were modified with an adaptor overhang which allowed for barcoding in a second PCR step. During the first PCR step, all DNA samples (> 10 ng µL^{-1}) were amplified in a 20 µL reaction volume containing 10 µM of each primer, 0.67 µg µL^{-1} of BSA (bovine serum albumin), 5.67 µL nuclease-free water, and 10 µL HotStarTaq Master Mix (Qiagen, Hilden, Germany). The PCR conditions used consisted of an initial denaturation at 95 °C for 45 min, followed by 26 to 30 cycles of denaturation (94 °C for 45 s), annealing (55 °C for 45 s), and extension (72 °C for 45 s) and then a final extension step at 72 °C for 10 min. While samples from the AB and Bv horizon were amplified using 26 to 27 cycles, a few samples from the BvT depth with low DNA concentration were amplified using 30 cycles with the same

cycling conditions. All amplified sequences from the first PCR step were barcoded in a second PCR step using 1 µL of the initial PCR products, 0.5 µM of barcoded primer set from Illumina (sequences provided in Table S4 in the Supplement), and Ruby Taq Master Mix (Jena Bioscience, Germany) following the cycling conditions of 6 cycles at 95 °C for 45 s, 55 °C for 45 s, and 72 °C for 45 s for denaturing, annealing, and extension steps, respectively. All samples were analysed by gel electrophoresis using 1 % agarose gel to ensure all amplicons were ∼ 500 bp in length. Subsequently, prepared libraries were sequenced on a MiSeq (Illumina, Inc, San Diego, CA, USA) using v3 chemistry (2 × 250 bp).

The raw sequences generated were analysed using mothur (Schloss et al., 2009; http://www.mothur.org, last access: 19 January 2021) and the mothur MiSeq SOP as of 19 January 2021. Paired reads were combined, and sequences were trimmed, saving only sequences with the desired length of between 360 and 500 bp. Trimmed sequences were aligned to the SILVA reference database v132 release (Quast et al., 2013), and sequences with differences of up to four bases were pre-clustered. Chimeras were removed using UCHIME and the GOLD reference database implemented in mothur (Edgar et al., 2011). Subsequently, the taxonomic classification of the sequences against the SILVA database was performed.

2.7 Determination of chemolithoautotrophic CO_2 fixation potential in the Hummelshain forest soils

To determine the potential for chemolithoautotrophic CO_2 fixation among all soil samples, the abundance of functional genes involved in autotrophic CO_2 fixation was first predicted for all bacteria communities. Here, the representative sequences from operational taxonomic unit (OTUs) generated from mothur were analysed using version 2 (v2.2.0 beta) of the PICRUSt (Phylogenetic Investigation of Communities by Reconstruction of Unobserved States) software package (Douglas et al., 2020). All OTU sequences were de-gapped and placed in a reference taxonomic tree based on the Integrated Microbial Genomes database. EPA-ng and GAPPA tools were used to determine the best position of these placed OTUs in the reference phylogeny (Barbera et al., 2019; Czech and Stamatakis, 2019; http://www.hmmer.org, last access: 19 January 2021) after which KEGG orthologues for key enzymes involved in dark CO_2 fixation were predicted for each OTU. Using the derived KEGG Orthology (KO) numbers for different key genes for CO_2 fixation, the six known autotrophic pathways were deduced for all samples as previously done (Akinyede et al., 2022a, 2020). These include the Calvin–Benson–Bassham (CBB) pathway (or Calvin cycle), the reductive citric acid (rTCA) pathway, the Wood–Ljungdahl pathway (WLP), the 3-hydroxypropionate–malyl-CoA (3HP) cycle, the 3-hydroxypropionate–4-hydroxybutyrate (HP/HB) cycle, and the dicarboxylate–4-hydroxybutyrate (DC/HB) cycle.

Based on PICRUSt2 predictions, the abundance of functional genes belonging to two CO_2 fixation pathways, the Calvin cycle and the rTCA pathway, were determined by quantitative PCR for the bulk soil as well in all soil samples incubated at 4 and 14 °C. Gene abundance of bacterial *16S rRNA*, RuBisCO marker genes (*cbbL* IA, *cbbL* IC, *cbbM*) for the Calvin–Benson–Bassham cycle and ATP citrate lyase genes, and *aclA* belonging to the reductive citric acid cycle was determined by quantitative PCR (qPCR) on the CFX96 Touch Real-Time PCR system (Bio-Rad, Singapore) using Maxima SYBR Green Master Mix (Agilent, CA, USA). Primer pair Bac 8Fmod–Bac 338R was used to target the *16S rRNA* genes (Loy et al., 2002; Daims et al., 1999), while F-*cbbL* IA–R-*cbbL* IA, F-*cbbL* IC–R-*cbbL* IC, and F-*cbbM*–R-*cbbM* were used to target both the form-I (*cbbL* IA and *cbbL* IC) and form-II (*cbbM*) RuBisCO marker genes (Alfreider et al., 2012, 2003), which is specific to both obligate and facultative chemolithoautotrophic bacteria groups like Proteobacteria (Selesi et al., 2005). Primer pair F-g-acl-Nit–R-g-acl-Nit was used to target the alpha subunit of the ATP citrate lyase (*aclA*) gene, which is specific to nitrite-oxidizing bacteria and complete ammonia-oxidizing (comammox) bacteria, e.g. *Nitrospira* (Alfreider et al., 2018). All cycling conditions and standards used for quantification are found in Akinyede et al. (2020) and Herrmann et al. (2012, 2015). Due to the absence of a reliable standardized qPCR protocol and primer sets to target genes for the WLP and the rest of the other autotrophic pathways, the presence of these pathways was based only on the predictions by PICRUSt2.

2.8 Statistical analysis

We compared the CO_2 fixation rates per gram of soil and per gram of MBC between all soil samples incubated at 4 and 14 °C using Student's t test. To compare the respective Q_{10} values between the beech and spruce profile and across individual horizons, analysis of covariance (ANCOVA) and one-way ANOVA with Tukey's test were conducted, respectively. To compare other parameters between the beech and spruce soil profiles, e.g. net soil respiration rates between 4 and 14 °C and ^{13}C signal of SOC and MBC, ANCOVA was also conducted. When comparing parameters between the beech and spruce soils using ANCOVA, soil depth also accounted for the variability in the measured parameters and was used as the covariate in the analysis. When deriving the CO_2 fixation and net soil respiration rates under projected future temperatures increase (from 8 to 12 °C), the mean Q_{10} values for the beech and spruce profiles were used in the Q_{10} equation described in Eq. (6) of the method in Sect. 2.5. As rates at 4 °C were low and, in some samples, below the detection limit (e.g. net respiration rates at the beech soil BvT depth), the rates per gram of soil measured at 14 °C were used (as k_2, T_2) in the Q_{10} equation to derive rates at 8 °C (k_1, T_1). The derived rates at 8 °C were then used (as k_1, T_1) for the subsequent derivation of rates at 12 °C (k_2, T_2).

Following Geyer et al. (2020), we quantified the proportion of excess ^{13}C transferred into the SOC pool from the MBC pool via microbial residues as the total amount of excess ^{13}C fixed in the SOC pool minus the excess ^{13}C fixed in the intact MBC pool.

The variations in the bacterial community between the beech and spruce soil and with temperature were determined by measuring the beta diversity. Beta diversity was measured by performing principal coordinate analysis (PCoA) based on Bray–Curtis dissimilarity using the package vegan contained in R (Oksanen et al., 2008). Here, the bacterial communities from all beech and spruce soil samples were clustered based on their similarity and dissimilarity between the soils and with temperature. To determine the significance of the factors accounting for OTU variances shown in the PCoA plot between the two soils, across individual soil depth, and between temperatures, permutational multivariant analysis of variance (PERMANOVA) was performed with 999 permutations using "adonis" functions. Differences in the abundance of all predicted and quantified CO_2 fixation genes between the beech and spruce soil were analysed using ANOVA and Tukey's test. For all statistical tests, differences with $p < 0.05$ were considered statistically significant. All statistical analyses were conducted with the R environment (v.3.6.1) and RStudio (v1.1.463).

3 Results

3.1 Effects of temperature on dark CO_2 fixation rates in beech and spruce soils

All soil incubations exposed to $^{13}CO_2$ were significantly enriched in $\delta^{13}C$ relative to the controls at both 4 and 14 °C, indicating dark CO_2 fixation (Fig. S1 in the Supplement). In the top depths of both the beech and the spruce soils, significantly higher CO_2 fixation rates were observed at 14 °C than at 4 °C. For the top AB horizon of the beech soil, CO_2 fixation rates expressed in relation to soil dry weight ($\mu g\,C\,g^{-1}$ (dw) soil d^{-1}) (Fig. 1a) were almost 2 times higher with $0.033 \pm 0.006\,\mu g\,C\,g^{-1}$ (dw) soil d^{-1} at 14 °C compared to $0.018 \pm 0.006\,\mu g\,C\,g^{-1}$ (dw) soil d^{-1} at 4 °C ($p = 0.04$; Student's t test). Similarly, the top AB depth of the spruce soil also featured ~ 2 times higher fixation rates at 14 °C with $0.030 \pm 0.003\,\mu g\,C\,g^{-1}$ (dw) soil d^{-1} than at 4 °C with $0.014 \pm 0.002\,\mu g\,C\,g^{-1}$ (dw) soil d^{-1} ($p = 0.005$). In the lower depths, however, no significant differences in fixation rates expressed per gram of soil dry weight were observed between soils incubated at 4 and 14 °C for either the beech soils ($p = 0.3$ and $p = 0.6$ at the Bv and BvT horizons, respectively) or the spruce soils ($p = 0.2$ and $p = 0.4$ at the Bv and BvT horizons, respectively). While we observed an expected decrease in fixation rates per gram of soil with depth in both soils due to the decreasing SOC content, there were no significant differences in rates between the beech and spruce soil, neither at 4 nor at 14 °C. Across the depth profiles, changes in rates with temperature did not differ between the spruce (1.5–3.2-fold changes) and the beech soil (0.9–2.7-fold changes) ($p = 0.08$) as both soils showed a 70 %–90 % increase in the ^{13}C signal with temperature (Fig. S1).

When expressed in relation to microbial biomass carbon (MBC), dark CO_2 fixation rates in the top AB horizon of the spruce soil were 1.6 times higher at 14 °C with $145.95 \pm 27.13\,\mu g\,C\,g^{-1}\,MBC\,d^{-1}$ than at 4 °C with $88.29 \pm 17.12\,\mu g\,C\,g^{-1}\,MBC\,d^{-1}$ ($p = 0.04$) (Fig. 1b). For the beech soil, however, values in the top AB depth were similar at 4 and 14 °C ($p = 0.3$) with 108.18 ± 8.82 and $125.11 \pm 23.76\,\mu g\,C\,g^{-1}\,MBC\,d^{-1}$, respectively. In the lower horizons, no significant differences between temperature treatments were observed for the two soils. Rates expressed per gram of MBC were approximately constant with depth, excepting the BvT horizon of the beech soil, which had lower rates. Taken together across depth profiles, stronger differences with temperature were observed for the spruce (1.3–2.6-fold changes) than the beech soil (0.9–1.4-fold changes) ($p = 0.003$). These differences in rates reflect the observed difference in the ^{13}C signals of MBC with temperature between the soils. While up to a 124 % increase in the ^{13}C signal of MBC was found for the spruce soil, the beech soil showed no more than a 23 % increase in the ^{13}C signal of MBC with temperature (Fig. S1). These differences between the beech and spruce soil suggest that drivers of dark CO_2 fixation may differ between soils.

3.2 Q_{10} of dark CO_2 fixation rates for beech and spruce soil profiles

The Q_{10} values, the factor by which CO_2 fixation rates differed with the 10 °C rise in temperature, were 1.81 ± 0.17 across depths (for rates per gram of soil) for the beech soil, and 2.34 ± 0.21 for the spruce soil (Fig. 2a) with a mean Q_{10} value of 2.07 ± 0.34 for all beech and spruce soils. Both the beech and the spruce soils showed large variability in the Q_{10} values with depth with values ranging from 1.97 ± 0.84 at the AB depth and 1.63 ± 0.86 at the bottom BvT depth of the beech soil to 2.11 ± 0.07 and 2.53 ± 0.70 through the spruce soil profile. Thus, no significant differences between corresponding depths of both soil profiles were observed ($p = 0.81$, $p = 0.32$, and $p = 0.23$ for the AB, Bv, and BvT horizons, respectively). However, differing trends across individual depths for the beech and spruce soil were observed, with Q_{10} values decreasing with depth in beech soil but increasing with depth in spruce soil ($R^2 = 0.92$, $p = 3.2 \times 10^{-8}$, ANCOVA).

We also calculated the Q_{10} for rates per gram of MBC, as the microbial cells are responsible for dark CO_2 fixation and should be primarily affected by temperature. Compared to the Q_{10} based on soil dry weight, the Q_{10} based on MBC was lower in the beech soil ($p = 0.008$), which is linked to

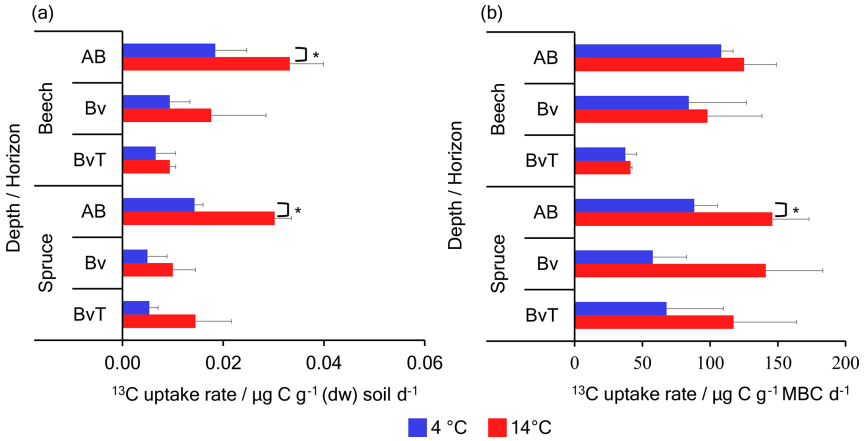

Figure 1. Dark CO_2 fixation rate measured from soil microcosms supplemented with 2 % $^{13}CO_2$ at 4 and 14 °C. Shown are **(a)** ^{13}C uptake rates in soil expressed in µg C g^{-1} (dw) soil d^{-1} (micrograms of carbon per gram dry weight (dw) of soil per day) and **(b)** ^{13}C uptake rates into MBC expressed in µg C g^{-1} MBC d^{-1} (micrograms of carbon per gram of microbial biomass carbon per day) after 21 d of incubation with 2 % $^{13}CO_2$ at 4 (blue bars) and 14 °C (red bars) across three horizons of the beech and spruce soils. Error bars indicate the standard deviation of incubations from three replicate soil cores. * denotes $p < 0.05$.

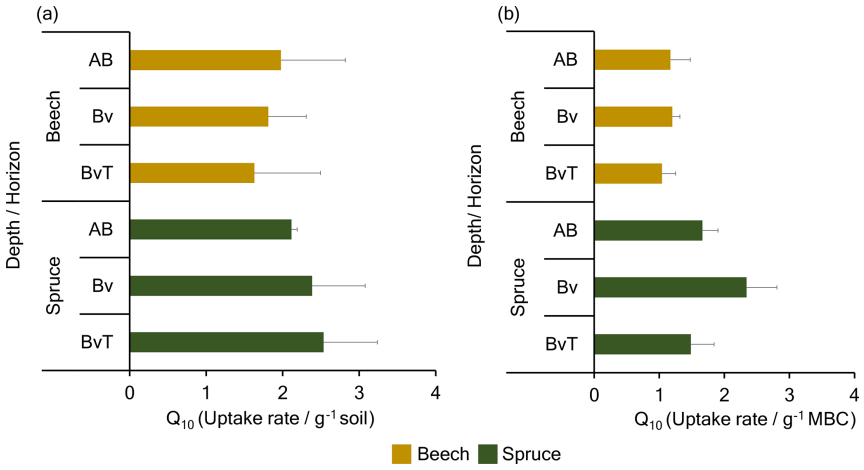

Figure 2. Temperature sensitivity (Q_{10}) of dark CO_2 fixation rate measured from soil microcosms supplemented with 2 % $^{13}CO_2$ at 4 and 14 °C. Shown are the Q_{10} (temperature sensitivity) values of dark CO_2 fixation rates derived from fixation rates expressed in **(a)** µg C g^{-1} (dw) soil d^{-1} (micrograms of carbon per gram dry weight (dw) of soil per day) and in **(b)** µg C g^{-1} MBC d^{-1} (micrograms of carbon per gram of microbial biomass carbon per day) after 21 d of incubation with 2 % $^{13}CO_2$ across three horizons in the beech and spruce soils.

the smaller differences in the ^{13}C signal of MBC and calculated CO_2 fixation rates with temperature. For the spruce soil, no difference between the Q_{10} based on MBC and the Q_{10} based on soil dry weight was observed ($p = 0.13$). As a result, the spruce soil profile featured a higher mean Q_{10} based on rates per gram of MBC with 1.9 ± 0.63 (Fig. 2b) than the beech soil profile with 1.1 ± 0.20 across depth ($p = 0.003$; ANOVA and Tukey's test).

3.3 Allocation of ^{13}C in the beech and spruce soils

As both the fixation rates and Q_{10} values differed between the beech and spruce soil, we aimed to determine if this was reflected by differences in the partitioning or transfer of the fixed ^{13}C via microbial residues between the MBC and SOC pools. On average, the ^{13}C signals of the MBC pool were significantly lower across the beech soil profile compared to the spruce soil profile at 14 °C ($R^2 = 0.91$, $p = 5.24 \times 10^{-8}$, ANCOVA) with no clear difference observed between forest types at 4 °C (Fig. S2 in the Supplement). In contrast, the ^{13}C

signatures measured in SOC were on average higher in the beech than in the spruce soil across depth for soils incubated both at 4 and at 14 °C ($R^2 = 0.98$ and $p = 3.90 \times 10^{-12}$ for 4 °C and $R^2 = 0.96$ and $p = 1.05 \times 10^{-10}$ for 14 °C, ANCOVA). As a result, a higher proportion of fixed ^{13}C was found to be allocated to the MBC pool in the spruce soil with up to 64 % compared to the beech soil with up to 32 % (Fig. 3). Hence, in the beech soil, a greater amount of ^{13}C allocation into the SOC pool was observed compared to the spruce soil. In general, higher temperatures were associated with a larger increase in ^{13}C allocation to SOC compared to MBC pools in the beech and spruce soils (Fig. 3). For instance, at the AB depth of the beech soil, ^{13}C fixed into SOC increased from 67 % to 81 %, and in the spruce soil, it went up from 36 % to 63 %.

3.4 Effects of temperature on net soil respiration rates

In addition to the CO_2 fixation rates, we also determined net soil respiration rates during the preincubation phase. As expected, net respiration rates across all beech and spruce soil samples were 20–70 times higher than CO_2 fixation rates ($p = 0.005$) with values as high as 2.89 ± 1.26 and $2.31 \pm 0.9\,\mu g\,C\,g^{-1}$ (dw) soil d^{-1} at 14 °C at the top AB horizon of the beech and spruce soils, respectively. Net respiration rates were higher in all soils incubated under 14 °C than at 4 °C for both the beech ($R^2 = 0.73$, $p = 0.03$, ANCOVA) and spruce ($R^2 = 0.58$, $p = 0.02$, ANCOVA) profiles (Fig. 4). As rates were highly variable across replicates, no significant differences between the beech and the spruce soil or with depth were observed.

In response to warming, the Q_{10} values of net respiration rates per gram of soil for the beech and spruce soils were 2.87 ± 0.81 and 3.06 ± 0.78, respectively. Taken together, the mean Q_{10} for net respiration rates across the beech and spruce soil profiles at 2.98 ± 0.69 was significantly higher than the Q_{10} of fixation rates relative to soil dry weight ($R^2 = 0.95$, $p = 3.0 \times 10^{-5}$, ANCOVA). Values ranged between 2.29 ± 0.004 and 3.44 ± 1.43 across the two AB and Bv depths in the beech soil and between 2.60 ± 0.12 and 3.96 ± 3.38 across all three depths of the spruce soil. Due to the high variations in net respiration rates among the soil samples, the Q_{10} values did not differ significantly between the beech and spruce soil and across the individual depth profiles. As net respiration rates were much higher than CO_2 fixation rates, the derived decomposition rates were nearly the same as the net respiration rates for the beech and spruce soils. Hence the Q_{10} values were also similar, having a mean value of 2.95 ± 1.34 (Table S3 in the Supplement).

3.5 Bacterial communities of the Hummelshain forest soils

The lower ^{13}C allocation in MBC but higher allocations to SOC for beech than for spruce soils indicated a higher turnover of fixed ^{13}C from MBC to SOC in the beech soil compared to the spruce soil. We thus further checked if this higher turnover was accompanied by differences in the overall bacterial community composition and abundance. We investigated the *16S rRNA* gene amplicons at OTU level and determined *16S rRNA* gene copies by qPCR (Table 1 and Fig. S3 in the Supplement). Principal coordinate analysis (PCoA) revealed differences in the composition between the beech and spruce soil ($R^2 = 0.23$, $p = 0.001$, PERMANOVA, Fig. 5a). This was most pronounced in the top AB horizon ($R^2 = 0.67$, $p = 0.003$). Furthermore, the bacterial community composition also differed with soil depth ($R^2 = 0.30$, $p = 0.001$). As expected, the microbial abundance decreased with depth in both soils (Table 1). However, no difference in the microbial abundance between soils was observed at comparable depths. With respect to temperature, no shifts in the community composition were found in either beech ($R^2 = 0.014$, $p = 0.99$) or spruce ($R^2 = 0.015$, $p = 0.98$) soils (Fig. 5b). Likewise, the microbial abundances did not differ with temperature (Table S2).

3.6 Abundance of genes for CO_2 fixation

Based on presumed differences in residue formation and in the community composition between the soils, we speculate that the potential key players in the beech soil were composed of a higher proportion of groups with faster life cycles when compared to the spruce soil. As the rich SOC content in forest soils generally promotes faster growth of heterotrophs over chemolithoautotrophs, we further hypothesized that the beech bulk soil contains lower fractions of autotrophs compared to the spruce soil. We used PICRUSt2 to predict and quantify the genetic potential for CO_2 fixation in both soils to test this hypothesis. Predicted autotrophic OTUs made up ~ 11 % of the total bacterial community in all samples. Most of the autotrophic OTUs were predicted to possess genes affiliated with RuBisCO of the CBB pathway for CO_2 fixation, with ~ 9 %, while genes of the WLP and the rTCA pathway were predicted in ~ 2 % and 0.1 % of the OTUs, respectively. The spruce bulk soil featured higher abundances of OTUs predicted to possess the RuBisCO gene than the beech bulk soil (Fig. 6a), with significantly higher proportions in the AB horizon ($p = 0.007$).

Quantitative PCR of marker gene coding for the CBB (RuBisCO (*cbbL* IA, *cbbL* IC, *cbbM*)) and the rTCA pathway (ATP citrate lyase alpha subunit (*aclA*)) was performed to confirm the predicted potential for autotrophic CO_2 fixation. Of the detected gene variants, the *cbbL* IC gene was the most abundant with up to 5 % of the bacterial *16S rRNA* gene copies in both soils, whereas other RuBisCO and *aclA* genes constituted less than 1 % (Fig. S4 in the Supplement). The proportions of *cbbL* IC genes across the depths were significantly higher in the spruce than in the beech soil at 4 and 14 °C ($p = 0.007$, $p = 1.03 \times 10^{-6}$, respectively) (Fig. 6b).

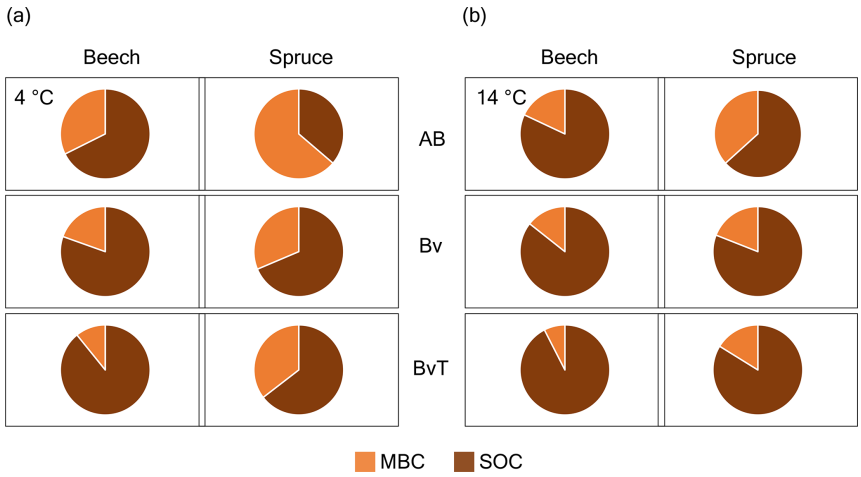

Figure 3. Proportion of fixed carbon recovered in MBC and SOC pools of the beech and spruce soils. The pie charts show the relative proportions of microbially derived $^{13}CO_2$ into MBC (orange fractions) and SOC (brown fractions) pools expressed as a percentage of the total fixed carbon after 21 d of incubation with 2 % $^{13}CO_2$ for soils incubated at **(a)** 4 and **(b)** 14 °C across three horizons (AB, Bv, BvT) in beech and spruce soils. Values are the mean of three replicate incubations.

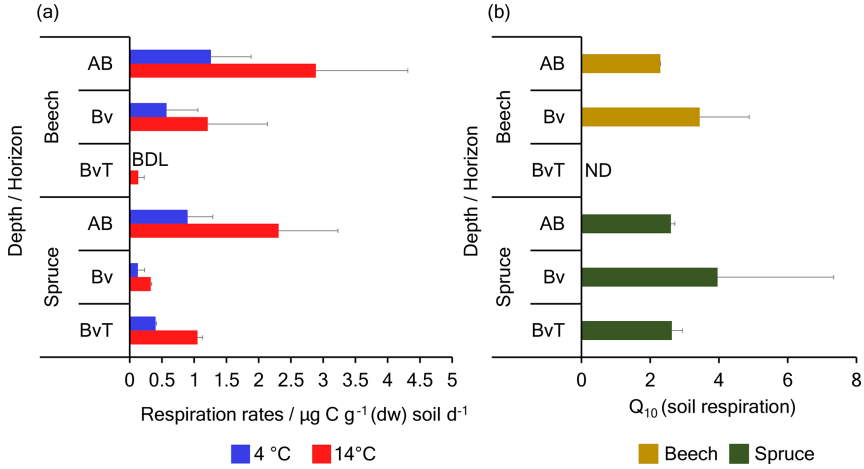

Figure 4. Net respiration rates and Q_{10} values measured from soil microcosms incubated at 4 and 14 °C. Shown are **(a)** net respiration rates in beech and spruce soils expressed in $\mu g\,C\,g^{-1}$ (dw) $soil\,d^{-1}$ (micrograms of carbon per gram dry weight (dw) of soil per day) at 4 (blue bars) and 14 °C (red bars) and **(b)** Q_{10} (temperature sensitivity) of net respiration rates measured after 4 d of preincubation in beech soils (yellow bars) and spruce soils (green bars) across depth. Error bars indicate the standard deviation of incubations from three replicate soil cores. BDL and ND denote values "below the detection limit" and values "not determined", respectively.

In the bulk soil, however, this was only observed in the BvT horizon ($p = 0.03$).

4 Discussion

This study shows that the derived Q_{10} values of dark CO_2 fixation rates per gram of soil, with a mean value of 2.07 across the beech and spruce soil depths, were significantly lower than the average Q_{10} of net soil respiration rates per gram of soil with 2.98 for both soils, which suggests that soil respiration is more sensitive to warming than CO_2 fixation. Our Q_{10} values of net soil respiration rates fall in the range of those reported for agricultural soils (1.5) and temperate mixed forest soils (3.1) (Fang et al., 2005; Conant et al., 2008; Hicks Pries et al., 2017; Li et al., 2021). For Q_{10} values of dark CO_2 fixation rates, a similar value of ~ 2.5 was extrapolated for afro-temperate forest soils (Nel and Cramer, 2019).

Comparing the responses of dark CO_2 fixation and net soil respiration to temperature for the same soil is important in

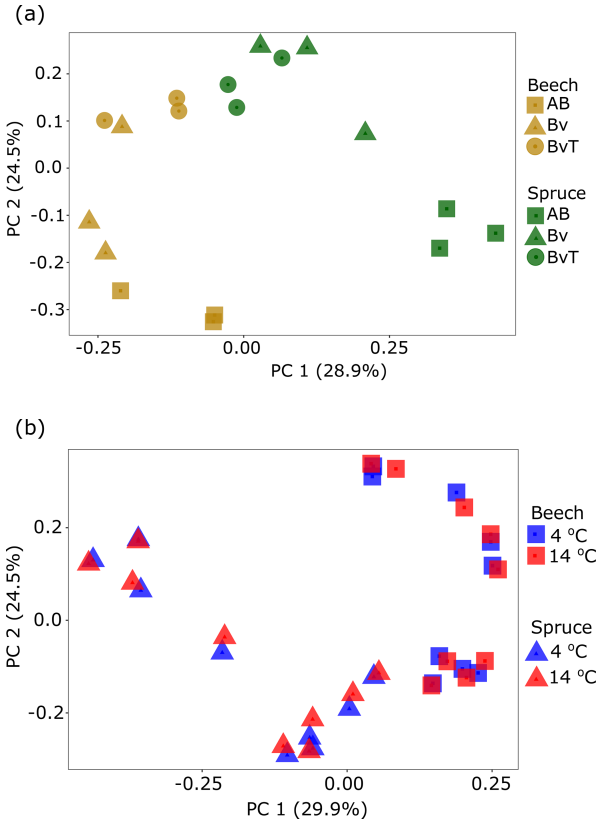

Figure 5. Bacterial community composition and community structure from beech and spruce bulk soil. Shown are the bacterial community structure of **(a)** the beech (yellow symbols) and spruce (green symbols) bulk soils before incubation and of **(b)** beech and spruce soils incubated with 2 % $^{13}CO_2$ at 4 (blue symbols) and 14 °C (red symbols). PCoA plots are based on OTU level analysis (Bray–Curtis dissimilarity) of *16S rRNA* gene amplicons generated by Illumina MiSeq sequencing with three independent data points per depth obtained from beech and spruce soils.

understanding the dynamics of SOC fluxes within the context of global climate change. Since dark CO_2 fixation can recycle up to 4 % of CO_2 respired from temperate forest soils (Spohn et al., 2019), higher CO_2 fixation rates might as well be affecting the magnitude of SOC losses from temperate forest soils under warming. By assuming a Q_{10} of 2.07 and 2.98 for dark CO_2 fixation rate and net soil respiration rates, respectively, we extrapolated the effect of future warming on the forest SOC fluxes. With a 4 °C increase in mean annual temperate forest soil temperature (∼ 8 now to 12 °C by 2100) to 1 m deep by the end of this century (IPCC, 2013; Soong et al., 2020), dark CO_2 fixation rates to 1 m depth would increase by 33 % while net soil respiration rates would increase by 55 %. This indicates that future increase in net soil respiration might be 1.16 times higher than CO_2 fixation upon 4 °C warming. Hence, the potential for dark CO_2 fixation to recycle or modulate carbon respired from temperate forest soils could decrease under future warming scenarios. However, the temperature response of dark CO_2 fixation and respiration in soils is likely also affected by varying temperatures occurring in different temperate forest biomes. Differences in carbon allocation between MBC and SOC also show that not all components of the soil carbon cycle will have the same response to soil temperature changes. Furthermore, higher temperature might alter primary production and root exudation, resulting in changes in soil carbon inputs and, consequently, soil pore space CO_2 concentrations and effluxes (Jakoby et al., 2020; Way and Oren, 2010; Yin et al., 2013). Thus, the estimates presented here are associated with a range of uncertainty.

Our measured soil CO_2 production in all soil incubations does not represent decomposition rates but the net soil respiration rates, as these rates include the effects of temperature on both CO_2 production (decomposition) and CO_2 fixation, with both processes occurring simultaneously (Braun et al., 2021). Thus, to accurately derive the decomposition rates, CO_2 fixation rates have to be added to measured net soil respiration rates. Although our measured CO_2 fixation rates were very small with only marginal effects on the Q_{10} of soil CO_2 production, that is, a Q_{10} of 2.98 vs. 2.95 for net soil respiration and decomposition rate, respectively, dark CO_2 fixation may result in an overestimation of Q_{10} of decomposition rates if only net soil respiration is measured. This is especially the case in scenarios where high CO_2 fixation rates are expected.

Unexpectedly, the two soils, beech and spruce, showed differences in their temperature response. Although Q_{10} values for CO_2 fixation rates per gram of soil were similar between the beech and spruce topsoil, the Q_{10} values differed in their depth trends, with decreasing Q_{10} with depth in the beech soil and increasing Q_{10} with depth in the spruce soil. Furthermore, while both soils showed similar temperature responses in terms of rates of CO_2 production per gram of soil, the temperature effect of CO_2 fixation rates expressed per gram of MBC was smaller in the beech than in the spruce soil. The lower Q_{10} in the beech soil was accompanied by higher proportions of newly fixed ^{13}C in the SOC pool but lower proportions in the MBC pool when compared to the spruce soil, especially for soils incubated at 14 °C. This suggested that there was a higher transfer of microbially derived carbon from the MBC pool into the SOC pool in the beech soil. Through microbial residue formation, fixed ^{13}C is transferred from the MBC into the SOC pool (Geyer et al., 2020; Miltner et al., 2012). A higher rate of residue formation in the beech soil will lead to a lower fraction of fixed ^{13}C remaining in the MBC pool and, thereby, an underestimation of the CO_2 fixation rates per gram of MBC when compared to the spruce soil. Hence, a higher rate of microbial residue transfer in our 21 d incubations might explain the lower Q_{10} of fixation rates per gram of MBC in the beech than in the spruce soil. Such rapid residue formation is not uncommon in soils

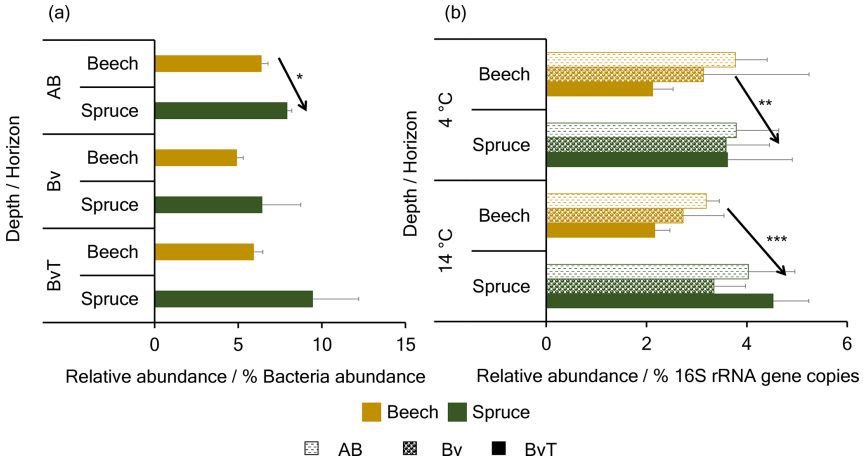

Figure 6. Relative abundance of RuBisCO genes in the beech and spruce soil. Shown are the relative abundances of **(a)** predicted and **(b)** quantified RuBisCO genes coding for the CBB pathway in the beech and spruce soil. Data in **(a)** are based on predictions by PICRUSt2 analysis of bacterial *16S rRNA* gene amplicon sequence data for the beech and spruce bulk soil, while data in **(b)** are acquired by qPCR of *cbbL* IC genes for both soils incubated at 4 and 14 °C. *, **, and *** denote $p < 0.05$, $p < 0.01$, and $p < 0.001$, respectively.

as it was observed in as little as 6 h in a temperate forest soil (Geyer et al., 2020). Microbial biomass can also turn over as necromass within a few days to weeks in soils (Kästner et al., 2021; Miltner et al., 2012) with turnover times of 18–21 d reported in agricultural soils (Cheng, 2009) and 33 d in temperate forest soils (Spohn et al., 2016). Thus, the formation of microbial residues can be observed within the timescale of our incubation experiment.

Accelerated microbial residue formation in the beech compared to the spruce soil might have been related to differences in soil abiotic parameters, in particular, factors differentially affecting either the lifespan (turnover) of microbial cells or the formation of extracellular metabolites from living cells. The biggest difference between the soils was soil texture, with lower clay and higher sand content in the beech compared to the spruce soil. Soil texture is known to affect microbial biomass turnover in soils (Van Veen et al., 1984; Sakamoto and Hodono, 2000; Prévost-Bouré et al., 2014), with high-clay-content soils often associated with slow biomass turnover into necromass compared to low-clay-content soils (Ali et al., 2020; Gregorich et al., 1991; Van Veen et al., 1985) due to the capacity of clay-rich soils to protect or preserve microbial cells, reducing overall the death rate (Van Veen et al., 1985, 1984). Interaction of microbial biomass with the negatively charged clay mineral particles was suggested as the mechanism causing biomass stability (Ali et al., 2020; Six et al., 2006). Clay–microbe interactions may promote microbial growth by maintaining an optimal pH range (Stotzky and Rem, 1966) and helping to adsorb metabolites inhibitory to microbial growth (Martin et al., 1976). The fine particles and small pore space characteristic of clay-rich soils also lead to a higher water-holding capacity (Fan et al., 2004; Jommi and Della Vecchia, 2016; Miltner et al., 2009; Tsubo et al., 2007), resulting in the observed higher moisture content in the spruce compared to the beech soil. This higher moisture typical of clay-rich soils might partly be responsible for protecting microbes against moisture limitations when compared to sandy soils (Meisner et al., 2018; Schnürer et al., 1986; Bitton et al., 1976). Furthermore, small pores also restrict the access of higher organisms like protozoa, providing protection against predation (Elliott et al., 1980; Rutherford and Juma, 1992). Microbial protection promotes recycling or transfer of microbial extracellular products among the living communities, thus preventing further release into the soil pool (Gregorich et al., 1991). All of these mechanisms imply that the formation of microbial residues in the more clay-rich spruce soils should be slower than in the beech soil, as we observed. Due to the presence of larger mineral surface areas of clay in the spruce soils, association with clay surfaces can also lower residue formation and the amount of ^{13}C label transferred would be a smaller proportion of total SOC. However, as the mineral composition of the soils was not measured, we cannot verify this assumption.

The higher microbial residue formation in the beech soil was accompanied by a different community composition and a lower proportion of genes for chemolithoautotrophic CO_2 fixation. Considering that both soils featured a similar abundance of the total bacterial community, this implied a higher proportion of heterotrophs among the beech soil communities. Growth of heterotrophs is favoured by high quantities of simple and complex carbon substrates released as root exudates (Huang et al., 2022; Li et al., 2018; Lladó et al., 2017; Vijay et al., 2019), whereas soils are usually deficient in reduced inorganic compounds (Jones et al., 2018) required as energy sources for autotrophic growth (Brock et al., 2003;

Berg, 2011). The redox potential of half reactions utilized by chemolithoautotrophs for energy often leads to lower energy yield than commonly observed for heterotrophs, causing chemolithoautotrophs to grow more slowly (Hooper and DiSpirito, 2013; Madigan et al., 2015; In't Zandt et al., 2018). As cell growth correlates with microbial residue formation (Geyer et al., 2020; Hagerty et al., 2014; Kästner et al., 2021), it is likely that heterotrophs in soils also form residues at faster rates than their chemolithoautotrophic counterparts. Hence, the suggested higher proportion of heterotrophs in the beech soil could also explain the higher rate of microbial residue formation observed when compared to the spruce soil. In both the beech and the spruce soil, the majority of the chemolithoautotrophic genes were affiliated to facultative autotrophs or mixotrophs which can also utilize SOC as a carbon source for growth (Yuan et al., 2012). This versatility allows them to be more active or grow faster than obligate autotrophs (Madigan et al., 2015). Hence, mixotrophs might contribute to microbial residue formation into the SOC pool especially in the beech soils.

The proportion of labelled carbon transferred to the SOC pool increased with temperature in both beech and spruce soils and across all depths, indicating higher inputs of microbial residues under warming. Higher temperatures have been often reported to increase inputs of microbial residues into soil (Ding et al., 2019; Hagerty et al., 2014; Li et al., 2019). Increasing soil temperature by 10 °C (15 to 25 °C) has been reported to double the specific death rate of microbial communities in soil due to increased protein turnover (Joergensen et al., 1990). Increased microbial residue formation of soil microbial biomass has been suggested to result from higher rates of enzymatic activities or changes in the abundance and composition of the soil microbial community (Ding et al., 2019; Hagerty et al., 2014). However, we did not find changes in the composition and abundance of the microbial community with warming in both the beech and the spruce soils during this short incubation time. Previous studies have shown that even after 4 or 5 years of warming, no increase in bacterial and fungal biomass is observed for a temperate forest soil (Schindlbacher et al., 2011) and it can take up to a decade to detect temperature-related changes in the soil community composition (Rinnan et al., 2009, 2007). In agreement, DeAngelis et al. (2015) revealed that 5 °C soil warming had a significant impact on bacterial community structure in mixed deciduous temperate forest soils only after 20 years of warming. Some authors have suggested that soil communities are more likely driven by gradual warming-induced changes in aboveground plant biomass and composition and associated shifts in carbon substrate, moisture, and nutrient conditions rather than just by elevated soil temperature effects (Sarathchandra et al., 1989; Rinnan et al., 2007; Frey et al., 2008; DeAngelis et al., 2015). This indicates that increases in dark CO_2 fixation in temperate forest soils as a response to short-term warming may not be caused by an increased microbial abundance or a shift in community composition but likely by an increase in the formation and release of microbial residues.

5 Conclusion

In response to warming, we measured an average Q_{10} of 2.07 for CO_2 fixation rates per gram of soil across 1 m depth profiles for soils dominated by deciduous beech and coniferous spruce trees. As net soil respiration rates across depth displayed a higher mean Q_{10} of 2.98, we estimated that net soil respiration might increase 1.16-fold more than CO_2 fixation rates under projected warming scenarios of 4 °C. The observed higher ^{13}C signatures in the SOC pool of the beech soil suggested higher microbial residue formation, and this was reflected in the lower Q_{10} values for CO_2 fixation rates per gram of microbial biomass for the beech than for the spruce soil. Also, the higher allocation of CO_2-derived carbon to the SOC pool at higher temperatures indicates that warming primarily results in an increased residue formation of microbial cells. Findings from this study indicate that dark CO_2 fixation in temperate forest soils might be less responsive to future warming than net respiration and, as a result, could recycle less CO_2 respired from temperate forest soils in the future than it does now.

Code availability. Data analysis was performed using only standard tests and plotting commands in R. These codes are available on request from the corresponding author.

Data availability. Raw data associated with this study can be accessed at https://doi.org/10.17617/3.EFHWIY (Akinyede et al., 2022b). Generated sequences obtained for all soil samples in this study are deposited in the NCBI Sequence Read Archive (SRA) database with accession numbers SAMN26148471, SAMN26148472, SAMN26148473, SAMN26148474, SAMN26148475, and SAMN26148476 under the BioProject accession number PRJNA607916 and submission SUB11118201 (https://submit.ncbi.nlm.nih.gov/subs/biosample/SUB11118201/overview, last access: 7 March 2022).

Supplement. The supplement related to this article is available online at: https://doi.org/10.5194/bg-19-4011-2022-supplement.

Author contributions. RA and KK planned the sampling campaign; RA carried out the campaign and performed the experiments and measurements; RA and MT analysed the data and wrote the manuscript draft. MS, ST, and KK reviewed and edited the manuscript.

Competing interests. The contact author has declared that none of the authors has any competing interests.

Acknowledgements. We thank Beate Michalzik and Florian Achilles for providing us with useful information on the soil properties and the history of the study site. We are grateful to Marco Pöhlmann, Jens Wurlitzer, and Stefan Riedel for soil sampling and incubation set-ups. We wish to acknowledge the contributions of Iris Kuhlmann for her support with CFE, Armin Jordan for helping with gas measurements, and members of the routine measurements and analytical departments of the Max Planck Institute for Biogeochemistry, Jena.

Financial support. This study was jointly supported by the Max Planck Institute for Biogeochemistry, Jena (MPI BGC); the International Max Planck Research School for Global Biogeochemical Cycles, Jena (IMPRS-gBGC); Deutscher Akademischer Austauschdienst (DAAD); and the Collaborative Research Centre 1076 AquaDiva (CRC AquaDiva), Germany. Funding by the DFG under Germany's Excellence Strategy – EXC 2051 – Project ID 390713860 was also provided.

Review statement. This paper was edited by Akihiko Ito and reviewed by two anonymous referees.

References

Achilles, F., Tischer, A., Bernhardt-Römermann, M., Heinze, M., Reinhardt, F., Makeschin, F., and Michalzik, B.: European beech leads to more bioactive humus forms but stronger mineral soil acidification as Norway spruce and Scots pine – Results of a repeated site assessment after 63 and 82 years of forest conversion in Central Germany, Forest Ecol. Manag., 483, 118769, https://doi.org/10.1016/j.foreco.2020.118769, 2020.

Adams, M. B., Kelly, C., Kabrick, J., and Schuler, J.: Temperate forests and soils, Chap. 6, in: Global Change and Forest Soils: Cultivating stewardship of a finite natural resource. Developments in Soil Science, edited by: Busse, M., Giardina, C. P., Morris, D. M., and Page, D. D. S., Elsevier, 36, 83–108, https://doi.org/10.1016/b978-0-444-63998-1.00006-9, 2019.

Akinyede, R., Taubert, M., Schrumpf, M., Trumbore, S., and Küsel, K.: Rates of dark CO_2 fixation are driven by microbial biomass in a temperate forest soil, Soil Biol. Biochem., 150, 107950, https://doi.org/10.1016/j.soilbio.2020.107950, 2020.

Akinyede, R., Taubert, M., Schrumpf, M., Trumbore, S., and Küsel, K.: Dark CO_2 fixation in temperate beech and pine forest soils, Soil Biol. Biochem., 165, 108526, https://doi.org/10.1016/j.soilbio.2021.108526, 2022a.

Akinyede, R., Taubert, M., Schrumpf, M., Trumbore, S., and Küsel, K.: Temperature sensitivity of dark CO_2 fixation in temperate forest soils, Edmond V1 [data set], https://doi.org/10.17617/3.EFHWIY, 2022b.

Alfreider, A., Vogt, C., Hoffmann, D., and Babel, W.: Diversity of ribulose-1,5-bisphosphate carboxylase/oxygenase large-subunit genes from groundwater and aquifer microorganisms, Microb. Ecol., 45, 317–328, https://doi.org/10.1007/s00248-003-2004-9, 2003.

Alfreider, A., Schirmer, M., and Vogt, C.: Diversity and expression of different forms of RubisCO genes in polluted groundwater under different redox conditions, FEMS Microbiol. Ecol., 79, 649–660, https://doi.org/10.1111/j.1574-6941.2011.01246.x, 2012.

Alfreider, A., Grimus, V., Luger, M., Ekblad, A., Salcher, M. M., and Summerer, M.: Autotrophic carbon fixation strategies used by nitrifying prokaryotes in freshwater lakes, FEMS Microbiol. Ecol., 94, 1–12, https://doi.org/10.1093/femsec/fiy163, 2018.

Ali, R. S., Poll, C., and Kandeler, E.: Soil Properties Control Microbial Carbon Assimilation and Its Mean Residence Time, Frontiers in Environmental Science, 8, 1–9, https://doi.org/10.3389/fenvs.2020.00033, 2020.

Arrhenius, S.: Über die Reaktionsgeschwindigkeit bei der Inversion von Rohrzucker durch Säuren, Z. Phys. Chem., 4, 226–248, 1889.

Barbera, P., Kozlov, A. M., Czech, L., Morel, B., Darriba, D., Flouri, T., and Stamatakis, A.: EPA-ng: Massively Parallel Evolutionary Placement of Genetic Sequences, Syst. Biol., 68, 365–369, https://doi.org/10.1093/sysbio/syy054, 2019.

Berg, I. A.: Ecological aspects of the distribution of different autotrophic CO_2 fixation pathways, Appl. Environ. Microb., 77, 1925–1936, https://doi.org/10.1128/AEM.02473-10, 2011.

Beulig, F., Urich, T., Nowak, M., Trumbore, S. E., Gleixner, G., Gilfillan, G. D., Fjelland, K. E., and Küsel, K.: Altered carbon turnover processes and microbiomes in soils under long-term extremely high CO_2 exposure, Nat. Microbiol., 1, 1–9, https://doi.org/10.1038/nmicrobiol.2015.25, 2016.

Bitton, G., Henis, Y., and Lahav, N.: Influence of clay minerals, humic acid and bacterial capsular polysaccharide on the survival of *Klebsiella aerogenes* exposed to drying and heating in soils, Plant Soil, 45, 65–74, 1976.

Bormann, H.: Analysis of the suitability of the German soil texture classification for the regional scale application of physical based hydrological model, Adv. Geosci., 11, 7–13, https://doi.org/10.5194/adgeo-11-7-2007, 2007.

Braun, A., Spona-Friedl, M., Avramov, M., Elsner, M., Baltar, F., Reinthaler, T., Herndl, G. J., and Griebler, C.: Reviews and syntheses: Heterotrophic fixation of inorganic carbon – significant but invisible flux in environmental carbon cycling, Biogeosciences, 18, 3689–3700, https://doi.org/10.5194/bg-18-3689-2021, 2021.

Brock, T. D., Madigan, M. T., Martinko, J. P., and Parker, J. (Eds.): Brock Biology of Microorganisms, 10th Edn., Prentice Hall, Upper Saddle River, New Jersey, 565–575, ISBN 0-13-049147-0, 2003.

Cheng, W.: Rhizosphere priming effect: Its functional relationships with microbial turnover, evapotranspiration, and C-N budgets, Soil Biol. Biochem., 41, 1795–1801, https://doi.org/10.1016/j.soilbio.2008.04.018, 2009.

Conant, R. T., Drijber, R. A., Haddix, M. L., Parton, W. J., Paul, E. A., Plante, A. F., Six, J., and Steinweg, M. J.: Sensitivity of organic matter decomposition to warming varies with its quality, Glob. Change Biol., 14, 868–877, https://doi.org/10.1111/j.1365-2486.2008.01541.x, 2008.

Coplen, T. B., Brand, W. A., Gehre, M., Gröning, M., Meljer, L. H. A. J., Toman, B., and Verkouteren, R. M.: New Guidelines for delta ^{13}C Measurements, Anal. Chem., 78, 2439–2441, 2006.

Czech, L. and Stamatakis, A.: Scalable methods for analyzing and visualizing phylogenetic placement of metagenomic samples, PLoS ONE, 14, 1–50, https://doi.org/10.1371/journal.pone.0217050, 2019.

Daims, H., Brühl, A., Amann, R., Schleifer, K.-H., and Wagner, M.: The domain-specific probe EUB338 is insufficient for the detection of all Bacteria: development and evaluation of a more comprehensive probe set, Syst. Appl. Microbiol., 22, 434–444, 1999.

Davidson, E. A. and Janssens, I. A.: Temperature sensitivity of soil carbon decomposition and feedbacks to climate change, Nature, 440, 165–173, https://doi.org/10.1038/nature04514, 2006.

DeAngelis, K. M., Pold, G., Topçuoglu, B. D., van Diepen, L. T. A., Varney, R. M., Blanchard, J. L., Melillo, J., and Frey, S. D.: Long-term forest soil warming alters microbial communities in temperate forest soils, Front. Microbiol., 6, 1–13, https://doi.org/10.3389/fmicb.2015.00104, 2015.

Ding, X., Chen, S., Zhang, B., Liang, C., He, H., and Horwath, W. R.: Warming increases microbial residue contribution to soil organic carbon in an alpine meadow, Soil Biol. Biochem., 135, 13–19, https://doi.org/10.1016/j.soilbio.2019.04.004, 2019.

Dossa, G. G. O., Paudel, E., Wang, H., Cao, K., Schaefer, D., and Harrison, R. D.: Correct calculation of CO_2 efflux using a closed-chamber linked to a non-dispersive infrared gas analyzer, Methods Ecol. Evol., 6, 1435–1442, https://doi.org/10.1111/2041-210X.12451, 2015.

Douglas, G. M., Maffei, V. J., Zaneveld, J. R., Yurgel, S. N., James, R., Taylor, C. M., Huttenhower, C., and Langille, M. G. I.: PICRUSt2 for prediction of metagenome functions, Nat. Biotechnol, 38, 685–688, https://doi.org/10.1038/s41587-020-0548-6, 2020.

Dreiss, L. M. and Volin, J. C.: Forests: temperate evergreen and deciduous, in: Encyclopedia of Natural Resources – Land – Volume 1, edited by: Yeqiao, W., 1st Edn., CRC Press, 214–223, ISBN 9780203757628, 2014.

Eckelmann, W., Sponagel, H., Grottenthaler, W., Hartmann, K.-J., Hartwich, R., Janetzko, P., Joisten, H., Kühn, D., Sabel, K.-J. and Traidl, R. (Eds.): Bodenkundliche Kartieranleitung, KA5, 5th Edn., Schweizerbart'sche Verlagsbuchhandlung, ISBN 978-3-510-95804-7, 2006.

Edgar, R. C., Haas, B. J., Clemente, J. C., Quince, C., and Knight, R.: UCHIME improves sensitivity and speed of chimera detection, Bioinformatics, 27, 2194–2200, https://doi.org/10.1093/bioinformatics/btr381, 2011.

Elliott, E. T., Anderson, R. V., Coleman, D. C., and Cole, C. V.: Habitable Pore Space and Microbial Trophic Interaction, Oikos, 35, 327–335, https://doi.org/10.2307/3544648, 1980.

Erb, T. J.: Carboxylases in natural and synthetic microbial pathways, Appl. Environ. Microb., 77, 8466–8477, https://doi.org/10.1128/AEM.05702-11, 2011.

Fan, T. W. M., Lane, A. N., Chekmenev, E., Wittebort, R. J., and Higashi, R. M.: Synthesis and physicochemical properties of peptides in soil humic substances, J. Pept. Res., 63, 253–264, https://doi.org/10.1111/j.1399-3011.2004.00142.x, 2004.

Fang, C., Smith, P., Moncrieff, J. B., and Smith, J. U.: Similar response of labile and resistant soil organic matter pools to changes in temperature, Nature, 433, 57–59, https://doi.org/10.1038/nature04044, 2005.

Frey, S. D., Drijber, R., Smith, H., and Melillo, J.: Microbial biomass, functional capacity, and community structure after 12 years of soil warming, Soil Biol. Biochem., 40, 2904–2907, https://doi.org/10.1016/j.soilbio.2008.07.020, 2008.

Geyer, K., Schnecker, J., Grandy, A. S., Richter, A., and Frey, S.: Assessing microbial residues in soil as a potential carbon sink and moderator of carbon use efficiency, Biogeochemistry, 151, 237–249, https://doi.org/10.1007/s10533-020-00720-4, 2020.

Graser, H.: Die Bewirtschaftung des erzgebirgischen Fichtenwaldes, Erster Band, Hofbuchhandlung H. Burdach, Dresden, 1928.

Gregorich, E. G., Voroney, R. P., and Kachanoski, R. G.: Turnover of carbon through the microbial biomass in soils with different texture, Soil Biol. Biochem., 23, 799–805, https://doi.org/10.1016/0038-0717(91)90152-A, 1991.

Hagerty, S. B., Van Groenigen, K. J., Allison, S. D., Hungate, B. A., Schwartz, E., Koch, G. W., Kolka, R. K., and Dijkstra, P.: Accelerated microbial turnover but constant growth efficiency with warming in soil, Nat. Clim. Change, 4, 903–906, https://doi.org/10.1038/nclimate2361, 2014.

Herrmann, M., Hädrich, A., and Küsel, K.: Predominance of thaumarchaeal ammonia oxidizer abundance and transcriptional activity in an acidic fen, Environ. Microbiol., 14, 3013–3025, https://doi.org/10.1111/j.1462-2920.2012.02882.x, 2012.

Herrmann, M., Rusznyák, A., Akob, D. M., Schulze, I., Opitz, S., Totsche, K. U., and Küsel, K.: Large fractions of CO_2-fixing microorganisms in pristine limestone aquifers appear to be involved in the oxidation of reduced sulfur and nitrogen compounds, Appl. Environ. Microb., 81, 2384–2394, https://doi.org/10.1128/AEM.03269-14, 2015.

Hicks Pries, C. E., Castanha, C., Porras, R., Phillips, C., and Torn, M. S.: The whole-soil carbon flux in response to warming, Science, 355, 1420–1423, https://doi.org/10.1126/science.aao0457, 2017.

Hooper, A. B. and DiSpirito, A. A.: Chemolithotrophy, Encyclopedia of Biological Chemistry, 1, 486–492, https://doi.org/10.1016/B978-0-12-378630-2.00219-X, 2013.

Huang, X., Duan, C., Yu, J., and Dong, W.: Transforming heterotrophic to autotrophic denitrification process: Insights into microbial community, interspecific interaction and nitrogen metabolism, Bioresource Technol., 345, 126471, https://doi.org/10.1016/j.biortech.2021.126471, 2022.

Hugelius, G., Strauss, J., Zubrzycki, S., Harden, J. W., Schuur, E. A. G., Ping, C.-L., Schirrmeister, L., Grosse, G., Michaelson, G. J., Koven, C. D., O'Donnell, J. A., Elberling, B., Mishra, U., Camill, P., Yu, Z., Palmtag, J., and Kuhry, P.: Estimated stocks of circumpolar permafrost carbon with quantified uncertainty ranges and identified data gaps, Biogeosciences, 11, 6573–6593, https://doi.org/10.5194/bg-11-6573-2014, 2014.

Hügler, M. and Sievert, S. M.: Beyond the Calvin Cycle: Autotrophic Carbon Fixation in the Ocean, Annu. Rev. Mar. Sci., 3, 261–289, https://doi.org/10.1306/06210404037, 2011.

In't Zandt, M. H., de Jong, A. E., Slomp, C. P., and Jetten, M. S.: The hunt for the most-wanted chemolithoautotrophic spookmicrobes, FEMS Microbiol. Ecol., 94, 1–17, https://doi.org/10.1093/femsec/fiy064, 2018.

IPCC: Summary for Policymakers, in: Climate Change – The Physical Science Basis. Contribution of Working Group I to the Fifth Assessment Report of the Intergovernmental Panel on Climate Change, edited by: Stocker, T. F., Qin, D., Plattner, G.-K., Tignor, M., Allen, S. K., Boschung, J., Nauels, A., Xia, Y., Bex, V., and Midgley, P. M., Cambridge University Press, Cambridge, United Kingdom and New York, NY, USA, 20–23, https://selectra.co.uk/sites/selectra.co.uk/files/pdf/Climate%20change%202013.pdf (last access: 25 August 2022), 2013.

IUSS Working Group WRB: World reference base for soil resources 2014, updated 2015, International soil classification system for naming soils and creating legends for soil maps, World Soil Resources Reports No. 106, https://doi.org/10.1017/S0014479706394902, 2015.

Jakoby, G., Rog, I., Megidish, S., and Klein, T.: Enhanced root exudation of mature broadleaf and conifer trees in a Mediterranean forest during the dry season, Tree Physiol., 40, 1595–1605, https://doi.org/10.1093/treephys/tpaa092, 2020.

Jobbágy, E. G. and Jackson, R. B.: The vertical distribution of soil organic carbon and its relation to climate and vegetation, Ecol. Appl., 10, 423–436, https://doi.org/10.1890/1051-0761(2000)010[0423:TVDOSO]2.0.CO;2, 2000.

Joergensen, R. G. and Mueller, T.: The fumigation-extraction method to estimate soil microbial biomass: Calibration of the kEN value, Soil Biol. Biochem., 28, 33–37, https://doi.org/10.1016/0038-0717(95)00101-8, 1996.

Joergensen, R. G., Brookes, P. C., and Jenkinson, D. S.: Survival of the soil microbial biomass at elevated temperatures, Soil Biol. Biochem., 22, 1129–1136, https://doi.org/10.1016/0038-0717(90)90039-3, 1990.

Joergensen, R. G., Wu, J., and Brookes, P. C.: Measuring soil microbial biomass using an automated procedure, Soil Biol. Biochem., 43, 873–876, https://doi.org/10.1016/j.soilbio.2010.09.024, 2011.

Jommi, C. and Della Vecchia, G.: Fabric and clay activity in soil water retention behaviour, E3S Web Conf., 9, 04022, https://doi.org/10.1051/e3sconf/20160904002, 2016.

Jones, R. M., Goordial, J. M., and Orcutt, B. N.: Low energy subsurface environments as extraterrestrial analogs, Front. Microbiol., 9, 1–18, https://doi.org/10.3389/fmicb.2018.01605, 2018.

Kaiser, K., Wemheuer, B., Korolkow, V., Wemheuer, F., Nacke, H., Schöning, I., Schrumpf, M., and Daniel, R.: Driving forces of soil bacterial community structure, diversity, and function in temperate grasslands and forests, Sci. Rep.-UK, 6, 1–12, https://doi.org/10.1038/srep33696, 2016.

Kästner, M., Miltner, A., Thiele-Bruhn, S., and Liang, C.: Microbial Necromass in Soils – Linking Microbes to Soil Processes and Carbon Turnover, Frontiers in Environmental Science, 9, 1–18, https://doi.org/10.3389/fenvs.2021.756378, 2021.

Klindworth, A., Pruesse, E., Schweer, T., Peplies, J., Quast, C., Horn, M., and Glöckner, F. O.: Evaluation of general 16S ribosomal RNA gene PCR primers for classical and next-generation sequencing-based diversity studies, Nucleic Acids Res., 41, 1–11, https://doi.org/10.1093/nar/gks808, 2013.

Lal, R.: Soil carbon sequestration to mitigate climate change, Geoderma, 123, 1–22, https://doi.org/10.1016/j.geoderma.2004.01.032, 2004.

Leifeld, J. and Fuhrer, J.: The temperature response of CO_2 production from bulk soils and soil fractions is related to soil organic matter quality, Biogeochemistry, 75, 433–453, https://doi.org/10.1007/s10533-005-2237-4, 2005.

Li, B., Li, Z., Sun, X., Wang, Q., Xiao, E., and Sun, W.: DNA-SIP Reveals the Diversity of Chemolithoautotrophic Bacteria Inhabiting Three Different Soil Types in Typical Karst Rocky Desertification Ecosystems in Southwest China, Microb. Ecol., 76, 976–990, https://doi.org/10.1007/s00248-018-1196-y, 2018.

Li, H., Yang, S., Semenov, M. V., Yao, F., Ye, J., Bu, R., Ma, R., Lin, J., Kurganova, I., Wang, X., Deng, Y., Kravchenko, I., Jiang, Y., and Kuzyakov, Y.: Temperature sensitivity of SOM decomposition is linked with a K-selected microbial community, Glob. Change Biol., 27, 2763–2779, https://doi.org/10.1111/gcb.15593, 2021.

Li, J., Wang, G., Mayes, M. A., Allison, S. D., Frey, S. D., Shi, Z., Hu, X. M., Luo, Y., and Melillo, J. M.: Reduced carbon use efficiency and increased microbial turnover with soil warming, Glob. Change Biol., 25, 900–910, https://doi.org/10.1111/gcb.14517, 2019.

Liu, Z., Sun, Y., Zhang, Y., Feng, W., Lai, Z., Fa, K., and Qin, S.: Metagenomic and ^{13}C tracing evidence for autotrophic atmospheric carbon absorption in a semiarid desert, Soil Biol. Biochem., 125, 156–166, https://doi.org/10.1016/j.soilbio.2018.07.012, 2018.

Lladó, S., López-Mondéjar, R., and Baldrian, P.: Forest Soil Bacteria: Diversity, Involvement in Ecosystem Processes, and Response to Global Change, Microbiol. Mol. Biol. R., 81, 1–27, https://doi.org/10.1128/MMBR.00063-16, 2017.

Long, X. E., Yao, H., Wang, J., Huang, Y., Singh, B. K., and Zhu, Y. G.: Community Structure and Soil pH Determine Chemoautotrophic Carbon Dioxide Fixation in Drained Paddy Soils, Environ. Sci. Technol., 49, 7152–7160, https://doi.org/10.1021/acs.est.5b00506, 2015.

Loy, A., Lehner, A., Lee, N., Adamczyk, J., Meier, H., Ernst, J., Schleifer, K. H., and Wagner, M.: Oligonucleotide microarray for 16S rRNA gene-based detection of all recognized lineages of sulfate-reducing prokaryotes in the environment, Appl. Environ. Microb., 68, 5064–5081, 2002.

Madigan, M. T., Martinko, J. M., Bender, K. S., Buckley, D. H., and Stahl, D. A. (Eds.): Brock Biology of Microorganisms, 14th Edn., Pearson Education, Inc, 79–83, ISBN 978-0-321-89739-8, 2015.

Martens, R.: Current methods for measuring microbial biomass C in soil: Potentials and limitations, Biol. Fert. Soils, 19, 87–99, https://doi.org/10.1007/BF00336142, 1995.

Martin, J., Filip, Z., and Haider, K.: Effect of Montmorillontte and Humate on Growth and Metabolic Activity of Some, Soil Biol. Biochem., 8, 409–413, 1976.

Meisner, A., Jacquiod, S., Snoek, B. L., Ten Hooven, F. C., and van der Putten, W. H.: Drought legacy effects on the composition of soil fungal and prokaryote communities, Front. Microbiol., 9, 1–12, https://doi.org/10.3389/fmicb.2018.00294, 2018.

Melillo, J. M., Steudler, P. A., Aber, J. D., Newkirk, K., Lux, H., Bowles, F. P., Catricala, C., Magill, A., Ahrens, T., and Morrisseau, S.: Soil warming and carbon-cycle feedbacks to the climate system, Science, 298, 2173–2176, https://doi.org/10.1126/science.1074153, 2002.

Melillo, J. M., Butler, S., Johnson, J., Mohan, J., Steudler, P., Lux, H., Burrows, E., Bowles, F., Smith, R., Scott, L., Vario, C., Hill, T., Burton, A., Zhouj, Y. M., and Tang, J.: Soil warming, carbon-nitrogen interactions, and forest carbon budgets, P. Natl. Acad. Sci. USA, 108, 9508–9512, https://doi.org/10.1073/pnas.1018189108, 2011.

Melillo, J. M., Frey, S. D., DeAngelis, K. M., Werner, W. J., Bernard, M. J., Bowles, F. P., Pold, G., Knorr, M. A., and Grandy, A. S.: Long-term pattern and magnitude of soil carbon feedback to the climate system in a warming world, Science, 358, 101–105, https://doi.org/10.1126/science.aan2874, 2017.

Miltner, A., Richnow, H. H., Kopinke, F. D., and Kästner, M.: Assimilation of CO_2 by soil microorganisms and transformation into soil organic matter, Org. Geochem., 35, 1015–1024, https://doi.org/10.1016/j.orggeochem.2004.05.001, 2004.

Miltner, A., Kopinke, F. D., Kindler, R., Selesi, D., Hartmann, A., and Kästner, M.: Non-phototrophic CO_2 fixation by soil microorganisms, Plant Soil, 269, 193–203, https://doi.org/10.1007/s11104-004-0483-1, 2005.

Miltner, A., Kindler, R., Knicker, H., Richnow, H. H., and Kästner, M.: Fate of microbial biomass-derived amino acids in soil and their contribution to soil organic matter, Org. Geochem., 40, 978–985, https://doi.org/10.1016/j.orggeochem.2009.06.008, 2009.

Miltner, A., Bombach, P., Schmidt-Brücken, B., and Kästner, M.: SOM genesis: Microbial biomass as a significant source, Biogeochemistry, 111, 41–55, https://doi.org/10.1007/s10533-011-9658-z, 2012.

Nel, J. A. and Cramer, M. D.: Soil microbial anaplerotic CO_2 fixation in temperate soils, Geoderma, 335, 170–178, https://doi.org/10.1016/j.geoderma.2018.08.014, 2019.

Niederberger, T. D., Sohm, J. A., Gunderson, T., Tirindelli, J., Capone, D. G., Carpenter, E. J., and Cary, S. C.: Carbon-fixation rates and associated microbial communities residing in arid and ephemerally wet antarctic dry valley soils, Front. Microbiol., 6, 1–9, https://doi.org/10.3389/fmicb.2015.01347, 2015.

Nowak, M. E., Beulig, F., von Fischer, J., Muhr, J., Küsel, K., and Trumbore, S. E.: Autotrophic fixation of geogenic CO_2 by microorganisms contributes to soil organic matter formation and alters isotope signatures in a wetland mofette, Biogeosciences, 12, 7169–7183, https://doi.org/10.5194/bg-12-7169-2015, 2015.

Ocio, J. A. and Brookes, P. C.: An evaluation of methods for measuring the microbial biomass in soils following recent additions of wheat straw and the characterization of the biomass that develops, Soil Biol. Biochem., 22, 685–694, https://doi.org/10.1016/0038-0717(90)90016-S, 1990.

Oksanen, J., Kindt, R., Legendre, P., O'Hara, B., Simpson, G. L., Solymos, P. M., Stevens, M. H. H., and Wagner, H.: The Vegan Package, Community Ecology Package [code], 190, https://www.researchgate.net/profile/Gavin-Simpson-2/publication/228339454_The_vegan_Package/links/0912f50be86bc29a7f000000/The-vegan-Package.pdf (last access: 25 August 2022), 2008.

Prévost-Bouré, N. C., Dequiedt, S., Thioulouse, J., Lelièvre, M., Saby, N. P. A., Jolivet, C., Arrouays, D., Plassart, P., Lemanceau, P., and Ranjard, L.: Similar processes but different environmental filters for soil bacterial and fungal community composition turnover on a broad spatial scale, PLoS ONE, 9, 1–11, https://doi.org/10.1371/journal.pone.0111667, 2014.

Quast, C., Pruesse, E., Yilmaz, P., Gerken, J., Schweer, T., Yarza, P., Peplies, J., and Glöckner, F. O.: The SILVA ribosomal RNA gene database project: Improved data processing and web-based tools, Nucleic Acids Res., 41, 590–596, https://doi.org/10.1093/nar/gks1219, 2013.

Rastogi, M., Singh, S., and Pathak, H.: Emission of carbon dioxide from soil, Curr. Sci. India, 82, 510–517, 2002.

Rinnan, R., Michelsen, A., Bååth, E., and Jonasson, S.: Fifteen years of climate change manipulations alter soil microbial communities in a subarctic heath ecosystem, Glob. Change Biol., 13, 28–39, https://doi.org/10.1111/j.1365-2486.2006.01263.x, 2007.

Rinnan, R., Stark, S., and Tolvanen, A.: Responses of vegetation and soil microbial communities to warming and simulated herbivory in a subarctic heath, J. Ecol., 97, 788–800, https://doi.org/10.1111/j.1365-2745.2009.01506.x, 2009.

Rutherford, P. M. and Juma, N. G.: Influence of soil texture on protozoa-induced mineralization of bacterial carbon and nitrogen, Can. J. Soil Sci., 72, 183–200, https://doi.org/10.4141/cjss92-019, 1992.

Sakamoto, K. and Hodono, N.: Turnover time of microbial biomass carbon in japanese upland soils with different textures, Soil Sci. Plant Nutr., 46, 483–490, 2000.

Šantrůčková, H., Bird, M. I., Elhottová, D., Novák, J., Picek, T., Šimek, M., and Tykva, R.: Heterotrophic fixation of CO_2 in soil, Microb. Ecol., 49, 218–225, https://doi.org/10.1007/s00248-004-0164-x, 2005.

Šantrůčková, H., Kotas, P., Bárta, J., Urich, T., Čapek, P., Palmtag, J., Eloy Alves, R. J., Biasi, C., Diáková, K., Gentsch, N., Gittel, A., Guggenberger, G., Hugelius, G., Lashchinsky, N., Martikainen, P. J., Mikutta, R., Schleper, C., Schnecker, J., Schwab, C., Shibistova, O., Wild, B., and Richter, A.: Significance of dark CO_2 fixation in arctic soils, Soil Biol. Biochem., 119, 11–21, https://doi.org/10.1016/j.soilbio.2017.12.021, 2018.

Sarathchandra, S. U., Perrott, K. W., and Littler, R. A.: Soil microbial biomass: Influence of simulated temperature changes on size, activity and nutrient-content, Soil Biol. Biochem., 21, 987–993, https://doi.org/10.1016/0038-0717(89)90034-5, 1989.

Schindlbacher, A., Rodler, A., Kuffner, M., Kitzler, B., Sessitsch, A., and Zechmeister-Boltenstern, S.: Experimental warming effects on the microbial community of a temperate mountain forest soil, Soil Biol. Biochem., 43, 1417–1425, https://doi.org/10.1016/j.soilbio.2011.03.005, 2011.

Schloss, P. D., Westcott, S. L., Ryabin, T., Hall, J. R., Hartmann, M., Hollister, E. B., Lesniewski, R. A., Oakley, B. B., Parks, D. H., Robinson, C. J., Sahl, J. W., Stres, B., Thallinger, G. G., Van Horn, D. J., and Weber, C. F.: Introducing mothur: open-source, platform-independent, community-supported software for describing and comparing microbial communities, Appl. Environ. Microbiol., 75, 7537–7541, https://doi.org/10.1128/AEM.01541-09, 2009.

Schnürer, J., Clarholm, M., Boström, S., and Rosswall, T.: Effects of moisture on soil microorganisms and nematodes: A field experiment, Microb. Ecol., 12, 217–230, https://doi.org/10.1007/BF02011206, 1986.

Schuur, E. A. G., McGuire, A. D., Schädel, C., Grosse, G., Harden, J. W., Hayes, D. J., Hugelius, G., Koven, C. D., Kuhry, P., Lawrence, D. M., Natali, S. M., Olefeldt, D., Romanovsky, V. E., Schaefer, K., Turetsky, M. R., Treat, C. C., and Vonk, J. E.: Cli-

mate change and the permafrost carbon feedback, Nature, 520, 171–179, https://doi.org/10.1038/nature14338, 2015.

Selesi, D., Schmid, M., and Hartmann, A.: Diversity of Green-Like and Red-Like Genes (cbbL) in Differently Managed Agricultural Soils, Appl. Environ. Microb., 71, 175–184, https://doi.org/10.1128/AEM.71.1.175-184.2005, 2005.

Six, J., Frey, S. D., Thiet, R. K., and Batten, K. M.: Bacterial and Fungal Contributions to Carbon Sequestration in Agroecosystems, Soil Sci. Soc. Am. J., 70, 555–569, https://doi.org/10.2136/sssaj2004.0347, 2006.

Soong, J. L., Phillips, C. L., Ledna, C., Koven, C. D., and Torn, M. S.: CMIP5 Models Predict Rapid and Deep Soil Warming Over the 21st Century, J. Geophys. Res.-Biogeo., 125, e2019JG005266, https://doi.org/10.1029/2019JG005266, 2020.

Soong, J. L., Castanha, C., Hicks Pries, C. E., Ofiti, N., Porras, R. C., Riley, W. J., Schmidt, M. W. I., and Torn, M. S.: Five years of whole-soil warming led to loss of subsoil carbon stocks and increased CO_2 efflux, Science Advances, 7, 1–9, https://doi.org/10.1126/sciadv.abd1343, 2021.

Spohn, M., Klaus, K., Wanek, W., and Richter, A.: Microbial carbon use efficiency and biomass turnover times depending on soil depth – Implications for carbon cycling, Soil Biol. Biochem., 96, 74–81, https://doi.org/10.1016/j.soilbio.2016.01.016, 2016.

Spohn, M., Müller, K., Höschen, C., Mueller, C. W., and Marhan, S.: Dark microbial CO_2 fixation in temperate forest soils increases with CO_2 concentration, Glob. Change Biol., 26, 1926–1935, https://doi.org/10.1111/gcb.14937, 2019.

Stotzky, G. and Rem, L. T.: Influence of clay minerals on microorganizms. I. Montmorillonite and kaolinite on bacteria, Can. J. Microbiol, 12, 547–563, 1966.

Tsubo, M., Fukai, S., Basnayake, J., To, P. T., Bouman, B., and Harnpichitvitaya, D.: Effects of soil clay content on water balance and productivity in rainfed lowland rice ecosystem in Northeast Thailand, Plant Prod. Sci., 10, 232–241, https://doi.org/10.1626/pps.10.232, 2007.

Van 't Hoff, J. H.: Lectures on Theoretical and Physical Chemistry. Part 1. Chemical Dynamics, OCLC Number 220605730, Edward Arnold, London, 1898.

Van Veen, J. A., Ladd, J. N., and Frissel, M. J.: Modelling C and N turnover through the microbial biomass in soil, Plant Soil, 76, 257–274, 1984.

Van Veen, J. A., Ladd, J. N., and Amato, M.: Turnover of carbon and nitrogen through the microbial biomass in a sandy loam and a clay soil incubated with $[^{14}C(U)]$glucose and $[^{15}N](NH_4)_2SO_4$ under different moisture regimes, Soil Biol. Biochem., 17, 747–756, https://doi.org/10.1016/0038-0717(85)90128-2, 1985.

Vance, E. D., Brookes, P. C., and Jenkinson, D. S.: An extraction method for measuring soil microbial biomass C, Soil Biol. Biochem., 19, 703–707, https://doi.org/10.1016/0038-0717(87)90052-6, 1987.

Vijay, A., Chhabra, M., and Vincent, T.: Microbial community modulates electrochemical performance and denitrification rate in a biocathodic autotrophic and heterotrophic denitrifying microbial fuel cell, Bioresource Technol., 272, 217–225, https://doi.org/10.1016/j.biortech.2018.10.030, 2019.

Walker, T. W. N., Kaiser, C., Strasser, F., Herbold, C. W., Leblans, N. I. W., Woebken, D., Janssens, I. A., Sigurdsson, B. D., and Richter, A.: Microbial temperature sensitivity and biomass change explain soil carbon loss with warming, Nat. Clim. Change, 8, 885–889, https://doi.org/10.1038/s41558-018-0259-x, 2018.

Way, D. A. and Oren, R.: Differential responses to changes in growth temperature between trees from different functional groups and biomes: a review and synthesis of data, Tree Physiol., 30, 669–688, https://doi.org/10.1093/treephys/tpq015, 2010.

Werner, R. A. and Brand, W. A.: Referencing strategies and techniques in stable isotope ratio analysis, Rapid Commun. Mass Sp., 15, 501–519, https://doi.org/10.1002/rcm.258, 2001.

Winkler, J. P., Cherry, R. S., and Schlesinger, W. H.: The Q_{10} relationship of microbial respiration in a temperate forest soil, Soil Biol. Biochem., 28, 1067–1072, https://doi.org/10.1016/0038-0717(96)00076-4, 1996.

Wu, J., Joergensen, R. G., Pommerening, B., Chaussod, R., and Brookes, P. C.: Short Communication Measurement of Soil Microbial Biomassc Automated Procedure, Soil Biol. Biochem., 22, 1167–1169, 1990.

Wu, X., Ge, T., Yuan, H., Li, B., Zhu, H., Zhou, P., Sui, F., O'Donnell, A. G., and Wu, J.: Changes in bacterial CO_2 fixation with depth in agricultural soils, Appl. Microbiol. Biot., 98, 2309–2319, https://doi.org/10.1007/s00253-013-5179-0, 2014.

Xiao, H., Li, Z., Chang, X., Deng, L., Nie, X., Liu, C., Liu, L., Jiang, J., Chen, J., and Wang, D.: Microbial CO_2 assimilation is not limited by the decrease in autotrophic bacterial abundance and diversity in eroded watershed, Biol. Fert. Soils, 54, 595–605, https://doi.org/10.1007/s00374-018-1284-7, 2018.

Yin, H., Xiao, J., Li, Y., Chen, Z., Cheng, X., Zhao, C., and Liu, Q.: Warming effects on root morphological and physiological traits: The potential consequences on soil C dynamics as altered root exudation, Agr. Forest Meteorol., 180, 287–296, https://doi.org/10.1016/j.agrformet.2013.06.016, 2013.

Yuan, H., Ge, T., Chen, C., O'Donnell, A. G., and Wu, J.: Significant role for microbial autotrophy in the sequestration of soil carbon, Appl. Environ. Microb., 78, 2328–2336, https://doi.org/10.1128/AEM.06881-11, 2012.

Supplement of Biogeosciences, 19, 4011–4028, 2022
https://doi.org/10.5194/bg-19-4011-2022-supplement

Biogeosciences Open Access EGU

Supplement of

Temperature sensitivity of dark CO_2 fixation in temperate forest soils

Rachael Akinyede et al.

Correspondence to: Kirsten Küsel (kirsten.kuesel@uni-jena.de)

Supplementary methods

Determination of natural ^{14}C isotope signatures of the beech and spruce soil.

The radiocarbon signature of the bulk soil samples was measured using the accelerator mass spectrometry (AMS) with a 3-MV Tandetron ion accelerator (HVEE, Amersfoort, Netherlands) according to Steinhof et al. (2017). As with the ^{13}C isotope ratios, radiocarbon ratios were reported as the ‰ deviation of the $^{14}C/^{12}C$ ratio but from the international oxalic acid universal standard (ox1) in $\Delta^{14}C$. All $\Delta^{14}C$ value of the sample was then corrected appropriately as previously described (Trumbore, 2009; Mook and Van der Plicht, 1999). The measured bulk ^{14}C values of the beech and spruce soils are described in Table S1.

$$\Delta^{14}C = \left[\frac{\frac{^{14}C}{^{12}C} sample - 25}{0.95 \frac{^{14}C}{^{12}C} ox1 - 19 \times exp^{\left(y - \frac{1950}{8267}\right)}} \right] \times 1000 \quad \text{(S1)}$$

Supplementary figures

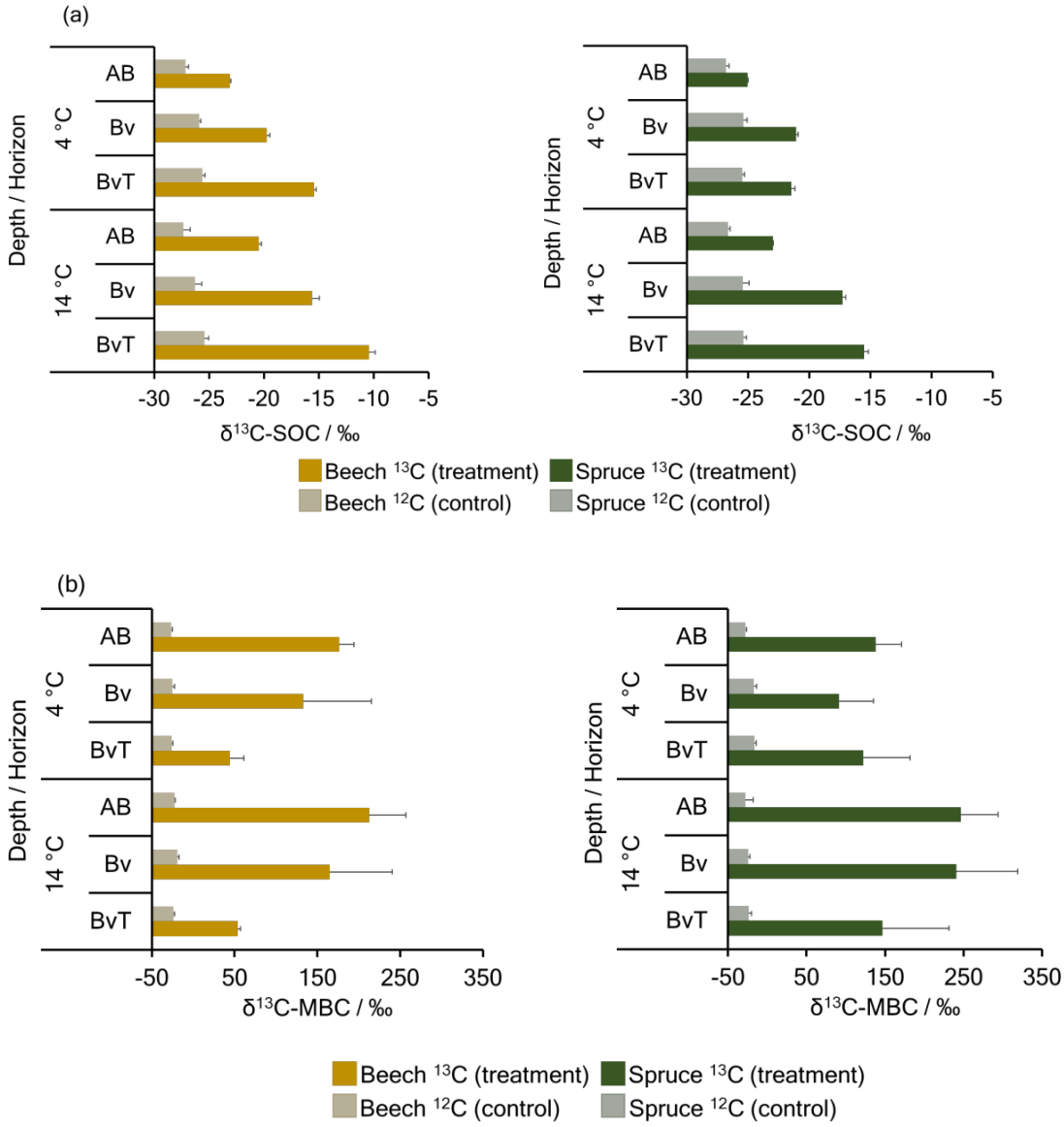

15 **Figure S1: δ^{13}C enrichment of SOC and MBC in soil microcosms supplemented with 2% $^{13}CO_2$ together with $^{12}CO_2$ labelled controls at 4 and 14 °C.** Shown are (a) ^{13}C signal in SOC and (b) ^{13}C signal in MBC after 21 days of incubation with 2% $^{13}CO_2$ at 4 and 14°C across three horizons in beech (yellow bars) and spruce (green bars) soils. Incubations with ^{13}C labelled CO_2 (treatment) are denoted with filled bars while incubations with ^{12}C (control/natural abundance) are denoted by shaded bars. Error bars indicate the standard deviation of incubations from three replicate soil cores.

90

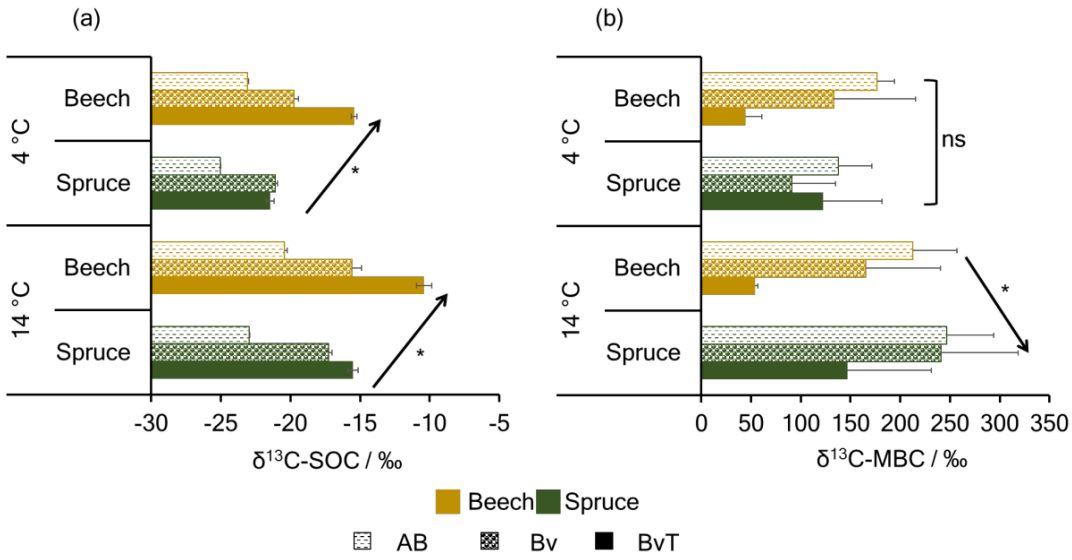

Figure S2: $\delta^{13}C$ signals of SOC and MBC in soil microcosms supplemented with 2% $^{13}CO_2$ at 4 and 14 °C from beech and spruce soils. Shown are (a) ^{13}C signal in SOC and (b) ^{13}C signal in MBC after 21 days of incubation with 2% $^{13}CO_2$ at 4 and 14°C across three horizons in beech (yellow bars) and spruce (green bars) soils. Error bars indicate the standard deviation of incubations from three replicate soil cores. * denote $p < 0.05$, ns denote not significant.

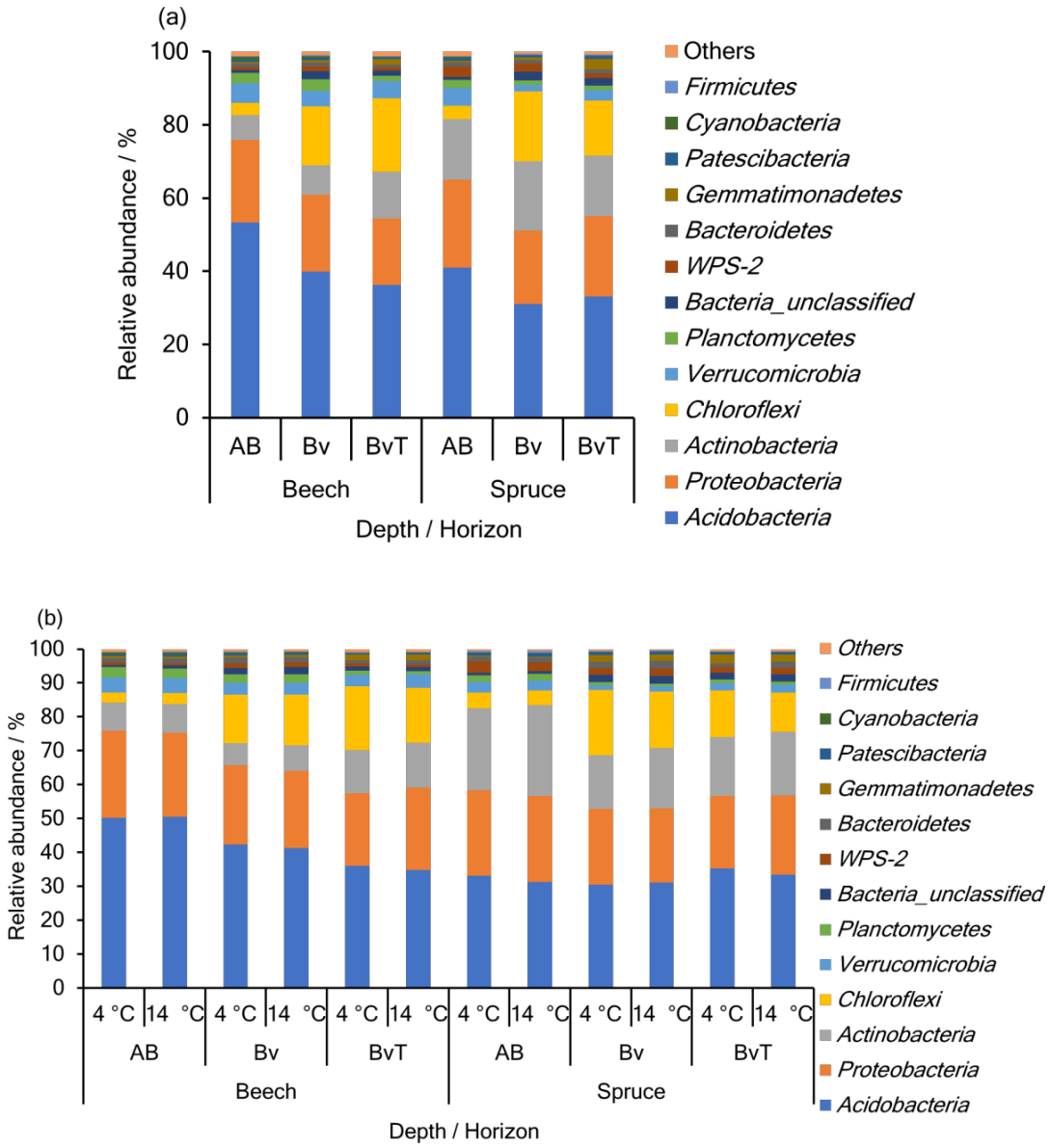

Figure S3: Bacterial community composition from beech and spruce soil. Shown are phylum-level relative abundances of assigned sequences for (a) the beech and spruce bulk soils and for (b) beech and spruce soils incubated with 2% $^{13}CO_2$ at 4 and 14°C. Bar plots are represented by three replicate soil cores per depth. Taxonomic assignment of OTUs is based on the SILVA database implemented on the MOTHUR sequence analysis pipeline. Data represent 3 replicate soil cores per depth for the beech and spruce soils.

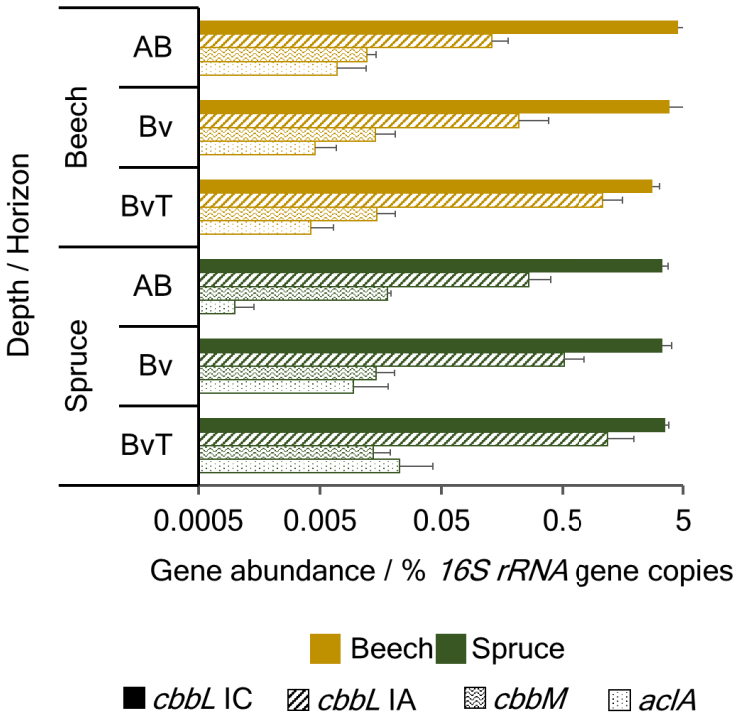

Figure S4: Abundance of chemolithoautotrophic marker genes potentially involved in dark CO_2 fixation in the beech and spruce bulk soi profiles. Shown are the abundances of RuBisCO (*cbbL* IA, *cbbL* IC, and *cbbM*) and ATP citrate lyase (*aclA*) genes relative to total bacterial abundance (*16S rRNA* gene copies) in the beech and spruce bulk soils. Data acquired by qPCR. The scale on the x-axis is logarithmic (base 10). Error bars indicate the standard deviation of incubations from three replicate soil cores.

Table S1: The $\Delta^{14}C$ signatures of SOC (‰) measured for soil cores obtained from beech and spruce soil plots at the Hummelshain forest. Each reported value represents the mean of three replicate soil cores taken from bulk soils during the sampling campaign.

Plot	Depth (Horizon)	$\Delta^{14}C$-SOC (‰)
Beech	AB	-2.68 ± 7.48
	Bv	-61.00 ± 30.96
	BvT	-170.10 ± 0.75
Spruce	AB	16.64 ± 18.18
	Bv	-92 .98 ± 28.82
	BvT	-201.89 ± 76.59

Table S2: Geochemical properties of soil cores obtained from beech and spruce soil plots at the Hummelshain forest measured under two temperature conditions. Soil organic carbon (SOC), Total nitrogen (TN), carbon/nitrogen (C/N) ratio, microbial biomass carbon (MBC), Moisture, and *16S rRNA* gene copies reported for 3 depths definitions for the beech and spruce soils at 4 and 14 °C. Each reported value represents the mean of three replicate soil cores taken after the soil incubation period.

		Beech			Spruce		
Depth (Horizon)		**AB**	**Bv**	**BvT**	**AB**	**Bv**	**BvT**
SOC (%)	**4 °C**	0.89 ± 0.09	0.27 ± 0.10	0.12 ± 0.02	1.50 ± 0.05	0.23 ± 0.04	0.30 ± 0.14
	14 °C	0.89 ± 0.1	0.29 ± 0.11	0.13 ± 0.03	1.56 ± 0.04	0.25 ± 0.05	0.30 ± 0.14
TN (%)	**4 °C**	0.04 ± 0.003	0.03 ± 0.004	0.02 ± 0.002	0.07 ± 0.01	0.03 ± 0.002	0.03 ± 0.005
	14 °C	0.04 ± 0.001	0.03 ± 0.003	0.02 ± 0.003	0.08 ± 0.002	0.03 ± 0.002	0.03 ± 0.003
C/N ratio	**4 °C**	20.82 ± 0.64	10.12 ± 3.24	5.22 ± 0.51	19.99 ± 1.96	8.74 ± 1.37	9.32 ± 3.24
	14 °C	19.81 ± 2.54	10.62 ± 2.82	5.16 ± 0.93	19.23 ± 0.39	9.12 ± 1.44	9.25 ± 3.55
MBC (µg C gdw^{-1})	**4 °C**	54.91 ± 4.91	24.04 ± 2.61	12.72 ± 1.78	101.53 ± 19.5	28.97 ± 9.56	27.61 ± 8.50
	14 °C	47.61 ± 2.95	23.90 ± 7.06	15.81 ± 2.51	73.69 ± 17.81	13.12 ± 3.95	26.62 ± 5.86
Moisture (%)	**4 °C**	8.92 ± 1.68	11.09 ± 1.32	11.96 ± 2.48	7.71 ± 1.68	11.23 ± 2.83	11.29 ± 1.97
	14 °C	7.49 ± 1.3	7.31 ± 0.44	10.65 ± 1.31	7.12 ± 1.00	7.42 ± 0.75	10.72 ± 1.07
***16S rRNA* (copies/gdw^{-1})**	**4 °C**	2.96 x 109 ± 9.69 x 108	8.49 x 108 ± 5.50 x 108	1.17 x 108 ± 4.27 x 108	2.19 x 109 ± 5.68 x 108	2.76 x 108 ± 1.32 x 108	2.92 x 108 ± 1.89 x 108
	14 °C	3.23 x 109 ± 7.41 x 108	8.67 x 108 ± 4.62 x 108	1.52 x 108 ± 1.02 x 108	2.54 x 109 ± 8.84 x 109	2.74 x 108 ± 1.06 x 108	2.98 x 108 ± 1.74 x 108

Table S3: Derived decomposition rates and the Q_{10} for the beech and spruce soils across depth. Decomposition rates (at 4 and 14 °C) were derived by adding the respective measured CO_2 fixation rates with the net respiration rates for all samples while the Q_{10} values were calculated as similarly done for the CO_2 fixation rates and the net respiration rates (Eq. (6) in method section 2.4). Each reported value represents the mean of three replicate soil cores taken after the soil incubation period. ND denotes values that were "not determined".

Plot	Depth (Horizon)	Decomposition rates (µg C g^{-1} (dw) soil d^{-1})		Q_{10}
		4 °C	14 °C	
Beech	AB	1.28 ± 0.63	2.92 ± 1.42	2.29 ± 0.02
	Bv	0.58 ± 0.49	1.23 ± 0.93	3.37 ± 1.34
	BvT	ND	0.14 ± 0.09	ND
Spruce	AB	0.91 ± 0.39	2.34 ± 0.92	2.59 ± 0.11
	Bv	0.13 ± 0.11	0.34 ± 0.01	3.89 ± 3.28
	BvT	0.41 ± 0.12	1.07 ± 0.07	2.63 ± 0.29

Table S4: Primers and adapter sequences used for two-step barcoding approach for Illumina MiSeq sequencing of the bacterial *16S rRNA* genes.

Primer	Sequences (5' – 3')	References
1st PCR step		
Bact_341F	[TCGTCGGCAGCGTCAGATGTGTATAAGAGACAG] CCTACGGGNGGCWGCAG	Klindworth et al., 2013
Bact_785R	[GTCTCGTGGGCTCGGAGATGTGTATAAGAGACAG] GACTACHVGGGTATCTAATCC	
2nd PCR step		
Index 1	CAAGCAGAAGACGGCATACGAGAT [i7] GTCTCGTGGGCTCGG	Illumina®
Index 2	AATGATACGGCGACCACCGAGATCTACAC [i5] TCGTCGGCAGCGTC	

References

Klindworth, A., Pruesse, E., Schweer, T., Peplies, J., Quast, C., Horn, M., Glöckner, F.O.: Evaluation of general 16S ribosomal RNA gene PCR primers for classical and next-generation sequencing-based diversity studies, Nucleic Acids Research, 41, 1–11, doi:10.1093/nar/gks808, 2013.

Mook, W. G., Van der Plicht, J.: Reporting ^{14}C activities and concentrations, Radiocarbon, 41, 227–239, 1999.

Steinhof, A., Altenburg, M., Machts, H.: Sample Preparation at the Jena 14C Laboratory, Radiocarbon, 59, 815–830. doi:10.1017/RDC.2017.50, 2017.

Trumbore, S.: Radiocarbon and Soil Carbon Dynamics, Annual Review of Earth and Planetary Sciences, 37, 47–66. doi:10.1146/annurev.earth.36.031207.124300, 2009.

5 General discussion

5.1 Dark CO_2 fixation and its inputs to temperate forest SOM across 1 m depth profiles

Dark CO_2 fixation occurs down to 1 m depth of soil. Based on the detection of ^{13}C from CO_2 in soil organic carbon (SOC) and microbial biomass carbon (MBC) reported in all three chapters, dark CO_2 fixation rates across 1 m depths profiles was measured in all forest plots investigated. Average rates per gram of soil dry weight ranged between ~0.7 ± 0.24 μg C g (dw) $soil^{-1}$ d^{-1} in the top depth (0 – 20 cm) and ~0.01 ± 0.002 μg C g (dw) $soil^{-1}$ d^{-1} in the lowest bottom depths (60 – 100 cm) across all forest soils (Figure 6). This supports the first hypothesis (**H_1**) that dark O_2 fixation occurs down to 1 m depth in temperate forest soils. The range of values measured was within the magnitude reported by other studies over a broad range of soil types, including agricultural soils, arctic soils, mofette soils, as well as soils of temperate forest regions (Beulig et al., 2014; Miltner et al., 2005; Nel and Cramer, 2019; Nowak et al., 2015; Šantrůčková et al., 2018; Spohn et al., 2019). A summary of these rates is given in Table 2 of **Chapter 2**. For instance, the highest measured fixation rates were up to 4 to 5 times higher than those of temperate agricultural soils (Miltner et al., 2005) and over 8 times higher than rates measured in tropical forest soils (Nowak et al., unpublished results) but 3 times lower than those reported for a wetland mofette (Beulig et al., 2016). Compared to other temperate forest soils reported in a recent study (Spohn et al., 2019), the contrast between the rates varied depending on the forest plots. For example, in the top depth of the Hainich forest soil, where the highest rates were measured, values at ~0.7 μg C g (dw) $soil^{-1}$ d^{-1} were 6 times higher than those recently reported by Spohn et al. (2019) at a similar depth. However, rates measured from the Schorfheide-Chorin topsoil with ~0.16 μg C g (dw) $soil^{-1}$ d^{-1} scaled with those of Spohn et al. (2019), and average rates measured from the Hummelshain forest topsoil at ~0.03 μg C g (dw) $soil^{-1}$ d^{-1} were 4 times lower in comparison to the Spohn et al. (2019) study. As discussed in **Chapter 2**, the differences in rates reported here when compared to other soils are likely a reflection of the variations in site-specific parameters like SOC and MBC content (Šantrůčková et al., 2018) and the abundance of specific chemolithoautotrophic groups (Beulig et al., 2016; Nowak et al., 2015). It could also result from differences in incubation conditions, e.g., duration (Miltner et al., 2005) and temperature (Nel and Cramer, 2019; Spohn et al., 2019).

Dark CO_2 fixation rates decrease with soil depth. Strikingly, the rates of dark CO_2 fixation normalized per gram of soil generally showed a decreasing trend with depth (Figure 6). In the Hainich soils, rates were as much as 17 times lower in bottom depth compared to the top depth

(**Chapter 2**). A similar magnitude with depth was observed in the Schorfheide-Chorin forest soils, with fixation rates being 7 and 14 and times lower in the deepest depths of the beech and spruce soils, respectively, in contrast to the top depth (**Chapter 3**). Less strong differences with depth were observed in the Hummelshain forest soils, with rates being 2 to 3 times lower in both the beech and spruce subsoils when compared to the rates measured at the topsoil (**Chapter 4**). This consistent decrease in CO_2 fixation rates across the profile partly disagrees with our assumption that the relative importance of chemolithoautotrophy will increase with depth due to limited amounts of SOC. A similar decrease in CO_2 fixation rates with soil depth has been observed in previous studies (Nowak et al., 2015; Spohn et al., 2019), suggesting this to be a common trend in soils.

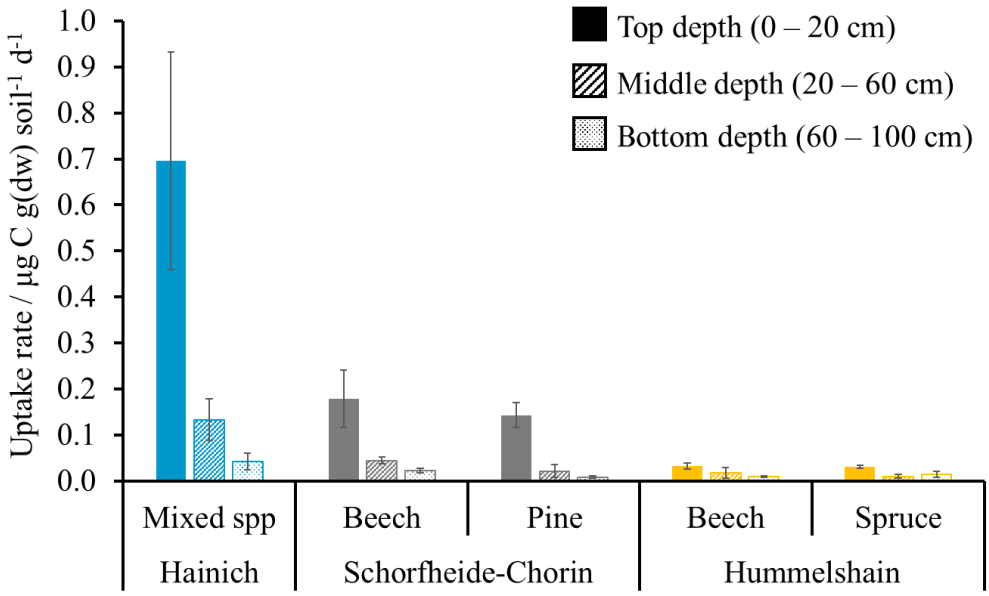

Figure 6| Dark CO_2 fixation rates measured down to 1 m depth profiles across three depth definitions from three temperate forest plots in Germany. Bars represent rates measured in soils incubated with 2% $^{13}CO_2$ at 20 °C. For the Hummelshain forest plots, values represent rates measured at 14 °C.

This decrease in fixation rates was consistently accompanied by a decrease in MBC and SOC content with increasing soil depth (Table 1), as commonly observed in soils (Jobbágy and Jackson, 2000; Xu et al., 2013). The decrease in rates with MBC suggests that microbial biomass as a whole chiefly contributed to fixing CO_2. Forest soil microbes largely depend on SOC for growth, and microbial biomass correlates strongly with SOC (Cleveland and Liptzin, 2007; Lladó et al., 2017). Hence, the decrease in SOC may explain why rates decreased with depth. In a study on non-phototrophic CO_2 fixation in agricultural soils, Miltner et al. (2005)

found that CO_2 fixation rates were enhanced in soils supplemented with acetate as an organic carbon source. Similar findings were observed in an arctic tundra soil supplemented with sucrose and lipids as an additional carbon substrate (Šantrůčková et al., 2018). Yuan et al. (2012, 2013) also reported higher CO_2 fixation rates in paddy soils characterized by high organic carbon content than upland soils with low SOC content. Because topsoil generally features the highest organic carbon content (Jobbágy and Jackson, 2000), this also indicates that dark CO_2 fixation is quantitatively most significant in the topsoil. Past studies have likewise shown higher CO_2 fixation rates in topsoils that feature higher SOC and MBC content compared to deeper profiles with lower SOC content (Nowak et al., 2015; Xiao et al., 2018).

Table 1| Average values of SOC (in %) and MBC (in µg C g $(dw)^{-1}$) content measured across all three temperate forest soil profiles.

Forest site	Tree species	Parameter	Depth		
			Top depth (0 – 20 cm)	Middle depth (20 – 60 cm)	Bottom depth (60 – 100 cm)
Hainich	Mixed (Mostly beech)	SOC /%	3.56 ± 0.65	0.85 ± 0.11	0.44 ± 0.14
		MBC/ µg C g $(dw)^{-1}$	367.97 ± 20.64	29.74 ± 10.49	20.15 ± 6.25
Schorfheide-Chorin	Beech	SOC/%	1.54 ± 0.40	0.40 ± 0.13	0.2 ± 0.04
		MBC/ µg C g $(dw)^{-1}$	224.70 ± 48.87	30.18 ± 9.22	35.21 ± 7.84
	Pine	SOC/%	2.33 ± 0.79	0.57 ± 0.08	0.08 ± 0.01
		MBC/ µg C g $(dw)^{-1}$	215.15 ± 63.35	90.64 ± 16.98	44.48 ± 3.88
Hummelshain	Beech	SOC/%	0.90 ± 0.12	0.28 ± 0.11	0.12 ± 0.03
		MBC/ µg C g $(dw)^{-1}$	74.14 ± 3.08	21.92 ± 6.53	14.26 ± 6.3
	Spruce	SOC/%	1.56 ± 0.07	0.33 ± 0.13	0.21 ± 0.05
		MBC/ µg C g $(dw)^{-1}$	84.83 ± 9.42	25.39 ± 12.85	19.43 ± 6.71

Dark CO_2 fixation contributes to soil organic matter. Despite that CO_2 fixation rates were lower in the deeper profiles, relative contributions to SOC content at these depths were only slightly lower than in the top depth with up to 0.01% in the Hainich and in the Schorfheide-Chorin forest soils **(Chapters 2 and 3**). For the Hummelshain forest soils, inputs to subsoil SOC were even 2 to 3 times higher than in the topsoil with up to 0.02% (**Chapter 4**). Such

contributions to SOC when comparing the top and subsoil profiles validate the recycling of CO_2 as an additional and important carbon source for microbes in the subsoil (Ehleringer, 2000). As the contributions of fixed carbon to SOC occurs via microbial inputs, dark CO_2 fixation contributed over 10 times more to MBC. Overall, across the profile, the contribution to MBC was mostly similar, with as much as 1% after 28 days in the Hainich forest soils (**Chapter 2**) and up to 0.2% after 7 days and 0.3 % after 21 days in the Schorfheide-Chorin soils (**Chapter 3**) and Hummelshain forest soils (**Chapter 4**) respectively.

Although the contributions of dark CO_2 fixation to SOC and MBC are small, they can be significant for SOC storage when considering the turnover of microbial biomass into the SOM pool (**Chapter 4**). When microbes die, microbial cells decay and lose their integrity (Lengler et al., 1999). Thus, part of the CO_2-derived carbon may leak out of their biomass and get transferred into non-living SOM pools (Miltner et al., 2012). Previous studies have shown that carbon derived from CO_2 fixation by microbes was found in microaggregate fractions of soil organic matter after only a 7-day incubation study (Spohn et al., 2019), and this is a relatively stable SOM pool (Totsche et al., 2017). Dead microbial biomass or microbial necromass (including fragments and macro-molecular residues) are considered to be as stable as plant detritus in soil (Miltner et al., 2012), with microbial residues like amino sugars described to be even more stabilized than plant lignin (Ma et al., 2018). Laboratory incubation studies also show that microbial biomass can even turnover at slower rates than some plant leaves and stems (Paul, 2016). Microbial biomolecules are stabilized due to macromolecular aggregations like in cell envelopes and the complex composition of these materials. They are further stabilized in soils by physical interaction, trapping within aggregates and matrix of soil, or by aggregation with themselves, limiting accessibility of the internal regions to degradation (Kästner et al., 2021). It is also suggested that subsoils have a high capacity to sequester significant amounts of SOC due to the longer turnover time and chemical recalcitrance of SOM (Lorenz and Lal, 2005). Since microbial necromass also makes up to 30% of temperate forest SOC (Liang et al., 2019), this makes microbial products derived from CO_2 fixation from surface to deep profiles a significant source of temperate forest SOM. Therefore, if the concept that microbial molecules have a long residence time in soils (Miltner et al., 2012) holds true and if CO_2 is fixed into stable SOM (Spohn et al., 2019), CO_2 derived carbon via necromass may, over time, contribute substantially to temperate forest SOC storage.

It should, however, be considered that the turnover of CO_2 derived carbon from MBC into SOM will ultimately depend on the persistence and turnover time of the living and dead

biomass (Liang et al., 2019; Miltner et al., 2012) as determined by various physicochemical factors like oxygen, nitrogen, moisture, clay content, and temperature, etc. (Ali et al., 2020; Hagerty et al., 2014; Liang et al., 2019; Zhang et al., 2019). For example, **Chapter 4** showed that the turnover of microbial biomass and its fixed carbon increased with temperature and was also higher in clay-rich spruce soils compared to clay-poor beech soils. Biomass turnover may also depend on the microbial taxa (Dong et al., 2021). Forest soils dominated by more heterotrophs were associated with a higher turnover of microbially fixed carbon than soils with less proportion of heterotrophs due to their fast growth (**Chapter 4**). Furthermore, in soils, the stabilization of different biomolecules to which CO_2 can be fixed may vary partly due to postmortem modification of the biomolecules, with proteins being more stable than bulk MBC and phospholipid fatty acid (PLFA) (proteins > bulk MBC > PLFA) (Fan et al., 2004; Kästner et al., 2021). As this thesis did not evaluate the amount of CO_2-derived carbon in different microbial cell components, the process underlying the contribution of dark CO_2 fixation to SOM via microbial biomass remains elusive. A full understanding of such contributions to SOM would require knowledge of the stability and turnover of different components of microbial biomass and necromass to which CO_2 is fixed and how this change under varying ecosystem and ecological conditions. The contributions to SOM via dark CO_2 fixation into MBC as reported here may only reflect the possible fate and significance of CO_2-derived carbon for temperate forest SOC storage.

H_1| The findings confirm the first hypothesis that dark CO_2 fixation occurs down to 1 m depth in temperate forest soils.

Dark CO_2 fixation was observed down to 1 m depth in all three temperate forest soil profiles. Dark CO_2 fixation rates across the profiles mirrored the decrease in MBC and SOC content with depth. This finding may suggest that microbial biomass as a whole (which depends on SOC) contributed towards CO_2 fixation. Despite the decrease in CO_2 fixation rates with depth, the relatively uniform contributions to the microbial biomass carbon and soil organic carbon pools from the surface to the subsoil provide insights into the significance of this process for carbon cycling across deep soil profiles as well as on the possible fate of the SOC derived via dark CO_2 fixation by microbial biomass.

5.2 The genomic potential for dark CO_2 fixation in temperate forest soils.

The genomic potential for chemolithoautotrophy does not increase with depth. The data from all three forest sites investigated disagrees with our second hypothesis (**H_2**) that the genomic potential for chemolithoautotrophy will increase with soil depth. PICRUSt2 predictions showed that the OTUs of putative autotrophs displayed a constant to decreasing relative abundance across the profile for all forest plots. While the abundance of putative autotrophic OTUs maintained a uniform proportion across depth in the Hainich forest soils and in the pine soil profiles of the Schorheide-Chorin soils (**Chapters 2 and 3**), they decreased with depth in the beech soils of the Schorfheide-Chorin forest and in the Hummelshain forest soils (**Chapters 3 and 4**). The abundance of marker genes for CBB and rTCA pathways was further determined by qPCR to verify the predicted potential for chemolithoautotrophy. The *cbbL* IC genes of the CBB pathway, being quantitatively the most dominant in all forest soils, mostly maintained a uniform proportion across most forest soil profiles (**Chapters 2, 3, and 4**). Only the beech profiles of the Hummelshain forest soils were an exception, where a slight decrease in abundance with depth was observed (**Chapter 4**). Consequently, the abundance of the dominant autotrophic genes (*cbbL* IC) quantified did not correlate with the measured CO_2 fixation rates across depth (Figure 7). This suggests that chemolithoautotrophy might not completely explain the CO_2 fixation rates measured from these soils.

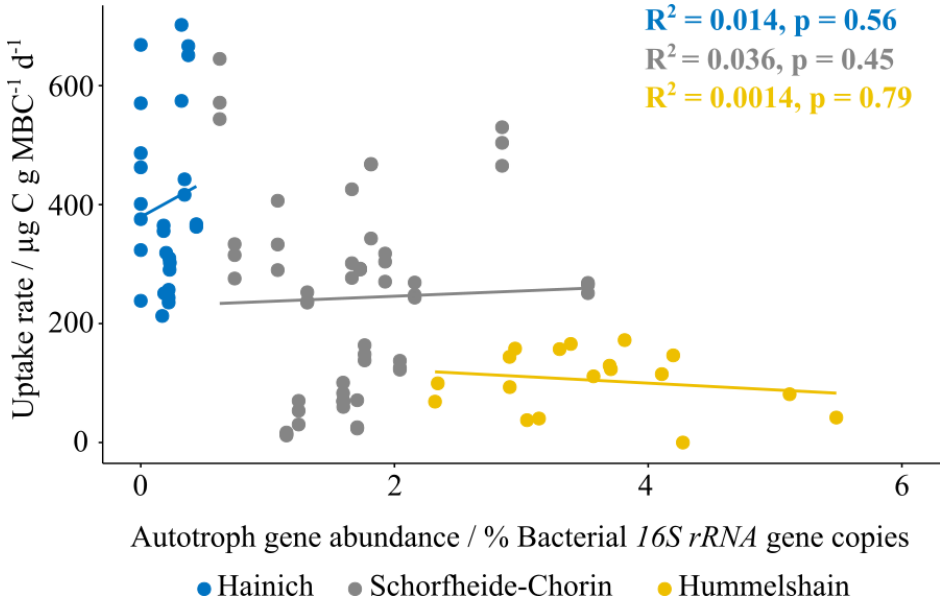

Figure 7| Relationship between dark CO_2 fixation rates and autotroph gene abundance. Data represent measurements from the three forest soil profiles investigated in Chapters 2, 3, and 4.

Dark CO_2 fixation rates correlate positively with microbial biomass. Although CO_2 fixation did not correlate with the abundance of autotrophs with depth, we found a strong relationship between the rates and microbial biomass carbon content. **Chapter 2** first showed that in the Hainich forest, dark CO_2 fixation rates normalized to MBC remained similar with depth regardless of changes in the SOC content and community composition across the profile. Based on this observation, microbial biomass was suggested as the main driver of dark CO_2 fixation in the soils. But for a few exceptions, a similar linear relationship between microbial biomass and dark CO_2 fixation rates, as reflected by the uniformity of rates per gram MBC across depth, was observed in the other forest plots (Figure 8). This was independent of the differences in the site conditions observed between the forest plots (**Chapters 2, 3 and 4**), indicating that the relationship between microbial biomass and dark CO_2 fixation is likely to occur in other temperate forest soils. Multiple stepwise regression analysis provided further information on the relationship between microbial biomass and CO_2 fixation rates over a range of temperate deciduous and coniferous forest soils (**Chapter 3**). Here, MBC significantly explained ~70% of the variations in the rates, further emphasizing the dominance of the microbial biomass on CO_2 fixation dynamics in temperate forest soils. Consequently, the Hainich forest soils featuring the highest MBC content (Table 1) also featured the highest CO_2 fixation rate compared to the Schorfheide-Chorin and Hummelshain forest soils (Figure 6). In agreement, soils with high microbial biomass content have been shown to feature higher dark CO_2 fixation rates compared to soils with low biomass (Nowak et al., 2015; Spohn et al., 2019).

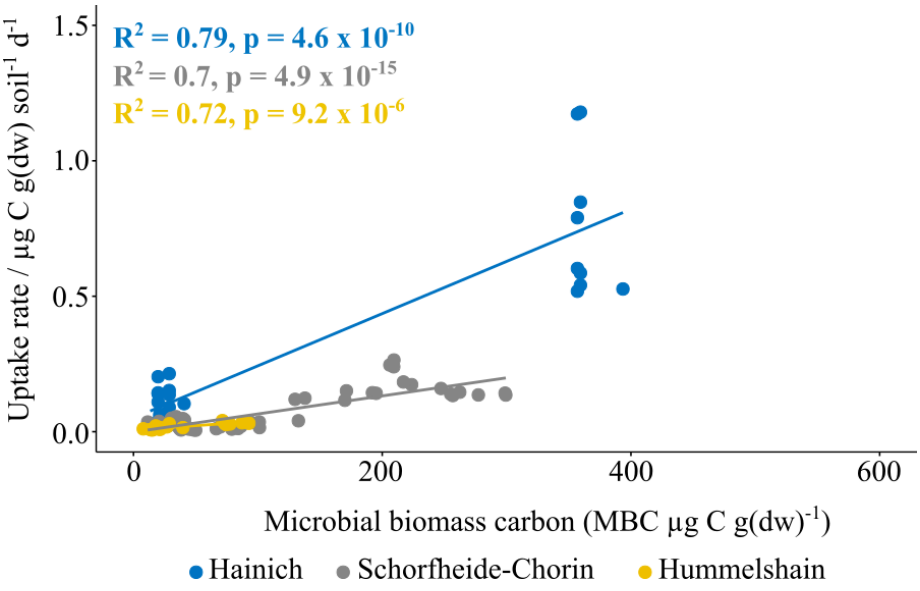

Figure 8| Relationship between dark CO_2 fixation rates and microbial biomass carbon. Data represent measurements from the three forest soil profiles investigated as given in Chapters 2, 3 and 4.

Constituting a small fraction (<5%) of SOC, the biomass of microbial communities is the most labile and biologically active pool of carbon in soils (Dalal, 1998; Jiang-shan et al., 2005; St. Luce et al., 2011; Rössner et al., 1996). Microbial biomass is the main energy transfer agent in soil (Bauhus and Khanna, 1999) and thus is mainly responsible for the cycling of SOC via the fixation and emission of CO_2 (Ehleringer et al., 2000; Nowak et al., 2015; Rastogi et al., 2002; Walker et al., 2018). For this reason, MBC is considered an important indicator of soil ecosystem changes (Bauhus and Khanna, 1999). This means that MBC can be potentially used as a proxy parameter when evaluating changes in dark CO_2 fixation activity across temperate forest soils. If we consider the relationship between MBC and dark CO_2 fixation across all the forest soils put together ($R^2 = 0.61$ $p = 2.2 \times 10^{-21}$), we can estimate how much carbon from CO_2 can be fixed through dark CO_2 fixation based on a specific amount of MBC. Based on this simple linear relationship, it can be roughly estimated that for every 100 µg of MBC in a gram of temperate forest soil, there is the potential for the incorporation of ~0.1 µg C g soil^{-1} from CO_2 via dark CO_2 fixation. With this given estimate, it is still difficult to accurately quantify the effects of microbial biomass on CO_2 fixation rates and inputs to SOM in temperate forest soils as CO_2 fixation rates may also depend on the composition of the microbial community and their response to external factors (Xiao et al., 2018). An additional factor to consider is the turnover of both living and dead biomass components (Kästner et al., 2021; Liang et al., 2019; Miltner et al., 2012) in light of their contributions to SOC as discussed in section 5.1. These estimates should thus, be treated cautiously and be primarily used for hypothesis generation.

The genomic potential for dark CO_2 fixation is associated with a common metabolism among the soil microbial communities. The consistent correlation between dark CO_2 fixation and microbial biomass suggested that most of the microbial communities and not just chemolithoautotrophs were potentially involved in fixing CO_2. Thus, further evaluation of the genomic potential for both autotrophic and non-autotrophic CO_2 fixation among the microbial communities was done. High throughput sequencing of the bacteria *16S rRNA* profiles provided a first snapshot of the microbial community composition in the temperate forest soils investigated. This analysis showed the dominance of bacterial groups belonging to four main phyla; *Proteobacteria*, *Actinobacteria*, *Acidobacteria,* and *Chloroflexi*, among the bacterial community (**Chapters 2, 3, and 4**), and these are the typical groups found in forest soils (Dukunde et al., 2019; Kaiser et al., 2016; Lladó et al., 2017; Urbanová et al., 2015).

The predictions of CO_2 fixation potentials for all generated *16S rRNA* sequences using PICRUSt2 showed a low abundance of chemolithoautotrophic genes, constituting no more than 20% of the total bacterial community across the profile (**Chapters 2, 3, and 4**). These were mostly affiliated with the CBB (~15%), followed by the WLP (<2%) and the rTCA (<1%) pathway (Figure 9). Bacterial phyla with the most abundant putative autotrophic OTUs were mostly *Proteobacteria* (CBB and WLP) and a few *Nitrospira* (rTCA), and many members of these groups are known to fix CO_2 in a diverse range of soils (Li et al., 2018; Liu et al., 2018; Niederberger et al., 2015; Šantrůčková et al., 2018; Wu et al., 2014; Xiao et al., 2018). Subsequent verification using qPCR analysis of functional genes as reported in all three chapters, pointed towards the presence of the same predicted autotrophic pathways in the same order except the WLP pathway, which was not quantified by qPCR due to the lack of reliable, standardized qPCR protocols and primer set targeting the key genes of this pathway. Among the genes quantified, the *cbbL* IC gene of the CBB pathway was also the most dominant ranging from 0.2% to <5% of the bacterial community across all forest plots. This was followed by *cbbL* IA (CBB) and the *aclA* gene of the rTCA pathway, each constituting no more than 0.2%. Altogether, all chemolithoautotrophic genes quantified by qPCR accounted for ~5% of the total bacterial community, thus, further confirming the low autotrophic CO_2 fixation potential predicted by PICRUSt2. In contrast to the genetic potential for chemolithoautotrophy, over 3 times higher abundance of PEPC and PC genes were predicted across depth, making up to 70% of the total bacterial community. These genes are markers of non-autotrophic anaplerotic CO_2 fixation (Erb, 2011b) and were mostly affiliated with three of the most dominant bacterial groups; *Proteobacteria, Actinobacteria, and Acidobacteria* (Figure 9). The potential for non-phototrophic anaplerotic CO_2 fixation has been reported in Arctic soils (Šantrůčková et al., 2018).

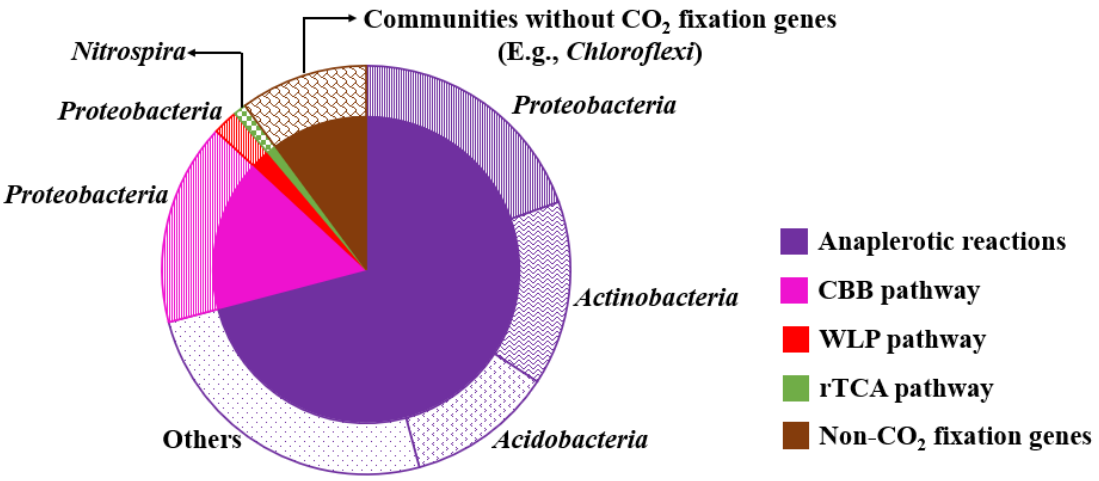

Figure 9| Figure showing the prevalent CO_2 fixation pathways and key players (phylum level) potentially involved in CO_2 fixation predicted for the microbial communities across the three temperate forest soils investigated. Inner pie chat shows the prevalent pathways identified based on PICRUSt2 predictions of the pathways' key genes for all bacterial OTUs. The outer ring chart shows the proportion of the dominant bacteria phyla affiliated with each of the predicted pathways.

This low potential for chemolithoautotrophy in all temperate forest soils investigated might be linked to a limited supply of reduced inorganic compounds as these compounds might be limited in soils (Jones et al., 2018). Obligate and facultative chemolithoautotrophs require a sufficient supply of inorganic compounds, e.g., reduced nitrogen or sulfur compounds, as energy sources for their growth (Brock et al., 2003; Yuan et al., 2012). In agreement, chemolithoautotrophic CO_2 fixation was stimulated in soils when amended with thiosulphate as an energy source (Hart et al., 2013; Zhao et al., 2020). As a result, fixation rates over 1000-fold higher were observed compared to previously documented studies where additional energy sources were not provided (Miltner et al., 2005; Nowak et al., 2015). Reduced inorganic substrates are mostly produced anaerobically in harsh environments (e.g., sediments), mainly as a result of industrial, agricultural, and volcanic activities (Shively et al., 1998). Hence, the supply of inorganic substrates might be limited in the more managed soil plots of the Hainich, Schorfheide-Chorin, and Hummelshain forests. This limited energy supply might partly explain why chemolithoautotrophs were suggested to contribute little towards dark CO_2 fixation in other managed temperate forest soils (Spohn et al., 2019) and in afro-temperate forest and field soils (Nel and Cramer, 2019).

Among the chemolithoautotrophic genes quantified, the high prevalence of *cbbL* IC genes suggests a high potential for autotrophic CO_2 fixation by microbial groups possessing this gene. The *cbbL* IC gene is employed by facultative autotrophs (Xiao et al., 2018). Facultative autotrophs are mixotrophic, requiring SOC for growth (Yuan et al., 2012), and are often the most prevalent autotrophs found in other soils (Tcherkez et al., 2006; Wu et al., 2014; Yuan et al., 2012). Thus, carbon inputs as exudates from tree roots might favor the prevalence of facultative autotrophs in temperate forest soils. The *cbbL* IA genes (CBB pathway), aclA genes (rTCA pathway), and genes for the WLP pathways are mostly found among obligate autotrophs inhabiting microoxic to anoxic soil environments (Alfreider et al., 2018; Nowak et al., 2015; Xiao et al., 2018). In addition to the presumably limited supply of electron donors, temperate forest soils are mostly aerated (Baas et al., 2019; Yavitt et al., 1990). Hence it is not surprising that these genes were less prevalent in all the temperate forest soils investigated.

In contrast to chemolithoautotrophy, the higher genomic potential for anaplerotic CO_2 fixation and its prevalence among the dominant microbial communities in all temperate forest soils investigated (**Chapters 2, 3, and 4**) suggests the dominant use of anaplerotic mechanisms for CO_2 fixation in temperate forest soils. Even in the subsoil where genes for chemolithoautotrophic CO_2 fixation maintained a low abundance and where SOC is limiting, PEPC and PC genes were still high in abundance (at least 30%) (**Chapter 3**). This may point toward the importance of CO_2 via anaplerotic fixation as a carbon source for microbes inhabiting the subsoil. A high potential for anaplerotic CO_2 fixation in subsoils has been suggested in other studies (Miltner et al., 2005; Spohn et al., 2019). Santruckova et al. (2018) showed a high abundance of PEPC genes in arctic permafrost soils and suggested that dark CO_2 fixation in extreme environments must be driven by heterotrophs (Selesi et al., 2005). Low SOC content has been shown to increase the demand for CO_2 by heterotrophs as an alternative carbon source via anaplerotic reactions to maintain optimum cellular biosynthesis (Alonso-Sáez et al., 2010; Eloka-Eboka and Inambao, 2017; Merlin et al., 2003). However, both PEPC and PC genes are typically found in all microbial groups with a complete TCA cycle including autotrophs and heterotrophs (Eichorst et al., 2018; Martins et al., 2019). Thus, the high genomic potential for anaplerotic CO_2 fixation throughout the forest soil profiles may suggest that dark CO_2 fixation in temperate forest soils is associated with a common metabolism among the soil microbial biomass. This might explain why dark CO_2 fixation rates correlated with microbial biomass carbon in all the forest soils investigated.

In this thesis, identification of the key players and metabolic pathways was not a result of the direct incorporation of labelled ^{13}C into specific microbial groups as the incorporated ^{13}C in metabolic labelling incubations were traced into the entire microbial biomass pool. Assessment of the CO_2 fixation potential was only based on the detection of specific marker genes in the bulk soil as assessed by qPCR and PICRUSt2 predictions of the bacterial *16S rRNA* genes. PICRUSt2 employs OTUs of generated *16S rRNA* gene amplicon sequences as the basis of functional predictions where hidden state predictions are used to infer (based on KEGG Orthology) genomic functional potentials (individual gene family and gene copy numbers) for each OTU (Douglas et al., 2020). On the other hand, qPCR involved the use of primer pairs specific for the quantification of functional genes present (Agrawal et al., 2019; Baptista et al., 2014). Hence, both methods did not provide an actual measure of the activity of the detected genes in the soils but measured only the genetic potential. Since the presence of a gene does not always infer activity and provides no information about its level of expression (Milanese et al., 2019), the genomic potential for CO_2 fixation described in all three studies (**Chapters 2, 3, and 4**) cannot be directly linked to CO_2 fixation activity. Additional direct measurements targeting the activity of the detected genes and expression in real-time are required to validate the use of these pathways amongst the microbial communities in temperate forest soils.

H_2| The findings in this thesis did not confirm the second hypothesis that the genomic potential for chemolithoautotrophy will increase with soil depth.

The genomic potential for chemolithoautotrophy was mostly constant with depth and did not correlate with dark CO_2 fixation rates. CO_2 fixation rates across soil depth are instead dependent on the microbial biomass carbon content. Microbial biomass carbon could thus be a proxy for predicting CO_2 fixation rates in temperate forest soils. Compared to autotrophy, all soils displayed a higher potential for non-autotrophic anaplerotic CO_2 fixation, and this was prevalent among the dominant taxa, *Proteobacteria, Acidobacteria, and Actinobacteria*. This indicates that dark CO_2 fixation in temperate forest soils is likely a common cellular mechanism within the soil microbiome. Further investigation is required to confirm the use of these pathways and the active microbial groups involved.

5.3 Influence of tree species-specific parameters on dark CO_2 fixation activity.

Lower SOC inputs in coniferous compared to deciduous dominated soils lead to lower CO_2 fixation activity. Across most soils investigated, microbial biomass was observed to strongly influence dark CO_2 fixation rates across depth due to a general metabolic potential to fix CO_2 via anaplerotic reactions. However, in pine subsoils of the Schorfheide-Chorin forest, dark CO_2 did not correlate with microbial biomass in the subsoil profiles (**Chapter 3**). The results in **Chapter 3** clearly showed that despite the similarity in microbial biomass carbon content, CO_2 fixation rates per gram of MBC were uniform across soil depths for the beech as well as the topsoil of the pine plot, but by contrast, pine subsoils featured significantly lower fixation rates. Similarly, fixation rates per gram of soil were also lower in the pine than in the beech subsoils. Linear correlation analysis and further comparison with the Hainich forest soil, a beech-dominated soil, revealed that the lower CO_2 fixation rates in pine soils could be explained by the lower SOC inputs evoked by coniferous compared to deciduous trees (**Chapter 3**). This finding thus disagreed with our third hypothesis (**H_3**) that lower SOC inputs in coniferous compared to deciduous dominated soils will lead to higher CO_2 fixation activity.

The relationship between SOC and the rates of CO_2 fixation in different soils has been explored (Miltner et al., 2005; Nowak et al., 2015; Šantrůčková et al., 2018; Xiao et al., 2018) and as discussed in section 5.1, some of these authors reported higher rates under higher SOC content (Miltner et al., 2005; Šantrůčková et al., 2018). In contrast to this thesis, these studies were mostly based on carbon amendment experiments and did not causally link the effects of the natural variations in SOC associated with vegetation type on CO_2 fixation rates. Recently, differences in fixation rates with respect to vegetation type were documented by Spohn et al. (2019), who investigated CO_2 fixation rates in soil profiles dominated by beech vs. spruce trees. Similarly, Wu et al. (2015) also determined CO_2 fixation rates in soils under different plants and cropping systems, but unlike the findings presented here, no link to SOC input was made.

Differences in tree species and, correspondingly, SOC content and quality, have been documented to affect soil microbial communities and their activities (Liu et al., 2019; Thoms et al., 2010; Zhang et al., 2016). Thus, we used molecular analysis to assess if differences in SOC and corresponding CO_2 fixation rates between the pine and the beech subsoils can be linked to the community composition. The pine subsoils featured a lower bacterial diversity than the beech soils despite a similar abundance of microbial biomass. The results presented in **Chapter 3** further showed that the high abundance of the *Chloroflexi* bacteria groups in the lower depths of the pine soils was the main group that led to the lower diversity, causing the

community to differ between the beech and pine soils. Members of this phylum are considered indicators of communities under coniferous soils (Nacke et al., 2016). The beech soils were instead more enriched in *Proteobacteria, Acidobacteria,* and *Actinobacteria* communities even till the deep horizons, and this has also been reported for other temperate forest soils dominated by deciduous trees (Dukunde et al., 2019; Eilers et al., 2010; Urbanová et al., 2015; Uroz et al., 2013). As opposed to these three dominant groups in the beech soils, PICRUSt2 predicted low anaplerotic CO_2 fixation potential for members of the *Chloroflexi* community.

Like other obligate fermenters of complex carbon substrates, e.g., Firmicutes, many *Chloroflexi* members are not adapted to fix CO_2 by anaplerotic reactions. They mostly live an acetogenic lifestyle due to the lack of a complete TCA cycle (Hug et al., 2013; Sewell et al., 2017). Heterotrophically, they are known to degrade complex carbon substrates like plant-derived polymers, e.g., polysaccharides, pyrogallol, and organic acids (Kragelund et al., 2007; Okabe et al., 2005; Xia et al., 2007). However, *Proteobacteria, Acidobacteria,* and *Actinobacteria* communities are mostly copiotrophs that prefer simpler carbon substrates (Llado et al., 2017). Also, most autotrophic *Chloroflexi* communities fix CO_2 by anoxygenic photosynthesis or via the WLP pathway, and these pathways are unlikely for the forest soils due to lack of light and a likely limited supply of electron donors like H_2 (Berg, 2011; Beulig et al., 2014). Hence, the higher abundance of *Chloroflexi* led to the lower fixation in the pine subsoils where SOC inputs were low. The lower SOC content, higher C/N ratios, and lower ^{14}C signatures indicating lower SOC quality in the pine soils were significant parameters in explaining the lower SOC inputs in the subsoils of the pine compared to beech tree stands. Coniferous soils are characterized by complex carbon fractions and lower carbon content when compared to deciduous soils (Lorenz et al., 2004; Thieme et al., 2019). This may lower microbial activity and cause more accumulation of complex carbon substrates (Tefs and Gleixner, 2012; Vesterdal et al., 2013) compared to soils under deciduous species. Based on these findings, we speculated that the lower organic carbon content and quality of pine subsoils favored the dominance of complex carbon utilizers like *Chloroflex*i with a low CO_2 fixation potential, leading to the low fixation rates (**Chapter 3**). However, in the beech soils, the higher carbon content and less complex SOC in these soils likely led to the dominance of microbial communities that fix CO_2 via anaplerotic reactions. This pile of evidence implies that tree species-derived SOC inputs affect dark CO_2 fixation rates in temperate forest soils via its influence on the composition of the microbial community (Figure 10).

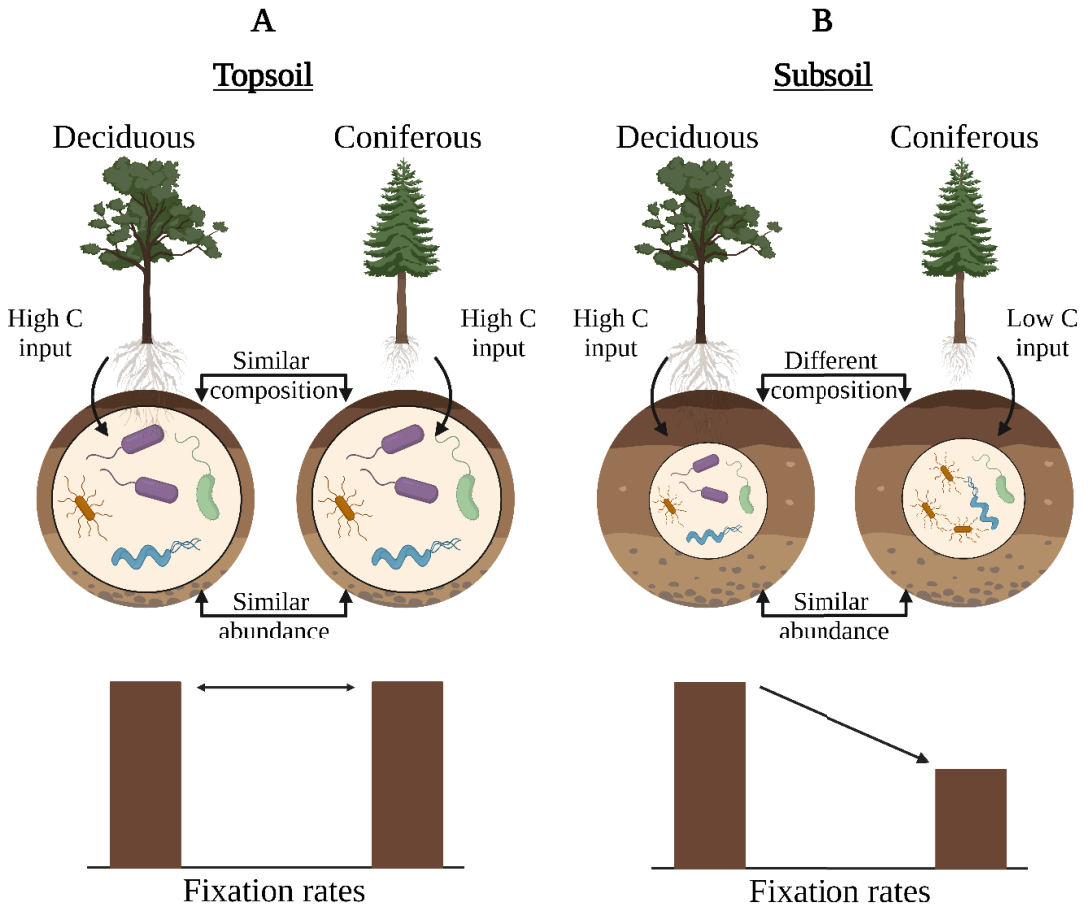

Figure 10| Schematic showing the relationship between dark CO_2 fixation rates and tree species derived SOC inputs between soils under deciduous and coniferous trees. Similar SOC input between the topsoil of deciduous and coniferous tree species can result in similar microbial community composition and lead to uniformity in fixation rates (A). However, lower inputs in coniferous subsoils can alter microbial community composition favoring groups with lower CO_2 fixation potential. This leads to lower fixation rates in coniferous than in deciduous subsoils even if microbial biomass abundance is similar (B).

Species-specific differences in SOC inputs between beech and pine forests agree with previous findings (Finzi et al., 1998; Vesterdal et al., 2013) and may result from differences in above-ground litter chemistry (Cuss and Guéguen, 2013; Don and Kalbitz, 2005). However, differences in subsoil SOC between these tree species predominantly result from differences in root inputs (Liu et al., 2019). In temperate forest ecosystems, mineral soil properties are strongly influenced by the tree root systems (Achilles et al., 2020; Binkley and Giardina, 2014). Since deciduous trees have greater root biomass than coniferous trees (Finér et al., 2007; Ostonen et al., 2007), higher carbon inputs are expected in the deeper horizons of soils under deciduous compared to coniferous trees (Vesterdal et al., 2013). Interestingly, **Chapter 4**

showed that the observed variations in SOC could be independent of tree species as similar effects of tree species on SOC inputs and, consequently, on dark CO_2 fixation rates between beech and spruce (another coniferous tree species) soils were not observed in the Hummelshain forest. Here, the beech and spruce forest plots had very similar SOC content and quality. This is probably because the beech plots were a recently converted coniferous monoculture plantation (Graser et al., 1928). The trees were around 70 years old as opposed to the Schorfheide-Chorin forest plots, where stand ages ranged between 98 and 100 years. Hence less tree species' influence on the organic carbon may have resulted. Trees >100 years old have a stronger influence on SOM than younger trees (~60 years) (Setälä et al., 2016). In agreement, for the Hummelshain forest, no differences in SOC properties were observed since its conversion (Achilles et al., 2020). This may further indicate that forest conversion strategies can mask or alter tree species-derived SOC inputs across soil profiles, and this could alter the expected influence on dark CO_2 fixation activity in temperate forest soils.

H_3| These findings contradict the third hypothesis that lower SOC inputs in coniferous compared to deciduous dominated soils will lead to higher CO_2 fixation activity

Dark CO_2 fixation rates differed between soils of different SOC inputs. Lower SOC inputs lead to lower fixation rates due to the strong influence on the composition and abundance of the microbial community and their CO_2 fixation potential. While SOC content and quality were believed to be tree species-specific, forest management regimes can alter the expected influence on SOC inputs and corresponding CO_2 fixation activity.

Dark CO_2 fixation rates increase with increasing soil pH. Besides the influence of tree species-derived SOC inputs on dark CO_2 fixation rates, variations in CO_2 fixation rates along with soil pH across the forest sites were observed. The Hainich forest profiles featured the highest pH gradient of 4 – 7 (**Chapter 2**), those of Schorfheide-Chorin Exploratory showed an intermediate pH range of 3 – 4 (**Chapter 3**), and those of the Hummelshain forest in Germany had the lowest pH range of 2 – 3 (**Chapter 4**). Among the three forest study sites, average fixation rates across depth were highest in the Hainich forest soils. Rates in the Hainich forest soils were 4 to 5 times higher than rates measured in the Schorfheide-Chorin forest soils and ~10 times higher than rates measured in the Hummelshain forest soils, as seen in Figure 6. Hence, taken together across depth, the soils showed an increase in CO_2 fixation rates with decreasing soil acidity (Figure 11).

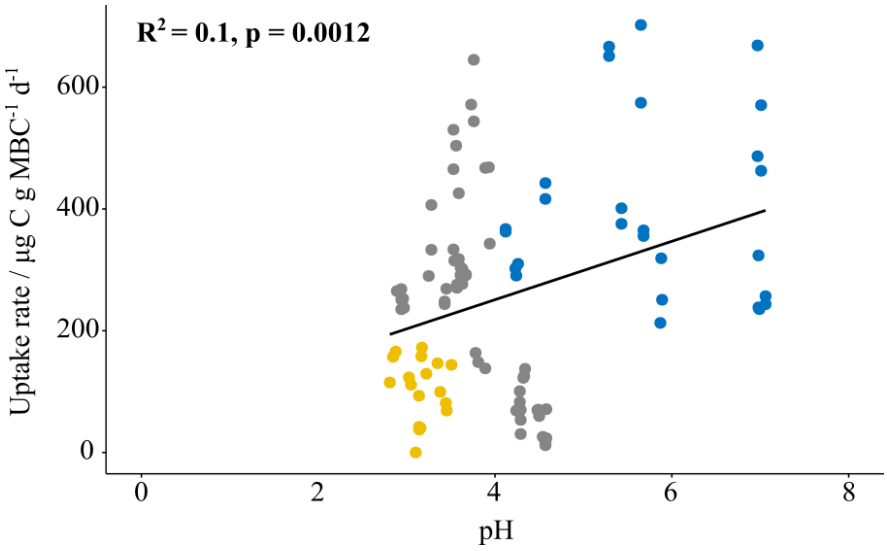

Figure 11| Relationship between dark CO_2 fixation rates and soil pH. Data represent measurements from the three forest soil profiles investigated as given in Chapters 2, 3 and 4.

Past studies have shown that dark CO_2 fixation rates are higher in neutral to alkaline soils than in acidic soils (Long et al., 2015; Santruckova et al., 2005). According to Long et al. (2015), the high bacterial diversity and a positive correlation with the abundance of specific bacteria groups like *Proteobacteria* was the underlying cause of the positive influence of increasing pH on CO_2 fixation rates in paddy soils. In agreement, the Hainich forest soils featured a higher bacterial diversity (Shannon index) in comparison to the Schorfheide-Chorin forest (**Chapter 3)** and, likewise, the Hummelshain forest soils (**Chapter 4**). Interestingly, the Hainich forest soils featured higher microbial biomass when compared to both the Schorfheide-Chorin and Hummelshain forest soils (Table 1). Microbes are sensitive to acidic conditions and studies

have demonstrated that microbial biomass and their activity decline with decreasing soil pH (Bauhus and Khanna, 1999; Tian et al., 2008). pH is important for the carbon utilization efficiency of microbial biomass and the incorporation of carbon into microbial tissues (Malik et al., 2018). It is suggested that the optimum pH for microbial cellular function is 6 – 7 since it is the pH of microbial cytoplasm (Madigan et al., 2015). This pH range is also considered the optimum for CO_2 reduction reactions (Bar-Even et al., 2012a).

Furthermore, soil pH can affect CO_2 fixation rates due to a positive correlation with SOM quality, indicative of the availability and input of organic carbon to microbial communities (Bauhus and Khanna, 1999). Forest soils with low pH conditions may feature low decomposition rates (Joly et al., 2017). This is because low pH can be inhibitory to the activity of phenol-oxidase, causing the accumulation of phenolic compounds (Tahvanainen and Haraguchi, 2013). These phenolic compounds inhibit the activity of hydrolase enzymes, thus slowing organic matter decomposition (Davidson and Janssens, 2006). Consequently, low pH might limit the input of SOC for facultative autotrophs and heterotrophs fixing CO_2 in soils. In agreement, the Hainich forest soils featuring the highest pH also showed lower CN ratios, indicative of a higher SOC input when compared to the other forest soils (**Chapter 2**). In **Chapter 3**, higher SOC inputs were shown to favour CO_2 fixation rates. Thus, the effect of pH on SOC inputs might also explain the higher rates observed in the Hainich forest soils compared to the rest of the plots.

Like SOC inputs, the significant difference in pH between the Hainich forest soil and the other two forest plots might be linked to their dominant tree species. The Hainich soils were dominated by a mixture of deciduous tree species, mostly beech. Deciduous trees are known to be less acidifying than coniferous trees (Lladó et al., 2017) due to differences in litter chemistry, especially at the topsoil (Thieme et al., 2019). Although soils of both the deciduous and coniferous forest plots of the Schorfheide-Chorin and the Hummelshain were more acidic than soils of the Hainich forest, the pH of the deciduous soils of the Schorfheide-Chorin and Hummelshain forests was still higher than those of their corresponding coniferous plots (**Chapters 2 and 3**). The reason for the lower soil pH in the deciduous soils of the Schorfheide-Chorin and Hummelshain forests compared to the Hainich forest soils might be linked to differences in their parent material, rate of atmospheric deposition of acidifying compounds, historical management of the forest sites, or fertilizer application as reported by other studies (Achilles et al., 2020; Fischer et al., 2010; Meesenburg et al., 2019).

5.4 Influences of global parameters on dark CO_2 fixation and its impact on temperate forest soil CO_2 fluxes

Dark CO_2 fixation modulates soil CO_2 fluxes. Despite the observed variations in dark CO_2 fixation activity in response to soil parameters like SOC and pH, contributions to CO_2 fluxes among the investigated forest plots occurred within similar magnitudes. Extrapolating dark CO_2 fixation rates per unit area and at in-situ field temperature conditions (8 °C) resulted in a fixation rate of up to 25 ± 7.2 g C m^{-2} yr^{-1} to 1 m depth (**Chapter 2**). At this rate, dark CO_2 fixation was estimated to recycle 5.6% of CO_2 from Hainich forest net soil respiration. This suggests that without dark CO_2 fixation in the Hainich forest soils, CO_2 emissions in these soils would be 5.6% higher (**Chapter 2**). In the Hummelshain forest soils, comparing the CO_2 fixation rates to respiration rates measured suggested that CO_2 fixation accounted for up to 3% of soil respiration in these soils. Although a direct comparison of CO_2 fixation rates to respiration rates measured from the Schorfheide Chorin plots was not possible due to a lack of respiration rate measurement. However, based on respiration rate from previous incubation studies conducted at the same sites for the topsoil with ~1.21 – 1.87 µg C g (dw) $soil^{-1}$ d^{-1} (Schoening et al., 2013), dark CO_2 fixation rates in the Schorfheide-Chorin could account for ~10% of net soil respiration rates in these soils. These estimated relative modulation of CO_2 from soil respiration rates are similar to the estimated 4% observed in other temperate forest soils (Spohn et al., 2019), around 3% in agricultural soils (Miltner et al., 2005), and 1.1% and 16% reported for mineral and permafrost soils respectively of the arctic regions (Šantrůčková et al., 2018). CO_2 recycling via dark CO_2 fixation was suggested to have a significant influence on the carbon isotope signatures of SOC (Ehleringer, 2000). Negative shifts in $\Delta^{14}C$ and positive shifts in $\delta^{13}C$ signals across soil profiles as a result of dark CO_2 fixation have been justified by previous findings (Nowak et al., 2015; Šantrůčková et al., 2018), throwing more light on the role of microbial processes in carbon cycling within the subsurface.

Further global upscaling of the rates reported for the Hainich forest soils revealed an estimated fixation rate of up to 0.26 ± 0.07 Pg C yr^{-1} to 1 m depth across the global temperate forests area (**Chapter 2**). At this rate, dark CO_2 fixation was suggested to modulate up to 2.3% of the total global anthropogenic carbon emissions (~11.5 ± 0.9 Pg C; Friedlingstein et al., 2019) (**Chapter 2**). This rate could also account for ~2% of soil respiration rates from temperate forest soils globally (assuming a global temperate forest soil respiration rate of 12.9 Pg C yr^{-1}; (Martin and Bolstad, 2005)). Strikingly, this estimated global fixation rate corresponds precisely to the mean annual net carbon flux absorbed in all mid-latitude forests on Earth (Dixon et al., 1994;

Lal, 2005). This indicates that without the dark CO_2 fixation in the soil, the world's temperate forests will lose their capacity to be a net sink of carbon. Thus dark CO_2 fixation might maintain the carbon sink in world's temperate forests. However, it should be noted that lower CO_2 fixation rates were observed in other forest soils (**Chapters 3 and 4**), indicating an overestimate of the global upscaling reported in **Chapter 2**. Also, based on reports from previous FACE experiments (Norby et al., 2005; Bernhardt et al., 2006), there have likely been an increase in soil CO_2 concentration in response to atmospheric CO_2 rise since the period the global temperate forest carbon sink was estimated (early 1990s) until now and this may have increased CO_2 fixation rates. Nonetheless, such global extrapolations may provide a first-hand insight on the quantitative role of dark CO_2 fixation for global temperate forest CO_2 fluxes.

Increase in CO_2 concentration increases dark CO_2 fixation rates and its influence on soil CO_2 fluxes. The impact of dark CO_2 fixation on temperate forest soil CO_2 fluxes can be significant in scenarios of increased atmospheric and soil CO_2, especially within the context of global climate change. An intriguing outcome of this thesis was the observed positive correlation between dark CO_2 fixation rates and CO_2 concentrations across the soil profiles (**Chapter 2**). An increase in CO_2 concentration has been shown to increase dark CO_2 fixation rates in temperate forest subsoils, where a linear relationship with soil CO_2 concentration between 1 and 6.1% was reported (Spohn et al., 2019). Findings from this thesis showed that across the entire 1 m depth profile, dark CO_2 fixation rates increased linearly by more than 2-folds, that is 120%, when CO_2 concentrations increased from 2 to 10% after 7 days of incubation, extending results reported by Spohn et al. (2019). This increase under higher CO_2 levels indicates that microbial communities in temperate forest soils can respond swiftly to short-term changes in soil CO_2 concentration.

The increase in fixation rates was observed to diminish when CO_2 concentration reached 20%. It is important to consider that O_2 was not limited as soil incubations under 20% CO_2 were done under oxic conditions (~20% O_2). Hence, a substrate saturation effect similar to Michaelis-Menten kinetics, indicating a subjection to the enzymatic limitations, might have set in (Michaelis and Menten, 1913). Based on this assumption, it is likely that at concentrations above 10%, CO_2 no longer becomes a rate-limiting factor. Instead, if other requirements are lacking, this might be inhibitory to the CO_2 fixation process. For example, diminishing rates could be a result of a limited supply of inorganic compounds or organic carbon as electron donors required as energy sources by autotrophs and heterotrophs, respectively, when fixing

CO_2 (Brock et al., 2003; Madigan et al., 2015; Miltner et al., 2005). A decrease in CO_2 fixation rates under energy limiting conditions is not surprising as microbes should require more nutrients to maintain their stoichiometry when fixing CO_2 at concentrations as high as 20% compared to 2% or 10%. However, a few exceptions might exist. Past studies showed an increase in dark CO_2 fixation rates in a mofette soil under increasing CO_2 concentration, with saturation effects observed when CO_2 concentrations reached 100% (Beulig et al., 2016). One possible explanation is that the communities are likely more adapted to the high CO_2 concentration (90% partial pressure) in this extreme environment compared to temperate forest soil communities. Also, the water-saturated, anoxic conditions in mofettes may support high proportions of anaerobic obligate autotrophs like acetogens and methanogens, which also fix CO_2 using energy-efficient pathways like the WLP pathway (Beulig et al., 2016, 2014).

Although CO_2 concentrations in well-drained or aerated soils such as in temperate forests are usually far less than 20% (Amundson and Davidson, 1990), with concentrations typically ranging between 1 and 5% (Andrews and Schlesinger, 2001; Richter and Markewitz, 1995). However, such an increase under elevated CO_2 beyond levels typically found in soils suggests that CO_2 fixation will respond to short-term to seasonal periods of high moisture and temperature conditions that might spike soil CO_2 concentration (Davidson et al., 2006; Lu et al., 2013) and possibly, soil CO_2 emissions into the atmosphere (Oh et al., 2005).

Studies show that elevating atmospheric CO_2 concentration by 1ppm can cause a linear increase in soil CO_2 levels by as much as 35 ppm (Bernhardt et al., 2006). Thus, considering the observed 120% linear increase in fixation rates between 2 and 10% CO_2 (400% increase in CO_2), **Chapter 2** further evaluated the effect of increased atmospheric CO_2 from the pre-industrial era (that is, the year 1750) until now on the estimated global dark CO_2 fixation rates. Here, we found that due to the rise in atmospheric CO_2 concentration since 1750, dark CO_2 fixation could be currently 6.3% higher than they were pre-industrially. As atmospheric CO_2 concentrations are proposed to almost triple preindustrial levels by 2100 (IPCC, 2001), it can be further estimated by how much dark CO_2 fixation rates will increase and consequently affect soil CO_2 fluxes in the future. If we assume the same linear relationship of Bernhardt et al. (2006), a 164% increase in atmospheric CO_2 by 2100 compared to current levels (416 ppm), that is, from 416 ppm to 1099 ppm (IPCC, 2000), could increase soil CO_2 by ~2.4% (23,905 ppm). Again, based on the observed 120% increase in fixation rates reported, dark CO_2 fixation rates in temperate forest soils globally could, as a result, be ~35% higher in 2100 than it is now.

Thus, due to future rise in atmospheric CO_2 levels, dark CO_2 fixation by the soil microbial community would likely fix ~0.09 Pg C yr^{-1} to 1 m depth more in 2100 than it does now.

But what could be the implication of this rate increase on future soil CO_2 fluxes? Suppose global temperate forest soil CO_2 emission also increases by 23,905 ppm (representing a 120% increase assuming that mean soil CO_2 concentration is currently at 20,000 ppm (Richter and Markewitz,, 1995)), that is, from 12.9 Pg C yr^{-1} (Martin and Bolstad, 2005) currently to ~28.4 Pg C yr^{-1} in the year 2100. This means that projected increase in global temperate forest soil respiration would likely be ~1.6-folds higher than the calculated increase in global temperate forest soil dark CO_2 fixation rate with 35% as stated above. Hence dark CO_2 fixation at a future rate of 0.35 Pg C yr^{-1} would modulate only ~1.2% of CO_2 global temperate forest soil respiration in 2100, instead of the 2%, the current estimated recycling rate. However, the relationship of CO_2 concentration with dark CO_2 fixation rate and soil respiration might depend on a broad spectrum of environmental conditions, e.g., soil moisture, diffusivity, the amount and depth distributions of roots, microbial activities and communities present, and rates of soil CO_2 production. Additionally, the geochemical conditions such as temperature and moisture of all temperate forest soils globally were not accounted for. Hence, these values represent rough estimates associated with some degree of uncertainty.

Dark CO_2 fixation and its temperature sensitivity. Temperature is an important driver of microbial activities (Biederbeck and Campbell, 1973; Pietikäinen et al., 2005) and SOC dynamics in soil (Melillo et al., 2011). Authors agree that understanding the response of microbial metabolism to increased temperature is critical to predicting the future size of the terrestrial carbon sink (Davidson and Janssens, 2006) and fluxes (Schimel, 2013). Thus, by comparing the responses of dark CO_2 fixation and respiration to an increase in temperature of the same soil, this thesis provides new insights for understanding the dynamics of SOC fluxes under global climate change.

The response of dark CO_2 fixation to temperature changes was tested and compared to those of soil respiration using short-term parallel ^{13}C soil incubation studies under different temperature regimes (**Chapter 4**). In this study, dark CO_2 fixation per unit of soil weight in beech and spruce-dominated soils increased by up to 2 folds under 10 °C warming (from 4 to 14 °C). Based on the measured rates, the sensitivity of dark CO_2 fixation rates to warming was derived using the known Q_{10} coefficient (Hicks Pries et al., 2018; Leifeld and Fuhrer, 2005) and compared to the Q_{10} of net soil respiration rates. Dark CO_2 fixation rates per unit of soil

weight featured a mean Q_{10} of 2.07 across soil depth, but this was significantly lower than the Q_{10} of net respiration rates, with 2.98. This finding thus contradicts our fourth hypothesis (**H_4**) that dark CO_2 fixation is as sensitive to warming as soil respiration. The measured Q_{10} of dark CO_2 fixation rates is similar to that reported for afro-temperate forest soils extrapolated as ~2.5 (Nel and Cramer, 2019). Similarly, the Q_{10} values of net soil respiration rates lie within the range of 1.5 and 3.1 reported for agricultural and temperate forest soils (Fang et al., 2005; Hicks Pries et al., 2017; Li et al., 2021). One possible reason for the lower Q_{10} value of dark CO_2 fixation rate than that of soil respiration rate could be linked to differences in the kinetics of their respective enzymes. Hydrolase enzymes like phenol oxidase (involved in SOM degradation) tend to have higher specific activity for their substrate (100 μmol mg^{-1} min^{-1}) (Dunn et al., 2014) compared to enzymes involved in CO_2 fixation like PEPC (25 μmol mg^{-1} min^{-1}) and RuBisCO (2 – 4 μmol mg^{-1} min^{-1}) (Bar-Even et al., 2010).The order and significance of these processes within the microbial cell might also explain the difference in Q_{10}. Respiration is the primary energy-generating process in microbial cells from which ATP (the main energy currency) is synthesized to drive other processes within the cell (Madigan et al., 2015). On the other hand, CO_2 fixation mechanisms usually depend on energy inputs from ATP (Bar-Even et al., 2012b; Berg, 2011). At higher temperatures, there is always an increase in the kinetic energies of cellular biomolecules to react (Arrhenius, 1898; Davidson and Janssens, 2006). To meet the energy demand for these reactions, a boost in central cellular metabolic rates, that is, cellular respiration occurs within the cell (Boscolo-Galazzo et al., 2018) to produce ATP (Dijkstra et al., 2011), which can be deployed to further power energy-driven metabolic processes like CO_2 fixation. It is thus likely that the response of soil respiration to warming will always be stronger than dark CO_2 fixation due to the need to initially meet ATP demands.

Based on the mean Q_{10} of 2.1 for fixation rates and 3.0 for respiration rates per gram of soil, **Chapter 4** predicted that a projected 4 °C warming by 2100 (Soong et al., 2020) would likely increase CO_2 fixation rates by ~33%. But as respiration rates will increase by 55%, dark CO_2 fixation might increase 1.16-fold less than soil respiration under 4 °C warming. This translates to the recycling of 1.7% of global temperate forest soil CO_2, which is less than the current extrapolations of 2% stated above. Hicks Pries et al. (2017) reported a 37% increase in soil respiration from a coniferous forest in response to 4 °C warming. This is still higher than the expected increase in CO_2 fixation rates reported in **Chapter 4**. This suggests that the potential for dark CO_2 fixation to modulate CO_2 emissions from temperate forest soils might decrease under future warming scenarios. However, the responses of dark CO_2 fixation and soil

respiration likely also depend on varying temperature ranges across different temperate forest biomes including corresponding changes in primary production, root exudation and soil CO_2 concentration. Therefore, these estimates are likely associated with a range of uncertainty.

It should be noted that much of the soil CO_2 available for microbial assimilation in-situ is derived from soil respiration (Kuzyakov, 2006). We know that future warming would accelerate SOM decomposition and respiration rates and lead to higher CO_2 release in temperate forest soils (Hicks Pries et al., 2017; Melillo et al., 2017). Also, dark CO_2 fixation rates scale with soil respiration and CO_2 concentration (Beulig et al., 2014; Miltner et al., 2005; Spohn et al., 2019) (**Chapter 2**). Thus, the actual effect of warming on dark CO_2 fixation rates might occur via an influence of increased soil respiration rates and soil CO_2 concentration. This might result in lower Q_{10} values for CO_2 fixation under in-situ conditions compared to what was experimentally measured. Furthermore, the Q_{10} of soil respiration may depend on SOM quality (Conant et al., 2008), with labile topsoil SOC decomposition suggested as being more responsive to warming than complex subsoil SOC (Melillo et al., 2002). Thus, under warming and assuming a scenario of initial depletion of the labile SOC pool over time in the real world, a reduction in soil CO_2 production might occur (Melillo et al., 2002), leading to lower CO_2 fixation rates. Therefore, even if global soil temperature increases in the future, temporal declines in the amount of labile SOC (and consequently lower soil CO_2 concentrations) might result in lower dark CO_2 fixation rates across temperate forest soil profiles. It would be promising to consider the effects of elevated temperature together with the effect of elevated CO_2 concentrations and their potential interactions to fully understand the dynamics of dark CO_2 fixation in soils of temperate forest biomes in the light of global climate change.

H_4| The findings from this thesis contradict the fourth hypothesis that dark CO_2 fixation has a similar sensitivity to higher temperatures as soil respiration.

Dark CO_2 fixation featured a lower temperature sensitivity than soil respiration. This suggests that dark CO_2 fixation in temperate forest soils might be less responsive under future warming scenarios than net soil respiration. As a result, the amount of recycled CO_2 in temperate forest soils would likely decrease in the future. Because temperature also affects CO_2 release in soil, it is necessary to consider the interactions between temperature and CO_2 when evaluating the response of dark CO_2 fixation to global climate change.

6 Conclusion and outlook

This thesis demonstrates that dark CO_2 fixation is a significant and dynamic microbial process in soils of various temperate forest settings (Figure 12). The relevance of this process is reflected in the modulation of CO_2 fluxes from soils and its contributions to SOM from the surface to the subsoil. Carbon input to microbial biomass is significant in the deep soil layers where organic carbon is limited and should be considered when modelling soil carbon storage and fluxes. This study marks the first steps to understanding the role of CO_2 fixation for carbon inputs and fluxes in soils. Further studies on the persistence and turnover of CO_2-derived carbon from microbial biomass into various non-living SOM components (Spohn et al., 2019) will go a long way toward understanding its contributions towards long term SOM storage. We were able to show that the genomic potential for chemolithoautotrophy did not increase with depth, but that microbial biomass correlated with dark CO_2 fixation rates. Hence, future research could use this relationship as a guide to roughly predict CO_2 fixation rates in other temperate forest soils. Using PICRUSt predictions and qPCR of functional genes, this thesis provided information on the genomic potential for CO_2 fixation in temperate forest soils. Based on these approaches, we suggest that anaplerotic CO_2 fixation is a dominant mechanism among the temperate forest soil bacteria community. The methods used to elucidate the genomic potential for CO_2 fixation are limited in revealing actual gene activity. Hence, there are still unknowns about the active key players and metabolic pathways involved. Further study using state-of-the-art genome-resolved techniques like metaproteomics and metatranscriptomics in combination with stable isotope probing would enable phylogenetic identification of the active microbial communities at different levels as well as the key genes expressed to determine the metabolic pathways involved (Galambos et al., 2019). This thesis focused on CO_2 fixation by bacteria as these are the main key players of this process in soils (Miltner et al., 2004, Šantrůčková et al., 2018). However, contributions from fungi and archaea should still be considered. Forest soils habour a large community of fungi (Llado et al., 2017) and some fungal communities require CO_2 fixation for growth (Hartman et al., 1972). Also, methanogenic archaea are ubiquitous in aerated soils and can become active under wet anoxic conditions, e.g., seasonal changes in soil moisture (Angel et al., 2012). By comparing CO_2 fixation rates between deciduous-beech and coniferous-pine soils, we showed that correlations between CO_2 fixation rates and microbial biomass was not universal due to the influence of SOC inputs on the community composition and the CO_2 fixation potential. We further highlighted the influence of soil pH on dark CO_2 fixation rates due to the potential effect of pH on the microbial community and this further stresses that tree-species specific parameters govern CO_2 fixation

in temperate forest soils. This thesis showed that dark CO_2 fixation responds to higher CO_2 concentration and as a result might modulate less CO_2 fluxes from temperate forest soils under future global climate change. The presented findings also illustrate the temperature sensitivity of dark CO_2 fixation in comparison to the temperature sensitivity of net soil respiration. We were able to show that CO_2 fixation in temperate forest soils will likely be less responsive than soil respiration to warming. Consequently, there might be a reduced potential to modulate CO_2 emissions from temperate forest soils under future warming. As CO_2 and temperature are strongly correlated, further studies on the effects of their interactions on CO_2 fixation is needed to fully understand the dynamics of dark CO_2 fixation in the light of global climate change.

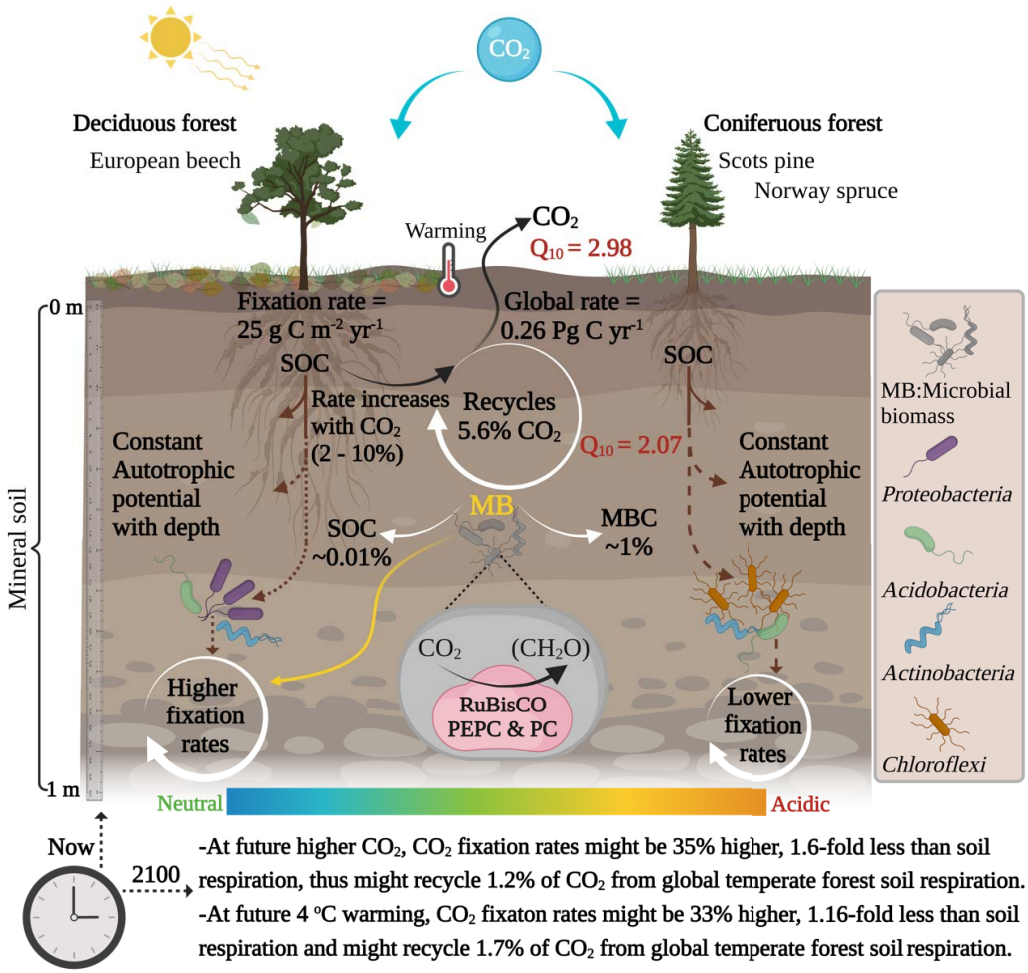

Figure 12| Scheme highlighting the new findings on dark CO_2 fixation in temperate forest soils. Black arrows close to the surface show soil respiration and while white circular arrows denote dark CO_2 fixation. Microbial biomass (MB) is a key driver of CO_2 fixation rates, as denoted by the yellow arrow. SOC inputs (broken brown arrows) decrease with depth and are higher in deciduous than coniferous-dominated soils shown by varying degrees of broken lines These affect soil microbial communities leading to differences in dark CO_2 fixation rates between deciduous and coniferous dominated soils.

7 References

Achilles, F., Tischer, A., Bernhardt-Römermann, M., Heinze, M., Reinhardt, F., Makeschin, F., Michalzik, B., 2020. European beech leads to more bioactive humus forms but stronger mineral soil acidification as Norway spruce and Scots pine – Results of a repeated site assessment after 63 and 82 years of forest conversion in Central Germany. Forest Ecology and Management. Forest Ecology and Management. 483, 118769.

Agrawal, S., Kinh, C.T., Schwartz, T., Hosomi, M., Terada, A., Lackner, S., 2019. Determining uncertainties in PICRUSt analysis – An easy approach for autotrophic nitrogen removal. Biochemical Engineering Journal 152, 107328.

Akinyede, R., Taubert, M., Schrumpf, M., Trumbore, S., Küsel, K., 2020. Rates of dark CO_2 fixation are driven by microbial biomass in a temperate forest soil. Soil Biology & Biochemistry 150, 107950.

Akinyede, R., Taubert, M., Schrumpf, M., Trumbore, S., Küsel, K., 2022 Dark CO_2 fixation in temperate beech and 585 pine forest soils, Soil Biology & Biochemistry, 165, 108526.

Alfreider, A., Baumer, A., Bogensperger, T., Posch, T., Salcher, M.M., Summerer, M., 2017. CO_2 assimilation strategies in stratified lakes: Diversity and distribution patterns of chemolithoautotrophs. Environmental Microbiology 19, 2754–2768.

Alfreider, A., Grimus, V., Luger, M., Ekblad, A., Salcher, M.M., Summerer, M., 2018. Autotrophic carbon fixation strategies used by nitrifying prokaryotes in freshwater lakes. FEMS Microbiology Ecology 94, 1–12.

Alfreider, A., Schirmer, M., Vogt, C., 2012. Diversity and expression of different forms of RubisCO genes in polluted groundwater under different redox conditions. FEMS Microbiology Ecology 79, 649–660.

Alfreider, A., Vogt, C., Hoffmann, D., Babel, W., 2003. Diversity of ribulose-1,5-bisphosphate carboxylase/oxygenase large-subunit genes from groundwater and aquifer microorganisms. Microbial Ecology 45, 317–328.

Ali, R.S., Poll, C., Kandeler, E., 2020. Soil Properties Control Microbial Carbon Assimilation and Its Mean Residence Time. Frontiers in Environmental Science 8, 1–9.

Allison, S.D., Treseder, K.K., 2011. Climate change feedbacks to microbial decomposition in boreal soils. Fungal Ecology 4, 362–374.

Alonso-Sáez, L., Galand, P.E., Casamayor, E.O., Pedrós-Alió, C., Bertilsson, S., 2010. High bicarbonate assimilation in the dark by Arctic bacteria. ISME Journal 4, 1581–1590.

Amundson, R.G., Davidson, E.A., 1990. Carbon dioxide and nitrogenous gases in the soil atmosphere. Journal of Geochemical Exploration 38, 13–41.

Anderson J.P.E. 1982. Soil respiration. In: Page, A.L., Miller, R.H., Keeney, D.R. (eds) Methods of soil analysis, part 2. Am Soc Agron, Soil Sci Soc Am, Madison Wisconsin, pp 831 – 871

Andrews, J.A., Schlesinger, W.H., 2001. Soil dynamics, acidification, and chemical weathering in a temperature forest with experimental enrichment. Global Biogeochemical Cycles 15, 149–162.

Angel, R., Claus, P., Conrad, R., 2012. Methanogenic archaea are globally ubiquitous in

aerated soils and become active under wet anoxic conditions. ISME Journal 6, 847–862. doi:10.1038/ismej.2011.141

Arrhenius, S. 1889. Uber die Reaktionsgeschwindigkeit bei der Inversion von Rohrzucker durch Sauren. Z. Phys. Chem. 4, 226-248

Baas, P., Knoepp, J.D., Mohan, J.E., 2019. Well-aerated southern appalachian forest soils demonstrate significant potential for gaseous nitrogen loss. Forests 10, 1–13.

Badger, M.R., Bek, E.J. 2008. Multiple Rubisco forms in proteobacteria: Their functional significance in relation to CO_2 acquisition by the CBB cycle. Journal of Experimental Botany 59, 1525–1541.

Baptista, J.D.C., Lunn, M., Davenport, R.J., Swan, D.L., Read, L.F., Brown, M.R., Morais, C., Curtis, T.P., 2014. Agreement between amoA gene-specific quantitative PCR and fluorescence in situ hybridization in the measurement of ammonia-oxidizing bacteria in activated sludge. Applied and Environmental Microbiology 80, 5901–5910.

Bar-Even, A., Flamholz, A., Noor, E., Milo, R., 2012a. Thermodynamic constraints shape the structure of carbon fixation pathways. Biochimica et Biophysica Acta - Bioenergetics 1817, 1646–1659.

Bar-Even, A., Noor, E., Lewis, N.E., Milo, R., 2010. Design and analysis of synthetic carbon fixation pathways. Proceedings of the National Academy of Sciences of the United States of America 107, 8889–8894.

Bar-Even, A., Noor, E., Milo, R., 2012b. A survey of carbon fixation pathways through a quantitative lens. Journal of Experimental Botany 63, 2325–2342.

Bassham JA, Benson AA, Kay LD, Harris AZ, Wilson AT, Calvin M. 1954. The path of carbon in photosynthesis. XXI. The cyclic regeneration of carbon dioxide acceptor. J. Am. Chem. Soc. 76:1760-1770

Batjes, N.H., 1996. Total carbon and nitrogen in the soils of the world. European Journal of Soil Science 47, 151–163.

Bauhus, J., Khanna, P.K., 1999. The significance of microbial biomass and activity in forest soils. Going Underground - Ecological Studies in Forest Soils 77–110.

Berg, I.A., 2011. Ecological aspects of the distribution of different autotrophic CO_2 fixation pathways. Applied and Environmental Microbiology 77, 1925–1936.

Berg, I.A., Kockelkorn, D., Buckel, W., Fuchs, G., 2007. A 3-hydroxypropionate/4-hydroxybutyrate autotrophic carbon dioxide assimilation pathway in archaea. Science 318, 1782–1786.

Berg, I.A., Kockelkorn, D., Ramos-Vera, W.H., Say, R.F., Zarzycki, J., Hügler, M., Alber, B.E., Fuchs, G., 2010. Autotrophic carbon fixation in archaea. Nature Reviews Microbiology 8, 447–460.

Bernhardt, E.S., Barber, J.J., Pippen, J.S., Taneva, L., Andrews, J.A., Schlesinger, W.H., 2006. Long-term effects of free air CO_2 enrichment (FACE) on soil respiration. Biogeochemistry 77, 91–116.

Beulig, F., Heuer, V.B., Akob, D.M., Viehweger, B., Elvert, M., Herrmann, M., Hinrichs, K.U., Küsel, K., 2014. Carbon flow from volcanic CO_2 into soil microbial communities

of a wetland mofette. ISME Journal 9, 746–759.

Beulig, F., Urich, T., Nowak, M., Trumbore, S.E., Gleixner, G., Gilfillan, G.D., Fjelland, K.E., Küsel, K., 2016. Altered carbon turnover processes and microbiomes in soils under long-term extremely high CO2exposure. Nature Microbiology 1, 1–9.

Biederbeck, V.O., Campbell, C.A., 1973. Soil Microbial Activity As Influenced By Temperature Trends and Fluctuations. Canadian Journal of Soil Science 53, 363–376.

Billings, S.A., Richter, D.D., 2006. Changes in stable isotopic signatures of soil nitrogen and carbon during 40 years of forest development. Oecologia 148, 325–333.

Binkley, D.A.N., Giardina, C., 2014. Why do tree species affect soils ? The Warp and Woof of tree-soil interactions. Biogeosciences 42, 89–106

Boscolo-Galazzo, F., Crichton, K.A., Barker, S., Pearson, P.N., 2018. Temperature dependency of metabolic rates in the upper ocean: A positive feedback to global climate change? Global and Planetary Change 170, 201–212.

Brock, T.D., Madigan, M.T., Martinko, J.P., Parker, J., 2003. Brock Biology of Microorganisms, tenth ed. Prentice Hall, Upper Saddle River, New Jersey, pp. 565-575

Brockett, B.F.T., Prescott, C.E., Grayston, S.J., 2012. Soil moisture is the major factor influencing microbial community structure and enzyme activities across seven biogeoclimatic zones in western Canada. Soil Biology and Biochemistry 44, 9–20.

Brunn, M., Spielvogel, S., Sauer, T., Oelmann, Y., 2014. Temperature and precipitation effects on δ13C depth profiles in SOM under temperate beech forests. Geoderma 235–236, 146–153.

Buchanan, B.B., Arnon, D.I., 1990. A reverse KREBS cycle in photosynthesis: consensus at last. Photosynthesis Research 24, 47–53.

Campbell, B.J., Craig Cary, S., 2004. Abundance of Reverse Tricarboxylic Acid Cycle Genes in Free-LivingMicroorganisms at Deep-Sea Hydrothermal Vents. Appl Environ Microbiol 70, 6282–6289.

Cerling, T.E., Solomon, D.K., Quade, J., Bowman, J.R., 1991. On the isotopic composition of carbon in soil carbon dioxide. Geochimica et Cosmochimica Acta 55, 3403–3405.

Chen, M., Wang, C., Wang, B., Bai, X., Gao, H., Huang, Y., 2019. Enzymatic mechanism of organic nitrogen conversion and ammonia formation during vegetable waste composting using two amendments. Waste Management 95, 306–315.

Cheng, J., Zhao, M., Cong, J., Qi, Q., Xiao, Y., Cong, W., Deng, Y., Zhou, J., Zhang, Y., 2020. Soil pH exerts stronger impacts than vegetation type and plant diversity on soil bacterial community composition in subtropical broad-leaved forests. Plant and Soil. 450, 273–286

Cleveland, C.C., Liptzin, D., 2007. C:N:P stoichiometry in soil: Is there a “Redfield ratio” for the microbial biomass? Biogeochemistry 85, 235–252.

Conant, R.T., Drijber, R.A., Haddix, M.L., Parton, W.J., Paul, E.A., Plante, A.F., Six, J., Steinweg, M.J., 2008. Sensitivity of organic matter decomposition to warming varies with its quality. Global Change Biology 14, 868–877.

Craig, H., 1953. The geochemistry of the stable carbon isotopes. Geochimica et

Cosmochimica Acta 3, 53–92.

Cuss, C.W., Guéguen, C., 2013. Distinguishing dissolved organic matter at its origin: Size and optical properties of leaf-litter leachates. Chemosphere 92, 1483–1489.

Dalal, R.C., 1998. Soil microbial biomass - What do the numbers really mean? Australian Journal of Experimental Agriculture 38, 649–665.

Davidson, E.A., Janssens, I.A., 2006. Temperature sensitivity of soil carbon decomposition and feedbacks to climate change. Nature 440, 165–173.

Davidson, E.A., Savage, K.E., Trumbore, S.E., Borken, W., 2006. Vertical partitioning of within a temperate forest soil. Global Change Biology 12, 944–956.

Dell'Abate, M.T., Biro, B., 2015. Soil microbes and soil organic matter dynamics. EIP-AGRI. 1–14.

Dijkstra, P., Thomas, S.C., Heinrich, P.L., Koch, G.W., Schwartz, E., Hungate, B.A., 2011. Effect of temperature on metabolic activity of intact microbial communities: Evidence for altered metabolic pathway activity but not for increased maintenance respiration and reduced carbon use efficiency. Soil Biology and Biochemistry 43, 2023–2031.

Diochon, A., Kellman, L., 2008. Natural abundance measurements of ^{13}C indicate increased deep soil carbon mineralization after forest disturbance. Geophysical Research Letters 35, 1–5.

Dixon, R.K., Brown, S., Houghton, R.A., Solomon, A.M., Trexler, M.C., Wisniewski, J., 1994. Carbon pools and flux of global forest ecosystems. Science 263, 185–190.

Don, A., Kalbitz, K., 2005. Amounts and degradability of dissolved organic carbon from foliar litter at different decomposition stages. Soil Biology and Biochemistry 37, 2171–2179.

Dong, W., Song, A., Yin, H., Liu, X., Li, J., Fan, F., 2021. Decomposition of Microbial Necromass Is Divergent at the Individual Taxonomic Level in Soil. Frontiers in Microbiology 12, 1–11.

Douglas, G.M., Maffei, V.J., Zaneveld, J.R., Yurgel, S.N., James, R., Taylor, C.M., Huttenhower, C., Langille, M.G.I., 2020. PICRUSt2 for prediction of metagenome functions 38, 685–688.

Drake HL, Kirsten K, Matthies C. 2006. Acetogenic prokaryotes. In: The Prokaryotes. New York: Springer, 354–420.

Dukunde, A., Schneider, D., Schmidt, M., Veldkamp, E., Daniel, R., 2019. Tree Species Shape Soil Bacterial Community Structure and Function in Temperate Deciduous Forests. Frontiers in Microbiology 10, 1–17.

Dunn, C., Jones, T.G., Girard, A., Freeman, C., 2014. Methodologies for extracellular enzyme assays from wetland soils. Wetlands 34, 9–17. doi:10.1007/s13157-013-0475-0

Ehleringer, J.R., Buchmann, N., Flanagan, L.B., 2000. Carbon isotope ratios in belowground carbon cycle processes. Ecological Applications 10, 412-422

Eichorst, S.A., Trojan, D., Roux, S., Herbold, C., Rattei, T., Woebken, D., 2018. Genomic insights into the Acidobacteria reveal strategies for their success in terrestrial environments. Environmental Microbiology 20, 1041–1063.

Eilers, K.G., Lauber, C.L., Knight, R., Fierer, N., 2010. Shifts in bacterial community structure associated with inputs of low molecular weight carbon compounds to soil. Soil Biology and Biochemistry 42, 896–903.

Eloka-Eboka, A.C., Inambao, F.L., 2017. Effects of CO_2 sequestration on lipid and biomass productivity in microalgal biomass production. Applied Energy 195, 1100–1111.

Erb, T.J., Carboxylases in natural and synthetic microbial pathways. Applied and Environmental Microbiology 77, 8466–8477.

Fan, T.W.M., Lane, A.N., Chekmenev, E., Wittebort, R.J., Higashi, R.M., 2004. Synthesis and physicochemical properties of peptides in soil humic substances. Journal of Peptide Research 63, 253–264.

Fang, C., Smith, P., Moncrieff, J.B., Smith, J.U., 2005. Similar response of labile and resistant soil organic matter pools to changes in temperature Nature 433, 57–59.

Finér, L., Helmisaari, H.S., Lõhmus, K., Majdi, H., Brunner, I., Børja, I., Eldhuset, T., Godbold, D., Grebenc, T., Konôpka, B., Kraigher, H., Möttönen, M.R., Ohashi, M., Oleksyn, J., Ostonen, I., Uri, V., Vanguelova, E., 2007. Variation in fine root biomass of three European tree species: Beech (Fagus sylvatica L.), Norway spruce (Picea abies L. Karst.), and Scots pine (Pinus sylvestris L.). Plant Biosystems 141, 394–405.

Finzi, A.C., Breemen, N. Van, Canham, C.D., 1998. Canopy Tree-Soil Interactions within Temperate Forests: Species Effects on Soil Carbon and Nitrogen. Ecological Applications 8, 440–446.

Fischer, M., Bossdorf, O., Gockel, S., Hänsel, F., Hemp, A., Hessenmöller, D., Korte, G., Nieschulze, J., Pfeiffer, S., Prati, D., Renner, S., Schöning, I., Schumacher, U., Wells, K., Buscot, F., Kalko, E.K.V., Linsenmair, K.E., Schulze, E.D., Weisser, W.W., 2010. Implementing large-scale and long-term functional biodiversity research: The Biodiversity Exploratories. Basic and Applied Ecology 11, 473–485.

Friedlingstein, P., Jones, M.W., O'Sullivan, M., Andrew, R.M., Hauck, J., Peters, G.P., Peters, W., Pongratz, J., Sitch, S., Le Quéré, C., DBakker, O.C.E., Canadell1, J.G., Ciais1, P., Jackson, R.B., Anthoni1, P., Barbero, L., Bastos, A., Bastrikov, V., Becker, M., Bopp, L., Buitenhuis, E., Chandra, N., Chevallier, F., Chini, L.P., Currie, K.I., Feely, R.A., Gehlen, M., Gilfillan, D., Gkritzalis, T., Goll, D.S., Gruber, N., Gutekunst, S., Harris, I., Haverd, V., Houghton, R.A., Hurtt, G., Ilyina, T., Jain, A.K., Joetzjer, E., Kaplan, J.O., Kato, E., Goldewijk, K.K., Korsbakken, J.I., Landschützer, P., Lauvset, S.K., Lefèvre, N., Lenton, A., Lienert, S., Lombardozzi, D., Marland, G., McGuire, P.C., Melton, J.R., Metzl, N., Munro, D.R., Nabel, J.E.M.S., Nakaoka, S.I., Neill, C., Omar, A.M., Ono, T., Peregon, A., Pierrot, D., Poulter, B., Rehder, G., Resplandy, L., Robertson, E., Rödenbeck, C., Séférian, R., Schwinger, J., Smith, N., Tans, P.P., Tian, H., Tilbrook, B., Tubiello, F.N., Van Der Werf, G.R., Wiltshire, A.J., Zaehle, S., 2019. Global carbon budget 2019. Earth System Science Data 11, 1783–1838.

Fuchs, G., 2011. Alternative Pathways of Carbon Dioxide Fixation: Insights into the Early Evolution of Life?, Annual Review of Microbiology. 65, 631–658.

Galambos, D., Anderson, R.E., Reveillaud, J., Huber, J.A., 2019. Genome-resolved metagenomics and metatranscriptomics reveal niche differentiation in functionally redundant microbial communities at deep-sea hydrothermal vents. Environmental Microbiology 21, 4395–4410.

Ge, T., Wu, X., Liu, Q., Zhu, Z., Yuan, H., Wang, W., Whiteley, A.S., Wu, J., 2016. Effect of simulated tillage on microbial autotrophic CO_2 fixation in paddy and upland soils. Scientific Reports 6, 1–9.

Gleixner, G., 2013. Soil organic matter dynamics: A biological perspective derived from the use of compound-specific isotopes studies. Ecological Research 28, 683–695.

Gleixner, G., Poirier, N., Bol, R., Balesdent, J., 2002. Molecular dynamics of organic matter in a cultivated soil. Organic Geochemistry 33, 357–366.

Goodale, C.L., Apps, M.J., Birdsey, R.A., Field, C.B., Heath, L.S., Houghton, R.A., Jenkins, J.C., Kohlmaier, G.H., Kurz, W., Liu, S., Nabuurs, G.J., Nilsson, S., Shvidenko, A.Z., 2002. Forest carbon sinks in the Northern Hemisphere. Ecological Applications 12, 891–899.

Graser, H., 1928. Die Bewirtschaftung des erzgebirgischen Fichtenwaldes. Erster Band. Hifbuchhandlung H.Burdach, Dresden.

Grüneberg, E., Ziche, D., Wellbrock, N., 2014. Organic carbon stocks and sequestration rates of forest soils in Germany. Global Change Biology 20, 2644–2662.

Hackl, E., Pfeffer, M., Donat, C., Bachmann, G., Zechmeister-Boltenstern, S., 2005. Composition of the microbial communities in the mineral soil under different types of natural forest. Soil Biology and Biochemistry 37, 661–671.

Hagerty, S.B., Van Groenigen, K.J., Allison, S.D., Hungate, B.A., Schwartz, E., Koch, G.W., Kolka, R.K., Dijkstra, P., 2014. Accelerated microbial turnover but constant growth efficiency with warming in soil. Nature Climate Change 4, 903–906.

Hart, K.M., Kulakova, A.N., Allen, C.C.R., Simpson, A.J., Oppenheimer, S.F., Masoom, H., Courtier-Murias, D., Soong, R., Kulakov, L.A., Flanagan, P. V., Murphy, B.T., Kelleher, B.P., 2013. Tracking the fate of microbially sequestered carbon dioxide in soil organic matter. Environmental Science and Technology 47, 5128–5137.

Herrmann, M., Rusznyák, A., Akob, D.M., Schulze, I., Opitz, S., Totsche, K.U., Küsel, K., 2015. Large fractions of CO_2-fixing microorganisms in pristine limestone aquifers appear to be involved in the oxidation of reduced sulfur and nitrogen compounds. Applied and Environmental Microbiology 81, 2384–2394.

Hicks Pries, C.E., Castanha, C., Porras, R., Phillips, C., Torn, M.S., 2017. The whole-soil carbon flux in response to warming. Science 355, 1420–1423.

Huber, H., Gallenberger, M., Jahn, U., Eylert, E., Berg, I.A., Kockelkorn, D., Eisenreich, W., Fuchs, G., 2008. A dicarboxylate/4-hydroxybutyrate autotrophic carbon assimilation cycle in the hyperthermophilic Archaeum Ignicoccus hospitalis. Proceedings of the National Academy of Sciences of the United States of America 105, 7851–7856.

Hug, L.A., Castelle, C.J., Wrighton, K.C., Thomas, B.C., Sharon, I., Frischkorn, K.R., Williams, K.H., Tringe, S.G., Banfield, J.F., 2013. Community genomic analyses constrain the distribution of metabolic traits across the Chloroflexi phylum and indicate roles in sediment carbon cycling. Microbiome 1, 1–17.

Hügler, M., Huber, H., Stetter, K.O., Fuchs, G., 2003. Autotrophic CO_2 fixation pathways in archaea (Crenarchaeota). Archives of Microbiology 179, 160–173.

Hügler, M., Sievert, S.M., 2011. Beyond the Calvin Cycle: Autotrophic Carbon Fixation in

the Ocean. Annual Review of Marine Science 3, 261–289.

Hügler, M., Wirsen, C.O., Fuchs, G., Taylor, C.D., Sievert, S.M., 2005. Evidence for autotrophic via the reductive tricarboxylic acid cycle by members of the ε subdivision of proteobacteria. Journal of Bacteriology 187, 3020–3027.

IPCC, 2000. Robert T. Watson, Ian R. Noble, Bert Bolin, N. H. Ravindranath, David J. Verardo and David J. Dokken (Eds.) Cambridge University Press, UK. pp 375.

IPCC, 2001. Climate change 2001: impacts, adaptation and vulnerability, Contribution of Working Group II to the Third Assessment Report of the Intergovernmental Panel on Climate Change. J. J. McCarthy, O. F. Canziani, N. A. Leary, D. J. Dokken and K. S. White (eds). Cambridge University Press, Cambridge, UK, and New York, USA.

IPCC, 2007: Climate Change 2007: Synthesis Report. Contribution of Working Groups I, II and III to the Fourth Assessment Report of the Intergovernmental Panel on Climate Change [Core Writing Team, Pachauri, R.K and Reisinger, A. (eds.)]. IPCC, Geneva, Switzerland, 104 pp

Jobbágy, E.G., Jackson, R.B., 2000. The vertical distribution of soil organic carbon and its relation to climate and vegetation. Ecological Applications 10, 423–436.

Joly, F.X., Milcu, A., Scherer-Lorenzen, M., Jean, L.K., Bussotti, F., Dawud, S.M., Müller, S., Pollastrini, M., Raulund-Rasmussen, K., Vesterdal, L., Hättenschwiler, S., 2017. Tree species diversity affects decomposition through modified micro-environmental conditions across European forests. New Phytologist 214, 1281–1293.

Jones, R.M., Goordial, J.M., Orcutt, B.N., 2018. Low energy subsurface environments as extraterrestrial analogs. Frontiers in Microbiology 9, 1–18.

Kaiser, K., Wemheuer, B., Korolkow, V., Wemheuer, F., Nacke, H., Schöning, I., Schrumpf, M., Daniel, R., 2016. Driving forces of soil bacterial community structure, diversity, and function in temperate grasslands and forests. Scientific Reports 6, 1–12.

Kallenbach, C.M., Frey, S.D., Grandy, A.S., 2016. Direct evidence for microbial-derived soil organic matter formation and its ecophysiological controls. Nature Communications 7, 1–10.

Kästner, M., Miltner, A., Thiele-Bruhn, S., Liang, C., 2021. Microbial Necromass in Soils—Linking Microbes to Soil Processes and Carbon Turnover. Frontiers in Environmental Science 9, 1–18.

Kirschbaum, M.U.F., 1995. The temperature dependence of soil organic matter decomposition, and the effect of global warming on soil organic C storage. Soil Biology and Biochemistry 27, 753–760.

Knohl, A., Schulze, E.D., Kolle, O., Buchmann, N., 2003. Large carbon uptake by an unmanaged 250-year-old deciduous forest in Central Germany. Agricultural and Forest Meteorology 118, 151–167.

Kögel-Knabner, I., 2001. The macromolecular organic composition of plant and microbial residues as inputs to soil organic matter. Soil Biology & Biochemistry 34, 139–162.

Kragelund, C., Levantesi, C., Borger, A., Thelen, K., Eikelboom, D., Tandoi, V., Kong, Y., Van Der Waarde, J., Krooneman, J., Rossetti, S., Thomsen, T.R., Nielsen, P.H., 2007. Identity, abundance and ecophysiology of filamentous Chloroflexi species present in

activated sludge treatment plants. FEMS Microbiology Ecology 59, 671–682.

Krebs, H.A., 1941. Carbon dioxide assimilation in heterotrophic organisms. Nature (London) 147, 560 – 563

Kuzyakov, Y., 2006. Sources of CO_2 efflux from soil and review of partitioning methods. Soil Biology and Biochemistry 38, 425–448.

Lal, R., 2008. Carbon sequestration Rattan Lal Email alerting service Carbon sequestration. Management 815–830.

Lal, R., 2005. Forest soils and carbon sequestration. Forest Ecology and Management 220, 242–258.

Lal, R., 2004. Soil carbon sequestration to mitigate climate change. Geoderma 123, 1–22.

Lauber, C.L., Hamady, M., Knight, R., Fierer, N., 2009. Pyrosequencing-based assessment of soil pH as a predictor of soil bacterial community structure at the continental scale. Applied and Environmental Microbiology 75, 5111–5120.

Leifeld, J., Fuhrer, J., 2005. The temperature response of CO_2 production from bulk soils and soil fractions is related to soil organic matter quality. Biogeochemistry 75, 433–453.

Lengler, J. W., Drews, G., and Schlegel, H. G. (1999). Biology of the Prokaryotes. Willey-Blackwell, Oxford, pp. 166.

Li, B., Li, Z., Sun, X., Wang, Q., Xiao, E., Sun, W., 2018. DNA-SIP Reveals the Diversity of Chemolithoautotrophic Bacteria Inhabiting Three Different Soil Types in Typical Karst Rocky Desertification Ecosystems in Southwest China. Microbial Ecology 76, 976–990.

Li, H., Yang, S., Semenov, M. V., Yao, F., Ye, J., Bu, R., Ma, R., Lin, J., Kurganova, I., Wang, X., Deng, Y., Kravchenko, I., Jiang, Y., Kuzyakov, Y., 2021. Temperature sensitivity of SOM decomposition is linked with a K-selected microbial community. Global Change Biology 27, 2763–2779.

Liang, C., Amelung, W., Lehmann, J., Kästner, M., 2019. Quantitative assessment of microbial necromass contribution to soil organic matter. Global Change Biology 25, 3578–3590.

Liu, X., Lin, T.-C., Vadeboncoeur, M.A., Yang, Z., Chen, S., Xiong, D., Xu, C., Li, Y., Yang, Y., 2019. Root litter inputs exert greater influence over soil C than does aboveground litter in a subtropical natural forest. Plant and Soil 444, 489–499.

Liu, X., Trogisch, S., He, J.S., Niklaus, P.A., Bruelheide, H., Tang, Z., Erfmeier, A., Scherer-Lorenzen, M., Pietsch, K.A., Yang, B., Kühn, P., Scholten, T., Huang, Y., Wang, C., Staab, M., Leppert, K.N., Wirth, C., Schmid, B., Ma, K., 2018. Tree species richness increases ecosystem carbon storage in subtropical forests. Proceedings of the Royal Society B: Biological Sciences 285.

Liu, Z., Sun, Y., Zhang, Y., Feng, W., Lai, Z., Fa, K., Qin, S., 2018. Metagenomic and ^{13}C tracing evidence for autotrophic atmospheric carbon absorption in a semiarid desert. Soil Biology and Biochemistry 125, 156–166.

Ljungdahl, L.G., 1986. The autotrophic pathway of acetate synthesis in acetogenic bacteria. Annual Review of Microbiology 40, 415–450.

Lladó, S., López-Mondéjar, R., Baldrian, P., 2017. Forest Soil Bacteria: Diversity,

Involvement in Ecosystem Processes, and Response to Global Change. Microbiology and Molecular Biology Reviews 81, 1–27.

Long, X.E., Yao, H., Wang, J., Huang, Y., Singh, B.K., Zhu, Y.G., 2015. Community Structure and Soil pH Determine Chemoautotrophic Carbon Dioxide Fixation in Drained Paddy Soils. Environmental Science and Technology 49, 7152–7160.

Lorenz, K., Lal, R., 2005. The Depth Distribution of Soil Organic Carbon in Relation to Land Use and Management and the Potential of Carbon Sequestration in Subsoil Horizons. Advances in Agronomy 88, 35–66.

Lorenz, K., Lal, R., Shipitalo, M.J., 2011. Stabilized soil organic carbon pools in subsoils under forest are potential sinks for atmospheric CO_2. Forest Science 57, 19–25.

Lorenz, K., Preston, C.M., Krumrei, S., Feger, K.H., 2004. Decomposition of needle/leaf litter from Scots pine, black cherry, common oak and European beech at a conurbation forest site. European Journal of Forest Research 123, 177–188.

Lorimer, G.H., Andrews, T.J., 1973. Plant photorespiration - An inevitable consequence of the existence of atmospheric oxygen. Nature 243, 359–360.

Lu, X., Fan, J., Yan, Y., Wang, X., 2013. Responses of Soil CO_2 Fluxes to Short-Term Experimental Warming in Alpine Steppe Ecosystem, Northern Tibet. PLoS ONE 8, 8(3): e59054.

Lynn, T.M., Ge, T., Yuan, H., Wei, X., Wu, X., Xiao, K., Kumaresan, D., Yu, S.S., Wu, J., Whiteley, A.S., 2017. Soil Carbon-Fixation Rates and Associated Bacterial Diversity and Abundance in Three Natural Ecosystems. Microbial Ecology 73, 645–657.

Ma, T., Zhu, S., Wang, Z., Chen, D., Dai, G., Feng, B., Su, X., Hu, H., Li, K., Han, W., Liang, C., Bai, Y., Feng, X., 2018. Divergent accumulation of microbial necromass and plant lignin components in grassland soils. Nature Communications 9, 3480.

Madigan, M.T., Martinko, J.M., Bender, K.S., Buckley, D.H., Stahl, D.A. 2015. Brock Biology of Microorganisms, fourteenth ed. Pearson Education, Inc, pp. 79-83

Malik, A.A., Puissant, J., Buckeridge, K.M., Goodall, T., Jehmlich, N., Chowdhury, S., Gweon, H.S., Peyton, J.M., Mason, K.E., van Agtmaal, M., Blaud, A., Clark, I.M., Whitaker, J., Pywell, R.F., Ostle, N., Gleixner, G., Griffiths, R.I., 2018. Land use driven change in soil pH affects microbial carbon cycling processes. Nature Communications 9, 1–10.

Martin, J.G., Bolstad, P. V., 2005. Annual soil respiration in broadleaf forests of northern Wisconsin: Influence of moisture and site biological, chemical, and physical characteristics, Biogeochemistry 73, 149–182.

Martins, P.D., Frank, J., Mitchell, H., Markillie, L.M., Wilkins, M.J., 2019. Wetland sediments host diverse microbial taxa capable of cycling alcohols. Applied and Environmental Microbiology 85, 1–15.

Meesenburg, H., Riek, W., Ahrends, B., Eickenscheidt, N., Grüneberg, E., Evers, J., Fortmann, H., König, N., Lauer, A., Meiwes, K.J., Nagel, H.-D., Schimming, C.-G., Wellbrock, N., 2019. Soil Acidification in German Forest Soils 93–121.

Melillo, J.M., Butler, S., Johnson, J., Mohan, J., Steudler, P., Lux, H., Burrows, E., Bowles, F., Smith, R., Scott, L., Vario, C., Hill, T., Burton, A., Zhouj, Y.M., Tang, J., 2011. Soil

warming, carbon-nitrogen interactions, and forest carbon budgets. Proceedings of the National Academy of Sciences of the United States of America 108, 9508–9512.

Melillo, J.M., Frey, S.D., DeAngelis, K.M., Werner, W.J., Bernard, M.J., Bowles, F.P., Pold, G., Knorr, M.A., Grandy, A.S., 2017. Long-term pattern and magnitude of soil carbon feedback to the climate system in a warming world. Science 358, 101–105.

Melillo, J.M., Steudler, P.A., Aber, J.D., Newkirk, K., Lux, H., Bowles, F.P., Catricala, C., Magill, A., Ahrens, T., Morrisseau, S., 2002. Soil warming and carbon-cycle feedbacks to the climate system. Science 298, 2173–2176.

Merlin, C., Masters, M., Mcateer, S., Coulson, A., 2003. Why Is Carbonic Anhydrase Essential to Escherichia coli ? 185, 6415–6424.

Miao, R., Ma, J., Liu, Yinzhan, Liu, Yanchun, Yang, Z., Guo, M., 2019. Variability of aboveground litter inputs alters soil carbon and nitrogen in a coniferous-broadleaf mixed forest of Central China. Forests 10, 1–12.

Michaelis, L. & Menten, M. L. 1913. Die kinetik der invertin wirkung. 1913. Biochem. Z. 49, 334-336.

Milanese, A., Mende, D.R., Paoli, L., Salazar, G., Ruscheweyh, H.J., Cuenca, M., Hingamp, P., Alves, R., Costea, P.I., Coelho, L.P., Schmidt, T.S.B., Almeida, A., Mitchell, A.L., Finn, R.D., Huerta-Cepas, J., Bork, P., Zeller, G., Sunagawa, S., 2019. Microbial abundance, activity and population genomic profiling with mOTUs2. Nature Communications 10, 1014.

Miltner, A., Bombach, P., Schmidt-Brücken, B., Kästner, M., 2012. SOM genesis: Microbial biomass as a significant source. Biogeochemistry 111, 41–55.

Miltner, A., Kopinke, F.D., Kindler, R., Selesi, D., Hartmann, A., Kästner, M., Non-phototrophic CO_2 fixation by soil microorganisms. Plant and Soil 269, 193–203.

Miltner, A., Richnow, H.H., Kopinke, F.D., Kästner, M., 2004. Assimilation of CO_2 by soil microorganisms and transformation into soil organic matter. Organic Geochemistry 35, 1015–1024.

Miralles, I., Domingo, F., Cantón, Y., Trasar-Cepeda, C., Leirós, M.C., Gil-Sotres, F., 2012. Hydrolase enzyme activities in a successional gradient of biological soil crusts in arid and semi-arid zones. Soil Biology and Biochemistry 53, 124–132. doi:10.1016/j.soilbio.2012.05.016

Mobley, M.L., Lajtha, K., Kramer, M.G., Bacon, A.R., Heine, P.R., Richter, D.D., 2015. Surficial gains and subsoil losses of soil carbon and nitrogen during secondary forest development. Global Change Biology 21, 986–996.

Mölder, a, Bernhardt-Römermann, M., Schmidt, W., 2006. Forest ecosystem research in Hainich National Park (Thuringia): First results on flora and vegetation in stands with contrasting tree species diversity. Waldoekologie Online 3, 83–99.

Nacke, H., Goldmann, K., Schöning, I., Pfeiffer, B., Kaiser, K., 2016. Fine Spatial Scale Variation of Soil Microbial Communities under European Beech and Norway Spruce 7, 2067.

Nacke, H., Thürmer, A., Wollherr, A., Will, C., Hodac, L., Herold, N., Schöning, I., Schrumpf, M., Daniel, R., 2011. Pyrosequencing-based assessment of bacterial

community structure along different management types in German forest and grassland soils. PLoS ONE 6 6(2): e17000.

Nel, J.A., Cramer, M.D., 2019. Soil microbial anaplerotic CO2fixation in temperate soils. Geoderma 335, 170–178.

Niederberger, T.D., Sohm, J.A., Gunderson, T., Tirindelli, J., Capone, D.G., Carpenter, E.J., Cary, S.C., 2015. Carbon-fixation rates and associated microbial communities residing in arid and ephemerally wet antarctic dry valley soils. Frontiers in Microbiology 6, 1–9.

Nowak, M.E., Beulig, F., Von Fischer, J., Muhr, J., Küsel, K., Trumbore, S.E., 2015. Autotrophic fixation of geogenic CO2 by microorganisms contributes to soil organic matter formation and alters isotope signatures in a wetland mofette. Biogeosciences 12, 7169–7183.

Norby, R.J., DeLucia, E.H., Gielen, B., Calfapietra, C., Giardina, C.P., Kings, J.S., Ledford, J., McCarthy, H.R., Moore, D.J.P., Ceulemans, R., De Angelis, P., Finzi, A.C., Karnosky, D.F., Kubiske, M.E., Lukac, M., Pregitzer, K.S., Scarascia-Mugnozza, G.E., Schlesinger, W.H., Oren, R., 2005. Forest response to elevated CO2 is conserved across a broad range of productivity. Proceedings of the National Academy of Sciences of the United States of America 102, 18052–18056. doi:10.1073/pnas.0509478102

Oh, N.H., Kim, H.S., Richter, D.D., 2005. What regulates soil CO_2 concentrations? A modeling approach to CO2 diffusion in deep soil profiles. Environmental Engineering Science 22, 38–45.

Okabe, S., Kindaichi, T., Ito, T., 2005. Fate of ^{14}C-labeled microbial products derived from nitrifying bacteria in autotrophic nitrifying biofilms. Applied and Environmental Microbiology 71, 3987–3994.

Ostonen, I., Püttsepp, Ü., Biel, C., Alberton, O., Bakker, M.R., Lõhmus, K., Majdi, H., Metcalfe, D., Olsthoorn, A.F.M., Pronk, A., Vanguelova, E., Weih, M., Brunner, I., 2007. Specific root length as an indicator of environmental change. Plant Biosystems 141, 426–442.

Owen, O.E., Kalhan, S.C., Hanson, R.W., 2002. The key role of anaplerosis and cataplerosis for citric acid cycle function. Journal of Biological Chemistry 277, 30409–30412.

Palma, J.H.N., Graves, A.R., Bunce, R.G.H., Burgess, P.J., de Filippi, R., Keesman, K.J., van Keulen, H., Liagre, F., Mayus, M., Moreno, G., Reisner, Y., Herzog, F., 2007. Modeling environmental benefits of silvoarable agroforestry in Europe. Agriculture, Ecosystems and Environment 119, 320–334.

Paul, E.A., 2016. The nature and dynamics of soil organic matter: Plant inputs, microbial transformations, and organic matter stabilization. Soil Biology and Biochemistry 98, 109–126.

Peltoniemi, K., Laiho, R., Juottonen, H., Kiikkilä, O., Mäkiranta, P., Minkkinen, K., Pennanen, T., Penttilä, T., Sarjala, T., Tuittila, E.S., Tuomivirta, T., Fritze, H., 2015. Microbial ecology in a future climate: Effects of temperature and moisture on microbial communities of two boreal fens. FEMS Microbiology Ecology 91, 1–14.

Pendall, E., Leavitt, S.W., Brooks, T., Kimball, B.A., Pinter, P.J., Wall, G.W., LaMorte, R.L., Wechsung, G., Wechsung, F., Adamsen, F., Matthias, A.D., Thompson, T.L., 2001. Elevated CO_2 stimulates soil respiration in a FACE wheat field. Basic and Applied

Ecology 2, 193–201.

Pietikäinen, J., Pettersson, M., Bååth, E., 2005. Comparison of temperature effects on soil respiration and bacterial and fungal growth rates. FEMS Microbiology Ecology 52, 49–58.

Probst, A.J., Castelle, C.J., Singh, A., Brown, C.T., Anantharaman, K., Sharon, I., Hug, L.A., Burstein, D., Emerson, J.B., Thomas, B.C., Banfield, J.F., 2017. Genomic resolution of a cold subsurface aquifer community provides metabolic insights for novel microbes adapted to high CO_2 concentrations. Environmental Microbiology 19, 459–474.

Qualls, R.G., Haines, B.L., Swank, W.T., Tyler, S.W., 2000. Soluble Organic and Inorganic Nutrient Fluxes in Clearcut and Mature Deciduous Forests. Soil Science Society of America Journal 64, 1068–1077.

Ragsdale, S.W., Pierce, E., 2008. Acetogenesis and the Wood-Ljungdahl pathway of fixation.

Rasse, D.P., Longdoz, B., Ceulemans, R., 2001. TRAP: A modelling approach to below-ground carbon allocation in temperate forests. Plant and Soil 229, 281–293.

Rasse, D.P., Rumpel, C., Dignac, M.F., 2005. Is soil carbon mostly root carbon? Mechanisms for a specific stabilisation. Plant and Soil 269, 341–356.

Rastogi, M., Singh, S., Pathak, H., 2002. Emission of carbon dioxide from soil. Current Science 82, 510–517.

Ren, B., Hu, Y., Chen, B., Zhang, Y., Thiele, J., Shi, R., Liu, M., Bu, R., 2018. Soil pH and plant diversity shape soil bacterial community structure in the active layer across the latitudinal gradients in continuous permafrost region of Northeastern China. Scientific Reports 8, 1–10.

Richter, D.D., Markewitz, D., 1995. How Deep Is Soil? BioScience 45, 600–609.

Saini, R., Kapoor, R., Kumar, R., Siddiqi, T.O., Kumar, A., 2011. CO_2 utilizing microbes - A comprehensive review. Biotechnology Advances 29, 949–960.

Santruckova, H., Bird, M.I., Elhottová, D., Novák, J., Picek, T., Šimek, M., Tykva, R., 2005. Heterotrophic fixation of CO_2 in soil. Microbial Ecology 49, 218–225.

Santruckova, H., Bird, M.I., Lloyd, J., 2000. Microbial processes and carbon-isotope fractionation in. Functional Ecology 14, 108–114.

Šantrůčková, H., Kotas, P., Bárta, J., Urich, T., Čapek, P., Palmtag, J., Eloy Alves, R.J., Biasi, C., Diáková, K., Gentsch, N., Gittel, A., Guggenberger, G., Hugelius, G., Lashchinsky, N., Martikainen, P.J., Mikutta, R., Schleper, C., Schnecker, J., Schwab, C., Shibistova, O., Wild, B., Richter, A., 2018. Significance of dark CO_2 fixation in arctic soils. Soil Biology and Biochemistry 119, 11–21.

Sauer, U., Eikmanns, B.J., 2005. The PEP-pyruvate-oxaloacetate node as the switch point for carbon flux distribution in bacteria. FEMS Microbiology Reviews 29, 765–794.

Scharlemann, J.P.W., Tanner, E.V.J., Hiederer, R., Kapos, V., 2014. Global soil carbon: Understanding and managing the largest terrestrial carbon pool. Carbon Management 5, 81–91.

Schimel, J., 2013. Soil carbon: Microbes and global carbon. Nature Climate Change 3, 867–

868.

Schoonover, J.E., Crim, J.F., 2015. An Introduction to Soil Concepts and the Role of Soils in Watershed Management. Journal of Contemporary Water Research & Education 154, 21–47.

Schrumpf, M., Kaiser, K., Schulze, E.D., 2014. Soil organic carbon and total nitrogen gains in an old growth deciduous forest in Germany. PLoS ONE 9, 1–8.

Schwilch, G., Bernet, L., Claringbould, H., Fleskens, L., Giannakis, E., Leventon, J., Marañón, T., Mills, J., Short, C., Stolte, J., van Delden, H. and Verzandvoort, S. 2015. Soil Functions and Ecosystem Services. In: Stolte, J., Tesfai, M., Oygarden, L., Kvaerno, S., Keizer, J., Verheijen, F., Panagos, P., Ballabio, C., and Hessel, R. (2016). *Soil threats in Europe: status, methods, drivers and effects on ecosystem services: deliverable 2.1 RECARE project.* (98673 ed.) (JRC Technical reports). European Commission DG Joint Research Centre. pp.156-172.

Selesi, D., Schmid, M., Hartmann, A., 2005. Diversity of Green-Like and Red-Like Genes (cbbL) in Differently Managed Agricultural Soils. Applied and Environmental Microbiology 71, 175–184.

Setälä, H.M., Francini, G., Allen, J.A., Hui, N., Jumpponen, A., Kotze, D.J., 2016. Vegetation type and age drive changes in soil properties, nitrogen, and carbon sequestration in urban parks under cold climate. Frontiers in Ecology and Evolution 4, 1–14.

Sewell, H., Kaster, A.-K., Spormann, A., 2017. Homoacetogenesis in Deep-Sea Chloroflexi, as Inferred by Single-Cell Genomics, Provides a Link to Reductive Dehalogenation in Terrestrial Dehalococcoidetes 1–22.

Shively, J.M., Van Keulen, G., Meijer, W.G., 1998. Something from almost nothing: Carbon dioxide fixation in chemoautotrophs. Annual Review of Microbiology 52, 191–230.

Sierra, C.A., Hoyt, A.M., He, Y., Trumbore, S.E., 2018. Soil Organic Matter Persistence as a Stochastic Process: Age and Transit Time Distributions of Carbon in Soils. Global Biogeochemical Cycles 32, 1574–1588.

Six, J., Conant, R.T., Paul, E.A., Paustian, K., 2002. Six Stabilization nmechanisms of SOM implications for C saturation of soils.pdf. Plant and Soil 241, 155–176.

Soong, J.L., Phillips, C.L., Ledna, C., Koven, C.D., Torn, M.S., 2020. CMIP5 Models Predict Rapid and Deep Soil Warming Over the 21st Century. Journal of Geophysical Research: Biogeosciences 125.

Spohn, M., Müller, K., Höschen, C., Mueller, C.W., Marhan, S., 2019. Dark microbial CO_2 fixation in temperate forest soils increases with CO2 concentration. Global Change Biology 1926–1935.

Staelens, J., Rütting, T., Huygens, D., Schrijver, A. De, Müller, C., Verheyen, K., Boeckx, P., 2012. In situ gross nitrogen transformations differ between temperate deciduous and coniferous forest soils. Biogeochemistry 108, 259–277.

Su, Y., He, Z., Yang, Y., Jia, S., Yu, M., Chen, X., Shen, A., 2020. Linking soil microbial community dynamics to straw-carbon distribution in soil organic carbon. Scientific Reports 10, 1–12.

Szukics, U., Hackl, E., Zechmeister-Boltenstern, S., Sessitsch, A., 2012. Rapid and dissimilar response of ammonia oxidizing archaea and bacteria to nitrogen and water amendment in two temperate forest soils. Microbiological Research 167, 103–109.

Tabita, F.R., Satagopan, S., Hanson, T.E., Kreel, N.E., Scott, S.S., 2008. Distinct form I, II, III, and IV Rubisco proteins from the three kingdoms of life provide clues about Rubisco evolution and structure/function relationships. Journal of Experimental Botany 59, 1515–1524.

Taggart, R.E., Cross, A.T., 2009. Global greenhouse to icehouse and back again: The origin and future of the Boreal Forest biome. Global and Planetary Change 65, 115–121.

Tahvanainen, T., Haraguchi, A., 2013. Effect of pH on phenol oxidase activity on decaying Sphagnum mosses. European Journal of Soil Biology 54, 41–47.

Tcherkez, G.G.B., Farquhar, G.D., Andrews, T.J., 2006. Despite slow catalysis and confused substrate specificity, all ribulose bisphosphate carboxylases may be nearly perfectly optimized. Proceedings of the National Academy of Sciences of the United States of America 103, 7246–7251.

Tefs, C., Gleixner, G., 2012. Importance of root derived carbon for soil organic matter storage in a temperate old-growth beech forest - Evidence from C, N and ^{14}C content. Forest Ecology and Management 263, 131–137.

Thauer, R.K., Kaster, A.K., Seedorf, H., Buckel, W., Hedderich, R., 2008. Methanogenic archaea: Ecologically relevant differences in energy conservation. Nature Reviews Microbiology 6, 579–591.

Thieme, L., Graeber, D., Hofmann, D., Bischoff, S., Schwarz, M.T., Steffen, B., Meyer, U.N., Kaupenjohann, M., Wilcke, W., Michalzik, B., Siemens, J., 2019. Dissolved organic matter characteristics of deciduous and coniferous forests with variable management: Different at the source, aligned in the soil. Biogeosciences 16, 1411–1432.

Thoms, C., Gattinger, A., Jacob, M., Thomas, F.M., Gleixner, G., 2010. Direct and indirect effects of tree diversity drive soil microbial diversity in temperate deciduous forest. Soil Biology and Biochemistry 42, 1558–1565.

Tian, Y., Haibara, K., Toda, H., Ding, F., Liu, Y., Choi, D., 2008. Microbial biomass and activity along a natural pH gradient in forest soils in a karst region of the upper Yangtze River, China. Journal of Forest Research 13, 205–214.

Tolli, J., King, G.M., 2005. Diversity and structure of bacterial chemolithotrophic communities in pine forest and agroecosystem soils. Applied and Environmental Microbiology 71, 8411–8418.

Totsche, K.U., Amelung, W., Gerzabek, M.H., Guggenberger, G., Klumpp, E., Knief, C., Lehndorff, E., Mikutta, R., Peth, S., Prechtel, A., Ray, N., Kögel-Knabner, I., 2017. Microaggregates in soils. Journal of Plant Nutrition and Soil Science 000, 1–33.

Trumbore, S., 2009. Radiocarbon and Soil Carbon Dynamics. Annual Review of Earth and Planetary Sciences 37, 47–66.

Trumbore, S.E., Czimczik, C.I., 2008. Geology: An uncertain future for soil carbon. Science 321, 1455–1456.

Tyrrell, M.L., Ross, J., Kelty, M., 2012. Carbon dynamics in the temperate forest. In: Ashton,

M.S., Tyrrell, M.L., Spalding, D., Gentry, B. (Eds.), Managing Forest Carbon in a Changing Climate. Springer, Dordrecht, The Netherlands, pp. 77-107

Urbanová, M., Šnajdr, J., Baldrian, P., 2015. Composition of fungal and bacterial communities in forest litter and soil is largely determined by dominant trees. Soil Biology and Biochemistry 84, 53–64.

Uroz, S., Ioannidis, P., Lengelle, J., Cébron, A., Morin, E., Buée, M., Martin, F., 2013. Functional Assays and Metagenomic Analyses Reveals Differences between the Microbial Communities Inhabiting the Soil Horizons of a Norway Spruce Plantation. PLoS ONE 8(2): e55929.

Vance, E.D., Brookes, P.C., Jenkinson, D.S., 1987. An extraction method for measuring soil microbial biomass C. Soil Biology and Biochemistry 19, 703–707.

VanInsberghe, D., Maas, K.R., Cardenas, E., Strachan, C.R., Hallam, S.J., Mohn, W.W., 2015. Non-symbiotic Bradyrhizobium ecotypes dominate North American forest soils. ISME Journal 9, 2435–2441.

Vesterdal, L., Clarke, N., Sigurdsson, B.D., Gundersen, P., 2013. Do tree species influence soil carbon stocks in temperate and boreal forests? Forest Ecology and Management 309, 4–18.

Vesterdal, L., Schmidt, I.K., Callesen, I., Nilsson, L.O., Gundersen, P., 2008. Carbon and nitrogen in forest floor and mineral soil under six common European tree species. Forest Ecology and Management 255, 35–48.

Walker, T.W.N., Kaiser, C., Strasser, F., Herbold, C.W., Leblans, N.I.W., Woebken, D., Janssens, I.A., Sigurdsson, B.D., Richter, A., 2018. Microbial temperature sensitivity and biomass change explain soil carbon loss with warming. Nature Climate Change 8, 885–889.

Watson, G.M.F., Tabita, F.R., 1997. Microbial ribulose 1,5-bisphosphate carboxylase/oxygenase: A molecule for phylogenetic and enzymological investigation. FEMS Microbiology Letters 146, 13–22.

Winkler, J.P., Cherry, R.S., Schlesinger, W.H., 1996. The Q_{10} relationship of microbial respiration in a temperate forest soil. Soil Biology and Biochemistry 28, 1067–1072.

Wood M. 1995. Soil as a habitat for organisms. In: Environmental Soil Biology. Experimental and Clinical Neuroscience. Springer, Dordrecht.

Wu, X., Ge, T., Wang, W., Yuan, H., Wegner, C.E., Zhu, Z., Whiteley, A.S., Wu, J., 2015. Cropping systems modulate the rate and magnitude of soil microbial autotrophic in soil. Frontiers in Microbiology 6, 1–10.

Wu, X., Ge, T., Yuan, H., Li, B., Zhu, H., Zhou, P., Sui, F., O'Donnell, A.G., Wu, J., 2014. Changes in bacterial CO_2 fixation with depth in agricultural soils. Applied Microbiology and Biotechnology 98, 2309–2319.

Xia, Y., Kong, Y., Nielsen, P.H., 2007. In situ detection of protein-hydrolysing microorganisms in activated sludge. FEMS Microbiology Ecology 60, 156–165.

Xiao, H., Li, Z., Chang, X., Deng, L., Nie, X., Liu, C., Liu, L., Jiang, J., Chen, J., Wang, D., 2018. Microbial CO2 assimilation is not limited by the decrease in autotrophic bacterial abundance and diversity in eroded watershed. Biology and Fertility of Soils 54, 595–

605.

Xu, X., Thornton, P.E., Post, W.M., 2013. A global analysis of soil microbial biomass carbon, nitrogen and phosphorus in terrestrial ecosystems. Global Ecology and Biogeography 22, 737–749.

Yavitt, A.J.B., Downey, D.M., Lang, G.E., Sexstone, A.J. 1990. Methane Consumption in Two Temperate Forest Soils Published. Biogeosciences 9, 39 - 52.

Yuan, H., Ge, T., Chen, C., O'Donnell, A.G., Wu, J., 2012. Significant role for microbial autotrophy in the sequestration of soil carbon. Applied and Environmental Microbiology 78, 2328–2336.

Yuan, H., Ge, T., Zou, S., Wu, X., Liu, S., Zhou, P., Chen, X., Brookes, P., Wu, J., 2013. Effect of land use on the abundance and diversity of autotrophic bacteria as measured by ribulose-1,5-biphosphate carboxylase/oxygenase (RubisCO) large subunit gene abundance in soils. Biology and Fertility of Soils 49, 609–616.

Zarzycki, J., Brecht, V., Müller, M., Fuchs, G., 2009. Identifying the missing steps of the autotrophic 3-hydroxypropionate CO2 fixation cycle in Chloroflexus aurantiacus. Proceedings of the National Academy of Sciences of the United States of America 106, 21317–21322.

Zhang, C., Li, J., Wang, J., Liu, G., Wang, G., Guo, L., Peng, S., 2019. Decreased temporary turnover of bacterial communities along soil depth gradient during a 35-year grazing exclusion period in a semiarid grassland. Geoderma 351, 49–58.

Zhang, Z., Qiao, M., Li, D., Yin, H., Liu, Q., 2016. Do warming-induced changes in quantity and stoichiometry of root exudation promote soil N transformations via stimulation of soil nitrifiers, denitrifiers and ammonifiers? European Journal of Soil Biology 74, 60–68.

Zhao, Y., Liu, P., Rui, J., Cheng, L., Wang, Q., Liu, X., Yuan, Q., 2020. Dark carbon fixation and chemolithotrophic microbial community in surface sediments of the cascade reservoirs, Southwest China. Science of The Total Environment 698, 134316.

Žifčáková, L., Větrovský, T., Howe, A., Baldrian, P., 2016. Microbial activity in forest soil reflects the changes in ecosystem properties between summer and winter. Environmental Microbiology 18, 288–301.

Zifcakova L. 2020. Factors Affecting Soil Microbial Processes. In: Datta R., Meena R., Pathan S., Ceccherini M. (eds) Carbon and Nitrogen Cycling in Soil. Springer, Singapore

8 Acknowledgments

I am grateful to both the Institute of Biodiversity at the Friedrich Schiller University Jena and the Max Planck Institute for Biogeochemistry Jena for the enabling environment to carry out my doctoral studies by providing all necessary support and excellent working facilities. The funding from Deutscher Akademischer Austauschdienst (DAAD); Graduate School Scholarship program is gratefully acknowledged.

I like to foremostly express my gratitude to Prof. Dr. Kirsten Küsel and Professor Dr. Susan Trumbore. Thank you for the opportunity to conduct my Ph.D. under your supervision. I am indeed grateful for all your support throughout my Ph.D. time. The fruitful discussions from my experimental design up to the revision of my manuscripts and the many encouragements during the writing of my dissertation are part of what I will forever remain grateful for.

I am privileged to have received the constant supervision of Dr. Martin Taubert. You have been a huge pillar of support all through this project. I deeply appreciate your listening ear, the knowledge you impacted, and the numerous spontaneous discussions we had. You were of tremendous support when designing my experiments, analysing the data, and identifying the unique story. The many times you patiently looked through all my presentations and constructively criticized my manuscripts improved the quality of my work, and all of this would never be forgotten. I couldn't have completed this project without your help. Thank you!

I cannot just but thank you, Dr. Marion Schrumpf, for the extra support you gave me and for your willingness to come to my aid anytime I requested your help. Discussing my sampling plans and design, patiently helping me with soil characterisation, and looking through my fresh data was always fun with you. Thank you for not just helping to review my manuscripts but for giving me advice regarding my future career plans as well.

I owe special gratitude to Iris Kuhlmann for her support in various ways in the laboratory throughout my project with so much fun and laughter. Thank you, Ines Hilke, for every C and N measurement you did, Heike Geilmann and Heiko Moossen for isotope measurements of bulk soil carbon, Stefen Rühlow for isotope measurements of CFE extracts, Axel Steinhof for radiocarbon analyses, and Armin Jordan for CO_2 gas measurements. To Jens Wurlitzer, Stefan Riedel, and Marco Pöhlmann, thank you for your constant support in all my sampling sites and for the extra hands in the laboratory with Iris Kuhlmann. It would have been a daunting task without your helping hands.

I like to thank Prof. Dr. Beate Michalzik and Florian Achilles, who taught me a bit more about soils. To Prof. Dr. Gerd Gleixner, thank you for dealing with some of my spontaneous requests and impromptu questions and for your encouragement towards the end. I also appreciate Dr. Will Overholt for his many advice and suggestions with statistics and R scripts and Dr .Martina Herrmann for all qPCR and IT-related troubleshooting.

To my colleagues and friends both at the Institute of Biodiversity and the MPI-BGC, Dr. Qianqian Li, Constantinos Xenophontos, Markus Krüger, Dr. Patricia Geesink, Dr. Swatantar Kumar, Dr. Stefan Krüger, Beatrix Heinze, Linda Goniak, Alisha Sharma, Rasil Nafeh, Kevin Bisdorf, Dr. Annu Panwa, Dr. David Herrera, Dr. Kasun Gayanta, Dr. Antonios Apostolakis; thank you for making these institutes fun and conducive to work in, and for the many nice lunch breaks, summer grills and nice chats we had together.

To my dear friends and community here in Jena, Dr. Tomi Ibidapo-Obe, Dr. Tosin Abdulsalam, Damilola Akinyemi, Wisdom Maduabuchi, Timothy Imogore, Evans Iyamu, Anthony Chukwubuikem, Dr. Lawrence Yomade, Dr. Seun Akintola, Kirsten Schulze, Christus Gemeinde, Der Eckstein community, and the entire Encounter crew, you made Jena a home, and this kept me going all along, especially during the tough times.

Special thanks go to you, my four siblings, Nike, Samuel, Dami, and Isaac Akinyede, for all the inspiration and the hope I derived from you to finish. My indebted gratitude goes to my grandmother, Prof Lalage J. Bown (of blessed memory). Although you never got to see this work completed, you were always supportive with your encouraging words and kind advice in the many times you were able to. I can’t forget to thank all my in-laws, both young and old, for always making me smile and checking in to ensure everything was fine.

I am very grateful to my dear parents, Prof. Dr. and Mrs. Akinyede, without whom completing this doctoral study would be possible. Thank you for your love, your never lagging support, encouragement, prayers, and faith in me since the day I was born.

My dearest hugs go to my darling husband, Adeoye Adetoba. Coming aboard in the middle of this journey made the ride a whole lot smoother. Your trust in me and your supportive, kind, and encouraging words and shoulder, which I always needed to lean or cry on during my highs and lows, made all the difference.

Lastly, I am most grateful to my Lord and Saviour Jesus Christ, His love, guide and grace were and would always be my fuel!

9 Declaration of authorship

I hereby affirm the originality of this dissertation, “The dark side of primary production in temperate forest soils.” I confirm that I have cited the use of all used resource materials, data, personal communications, and literature used in the written text. All the assistance I received during the sampling campaigns, experimental set-ups, data analyses, presentations, and the writing of all the manuscripts have been provided as co-author contributions or mentioned in the acknowledgments in the respective published and prepared manuscripts.

I confirm that I have read and am familiar with the doctoral examination regulations by the Faculty of Biological Sciences of the Friedrich Schiller University Jena. I have not received any assistance from a consultant to write this dissertation. Also, no third party has received both indirectly and directly any financial rewards from me in relation to the entire contents of this doctoral dissertation. The whole or parts of this dissertation have not been previously submitted or accepted for either scientific survey or the award of a degree to the Friedrich Schiller University Jena or any other university or institution.

Jena, 26.04.2022

Rachael Oluwatoyin Akinyede

10 Contributions to published articles and manuscript

In this thesis, chapters 2 to 3 and chapter 4 were published and submitted respectively in international peer-reviewed journals. My contribution to each manuscript is as follows:

Chapter 2. **Rates of dark CO_2 fixation are driven by microbial biomass in a temperate forest soil** (Akinyede et al., 2020, published in *Soil Biology & Biochemistry*).

For this study, Trumbore, S. and Küsel, K designed the project and, together with Taubert, M and Schrumpf, M, designed the experiments. I, Akinyede, R, Küsel, K, and Schrumpf, M conducted the soil sampling campaigns. I performed all isotope measurements and molecular analysis, analyzed and discussed data (including all figures), and wrote the manuscript. Taubert, M helped with the experimental design, supervised DNA extraction and sequence analysis, and helped with the data visualization and discussion. Taubert, M also edited the manuscript draft. Schrumpf, M., Trumbore, S., Küsel, K helped review and edit the manuscript draft. My contributions are summarized as follows:

Study Design/Concept: 20%
Experimental Work: 70%
Data Analysis & Figures: 70%
Manuscript writing: 50%

Chapter 3. **Dark CO_2 fixation in temperate beech and pine forest soils** (Akinyede et al., 2022a, published in *Soil Biology & Biochemistry*).

In this study, I, Akinyede, R, Schrumpf, M and Küsel, K designed the concept and experiment. I conducted all soil sampling campaigns and laboratory experiments, performed all isotope measurements and molecular analysis, and analyzed all generated datasets, including the statistical modelling and figures. Taubert, M helped with experimental design, molecular analysis, and data visualization. He also edited the manuscript draft. Schrumpf, M., Trumbore, S., Küsel, K assisted with sampling design and editing the manuscript draft. The manuscript was written by me with contributions from all authors. My contributions are summarized as follows:

Study Design/Concept: 50%
Experimental Work: 80%

Data Analysis & Figures: 90%
Manuscript writing: 60%

Chapter 4. **Temperature sensitivity of dark CO_2 fixation in temperate forest soils** (Akinyede et al., 2022b, published in *Biogeosciences*).

For this manuscript, I, Akinyede, R, conceptualized the study with help from all co-authors. I designed and conducted the soil sampling and experiments. I performed all isotope measurements, analyzed the data, and produced all figures. I also wrote the manuscript draft. Taubert, M was part of the experimental design, data visualization and discussion, and editing of the manuscript. Schrumpf, M., Trumbore, S., Küsel, K helped with the study and experimental design, as well as reviewed and edited the manuscript draft. My contributions are summarized as follows:

Study Design/Concept: 70%
Experimental Work: 85%
Data Analysis & Figures: 90%
Manuscript writing: 70%

_____ _____

Jena, 26.04.2022 Jena, 26.04.2022

Rachael Oluwatoyin Akinyede Prof. Dr. Kirsten Küsel

11 Curriculum Vitae

Personal Details

Name: Rachael Oluwatoyin Akinyede

[redacted]

Education

[redacted]

Work Experience

[redacted]

Teaching at Institute of Biodiversity, Friedrich Schiller University Jena

[redacted]

Voluntary activities

[redacted]

Awards and Grant

[redacted]

Scientific training

[redacted]

Research-stay

Academic conferences

Publications/Manuscripts

Akinyede R., Taubert M., Schrumpf M., Trumbore S., Küsel K. 2022b. Temperature sensitivity of dark CO_2 fixation in temperate forest soils. *Biogeosciences* 2, 4011–4028. doi.org/10.5194/bg-19-4011-2022.

Akinyede R., Taubert M., Schrumpf M., Trumbore S., Küsel K. 2022a. Dark CO_2 fixation in temperate beech and pine forest soils. *Soil Biology & Biochemistry* 165, 108526. doi.org/10.1016/j.soilbio.2021.108526

Akinyede, R., Taubert, M., Schrumpf, M., Trumbore, S., Küsel, K., 2020. Rates of dark CO_2 fixation are driven by microbial biomass in a temperate forest soil. *Soil Biology & Biochemistry* 150, 107950. doi:10.1016/j.soilbio.2020.107950

Njoku, K.L., Akinyede, O.R., Obidi, O.F., 2020. Microbial remediation of heavy metals contaminated media by *Bacillus megaterium* and *Rhizopus stolonifer*. Scientific African 10, e00545. doi:https://doi.org/10.1016/j.sciaf.2020.e0054

Presentations/Posters in conferences

Akinyede R., Taubert M., Schrumpf M., Trumbore S., Küsel K. (2020). Significance and driving forces of dark CO_2 fixation for organic carbon inputs in temperate forest soils. European Geoscience Union (EGU), Online platform. (Presentation and poster).

Akinyede R., Taubert M., Schrumpf M., Trumbore S., Küsel K. (2019). Dark CO_2 fixation is driven by microbial biomass in temperate forest soils and enhanced over a sub-ambient to elevated CO_2 gradient. American Geophysical Union (AGU), San Francisco, USA. (Poster).

Akinyede R., Taubert M., Schrumpf M., Trumbore S., Küsel K. (2019). Dark CO_2 fixation by soil microbes contributes to soil organic matter formation in soils from an old-growth deciduous forest. European Geoscience Union (EGU), Vienna, Austria. (Presentation).

Akinyede R., Taubert M., Schrumpf M., Trumbore S., Küsel K. (2018). Dark CO_2 fixation by soil microbes contributes to soil organic matter formation in an old-growth deciduous forest soil. International Society for Microbial Ecology (ISME), Leipzig, Germany. (Poster).